



U.S. Department  
of Transportation  
**National Highway  
Traffic Safety  
Administration**

# The Minicars Research Safety Vehicle Program Phase III

---

## Volume II—Appendices

V. K. Ausherman  
A. V. Khadilkar  
S. R. Syson  
C. E. Strother  
D. E. Struble

Minicars, Inc.  
55 Depot Road  
Goleta, California 93117

Contract No. DOT HS-7-01552  
Contract Amount \$10,906,954

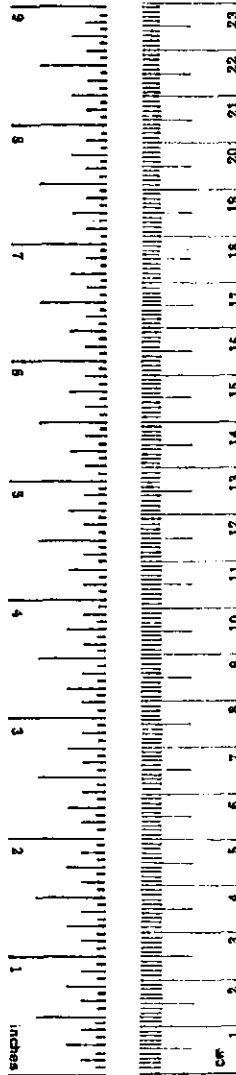
This document is disseminated under the sponsorship of the Department of Transportation in the interest of information exchange. The United States Government assumes no liability for its contents or use thereof.

1. Report No. DOT-HS-806 214		2. Government Accession No.		3. Recipient's Catalog No.	
4. Title and Subtitle The Minicars Research Safety Vehicle Program Phase III - Volume II, Appendices				5. Report Date September 1981	
				6. Performing Organization Code	
7. Author(s) V.K. Ausherman, A.V. Khadilkar, S.R. Syson C.E. Strother, D.E. Struble				8. Performing Organization Report No. RF-2100-09-81	
9. Performing Organization Name and Address Minicars, Inc. 55 Depot Road Goleta, California 93117				10. Work Unit No. (TRAIS)	
				11. Contract or Grant No. DOT-HS-7-01552	
12. Sponsoring Agency Name and Address U.S. Department of Transportation National Highway Traffic Safety Administration 400 Seventh Street, S.W. Washington, DC 20590				13. Type of Report and Period Covered Final Report Jan 1977 to Sep 1981	
				14. Sponsoring Agency Code	
15. Supplementary Notes					
16. Abstract <p>The objective of the RSV Program was to provide research and test data applicable to the automobile safety performance requirements for the mid-1980s, and to evaluate the compatibility of these requirements with environmental policies, efficient energy utilization, and consumer economic considerations. The program was designed to answer the question, "Can small fuel-efficient cars be made safe?" and to address such topics as: How safe should cars in general, and small cars in particular, be? What technologies will be required to make them this safe? Are these technologies feasible? Can they be, or have they been, sufficiently developed to justify the promulgation of more stringent safety standards?</p> <p>The RSV Program has demonstrated that it is possible to make cars much safer than they are presently. It has produced automobile designs that are consistent, at affordable cost, with the national objectives for fuel economy and environmental protection. It has indicated, at least to a limited degree, that the technological findings are applicable, at varying levels, to a variety of car designs. And it has provided evidence that these findings can be wrapped in a package of considerable appeal to the public.</p> <p>This Final Report is a comprehensive compilation of the findings of the Phase III efforts of Minicars, Inc. It describes the design and testing of the RSV systems, and the performance levels achieved. Specific topics include a vehicle description and performance specification, the structure, occupant restraints, braking and handling, propulsion, the vehicle exterior, driver controls, the radar and electronics, the Large Research Safety Vehicle, and the accident environment analysis.</p>					
17. Key Words RSV, Safety, Crashworthiness, Airbags, Radar, Large RSV, Foam-filling, High Technology RSV, Occupant Protection, Anti-skid Braking, Minicars, Automotive Electronics			18. Distribution Statement Document is available to the U.S. public through the National Technical Information Service, Springfield, Virginia 22161		
19. Security Classif. (of this report) Unclassified		20. Security Classif. (of this page) Unclassified		21. No. of Pages 301	22. Price

## METRIC CONVERSION FACTORS

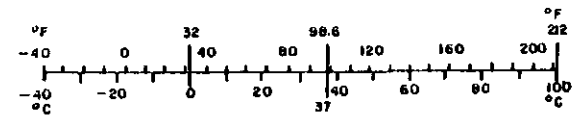
### Approximate Conversions to Metric Measures

Symbol	When You Know	Multiply by	To Find	Symbol
<b>LENGTH</b>				
in	inches	*2.5	centimeters	cm
ft	feet	30	centimeters	cm
yd	yards	0.9	meters	m
mi	miles	1.6	kilometers	km
<b>AREA</b>				
in <sup>2</sup>	square inches	6.5	square centimeters	cm <sup>2</sup>
ft <sup>2</sup>	square feet	0.09	square meters	m <sup>2</sup>
yd <sup>2</sup>	square yards	0.8	square meters	m <sup>2</sup>
mi <sup>2</sup>	square miles	2.6	square kilometers	km <sup>2</sup>
	acres	0.4	hectares	ha
<b>MASS (weight)</b>				
oz	ounces	28	grams	g
lb	pounds	0.45	kilograms	kg
	short tons (2000 lb)	0.9	tonnes	t
<b>VOLUME</b>				
tsp	teaspoons	5	milliliters	ml
Tbsp	tablespoons	15	milliliters	ml
fl oz	fluid ounces	30	milliliters	ml
c	cups	0.24	liters	l
pt	pints	0.47	liters	l
qt	quarts	0.96	liters	l
gal	gallons	3.8	liters	l
ft <sup>3</sup>	cubic feet	0.03	cubic meters	m <sup>3</sup>
yd <sup>3</sup>	cubic yards	0.76	cubic meters	m <sup>3</sup>
<b>TEMPERATURE (exact)</b>				
°F	Fahrenheit temperature	5/9 (after subtracting 32)	Celsius temperature	°C



### Approximate Conversions from Metric Measures

Symbol	When You Know	Multiply by	To Find	Symbol
<b>LENGTH</b>				
mm	millimeters	0.04	inches	in
cm	centimeters	0.4	inches	in
m	meters	3.3	feet	ft
m	meters	1.1	yards	yd
km	kilometers	0.6	miles	mi
<b>AREA</b>				
cm <sup>2</sup>	square centimeters	0.16	square inches	in <sup>2</sup>
m <sup>2</sup>	square meters	1.2	square yards	yd <sup>2</sup>
km <sup>2</sup>	square kilometers	0.4	square miles	mi <sup>2</sup>
ha	hectares (10,000 m <sup>2</sup> )	2.5	acres	
<b>MASS (weight)</b>				
g	grams	0.035	ounces	oz
kg	kilograms	2.2	pounds	lb
t	tonnes (1000 kg)	1.1	short tons	
<b>VOLUME</b>				
ml	milliliters	0.03	fluid ounces	fl oz
l	liters	2.1	pints	pt
l	liters	1.06	quarts	qt
l	liters	0.26	gallons	gal
m <sup>3</sup>	cubic meters	36	cubic feet	ft <sup>3</sup>
m <sup>3</sup>	cubic meters	1.3	cubic yards	yd <sup>3</sup>
<b>TEMPERATURE (exact)</b>				
°C	Celsius temperature	9/5 (then add 32)	Fahrenheit temperature	°F



\* 1 in = 2.54 (exactly). For other exact conversions and more detailed tables, see NBS Misc. Publ. 286, Units of Weights and Measures, Price \$2.25, SD Catalog No. C13.10 286.

APPENDIX A

RCA LABORATORIES FINAL REPORT

ELECTRONIC SUBSYSTEMS FOR THE RESEARCH SAFETY  
VEHICLE (PHASE III)

Report No. NHTSA-79-001

# **ELECTRONIC SUBSYSTEMS FOR THE RESEARCH SAFETY VEHICLE (PHASE III)**

RCA Laboratories  
Princeton, NJ 08540



MARCH 1980

FINAL REPORT

Document is available to the U.S. public through the National Technical Information Service, Springfield, Virginia 22161.

Prepared for  
Minicars, Inc.  
55 Depot Road  
Goleta, CA 93017

Prepared for the Department of Transportation, National Highway Traffic Safety Administration under Contract No. DOT-HS-01552. The opinions, findings, and conclusions expressed in this publication are those of the authors and not necessarily those of the National Highway Traffic Safety Administration.

The United States Government does not endorse products or manufacturers. Trade or manufacturer's names appear herein solely because they are considered essential to the object of this report.

This document is disseminated under the sponsorship of the Department of Transportation in the interest of information exchange. The United States Government assumes no liability for the contents or use thereof.

1. Report No.	2. Government Accession No.	3. Recipient's Catalog No.	
4. Title and Subtitle ELECTRONIC SUBSYSTEMS FOR THE RESEARCH SAFETY VEHICLE (PHASE III)		5. Report Date March 1980	6. Performing Organization Code
		8. Performing Organization Report No. PRRL-80-CR-8	
7. Author(s) E. F. Belohoubek, J. J. Risko, M. Ilovich J. Rosen, J. M. Cusack, R. E. Marx, and E. C. McDermott		10. Work Unit No.	11. Contract or Grant No.
9. Performing Organization Name and Address RCA Laboratories Princeton, New Jersey 08540		13. Type of Report and Period Covered Final Report 3/1/77 to 11/15/79	
		14. Sponsoring Agency Code	
12. Sponsoring Agency Name and Address Minicars, Inc. 55 Depot Road Goleta, California 93017		15. Supplementary Notes	
16. Abstract  <p>This final report covers Phase III of RCA's effort in the DOT sponsored development of the Research Safety Vehicle (RSV) for the mid 80's. Minicars, Inc., is the prime contractor on this program with RCA being responsible for the radar, sensor and display subsystems of the RSV. The radar, an FM/CW system interfaced with a microcomputer, is used to provide: (a) collision-mitigation braking, (b) automatic headway control, and (c) driving-related warning messages.</p> <p>The collision-mitigation function of the RSV involves the application of antiskid brakes under conditions where, based on radar and other sensor inputs, it is certain that a severe collision will take place. Other objects, not directly in the immediate path of the vehicle, must not trigger the brakes. The optimization of the radar processing hardware and associated computer algorithm for this function was performed with the help of tape recordings (both video and radar IF) for a large variety of road, traffic, and weather conditions. Separate, simulated collision tests were performed with an expendable target (corner reflector) to demonstrate the short reaction time of the system.</p> <p>The automatic headway-control system has the task to keep a safe distance with respect to the car ahead based on speed and range inputs. Without other vehicles close by, the system functions as a standard cruise control. Successful operation of the headway-control system interfaced with the car throttle was demonstrated on an RCA-owned station wagon. The integration of the system into the RSV is a separate follow-on task.</p> <p>Driving-related information, such as speed, mileage, fuel economy, fuel level, etc., together with warning messages such as water temperature too high, oil pressure too low, emergency brake on, doors open, etc., are shown on an alphanumeric plasma display which is interfaced through a micro-computer to various sensors.</p>			
17. Key Words (Selected by Author(s)) Research Safety Vehicle Collision-mitigation braking Automatic headway control Driving-related warning messages		18. Distribution Statement Document is available to the U.S. public through the National Technical Information Service, Springfield, Virginia 22161.	
19. Security Classif. (of this report) Unclassified	20. Security Classif. (of this page) Unclassified	21. No. of Pages 196	22. Price*

\*For sale by the Clearinghouse for Federal Scientific and Technical Information, Springfield, Virginia 22151.

## PREFACE

This Final Report describes work performed at the Microwave Technology Center of RCA Laboratories, Princeton, New Jersey, from March 1, 1977 to November 15, 1979, under subcontract P.O. 5062 from Minicars, Inc., Goleta, California. The prime contract for this effort was DOT-HS-7-01552, with Mr. Jerome Kossar from National Highway Traffic Safety Administration as contracting officer.

The program was carried out under the direction of Dr. Erwin F. Belohoubek, Head of the Microwave Circuits Technology. The following scientists participated in the development effort: John J. Risko, Mordechay Ilovich, Jerome Rosen, and Joseph M. Cusack (part-time consultant). The major portion of the effort on the radar headway control was carried out under separate RCA funding, with William R. Lile as project scientist.

## TABLE OF CONTENTS

Section	Page
I. INTRODUCTION .....	1
II. OVERALL SYSTEM LAYOUT .....	5
III. RADAR RF DESIGN .....	8
A. Ku-Band, Bistatic Noncooperative Radar .....	8
1. Block Diagram .....	8
2. System Parameters .....	10
a. RF Frequency Considerations .....	10
b. Bistatic Radar Considerations .....	12
c. Modulation Parameters .....	13
3. Range and Range-Rate Accuracy .....	15
4. Antenna Design and Measurement .....	20
5. Coverage Pattern Measurements .....	21
6. IF Amplifier Shaping for CMS .....	26
B. Dual-Mode X-Band Radar .....	28
1. Block Diagram .....	28
2. System Parameter Selection .....	30
3. Coverage Pattern Measurements .....	33
C. Radome for RSV Installation .....	37
IV. PROCESSOR HARDWARE .....	46
A. Radar Cards for CMS and Headway Control .....	46
1. Introduction .....	46
2. Phase II Radar Card .....	47
3. Phase III Radar Card .....	50
4. Revised Phase III Radar Card .....	52
5. Threshold Circuit .....	53
B. CPU and Memory .....	55
1. Introduction .....	55
2. Phase III Evaluation-Board System .....	56
3. CPU and Memory Card Cage for RSV Installation .....	59
4. Remote-Start Circuit for CPU .....	60
C. Display and Sensor Interfaces .....	65

TABLE OF CONTENTS (Continued)

Section	Page
V. CONTROL FUNCTIONS AND SOFTWARE IMPLEMENTATION .....	75
A. Collision-Mitigation Braking Considerations .....	75
B. Collision-Mitigation System .....	78
C. Headway/Cruise Control .....	82
1. Introduction .....	82
2. Design Considerations .....	83
3. Algorithm Flow Diagram .....	89
VI. PERFORMANCE TESTS .....	92
A. Test Van Instrumentation .....	92
B. Collision-Mitigation System Tests .....	97
C. Headway-Control Tests .....	104
1. System Optimization .....	104
2. Road Tests .....	105
3. Headway-Control Demonstration Vehicle .....	111
VII. INSTALLATION OF EQUIPMENT INTO THE RSV .....	115
A. General .....	115
B. Microcomputer and Sensor Installation .....	115
C. Radar Safety Considerations .....	118
VIII. COST ESTIMATES .....	120
IX. CONCLUSIONS AND RECOMMENDATIONS .....	122
APPENDIX A. COVERAGE PATTERN CALCULATIONS .....	A-1
APPENDIX B. SOFTWARE LISTING FOR CMS ALGORITHM .....	B-1
APPENDIX C. SOFTWARE LISTING FOR ARITHMETIC SUBROUTINE GETRAN .....	C-1
APPENDIX D. SOFTWARE LISTING FOR ELECTRONIC DASHBOARD DISPLAY .....	D-1
REFERENCES .....	R-1

## LIST OF ILLUSTRATIONS

Figure	Page
1. Block Diagram of Electronically Related Functions in RSV .....	6
2. Block Diagram of the Ku-Band FM/CW Radar .....	8
3. Front and Back View of the Radar Assembly .....	9
4. Asymmetric Triangular Modulation .....	16
5. Single Cycle of Nonlinear Modulation Waveform .....	18
6. Single Cycle of Distorted IF Frequency .....	20
7. Exploded View of Antenna .....	22
8. Azimuth Ku-Band Pattern .....	23
9. Elevation Ku-Band Pattern .....	23
10. Typical Radar-Target Configuration for Coverage Pattern Measurements .....	24
11. Coverage Pattern Ku-Band Radar - Output of Preamplifier .....	25
12. Coverage Pattern Ku-Band Radar - Output of Postamplifier .....	25
13. Transfer Characteristic of Ku-Band Preamplifier .....	26
14. Transfer Characteristic of CMS Postamplifier .....	27
15. Composite of Preamplifier and Postamplifier .....	27
16. Block Diagram of Dual-Mode Radar .....	30
17. (a) Typical IF Voltage Waveform for 0- to 180-Degree Phase Modulator. (b) Output of Envelope Detector .....	31
18. Cooperative Channel of Dual-Mode X-Band Radar .....	34
19. Baseband Channel of Dual-Mode X-Band Radar .....	34
20. Location of Microwave Tag Mounted on Vehicle .....	35
21. X-Band Dual-Mode Radar Mounted on Vehicle .....	36
22. Anechoic Chamber for Antenna Measurements .....	38
23. Azimuth Antenna Pattern (Nose and Air Scoop) .....	39
24. Elevation Antenna Pattern (Nose and Air Scoop) .....	39
25. Radome Construction .....	41
26. Azimuth Antenna Pattern With Radome .....	42
27. Elevation Antenna Pattern With Radome .....	43
28. Bistatic Ku-Band Radar with Radome .....	44
29. RSV With Radar and Radome in Place .....	45
30. Block Diagram of Phase II CMS Card .....	48

LIST OF ILLUSTRATIONS (Continued)

Figure	Page
31. Waveforms on Radar Interface Card .....	48
32. Signal-Processing Time Relations .....	49
33. Block Diagram of Phase III CMS Card .....	51
34. Revised Phase III CMS Card .....	53
35. Threshold Detection Circuits .....	54
36. Evaluation Board with Card Cage and Display .....	58
37. Evolution From Development Board to Full Card Cage System .....	59
38. Block Diagram of CPU Card .....	60
39. Photograph of CPU Card .....	61
40. Complete CMS Card Cage .....	62
41. CMS Card Cage with Cover Removed .....	63
42. Size Comparison - Microcomputer and CDS .....	64
43. Remote-Start Circuit .....	65
44. 8-Input Analog/Digital Circuit .....	67
45. Trip Odometer Circuit .....	67
46. Clock Circuit Diagram (Oscillator and Minute Counter) .....	69
47. Clock Circuit Diagram (Hour Advance) .....	69
48. Tachometer Interface Circuit .....	70
49. Fuel Economy Sensor Circuit .....	70
50. Schematic of Display Interface .....	72
51. Binary Input Card for Switches .....	73
52. Schematic of Airbag Indicator .....	73
53. Schematic of Velocity Indicator .....	74
54. Distance/Time Relation Between Two Vehicles, One of Which is Being Braked .....	75
55. Impact Velocity as Function of Distance Between Radar Car and Collision Object (System Delay 0.2 s; Braking Coefficient $\mu = 0.9$ ) .....	76
56. Energy Reduction as Function of Detection Distance and Closing Rate .....	77
57. Flow Chart of GETRAN (Data Acquisition) .....	79
58. Flow Chart of Main CMS Program .....	80
59. Comparison Between Cruise Control and Radar Headway Control .....	83

LIST OF ILLUSTRATIONS (Continued)

Figure	Page
60. Block Diagram of Headway-Control System .....	84
61. Automatic Cruise/Headway-Control Algorithm .....	85
62. State Transition Diagram .....	87
63. Capture Mode .....	88
64. Headway-Control Flow Chart .....	91
65. Test Van for Recording of Video and Radar Information .....	93
66. Interior of Test Van .....	94
67. View from Test Van During CMS Tests on Airport Runway .....	95
68. Block Diagram of Power Distribution in Test Van .....	96
69. Test Van During CMS Test with Expendable Target .....	97
70. Block Diagram and Waveforms of Recording System .....	99
71. Block Diagram of Playback System .....	101
72. System for Simultaneous Playback of Radar and Video Information .	102
73. Headway-Control Computer and Strip Chart Recorder Mounted in Front of RCA Station Wagon .....	106
74. Linear Throttle Activator .....	107
75. Early Recording of Cooperative Radar Car Following A Target Car Operating in Cruise Control at 45 mph .....	109
76. Noncooperative Ku-Band Radar Car Following Standard Passenger Car (Pinto) Using Optimized Algorithm .....	110
77. Headway-Control Radar Mounted on RCA Station Wagon .....	112
78. Display Format for Headway-Control Demonstration .....	114
79. Electromechanical Arrangement for Steering Angle Determinations .	117
80. Antenna Field Intensities .....	118
A-1 Calculated Detection Pattern (No Shaping) .....	132
A-2 Calculated Detection Pattern (High Pass: 1 Section, Cutoff at 30.7 m) .....	133
A-3 Calculated Detection Pattern (Low Pass: 4 Section, $R_c = 32.2$ m; High Pass: 1 Section, $R_c = 15.4$ m) .....	134
A-4 Cooperative Radar-Tag Geometry for Coverage Pattern Measure- ments .....	137
A-5 Detection Pattern for Cooperative Radar (Output of Detector) ....	139

LIST OF ILLUSTRATIONS (Continued)

Figure	Page
A-6 Detection Pattern of Cooperative Radar (Output of Post-amplifier) .....	140
A-7 Detection Pattern of Monostatic, X-band, Noncooperative Radar (Output of Preamplifier) .....	142

SECTION I  
INTRODUCTION

This report covers Phase III of the development effort, sponsored by the National Highway Traffic Safety Administration (NHTSA) under contract No. DOT-HS-7-01552, toward the demonstration of various electronic subsystems for the Research Safety Vehicle (RSV), for the mid-1980s time frame. Specifically, this effort encompassed extensions of the electronic functions that act as driver aids and that maximize the vehicle's collision avoidance and mitigation capabilities, with the final goal of installing these systems in the latest, high technology version of the RSV. This work was conducted by the Microwave Technology Center of RCA Laboratories in Princeton, New Jersey, under subcontract from Minicars, Inc., Goleta, California, during the period from March 1977 to November 1979.

The major effort during Phase III was directed toward the development of an FM/CW radar that, interfaced with a microcomputer, provides the following functions: (a) collision mitigation braking; (b) automatic safe headway control; and (c) driving-related warning messages. These warning messages are flashed on a self-scan alphanumeric plasma display which, driven by another microcomputer, also shows general operating and functional data such as speed, mileage, fuel level, oil pressure, water temperature, etc.

While the provision of safety and warning messages represented merely an extension and refinement of an existing system developed during Phase II, the collision-mitigation and headway-control systems required substantial development efforts to demonstrate their practical potentials in a real traffic environment. Early road tests with the initial radar system during Phase II had clearly shown the need for a more systematic approach to the optimization of the radar system to ensure proper operation and elimination of practically all false alarms under a wide variety of driving conditions. A large portion of Phase III was thus devoted to the tape recording of a wide variety of road, traffic, and weather conditions to permit a thorough optimization of the radar processing hardware and associated computer algorithm.

We also proceeded from initial headway-control experiments during Phase II that provided only speed-up or slow-down messages to a closed-loop system with the throttle of the car tied to the radar system for truly automatic headway

control. The inclusion of proportional braking into the automatic headway-control action, which would further enhance the acceptability of this function to the driver, was not yet included on the present test car.

The specific goals for the Phase III effort as originally formulated are listed below:

- Task 1 Installation of Phase II radar and display into RSV exhibition vehicle.
- Task 2 Radar improvements, including dual-mode operation (cooperative/noncooperative).
- Task 3 Road tests using tape recordings of radar output, together with video information of traffic conditions to optimize signal processing algorithm.
- Task 4 Final system integration and installation in high technology RSV.
- Task 5 Cost effectiveness studies.

During the early portion of the program it became apparent that a shift in the operating frequency of the radar to higher values would be beneficial. We also learned at that time of three major government-sponsored programs in Germany [1,2,3], all directed toward radar warning on high-speed expressways. Consequently, we concentrated our efforts mainly on collision mitigation and headway control, rather than long-range warning that was being explored by German companies very extensively using sophisticated 35-GHz radars. In addition, our program experienced a serious slow-down due to funding shortages that eventually led to a stretch of the program from the originally planned 18 months to 33 months.

1. D. Zur Heiden and H. Oehlen, "Radar Anticollision Warning System for Road Vehicles," *Electrical Communications* 52(2), 141 (1977).
2. G. Hahlganss and L. Hahn, "Headway Radar Using Pulse Techniques," *Int. Conf. on Automobile Electronics*, London, July 1976, pp. 132-135.
3. E. Dull and H. Peters, "Collision Avoidance System for Automobiles," *Society of Automotive Engineers*, Publication #780263, March 1978.

The above factors resulted in a redefinition of the program goals, as outlined in a new work statement dated May 1978 and listed in abbreviated form below:

Task 1 - Demonstration of Radar Functions in RCA-Owned Vehicles

- (a) Headway control using a cooperative X-band radar
- (b) Headway control using the new Ku-band noncooperative radar
- (c) Collision-mitigation function tests with expendable target

Task 2 - Radar Improvements

- (a) Design, fabricate, and test dual-mode (cooperative/noncooperative) radar at X-band
- (b) Develop noncooperative bistatic Ku-band radar
- (c) Improve processor algorithm and reliability of microcomputer system
- (d) Interface throttle and brakes to microprocessor

Task 3 - Road Test Program

- (a) Equip RCA test van with video recorder and synchronized radar IF output recorder
- (b) Perform tape recordings of test rides under a wide variety of traffic, road, and weather conditions
- (c) Optimize radar processing and computer algorithms of collision mitigation and headway-control\* functions
- (d) Perform final road tests of both systems in RCA cars under actual traffic conditions

Task 4 - Final System Integration

- (a) Fabricate and install Ku-band noncooperative bistatic radar, display, and associated microcomputers in a high-technology version of RSV
- (b) Calibrate all sensor functions, optimize radar performance and put all algorithms in the programmable read-only memory (PROM)

\*The development of a digital cruise control, the headway control, and fuel economy experiments with these systems were performed on RCA cars under separate RCA funding.

### Task 5 - Cost Study

Estimate the 1985 cost of individual systems in 1979 dollars using RCA's PRICE program

Practically all of the above tasks have been completed, except that in the present version of the high-technology RSV, the tie-in between the headway microcomputer and the automatic, electronically shifted transmission was not implemented. Due to a series of program delays and the unavailability in time of a properly functioning computer-controlled transmission, the final optimization of the automatic headway control could not be carried out in the RSV. The basic feasibility of this function was demonstrated instead on a separate RCA station wagon, which was refurbished specifically for demonstration purposes.

The final integration of the headway control into the RSV is the objective of a planned follow-up program which will be a joint effort between Dubner Computer Systems,\* Minicars, and RCA, and will be performed at RCA Laboratories in Princeton toward the middle of 1980. The results of this final integration will be reported separately.

---

\*Dubner Computer Systems, New York City, NY.

## SECTION II

### OVERALL SYSTEM LAYOUT

As mentioned before, the use of radars for long-range warning-only purposes has been explored extensively by several companies under government sponsorship in Germany. These radars are geared mainly toward warning the driver of impending dangerous situations and leaving the decision to react to this warning to the driver. Because of the relatively long reaction time of the driver (between 0.6 to 1 s), the warning has to be based on long-range information (typically 100 to 150 m) at the high speeds prevalent on many of Europe's expressways.

The situation in the United States, having a maximum speed limit of 90 km/h (55 mph) throughout, is substantially different. Here we try to effect a societal savings by mitigation of an inevitable collision. The key considerations are elimination of all false alarms and automatic application of antiskid brakes under conditions where, due to human error or mechanical failure, a severe collision is definitely unavoidable. This limits the action range of the radar to 25 to 30 m because for longer distances, the opportunities for false alarms increase rapidly and more importantly, a skilled driver possibly could still perform an avoidance maneuver which could be hampered by the application of antiskid brakes. Thus, the emphasis is on an automatic reaction only where a high-speed collision is unavoidable. This does not exclude the use of the radar for warning purposes over a longer range; the latter subject, however, has been covered extensively by the German radar development efforts and thus was not addressed in this program.

While the collision-mitigation function mentioned above is tailored mainly to safety aspects of the car, the automatic headway control could substantially improve the driver comfort and increase the throughput on high-density highways. Since the collision-mitigation function of the radar would not be used by the average driver so long as he is not involved in an accident, the simultaneous use of the radar for driver convenience is expected to lend a strong sales appeal to the inclusion of a radar in future cars.

In addition to the radar functions, the high-technology version of the RSV includes also a computer-controlled plasma display that provides driving-related information such as speed, mileage, fuel level, water temperature, etc., to the driver in either digital form or as analog bars. The selection

of the type of display format can be made through a switch by the driver. Malfunctions or safety hazards are indicated on the display by temporary flashing of warning messages which interrupt the normal display in 30-second intervals until the particular hazard has been corrected.

A block diagram of all electronically related functions in the RSV is shown in Figure 1. The processed radar signal is fed to two separate microprocessors, one for collision mitigation and one for headway control. A series of other sensor inputs, such as vehicle speed, steering angle, brake pedal position, and cruise control inputs are also interfaced with the respective microprocessors.

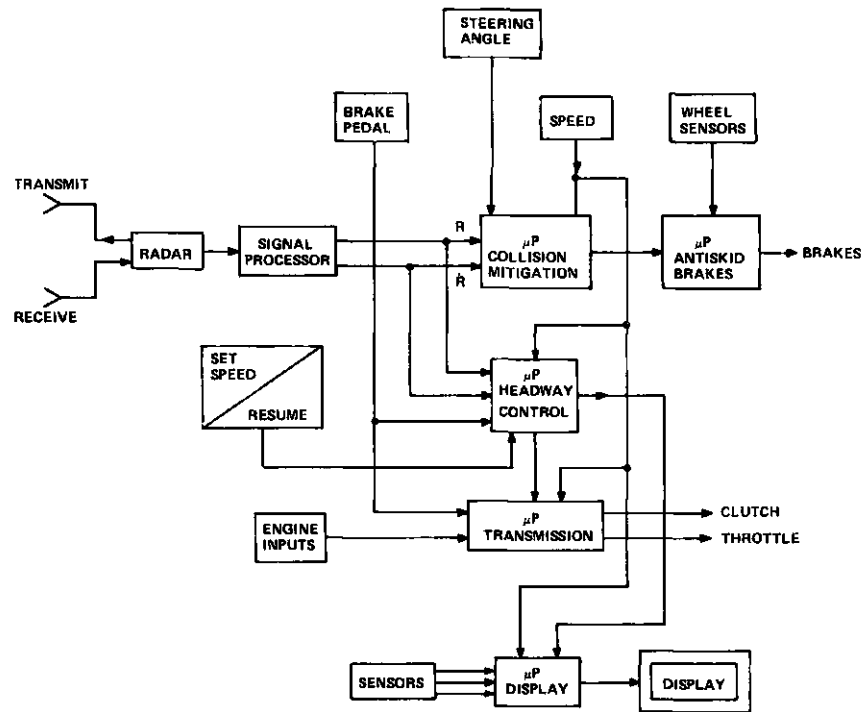


FIGURE 1. BLOCK DIAGRAM OF ELECTRONICALLY RELATED FUNCTIONS IN RSV.

At present, separate microprocessors are used for the collision-mitigation system (CMS), the headway control, the display, the antiskid system,\* and the automatic gear shift of the car. The latter function, being developed under subcontract to Minicars by Dubner Computer Systems, Inc., is important for

\*An experimental antiskid system, manufactured by Bendix, is used in the RSV.

improved fuel economy and interfaces directly with the commands from the automatic radar headway control. Later versions of the RSV could possibly use only two or three microprocessors, whereby one could perform certain vital functions in case of failure of the others to preserve a limp-home ability. Questions of time sharing between microprocessors and interleaving of programs, however, have not been addressed during this program.

SECTION III  
RADAR RF DESIGN

A. Ku-BAND, BISTATIC NONCOOPERATIVE RADAR

1. Block Diagram

The Ku-band radar is a forward-looking, bistatic noncooperative FM/CW radar. A block diagram of the system is shown in Figure 2. The RF section of the radar consists of a transmitter chain and receiver chain; each with its own antenna. The transmitter chain consists of a varactor-tuned oscillator and modulator, power divider, and printed circuit antenna. The receiver chain consists of a printed circuit antenna (same as in the transmit arm), isolator, and mixer. The IF section is made up of a shaped preamplifier and shaped postamplifier. Voltage regulators and ignition noise filters are included in the amplifiers.

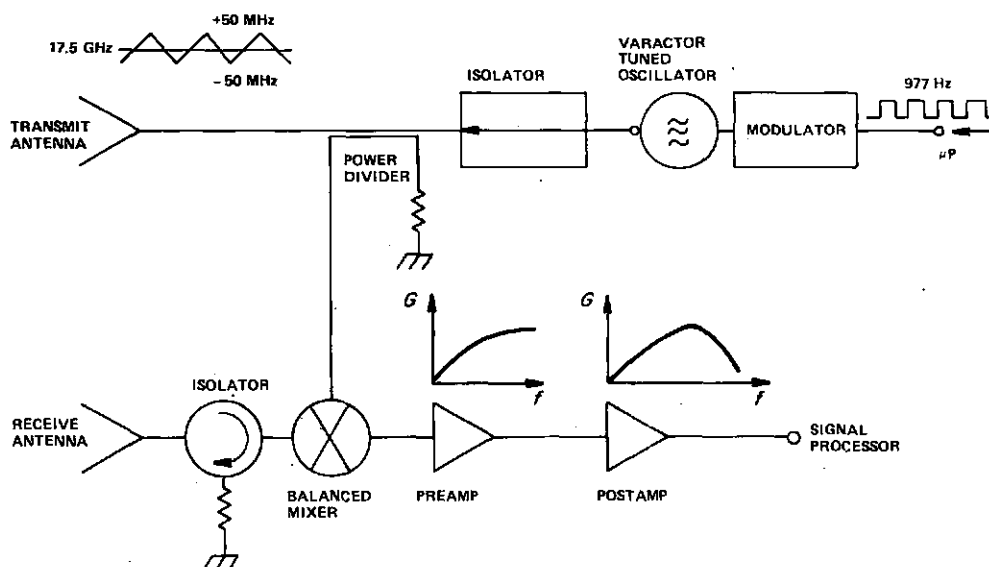


FIGURE 2. BLOCK DIAGRAM OF THE Ku-BAND FM/CW RADAR.

Figure 3 shows front and back views of the radar assembly with the radome removed. Also shown as part of the radar assembly are the radome supports, which serve as the transition members between the radar and the hood of the RSV. The radome conforms to the contour of the RSV and is made up of blocks of polystyrene covered with expanded polyethylene. The radome will be discussed in greater detail in subsection III.C below. The performance features of the radar are given in Table 1.

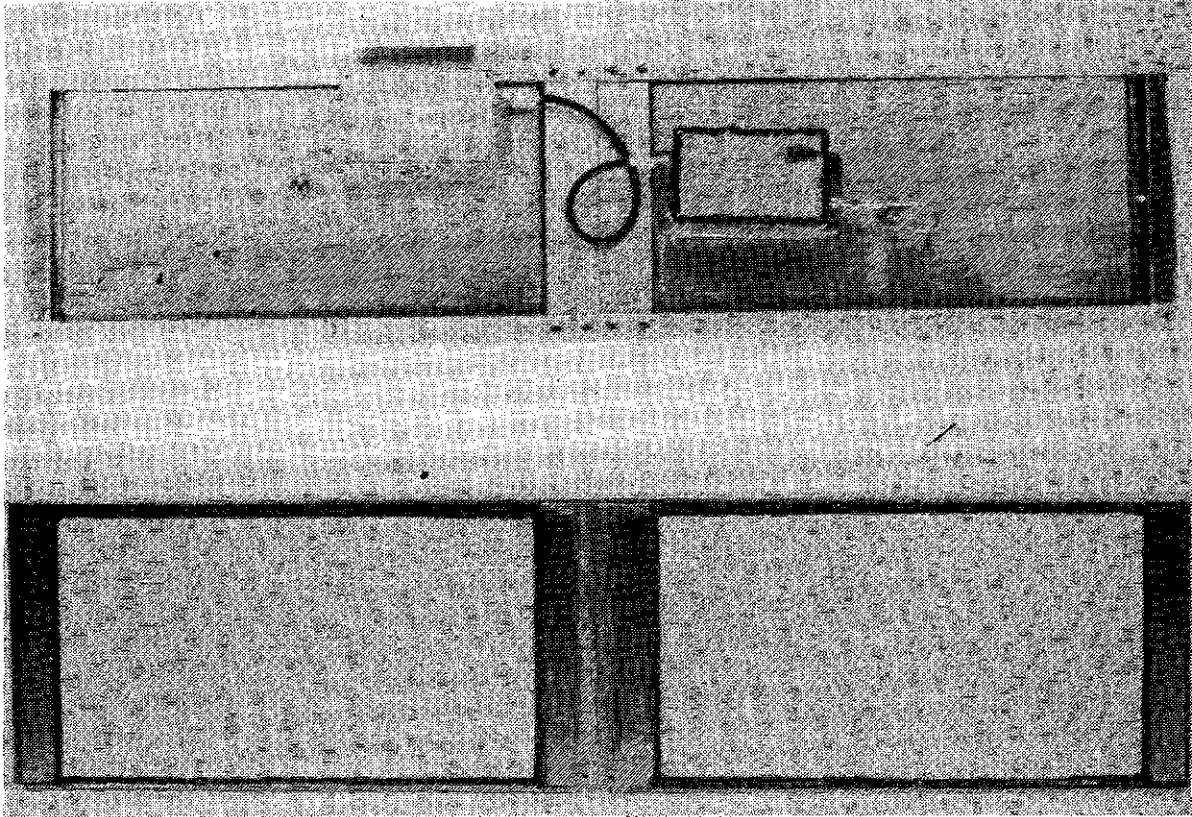


FIGURE 3. FRONT AND BACK VIEW OF THE RADAR ASSEMBLY.

TABLE 1. PERFORMANCE CHARACTERISTICS OF Ku-BAND RADAR

Parameter	Value
Frequency, $f_o$	17.5 GHz
Power Output, $P_o$	10 mW
Frequency Deviation, $\Delta f$	$\pm 50$ MHz
Modulation Rate, $f_m$	977 Hz
Beamwidth Horizontal, $\theta_H$	$3^\circ$
Beamwidth Vertical, $\theta_V$	$5^\circ$
Antenna Gain, G	30 dB
Bistatic Antenna Assembly Size	77 cm x 20.5 cm x 2.5 cm
Range	7 to 30 m, collision mitigation 8 to 50 m, headway control
Range-Rate	0-60 m/s

The operation of the radar is as follows: referring to Figure 2, the varactor-tuned oscillator and modulator furnish a 15-mW frequency-modulated carrier to the power divider. The carrier frequency is 17.5 GHz and has triangular modulation of  $\pm 50$  MHz deviation. One output of the power divider (11 mW) is directed to the antenna while the other output (2.75 mW) enters the local oscillator port of the mixer via a rigid cable. The power split is 6 dB to compensate for the 1.6-dB loss in the cable. The transmitted signal is reflected back to the radar from a target and coupled to the signal port of the mixer through the antenna and isolator in the receiver chain.

Due to the time delay between transmission and reception, the frequency of the received signal differs from the transmitted signal (local oscillator signal), and a beat frequency signal will be generated at the IF port of the mixer. The beat frequency contains the desired range and range-rate information which is recovered in the processing circuitry. The details of the signal processing are given in Section IV. Range and range-rate accuracy are discussed in subsection III.A.3 below. Range and range-rate information, speed of the radar-equipped vehicle, and steering angle are processed further to determine if a vehicle control action is necessary. The speed and steering angle are derived from transducers coupled to the speedometer and steering column of the vehicle, respectively. The software algorithms used for the control decisions are discussed in Section V.

## 2. System Parameters

### a. RF Frequency Considerations

To avoid false alarms from vehicles in adjacent lanes or roadside objects, a narrow antenna beam is desirable. For a narrow antenna beam, a large radiating surface is required, large with respect to a wavelength. For example, the X-band antenna used during Phase II is 28 x 17 cm (9.9 x 6 wavelengths) and provides a beam 5 degrees wide in azimuth and 10 degrees wide in elevation. Beamwidths are measured at the 3-dB points of the gain pattern. To decrease the beamwidth by a factor of two in azimuth and elevation, the required cross section becomes (19.9 x 12 wavelengths) or 56 x 34 cm at X-band. However, if the RF frequency were doubled, the same antenna area would provide an antenna pattern of half the beamwidths. Thus from both a size and ultimately cost standpoint, it is desirable to increase the RF frequency. The major limitation

to this trend is the availability and cost of RF components at the higher frequencies. The upper end of Ku-band (17.5 GHz) was chosen as a compromise frequency.

At 17.5 GHz, transferred electron oscillators (TEOs) are still state-of-the-art devices, and microstrip technology can be applied cost effectively to the other microwave components. In addition, microwave absorption through the atmosphere is still small, 0.02 dB/nautical mile for 1% water vapor and 6 dB/nautical mile for heavy rain. From the X-band reference of 10.575 GHz, a 40% size reduction is expected. The actual Ku-band antenna is 33 x 19 cm (19 x 11 wavelengths) and has a 3-degree beamwidth in azimuth and a 5-degree beamwidth in elevation.

A 3-degree beamwidth has been found to be a good compromise between beam confinement at far ranges and target acquisition at close range. For example, at 50 m the beam coverage is  $\pm 1.31$  m. Although the possibility of missing a target off to the side exists at close range, the decreased probability of false alarms in the far field is of greater importance.

For a well designed antenna, reducing the beamwidth will increase the gain. If the same current distribution would exist at X-band and Ku-band, reducing the beamwidths by a factor of two in azimuth and elevation would yield a 6-dB increase in gain. From the range equation the power returned to the radar is proportional to the square of the antenna gain, and square of the wavelength [4]. The net effect of increasing the gain by 6 dB and decreasing the wavelength would be a 8-dB increase in returned power for constant transmitted power. However, for the actual 17.5-GHz antenna, the gain only increased by 5 dB so that the returned power increased by 6 dB.

The location of multipath nulls is also dependent on the RF frequency. The range at which multipath nulls appear is given by, [5]

$$R = \frac{2h_1h_2}{\lambda N}, \quad N = 0, 1, 2, \dots \quad (1)$$

where  $\lambda$  is the wavelength,  $h_1$  is the effective height of the antenna above ground,  $h_2$  is the effective height of the target above ground, and  $N = 0$  corresponds to  $R = \infty$ .

4. F. E. Nathanson, Radar Design Principles, (McGraw-Hill Publishing Company, New York, 1969).
5. S. A. Hovanessian, Radar Detection and Tracking Systems, (Artech House, Inc., Massachusetts, 1973).

Experimentally it has been found that the farthest null from the radar, corresponding to  $N = 1$ , is the most severe. Assuming  $h_1 = h_2 = 0.675$  m, the first null occurs at 32 m in X-band. For a headway control system it is desirable to operate out to 50 m. A multipath null at 32 m would result in unstable operation around 32 m. To ensure smooth tracking out to 50 m, the multipath null should be moved beyond 50 m. By increasing the frequency to 17.5 GHz, the first null occurs at 53 m. This has been found to be acceptable.

b. Bistatic Radar Considerations

A shortcoming of CW radars is the lack of complete isolation between the transmitter and receiver. In a monostatic configuration (single antenna for transmit and receive), the antenna mismatch is the basic coupling mechanism between the transmitter and receiver. For example, an antenna with a VSWR of 1.2:1 will reflect 1% of the transmitter power to the receiver. By comparison in Ku-band, a  $1\text{-m}^2$  target 30 m from the radar returns only -67 dB to the receiver. Causes for the antenna reflection may be a slight mismatch between the feedline and the antenna or also the accumulation of snow or dirt on the front of the antenna radome.

The most serious problem caused by the coupled power, or spillover as it is more commonly called, is distortion of the IF amplifier output. In order to process the radar return and extract range and range-rate accurately, a flat amplifier response is required.

Because of spillover, the amplifier baseline is distorted and processing errors occur. Spillover also causes dynamic range problems when the spillover is orders of magnitude above the minimum detectable signal (MDS). A bistatic radar reduces this problem since separate antennas are used for transmit and receive. The basic coupling between transmitter and receiver for the bistatic system is through radiation from the transmit antenna to the receive antenna. The amount of radiation is a function of the antenna radiation pattern and the geometry of the antennas. For the stripline antennas mounted in the RSV that leakage is approximately -60 dB.

Another mode of spillover, even in bistatic radars, is through the mixer. Due to the finite isolation between the LO and signal port, some of the LO power is coupled to the signal port. An isolator before the receive antenna is used to reduce the effects of this source of spillover.

Although bistatic arrangements are larger and thus somewhat costlier, this configuration was chosen for the Ku-band radar to ensure reliable operation with high sensitivity.

c. Modulation Parameters

The general considerations made in choosing triangular FM modulation were given in the final report of Phase II [6] and will not be repeated here. Only the choice of modulation parameters for the Ku-band radar will be discussed.

Range accuracy is proportional to the bandwidth of the transmitted signal, while the range-rate accuracy is proportional to the processing time. Since the processing time is inversely proportional to the repetition frequency, some tradeoffs must be made between response time and range-rate accuracy. These tradeoffs are different for the CMS and the headway-control system. The CMS requires response times of the order of less than 100 ms while 0.5 s is adequate in the headway-control mode. For these response times, the 1-kHz repetition rate used previously for the X-band radar is adequate. In practice, because of greater stability, the 2-MHz crystal in the microprocessor is divided down to 977 Hz and serves as the repetition frequency.

The choice of the frequency deviation,  $\Delta f$ , about the center frequency is based on the following considerations:

The IF frequency,  $f_B$ , during the modulation upswing,  $f_{up}$ , and downswing,  $f_{down}$ , is given by [6]

$$\begin{aligned}
 f_{up} &= \left| \frac{8\Delta f f_m R}{c} \right| + \left| \frac{2 f_o \dot{R}}{c} \right| \\
 f_{down} &= \left| \frac{8\Delta f f_m R}{c} \right| - \left| \frac{2 f_o \dot{R}}{c} \right|
 \end{aligned}
 \tag{2}$$

The first term in equation (2) is often referred to as the range frequency,  $f_r$ , and the second term as the doppler frequency,  $f_d$ . Since  $\dot{R}$  can be positive or negative, depending on whether the target is inbound or outbound, equation (2) holds for an outbound target. For an inbound target, the sign of  $\dot{R}$

6. E. F. Belohoubek et al., "Electronic Subsystems for Research Safety Vehicle (RSV)," Final Report, Phase II, 1976.

is reversed and the beat frequency during upsweep is less than the beat frequency during the downsweep. This allows the determination of the direction of the range-rate during processing. When the range frequency,  $f_r$ , is greater than the doppler frequency,  $f_d$ , equation (2) becomes

$$\begin{aligned} f_{\text{up}} &= |f_r| + |f_d| \\ f_{\text{down}} &= |f_r| - |f_d| \end{aligned} \quad (3)$$

$$\begin{aligned} \text{and } |f_r| &= \frac{1}{2}(f_{\text{up}} + f_{\text{down}}) = f_{\text{B AVG}} \\ |f_d| &= \frac{1}{2}(f_{\text{up}} - f_{\text{down}}) \end{aligned} \quad (4)$$

From equation (4) it is seen that the range is proportional to the beat frequency averaged over a modulation cycle and the range-rate is proportional to the difference between upsweep and downsweep frequencies. When the doppler frequency is greater than the range frequency, the relations are reversed and the average beat frequency is proportional to the range-rate.

To ensure the condition of range frequency being greater than the doppler frequency over the complete set of range and range-rate of interest, the following inequality must hold

$$4\Delta f f_m R_{\text{min}} > v_{\text{max}} f_o \quad (5)$$

where  $f_m$  is the repetition frequency (977 Hz),  $R_{\text{min}}$  is the minimum range of interest (10 m),  $v_{\text{max}}$  is the maximum range-rate of interest (60 m/s), and  $f_o$  is the carrier frequency (17.5 GHz).

For the given parameters,

$$\Delta f > 27 \text{ MHz} \quad (6)$$

Equation (6) imposes one condition on the frequency deviation.

Another restriction arises from the spectral nature of the signal. Since the modulation is periodic in the repetition frequency,  $f_m$ , the transmitted signal can be represented as a Fourier series, with period  $1/f_m$ . The maximum signal strength occurs at  $f_m$  and decreases as the harmonic number increases. Unless filtering is included in the receiver, the receiver will be saturated by strong signal terms at  $f_m$  and the first two or three harmonics of  $f_m$ . To

simplify the filter problem, the IF frequency,  $f_B$ , should be much greater than  $f_m$ . Since  $f_B$  is proportional to  $\Delta f$ , a large value of  $\Delta f$  is desirable. For example, the minimum value of  $f_B$  that the receiver must pass is given by a target at the minimum range, traveling at the maximum velocity. Assuming a maximum velocity of 60 m/s at a range of 10 m and a frequency deviation of 27 MHz, the minimum IF frequency is 3.3 kHz; too close to  $3 f_m$ . A value of 50 MHz for  $\Delta f$  increases the minimum IF frequency to 6.2 kHz. This was considered a reasonable tradeoff between filter requirements and modulator complexity.

### 3. Range and Range-Rate Accuracy

Implicit in the derivation of equation (2) is the assumption that the modulating signal is a symmetric triangular wave. When the symmetry or the linearity of the triangular wave is perturbed, an error in range and range-rate will occur. To determine these errors, we use the more general equation relating the IF frequency,  $f_B$ , to modulation [6]

$$2\pi f_B = \ddot{\Psi}\tau + \dot{\Psi}\dot{\tau} \quad (7)$$

where

$$\begin{aligned} \Psi_{ch}(t) &= 2\pi \left\{ f_o t + \Delta f \int_0^t g(x) dx \right\} \\ \tau &= \frac{2R}{c} \end{aligned} \quad (8)$$

and  $\Delta f g(x)$  = frequency modulation

In the ideal case,

$$g(x) = 4f_m x \quad (9)$$

From equations (7) and (8)

$$f_B = +2\Delta f \dot{g}(t) \frac{R}{c} + (f_o + \Delta f g(x)) \frac{2\dot{R}}{c} \quad (10)$$

Neglecting second-order terms,

$$f_B = + \frac{2\Delta f \dot{g}(t) R}{c} + \frac{2\dot{R} f_o}{c} \quad (11)$$

As before, the first term is the range frequency and the second term the doppler frequency.

Equation (11) will be used to evaluate the error when the frequency modulation,  $\Delta f \dot{g}(t)$ , is not ideal.

When there is an asymmetry in the half-periods of the triangular modulation as shown in Figure 4,  $\dot{g}(t)$  will differ on the upsweep and downsweep of the modulation cycle. Therefore, a stationary target will exhibit a range-rate from equation (4). From Figure 4 the half-period during the upsweep  $T_u$ , is

$$T_u = \frac{T}{2} - \delta T \quad (12a)$$

and the half-period during the downsweep,  $T_d$ , is

$$T_d = \frac{T}{2} + \delta T \quad (12b)$$

Using equations (12a) and (12b) to calculate  $\dot{g}(t)$

$$\begin{aligned} f_{\text{up}} &\approx \frac{8\Delta f f_m R}{c} \left(1 + \frac{2\delta T}{T}\right) \\ f_{\text{down}} &\approx \frac{8\Delta f f_m R}{c} \left(1 - \frac{2\delta T}{T}\right) \end{aligned} \quad (13)$$

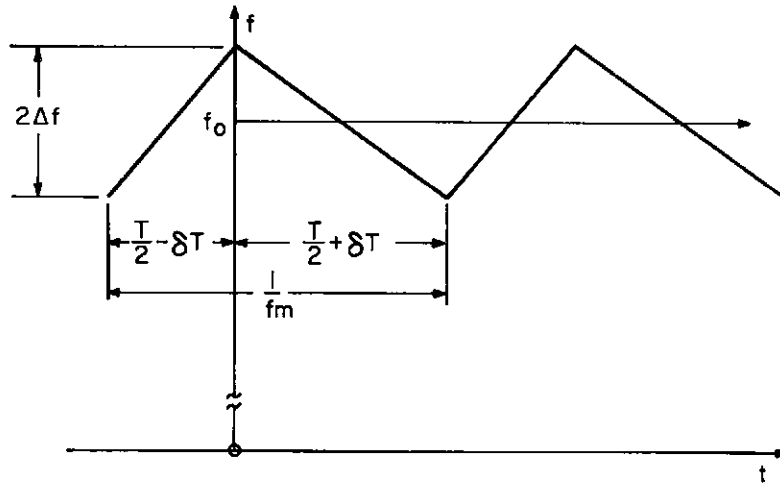


FIGURE 4. ASYMMETRIC TRIANGULAR MODULATION.

From equations (4) and (13), the range error is zero and the apparent doppler frequency,  $\delta f_d$ , is

$$\delta f_d = 2 f_r \frac{\delta T}{T} \quad (14)$$

Since 
$$f_d = \frac{2 R \dot{f}_o}{c} \quad (15)$$

The apparent range-rate,  $\delta \dot{R}$ , is

$$\delta \dot{R} = \frac{f_r c \delta T}{f_o T} \quad (16)$$

For the present modulation parameters and center frequency

$$\delta \dot{R} = 22.33 R \frac{\delta T}{T} \text{ m/s} \quad (17)$$

From equation (17), a 1% modulation asymmetry will cause an apparent range-rate of 6.7 m/s at 30 m. To eliminate this source of error, the repetition rate (and hence symmetry) is derived from the 2-MHz crystal of the microprocessor.

The effect of a nonlinear triangular wave can be derived from the model shown in Figure 5(a). From Figure 5(a), the RF frequency,  $f(t)$ , is

$$f(t) = f_o + 4\Delta f \frac{f_m}{f_o} t + \varepsilon(t) \quad (18)$$

where  $\varepsilon(t)$  is the time-dependent nonlinearity

Assuming the target to be stationary,

$$-\frac{T}{2} \leq t \leq 0$$

$$f_B = f_r + \frac{2 \dot{\varepsilon}(t) R}{c} \quad (19a)$$

$$0 \leq t \leq \frac{T}{2}$$

$$f_B = -f_r + \frac{1 \dot{\varepsilon}(t) R}{c} \quad (19b)$$

When  $f(t)$  has the form shown in Figure 5(a), the decomposition into  $\varepsilon(t)$  and  $f_o(t)$  is shown in Figures 5(b) and 5(c), respectively.  $f_o(t)$  is the ideal

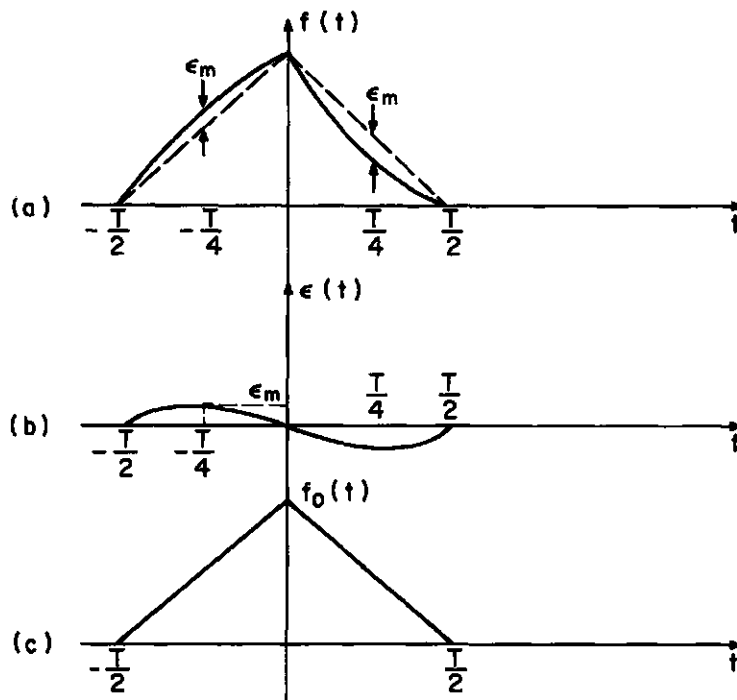


FIGURE 5. SINGLE CYCLE OF NONLINEAR MODULATION WAVEFORM.

linear waveform. If we assume  $\varepsilon(t)$  to be quadratic about  $T/4$ ,  $\varepsilon(t)$  can be written as

$$-\frac{T}{2} \leq t \leq 0$$

$$\varepsilon(t) = \varepsilon_m - \varepsilon_m \left(\frac{4}{T}\right)^2 \left(t + \frac{T}{4}\right)^2 \quad (20a)$$

$$0 \leq t \leq \frac{T}{2}$$

$$\varepsilon(t) = -\varepsilon_m + \varepsilon_m \left(\frac{4}{T}\right)^2 \left(t - \frac{T}{4}\right)^2 \quad (20b)$$

From equations (20a) and (20b)

$$-\frac{T}{2} \leq t \leq 0$$

$$\dot{\varepsilon}(t) = -2\varepsilon_m \left(\frac{4}{T}\right)^2 \left(t + \frac{T}{4}\right) \quad (21a)$$

$$0 \leq t \leq \frac{T}{2}$$

$$\dot{\varepsilon}(t) = 2\varepsilon_m \left(\frac{4}{T}\right)^2 \left(t - \frac{T}{4}\right) \quad (21b)$$

Substituting equation (21a) into equation (19a) and equation (21b) into equation (19b), we have

$$-\frac{T}{2} \leq t \leq 0$$

$$f_B = f_r - 4\varepsilon_m \left(\frac{4}{T}\right)^2 \left(t + \frac{T}{4}\right) \frac{R}{c}$$

$$0 \leq t \leq \frac{T}{2}$$

$$f_B = -f_r + 4\varepsilon_m \left(\frac{4}{T}\right)^2 \left(t - \frac{T}{4}\right) \frac{R}{c}$$

Assuming  $\varepsilon_m$  to be small so that  $f_r$  is the dominant term

$$f_{\text{up}} = f_r - 16\varepsilon_m f_m \frac{R}{c} - 64\varepsilon_m f_m^2 \frac{R}{c} t \quad -\frac{T}{2} \leq t \leq 0 \quad (22)$$

$$f_{\text{down}} = -f_r - 16\varepsilon_m f_m \frac{R}{c} - 64\varepsilon_m f_m^2 \frac{R}{c} t \quad 0 \leq t \leq \frac{T}{2}$$

Figure 6 is a plot of equation (22). From the figure it is seen that the IF frequency is frequency modulated. The modulating function is a sawtooth of amplitude  $\pm \frac{16\varepsilon_m f_m R}{c}$  about  $f_r$ . From the stationary phase one would expect

the IF frequency spectrum to be uniform about  $f_r$  and extending  $\pm \frac{16\varepsilon_m f_m R}{c}$  cycles on either side.

If we let  $\frac{\varepsilon_m}{2\Delta f}$  be a measure of the nonlinearity, then

$$\frac{16\varepsilon_m f_m R}{c} = \frac{16\varepsilon_m}{2\Delta f} (2\Delta f) f_m \frac{R}{c}$$

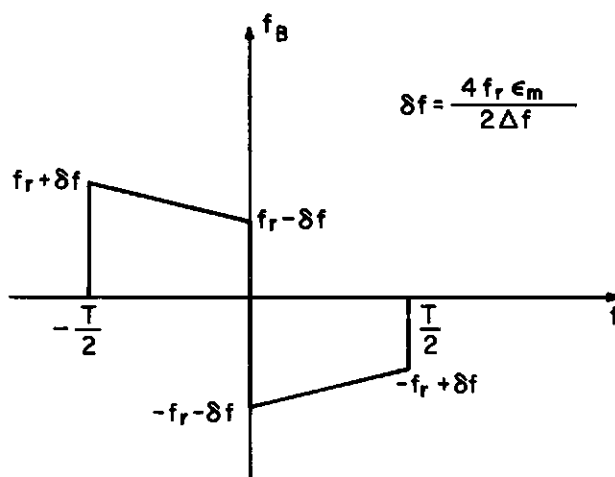


FIGURE 6. SINGLE CYCLE OF DISTORTED IF FREQUENCY.

or 
$$\frac{16\epsilon_m f_m R}{c} = 4f_r \frac{\epsilon_m}{2\Delta f} \quad (23)$$

From equation (23), we see that a 1% nonlinearity will lead to a +4% frequency spread. This has the net result of causing the IF response to appear noisy and difficult to process. Since the IF frequency is frequency modulated, the frequency between successive cycles will vary. If the variation is great enough, the measurement will be rejected by the signal processor. To avoid these problems a modulator with high linearity is used in conjunction with a linearized voltage-controlled oscillator.

#### 4. Antenna Design and Measurement

From our road test experience with the X-band antenna design from Phase II, improvements in beam definition were considered definitely desirable. The new design goals for beamwidth in azimuth and elevation were set at 3 and 5 degrees, respectively. This appeared to be the best compromise between avoiding interference from adjacent traffic lanes and not becoming so sensitive to beam alignment that slight steering angle corrections would lead to a temporary loss of target.

In addition, the new design was required to have lower side-lobe levels than the original X-band design, since large targets off to the side could otherwise still be detected. A uniformly illuminated rectangular aperture ideally has side-lobe levels of only -13 dB with respect to the main lobe [7]. To further reduce the side-lobe level, a predetermined current distribution

7. S. Silver, Microwave Antenna Theory and Design, Rad. Lab Series, Vol. 12, Boston Tech. Publications, 1964.

was established over the antenna aperture, consistent with the side-lobe level desired. A -30 dB Dolph-Chebyshev distribution was chosen for the azimuth pattern and -20 dB for the elevation pattern.

The new Ku-band antenna, shown in Figure 7, uses a construction similar to the original X-band design. The antenna consists of 512 fan-shaped dipoles printed together with the feed structure on both sides of a Duroid circuit board. A ground plane is located  $\lambda/4$  behind the printed board as a reflector. This arrangement provides a high-gain antenna in compact form (33 x 19 x 2 cm). Two identical printed circuit antennas, one for transmit and one for receive located next to each other, were used for the Ku-band bistatic radar.

Pattern measurements on the new antennas were performed in a special anechoic chamber. The azimuth and elevation patterns are shown in Figures 8 and 9, respectively. The measured side-lobe levels close to the main lobe were -22 dB in azimuth and -18 dB in elevation. These lower than theoretical levels are probably due mainly to the perturbing effects of the feed structure which is in the same plane as the radiating dipoles. The resulting side lobes are, however, much lower than for the previously used antenna with uniform excitation and should be adequate for the intended purpose.

The measured antenna beamwidth is close to the 3-degree azimuth and 5-degree elevation objective values. The gain is 30 dB above that of an isotropic radiator. For the 19 x 11 wavelength aperture, this represents an efficiency of 50%. Since a nonuniform current distribution is not as efficient as a uniform current distribution, 50% is a reasonable efficiency. By way of comparison, a parabolic reflector is also about 50% efficient.

## 5. Coverage Pattern Measurements

A coverage pattern of the radar is a series of equipower contours in the plane containing the radar and the target. A 10-m<sup>2</sup> corner reflector was used as target, mounted at the same height from the ground as the radar. Neglecting multipath effects for this position of the target, only the azimuth variation of the target and radar affects the power contours. Moreover, since the corner reflector is much less sensitive to azimuth changes than the antennas in the radar, the entire variation can be attributed to the radar. This allows a simpler mathematical model to be used, as discussed in Appendix A, where computer results are presented. A typical radar-target configuration is shown in Figure 10. The transmit and receive antennas are designated by their normals,

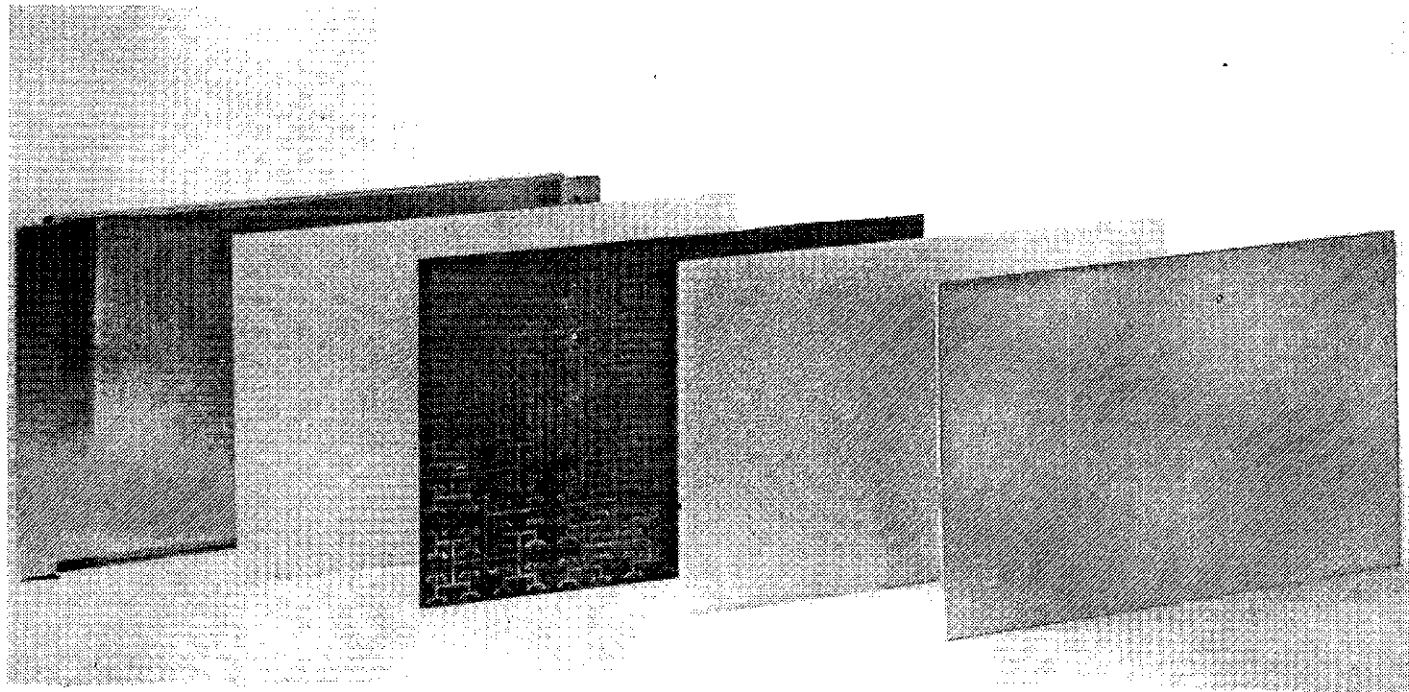


FIGURE 7. EXPLODED VIEW OF ANTENNA.

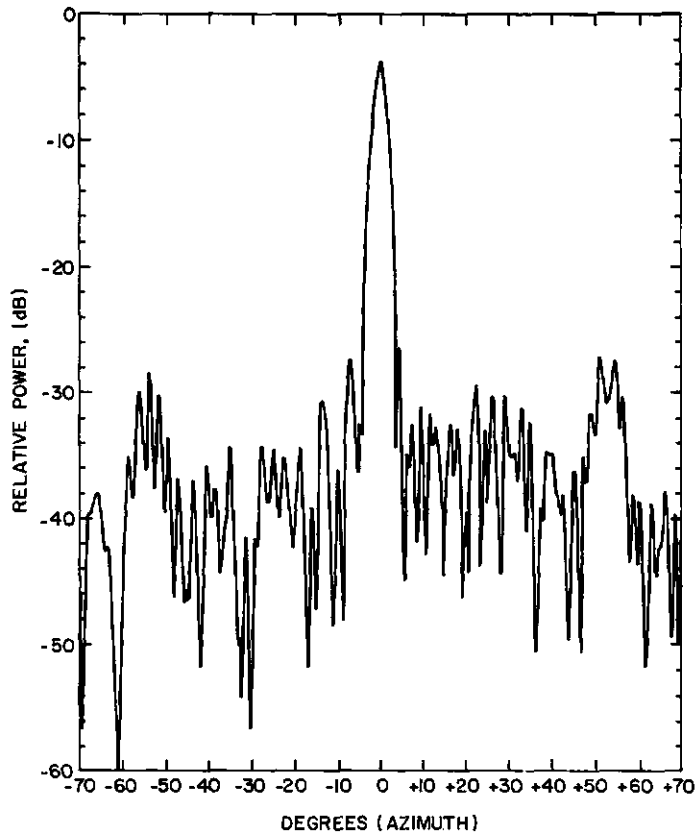


FIGURE 8. AZIMUTH Ku-BAND PATTERN.

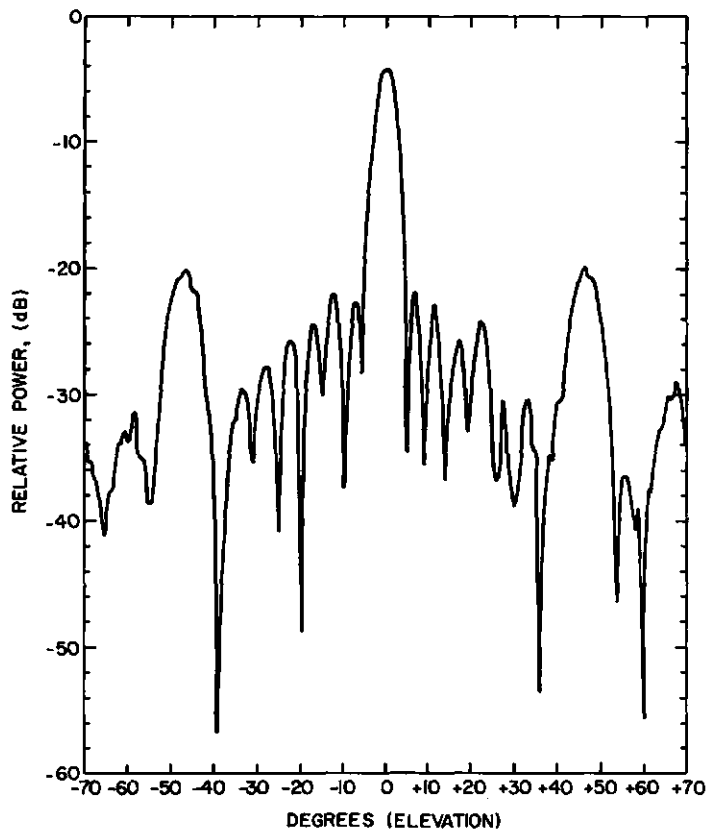


FIGURE 9. ELEVATION Ku-BAND PATTERN.

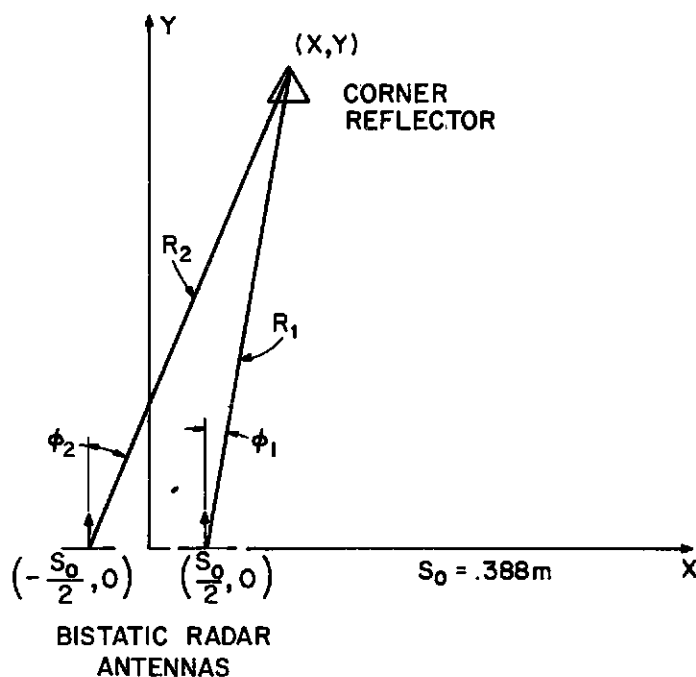


FIGURE 10. TYPICAL RADAR-TARGET CONFIGURATION FOR COVERAGE PATTERN MEASUREMENTS.

which are shown on the x axis at  $\pm s_0/2$ . The target is designated by the coordinates of the apex of the reflector. For a fixed separation,  $s_0$ , the geometry is completely defined by the coordinates of the corner reflector.

The determination of the equipower contours was made on a premarked range. Range markings consisted of parallel lines spaced 25 cm apart for the first  $\pm 1$  m from the center line ( $x = 0$ ) and 50 cm apart for  $x = \pm 1$  m to  $x = \pm 2.5$  m. Because of the narrow antenna beam the range markings were finer for the first  $\pm 1$  m. A spectrum analyzer was used as the readout device for the radar return. The analyzer has a wide dynamic range and can measure low-level signals, thus making it a natural candidate for this type of measurement.

Figure 11 shows a contour plot, where the radar return was monitored at the output of the preamplifier, shown in Figure 2. To confine the return to approximately 30 m as needed for CMS operation, a shaped postamplifier was designed with the aid of the computer program discussed in Appendix A. Figure 12 shows the power contour at the output of the shaped postamplifier. An inspection of Figure 12 shows that when the threshold level of detection is set for 30 m, the maximum coverage is within -1.0 m and +0.5 m off axis, a sharply defined microwave beam.

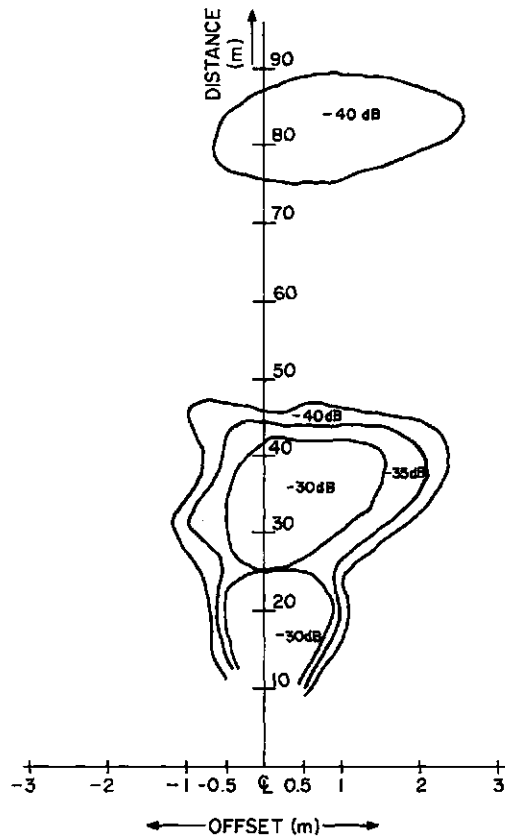


FIGURE 11. COVERAGE PATTERN Ku-BAND RADAR - OUTPUT OF PREAMPLIFIER.

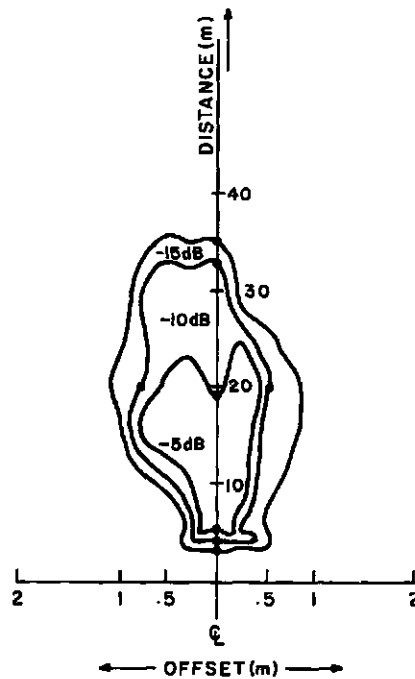


FIGURE 12. COVERAGE PATTERN Ku-BAND RADAR - OUTPUT OF POSTAMPLIFIER.

## 6. IF Amplifier Shaping for CMS

Two amplifiers are used between the radar receiver and the microprocessor. They are referred to as a preamplifier and a postamplifier. The combination of these amplifiers has three functions:

- (1) To amplify the return signal ( $f_B$ ),
- (2) To minimize unwanted signals, and
- (3) To limit the amplitude of the return signal.

A two-stage preamplifier and a five-stage postamplifier were designed for this purpose. They both use the CA3401 operational amplifier chip as the basic building block.

The preamplifier, located at the mixer output, consists of two stages. Its transfer characteristic is shown in Figure 13. The slope at the low-frequency end of the band is approximately 15 dB/octave, while in the operating band it is 5 dB/octave. The 15 dB/octave is intended to limit low-frequency noise and pickup of the harmonics of the modulating signal at 977 Hz. The 5 dB/octave helps compensate for the 12 dB/octave dropoff of the return signal. The high-frequency end is rolled off slightly to minimize unwanted signals beyond the desired range.

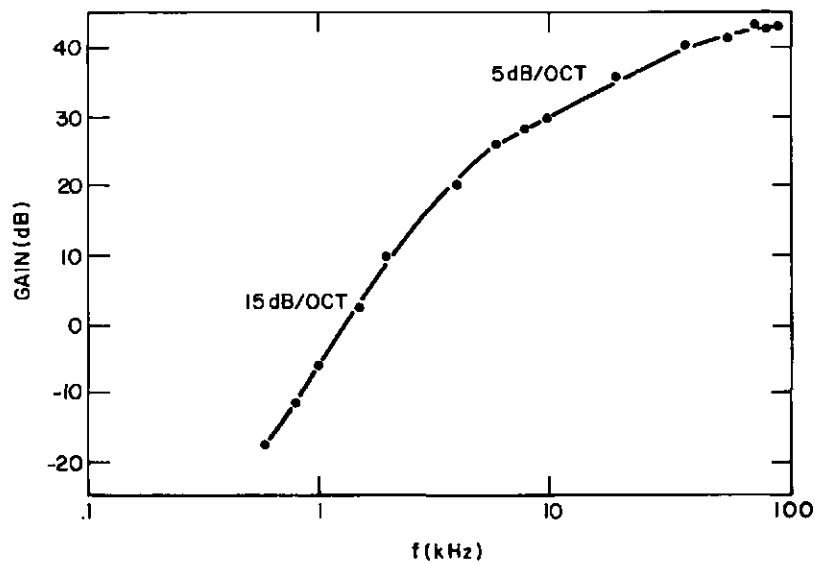


FIGURE 13. TRANSFER CHARACTERISTIC OF Ku-BAND PREAMPLIFIER.

The postamplifier designed for the CMS application has a transfer characteristic as shown in Figure 14. This amplifier consists of five stages. The

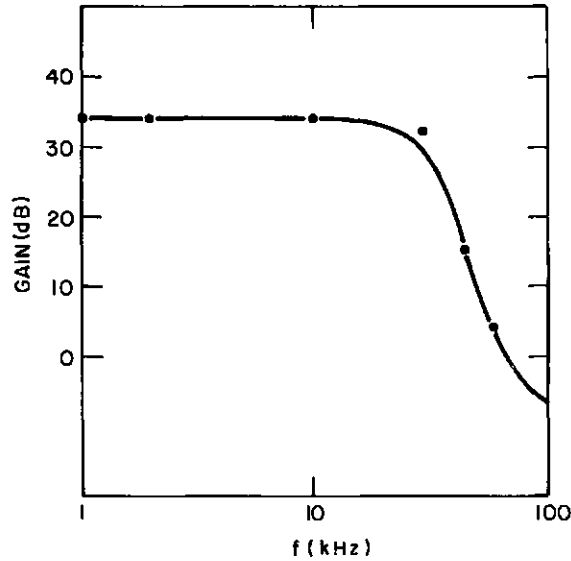


FIGURE 14. TRANSFER CHARACTERISTIC OF CMS POSTAMPLIFIER.

multiple stages are required to sharpen the roll-off at the high-frequency end of the passband to approximately 28 dB/octave. This roll-off minimizes spurious signals from beyond the range of interest.

The composite of the two sections, preamplifier and postamplifier, is shown in Figure 15. This composite band shaping gives us the required characteristics for operation out to a range of approximately 30 m.

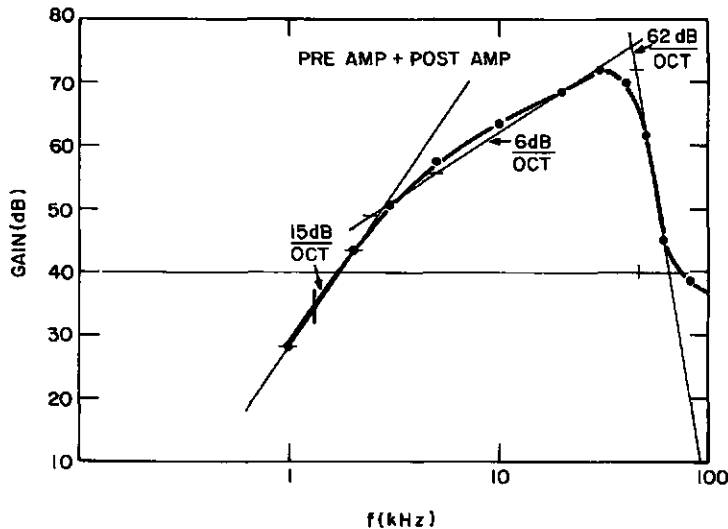


FIGURE 15. COMPOSITE OF PREAMPLIFIER AND POSTAMPLIFIER.

## B. DUAL-MODE X-BAND RADAR

### 1. Block Diagram

As part of this program, the operation of a cooperative radar was to be investigated and compared to the noncooperative radar. Cooperative means targets are identified by a special tag that affects the reflected RF energy in a unique way. The original cooperative radar system [8] demonstrated by RCA in 1973 used frequency doubling in the tag to differentiate the target return from regular backscattering clutter. In a more recent version of the cooperative principle [9], the tag provides phase modulation of the reflected signal.

Two of the major advantages of the cooperative system are the practical elimination of false alarms (only targets provided with a tag are being recognized by the radar) and an accurate, nonambiguous location capability of the target (the tag provides a clean single point of reflection). These characteristics appeared to be especially desirable for the development effort on the headway-control algorithm. Using a cooperative radar at least in the initial development phases has the advantage of eliminating a larger number of possible problem areas and permitting concentration on the actual algorithm development. In this way, the cooperative system would be exposed to a large variety of traffic conditions and its behavior could be conveniently evaluated and optimized. We, therefore, proceeded to modify the existing X-band monostatic radar for cooperative operation using the phase modulated tag principle. A second, higher frequency IF channel was added to the X-band radar to handle the modulated signal. The original baseband response remained unaltered to permit noncooperative operation also. A switch selects the desired mode.

With the cooperative system, alarms are only triggered by 'tagged' targets, so that false alarms due to road signs, bridges, guard rails, or generally any reflecting object in the radar beam are eliminated. Thus the useful warning range can be extended. Also since the radar cross section of the tag is constant, there is no problem with fluctuating returns and the dynamic range is

8. J. Shefer et al., "A New Kind of Radar For Collision Avoidance," SAE Automotive Engineering Congress and Exposition, Detroit, Michigan, February 26, 1974.
9. G. S. Kaplan and F. Sterzer, "Dual-Mode Automobile Collision Avoidance Radar," SAE Automotive Engineering Congress and Exposition, Detroit, Michigan, February 24-28, 1975.

reduced. A tag on a compact car will return as much signal as a tag on a truck. This feature was particularly attractive during the headway-control development. Because of the complex return from a target when a problem arose, it was not clear if the headway-control algorithm was at fault or if the signal had dropped out. With the tag this variable was eliminated. From a long-range view-point, the possibility of encoding other messages also exists. The license number of the car as well as emergency messages could be transmitted from the car via the tag [9].

Potential false-alarm situations which cannot be eliminated with the cooperative radar occur when the tagged vehicle is in the line of sight but is not a collision threat. A car in the adjacent lane rounding a curve is an often-cited example.

A block diagram of the dual-mode radar, including the tag, is shown in Figure 16. The tag consists of an antenna identical to the one used in the radar, terminated in a reflective modulator. The modulator is an inexpensive, low-drain varactor modulator which encodes a 0- to 180-degree phase sequence on the signal received from the radar. This phase-coded signal is reradiated back to the radar where it is preprocessed in the cooperative channel. The resulting baseband signal is processed further in the common processor. The modulation rate of 500 kHz was chosen so that  $T^2L$  logic could still be used. Ideally, a large separation between the modulation frequency and the highest expected baseband frequency is desired to eliminate false alarms from massive targets at far distances and to maintain signal fidelity of the modulated wave.

After the phase-coded signal is received by the radar, it is translated to IF via the homodyne mixer. The IF which is at the modulation frequency (500 kHz) is filtered through a bandpass filter. The bandwidth of the filter is twice the baseband frequency. The bandpass filter prevents the target's baseband signal from getting through the cooperative channel and removes harmonics of the modulation frequency. After filtering, the signal is amplified and envelope detected. Figure 17(a) shows the waveshape at the output of the mixer, and Figure 17(b) shows the waveshape at the output of the envelope detector. As seen from Figure 17(b), the output of the envelope detector is at twice the baseband frequency. A low-pass filter at the output of the envelope detector removes the high-frequency components and further conditions the detector output. A shaped postamplifier completes the preprocessing of the cooperative channel.

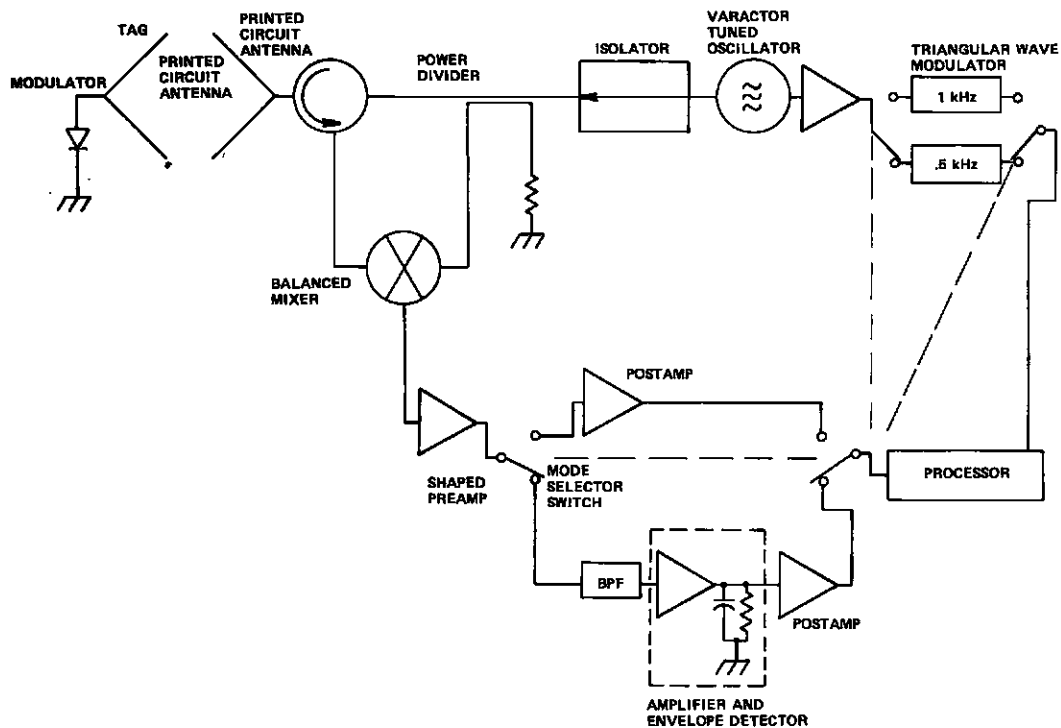


FIGURE 16. BLOCK DIAGRAM OF DUAL-MODE RADAR.

Earlier, it was mentioned that the output of the envelope detector is at twice the baseband frequency. Since it is desirable to use the same signal processor when the cooperative mode is selected, the frequency modulation repetition rate is reduced by a factor of two to 500 Hz to keep the final baseband frequency the same. When the mode of operation is selected by the switch, the modulation rate and the flow path are selected simultaneously.

## 2. System Parameter Selection

The cooperative channel of the dual-mode radar shares the RF front end with the noncooperative channel and, therefore, the modulation parameters with the exception of the repetition frequency,  $f_m$ . Because phase modulation doubles the baseband frequency (see Figure 17),  $f_m$  is reduced from 1 kHz to 500 Hz to keep the baseband constant. This permits the use of a single processor for the dual-mode radar. The frequency deviation  $\Delta f$  for the X-band radar remains at 25 MHz.

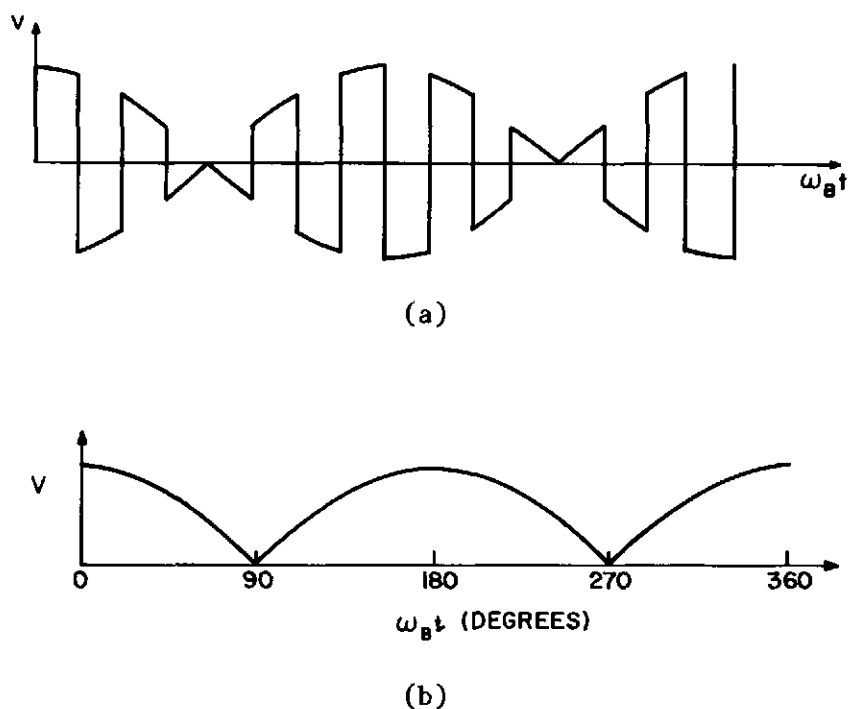


FIGURE 17. (a) TYPICAL IF VOLTAGE WAVEFORM FOR 0- to 180-DEGREE PHASE MODULATOR. (b) OUTPUT OF ENVELOPE DETECTOR.

A key parameter of the cooperative channel is the modulation rate,  $f_T$ . The reflected radar signal when phase modulated from 0 to 180 degrees can be represented as

$$\cos(\Psi(t) + \pi S'(t)) \quad (24)$$

where  $\Psi(t) = 2\pi\{f'_0 t \pm \Delta f \int_0^t g(x) dx\}$

and  $S'(t) = 0$  or  $1$  at the modulation rate

but  $\cos(\Psi(t) + \pi S'(t)) = \cos\Psi(t) \cos\pi S'(t)$

and  $\cos\pi S'(t) = S(t)$

where  $S(t) = 1$  or  $-1$  at the modulation rate.

therefore,  $\cos(\Psi(t) + \pi S'(t)) = S(t) \cos\Psi(t)$  (25)

When the modulated signal is translated to IF via a product mixer, the IF can be written as

$$u_{IF} = S(t) \cos[\Psi(t+\tau) - \Psi(t)] \quad (26)$$

because  $\Psi(t+\tau) - \Psi(t) = \dot{\Psi}\tau$

the IF response,  $u_{IF}$ , becomes

$$u_{IF} = S(t) \cos \dot{\Psi}\tau \quad (27)$$

When the modulation rate  $f_T$  is much greater than the range frequency,  $\dot{\Psi}\tau$ , equation (27) is the equation of an amplitude-modulated wave. That is, the square wave of amplitude 1 and -1 is amplitude modulated by the slowly varying baseband function  $\cos \dot{\Psi}\tau$ . Another point of view is that the cosine function is sampled by the square wave and must be at least twice the frequency of the cosine wave. For a range frequency,  $\dot{\Psi}\tau$  per meter of 333 Hz/m corresponding to  $\Delta f = 25$  MHz and  $f_m = 500$  Hz, the range frequency,  $f_r$ , at 100 m = 33.34 kHz. A tag modulation frequency of 500 kHz is 15 times larger than the maximum range frequency and thus is adequate.

In order to remove the baseband envelope,  $\cos \dot{\Psi}\tau$ , from the high-frequency carrier,  $S(t)$ , we make use of the fact that  $S(t)$  is periodic at the modulation rate,  $f_T$ , and can be represented as a Fourier series. Therefore,  $u_{IF}$  can be written as

$$u_{IF} = \cos \dot{\Psi}\tau \sum_{k=0}^{\infty} A_k \cos[2\pi(2k+1) f_T t - \phi_k] \quad (28)$$

$$u_{IF} = \frac{1}{2} \sum_{k=0}^{\infty} A_k \cos[2\pi(2k+1) f_T t + \dot{\Psi}\tau - \phi_k] + \frac{1}{2} \sum_{k=0}^{\infty} A_k \cos[2\pi(2k+1) f_T t - \dot{\Psi}\tau - \phi_k] \quad (29)$$

where  $A_k = \frac{4}{(2k+1)\pi}$  (30)

From equation (29) we see that each Fourier component is DSB modulated by  $\cos \dot{\Psi}\tau$ . The bandwidth around each line of the spectrum is  $\pm \frac{\dot{\Psi}\tau}{2\pi}$ . To prevent spectral overlap

$$f_T > \frac{\dot{\Psi}\tau}{2\pi} \quad (31)$$

Equation (31) is less restrictive than the condition derived earlier from sampling considerations. When  $u_{IF}$  is passed through a bandpass filter centered at  $f_T$  (500 kHz), the result is a DSB-modulated signal centered at 500 kHz.

The bandwidth of the filter must be wide enough to accommodate the highest frequency of  $\dot{\Psi}\tau$  or 70 kHz, and selective enough to remove the baseband response at the third harmonic. A three-section Butterworth filter, with a 3-dB bandwidth of 180 kHz was found to be adequate.

After filtering, an envelope detector is required to strip the baseband signal from the carrier. To improve the detector efficiency, the signal is amplified before detection. The signal-to-noise ratio of a linear detector is better than the signal-to-noise ratio of a square law detector in the region of low signal-to-noise [4]. Figure 17(b) shows a sketch of the signal after envelope detection. Because of the 0- to 180-degree modulation, the waveshape corresponds to a full wave rectified sine wave.

To eliminate the harmonics associated with a full wave rectified sine wave, a low pass filter follows the detector. Since the second harmonic of the rectified sine wave is 14 dB below the fundamental [10], a single R-C filter was used. A shaped amplifier provides the final signal conditioning before range and range-rate are derived in the common dual-mode processing circuitry. The shaping is similar to that used for the baseband amplifier of the noncooperative channel, the basic difference being that the bandwidth is increased to accommodate the anticipated range of up to 100 m.

### 3. Coverage Pattern Measurements

Coverage pattern measurements similar to those described in subsection III.A.5 above were made for both channels of the dual-mode radar. The tagged channel can be seen in Figure 18 and the baseband channel in Figure 19. The targets consisted of an electronic tag, mounted at license plate height (0.385 m), as shown in Figure 20, and a 10-dB corner reflector mounted at the radar height for baseband tests. A photograph of the radar mounted on an RCA vehicle is shown in Figure 21. The height of the target affects the position of the multipath nulls. For example, using equation (1), the first multipath null for the tagged channel should occur at 18.4 m, whereas the baseband channel null should occur at 32.6 m. This is in good agreement with the measured results shown in Figures 18 and 19.

---

10. A. G. Kandoian et al., Reference Data for Radio Engineers, International Telephone & Telegraph Corp., New York, 1964.

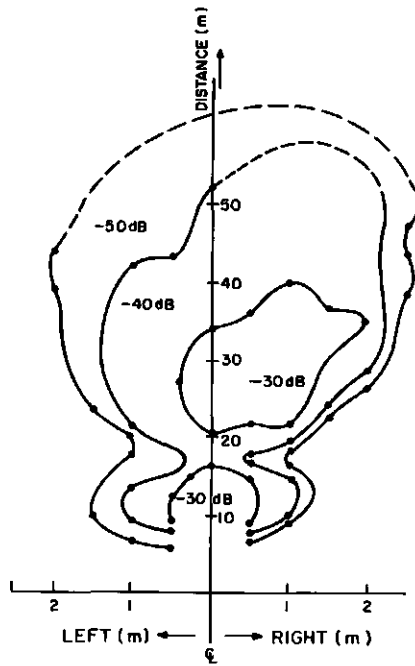


FIGURE 18. COOPERATIVE CHANNEL OF DUAL-MODE X-BAND RADAR.

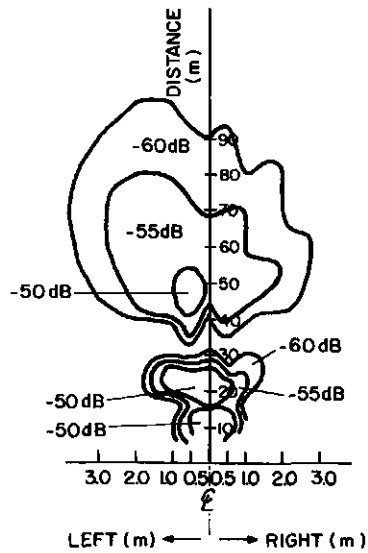


FIGURE 19. BASEBAND CHANNEL OF DUAL-MODE X-BAND RADAR.

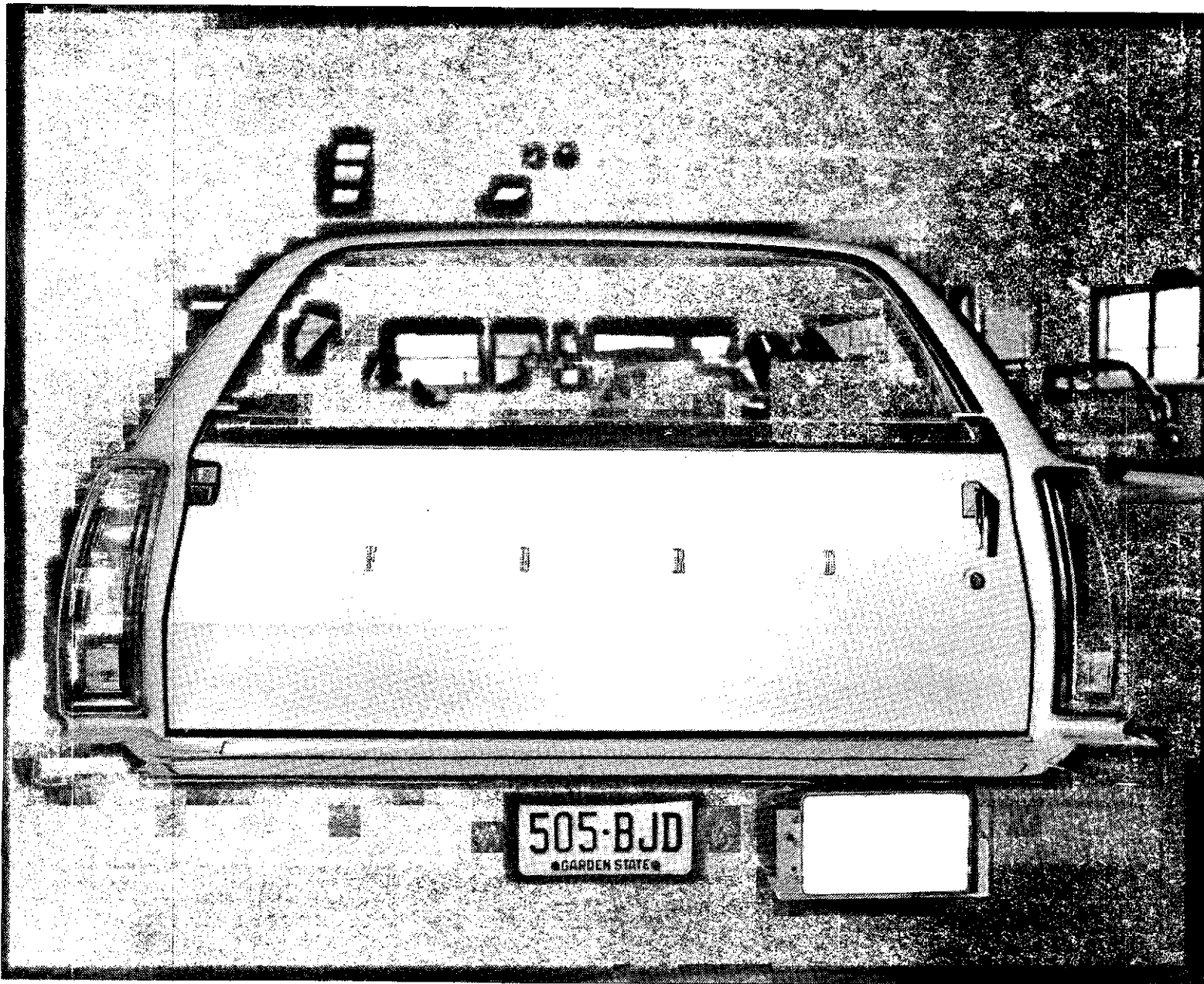


FIGURE 20. LOCATION OF MICROWAVE TAG MOUNTED ON VEHICLE.



FIGURE 21. X-BAND DUAL-MODE RADAR MOUNTED ON VEHICLE.

Although a complete one-to-one comparison between Figures 18 and 19 cannot be made due to the differences in amplifier gains and bandwidths between channels of the dual-mode radar (the tagged channel output was taken at the envelope detector and the preamplifier output was used for the baseband channel), it can be seen that the cooperative mode has no severe signal dropout and has a narrower coverage pattern out to 50 m. A theoretical treatment of coverage pattern is given in Appendix A which also indicates a narrower pattern for the tagged channel.

### C. RADOME FOR RSV INSTALLATION

To evaluate the various radome structures, we constructed a fixture that supports the entire nose of the RSV, as well as different radome structures under test. This mount was attached to a pedestal in the microwave anechoic chamber located at RCA's facility in Moorestown, NJ. The chamber, mount, and nose structure are illustrated in Figure 22. The pedestal on which the structure is mounted can be rotated  $360^\circ$  for azimuth measurements. At the top of the pedestal, the head to which the fixture is attached can also be tilted  $90^\circ$  for elevation measurements. The antenna is at the center of rotation so that it remains bore-sighted with the transmitting antenna located at the far end of the chamber.

Antenna patterns were originally taken on an antenna without a radome to be used as a bench mark. These patterns were shown in Figures 8 and 9. At first, an attempt was made to beam directly through the existing structure; that is, the RIM (Reaction Injection Molded outer skin of the RSV) and an ABS plastic air scoop. Due to the different dielectric properties of the two materials directly in the radar beam, the side lobes are degraded as shown in Figures 23 and 24. This is particularly severe in elevation. As can be seen from the illustrations, one of the side lobes comes within 6 dB of the main lobe. This could result in false targets from overhead structures such as bridges and signs. There is also an additional 5-dB insertion loss due to the lossiness of the material. Since the radome loss affects both transmit and receive, a total sensitivity reduction of 10 dB results. We, therefore, decided to investigate the development and fabrication of a separate radome structure.

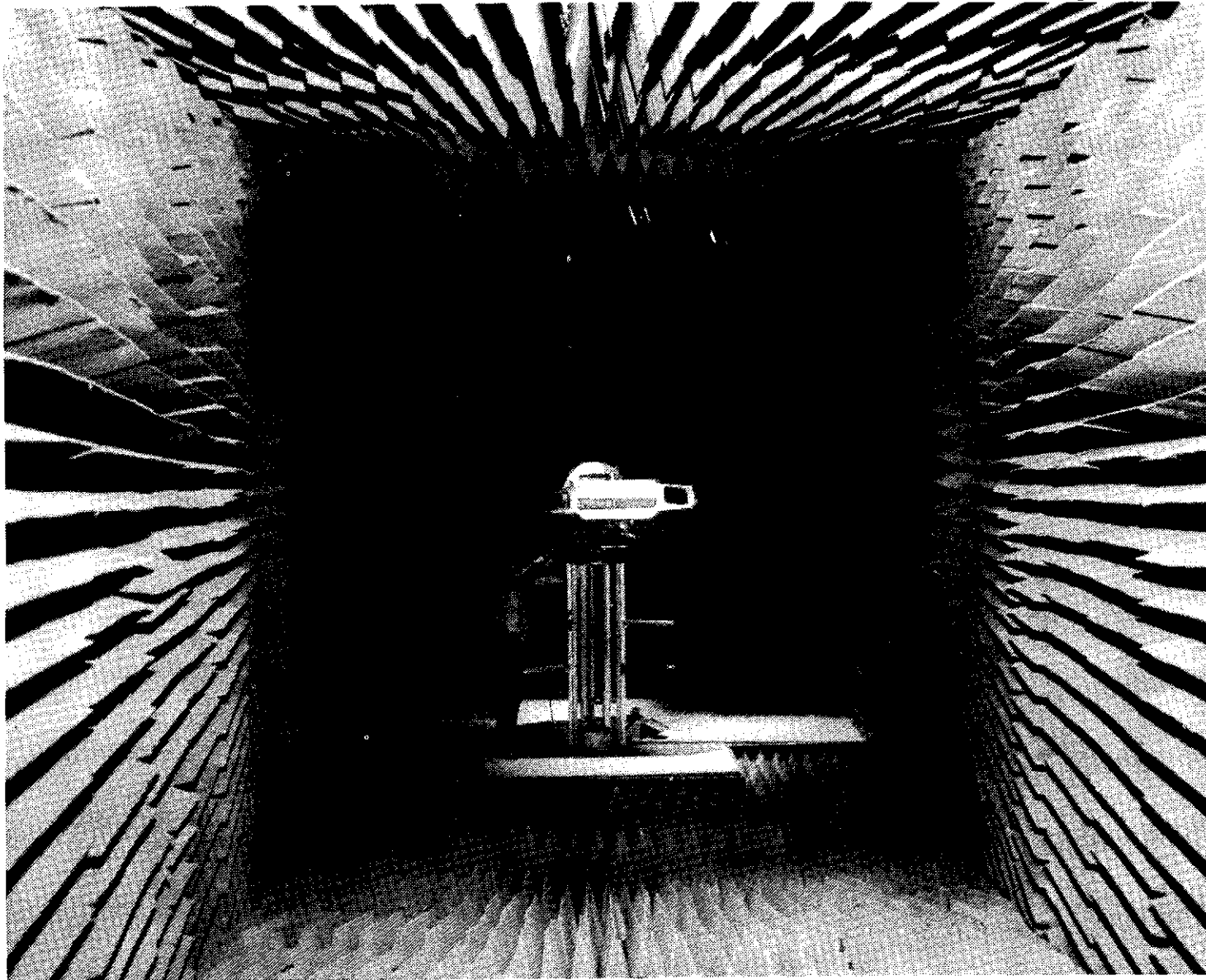


FIGURE 22. ANECHOIC CHAMBER FOR ANTENNA MEASUREMENTS.

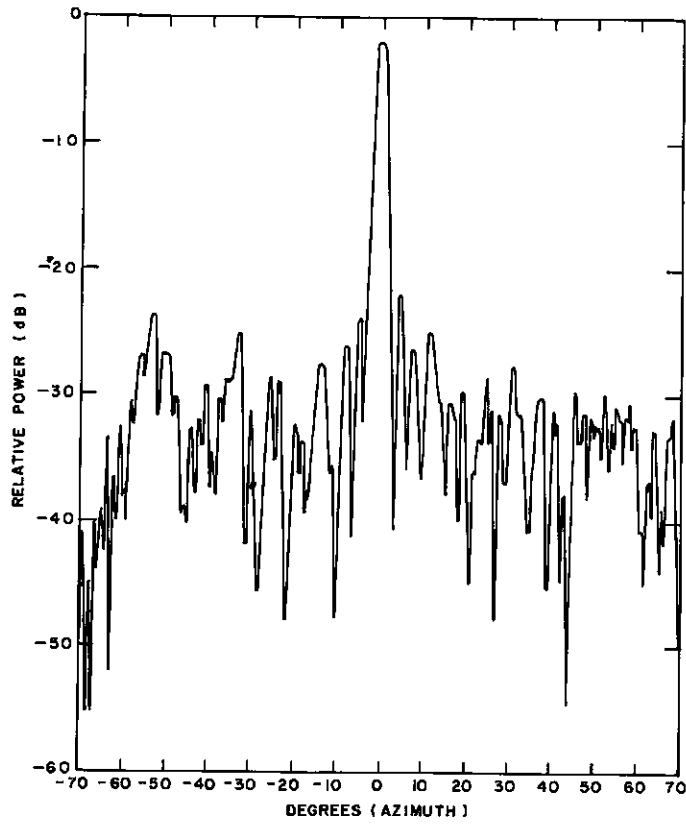


FIGURE 23. AZIMUTH ANTENNA PATTERN (NOSE AND AIR SCOOP).

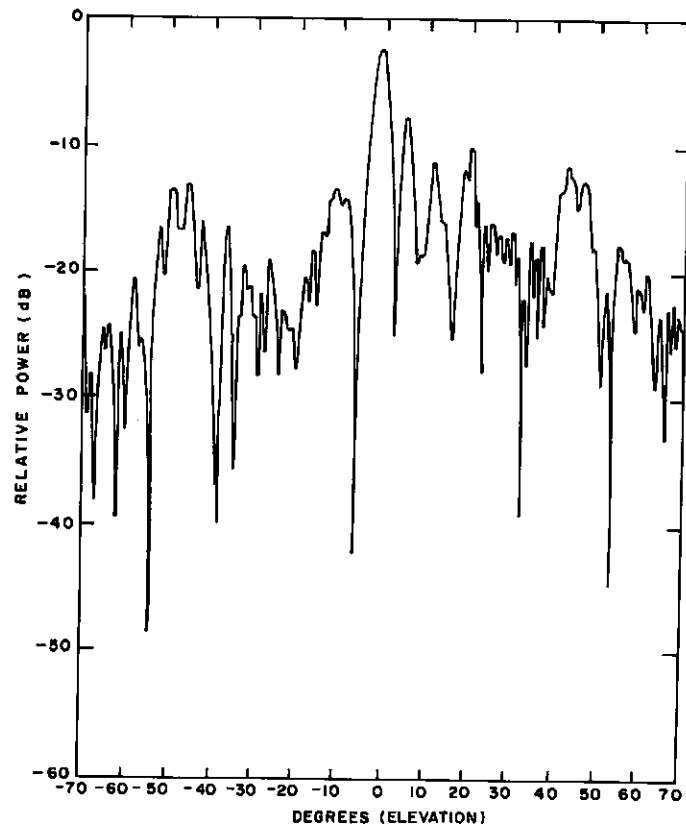


FIGURE 24. ELEVATION ANTENNA PATTERN (NOSE AND AIR SCOOP).

The radome has to conform to several requirements, such as:

- (1) It must have the same shape as the body of the vehicle;
- (2) It must have suitable electrical properties (low dielectric constant and low loss);
- (3) It must be environmentally sound (waterproof and fuel resistant).

Several materials were considered, as shown in Table 2, for this purpose. Early in the program, we approached Emerson & Cuming\* to cast a block of low dielectric, low loss, closed cell foam in a mold provided by RCA. After considerable delay, they declined to quote on small production numbers, and they recommended the use of Eccofoam FPH foam-in-place. We were, however, not equipped for handling a structure of this size and complexity by ourselves.

TABLE 2. CHARACTERISTICS OF MATERIALS CONSIDERED FOR RADOME CONSTRUCTION

<u>Material</u>	<u>Constant</u>	<u>Dielectric Loss Factor</u>	<u>Comment</u>
Hardman Epoweld 3672	~3	0.021	Hard/brittle
Foamed Polystyrene	1.03	0.0001	Light/porous
Polyethylene*	2.26	0.0031	Flexible/nonporous
Eccofoam FPH	1.04/1.25	0.001/0.005	Hard to handle
Eccoseal High-Q	2.55	<0.0004	Solvent attacks substrate
Eccocoat FP3	4.40	0.006	Too fluid/absorbed by substrate

\*The polyethylene used is expanded approximately 4:1, which reduces the dielectric constant and dissipation factor.

As the next best alternate to a solid block, we chose a laminated structure from standard blocks of foamed polystyrene, shaped to conform to the body contour, and sealed. The sealer is required to prevent moisture absorption into the foamed polystyrene which would deteriorate its electrical properties. Several sealers, listed in Table 2, were tested. The Eccoseal High-Q could not be used because its solvent dissolved the foamed polystyrene substrate.

\*Emerson & Cuming, Inc., Canton, MA.

The Eccocoat FP3 was better, but still too thin; it entered the cell structure of the foamed polystyrene, forming an irregular inner surface. The most promising coating was Hardman Epoweld 3672. A mock radome was constructed and tested. Electrically it was satisfactory, but, physically, the epoxy coating was too hard and shattered on minor impact.

The foamed polystyrene seemed the best building block because of its extremely low dielectric constant and dissipation factor. It still, however, required a suitable coating. A sheath of closed cell, cross linked, expanded polyethylene was finally selected as cover. This material does not absorb moisture and is highly resistant to automotive solvents as well as having acceptable electrical properties. A full scale radome was constructed, as shown in Figure 25.

The blocks of foamed polystyrene were shaped to conform to the contour of the RSV. The end and center supports are fastened to the antenna frame. The expanded polyethylene sheet is stretched over the foamed polystyrene and secured to the three solid polystyrene plates with plastic molding and nylon screws. The top and bottom edges are secured with aluminum battens. The natural gasket effect of the expanded polyethylene seals the edges while all other openings are sealed with RTV.

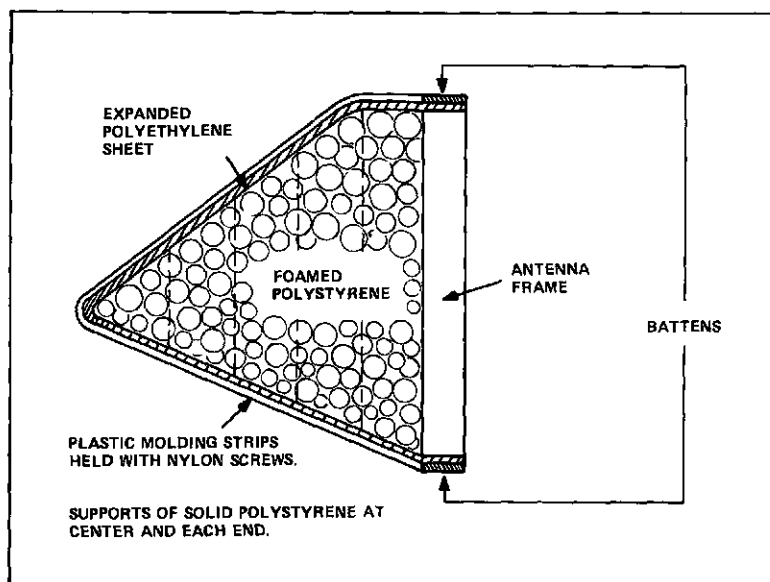


FIGURE 25. RADOME CONSTRUCTION.

The final structure was tested in the anechoic chamber with satisfactory results. Figures 26 and 27 show the resulting azimuth and elevation pattern. The side lobes in the worst case, elevation, are only 11 dB below the main lobe. This, however, occurs at an angle of  $40^\circ$  which is far removed from the general range of interest. The side lobes closer-in are at least 16 dB below the main lobe. There is also a loss of approximately 2 dB over an antenna without radome, but this is within acceptable limits.

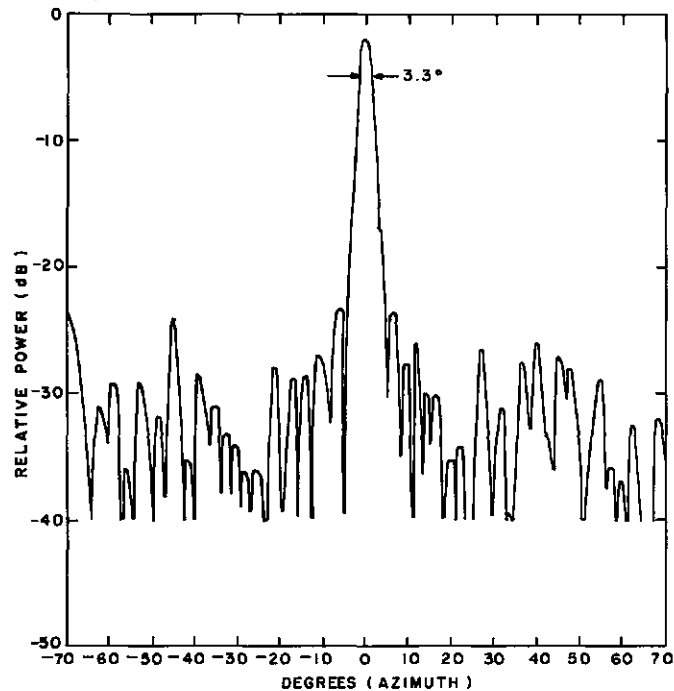


FIGURE 26. AZIMUTH ANTENNA PATTERN WITH RADOME.

The final configuration of the antenna and radome forms a separate unit, as shown in Figure 28, which fits into a cutout in the nose section of the RSV. A photograph of the RSV with the radar and radome inserted but before finishing off the joining areas is shown in Figure 29.

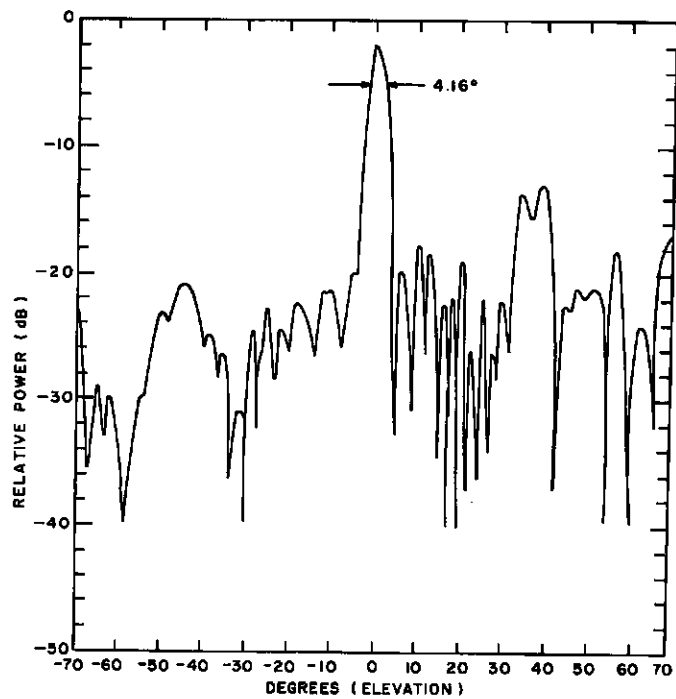


FIGURE 27. ELEVATION ANTENNA PATTERN WITH RADOME.

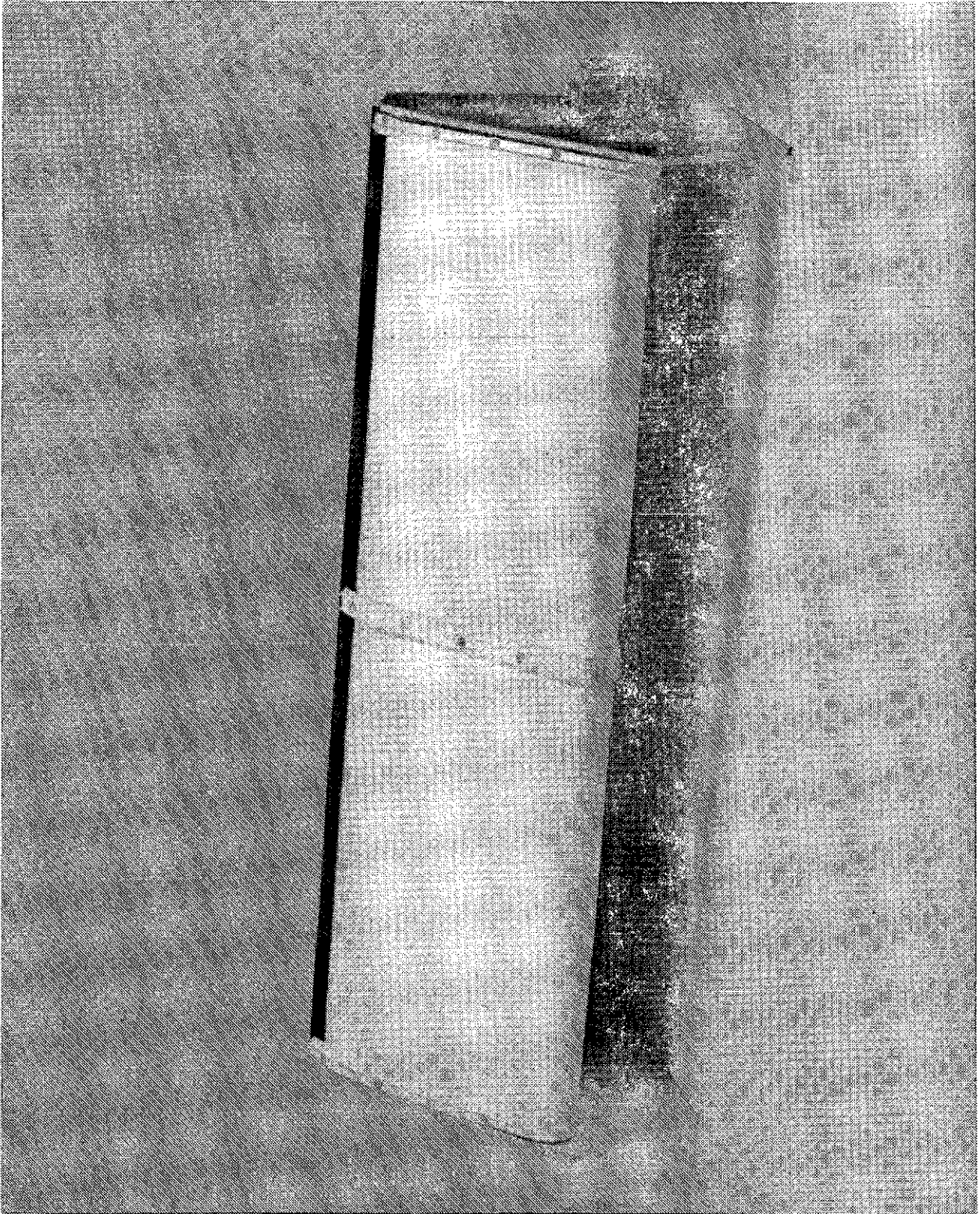


FIGURE 28. BISTATIC KU-BAND RADAR WITH RADOME.

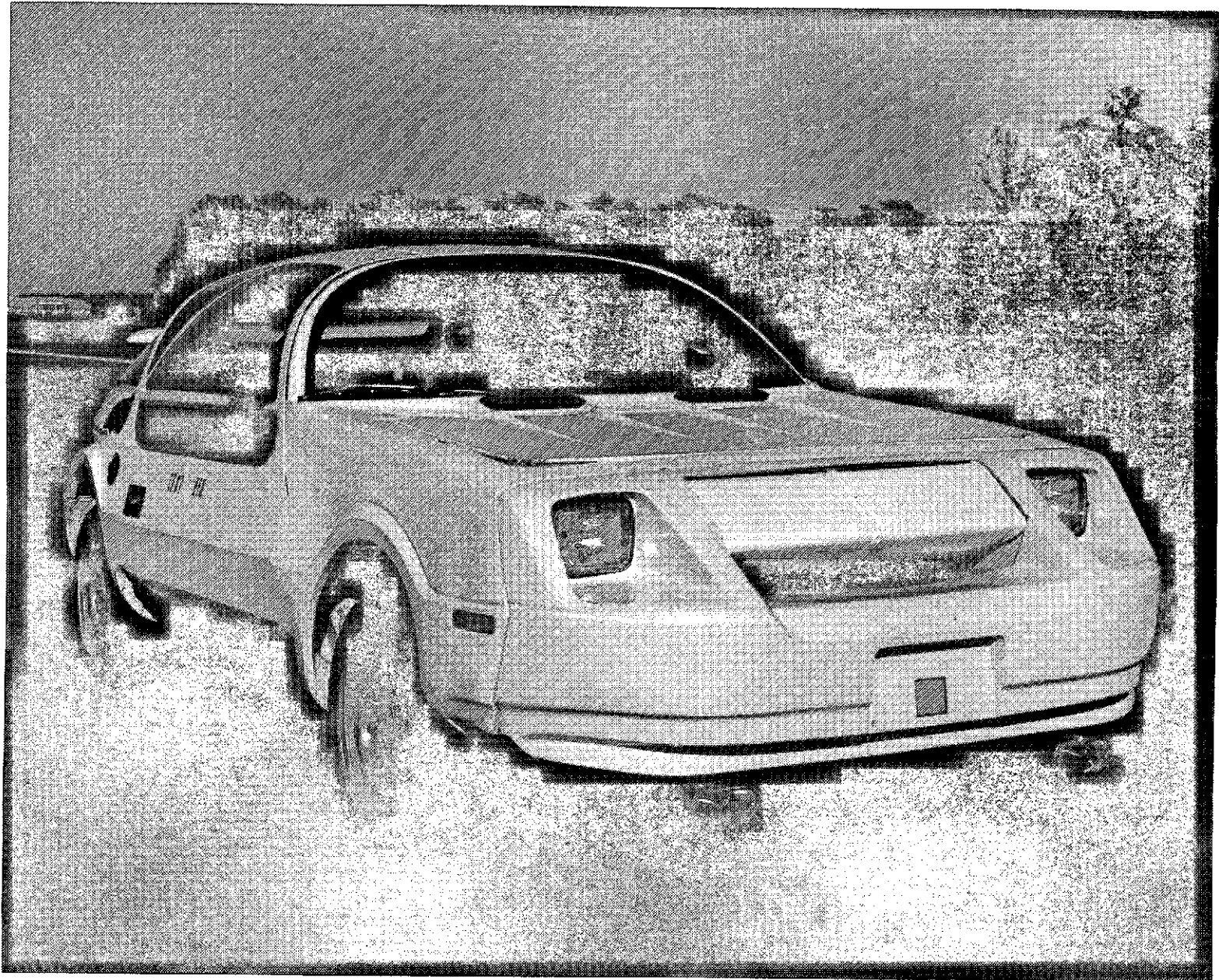


FIGURE 29. RSV WITH RADAR AND RADOME IN PLACE.

SECTION IV  
PROCESSOR HARDWARE

A. RADAR CARDS FOR CMS AND HEADWAY CONTROL

1. Introduction

The radar card is hardware that converts the analog signal input from the radar system to useable data for the microprocessor. During Phase II and Phase III of the Minicars program, three versions of radar interface cards were constructed. Each of the three cards during the course of their respective programs had minor modifications, as the need arose, to improve performance.

The first radar card, used in Phase II, measured an accumulated count over a predetermined number of periods selected by software within the measurement interval. The square wave that was used to generate the triangular wave for the TEO and blanking at the radar card originated at the radar system. The blanking of the turnaround transient started at the beginning of each turnaround transient for a set time period (hardware-determined). The weakness of this radar card was that it needed eight consecutive modulation cycles with the same number of periods within the measurement interval in order to obtain one processed data output of range and range-rate.

The second radar interface card (Phase III) measured each period individually within the measurement interval. The greater the range from the target to the radar, the greater the number of periods within the measurement interval and, therefore, the greater the number of periods individually measured. The second card was designed to not only measure each period within the measurement interval, but also the periods up to the time of a dropout that may occur. This type of adaptive processing improved the range accuracy and reduced the number of rejected readings. The blanking arrangement for the second radar card was the same as the first radar card, except that the square wave was now derived from the microprocessor by dividing down the 2-MHz clock frequency. This card was used in the headway-control processor to provide range data with high accuracy but slow update rate.

The third card tailored for CMS operation had to provide range and range-rate in very short time intervals. Range-rate was derived directly from the doppler information. To improve the accuracy of the range-rate information, a symmetrical blanking pulse had to be used that overlapped the turnaround

points of the triangular wave equally on both sides. The hardware of the card was simplified to accumulate a count through the measurement interval and up to any dropouts within the measurement intervals if they occurred.

The Phase III radar cards achieved increased responsiveness to all targets presented to the radar system. This increased system sensitivity placed the burden of false-alarm rejection in the case of the CMS system heavily on software.

## 2. Phase II Radar Card

A block diagram of the Phase II CMS radar card is shown in Figure 30. The radar provides a 1-kHz input and a sinusoidal signal input to the radar interface,  $f_B$ ; this is shown in Figure 31. The transitions of the 1-kHz square wave correspond to the turnaround points of the triangular modulation waveform. The positive transition of the 1-kHz square wave is the beginning of the positive-going slope of the triangular waveform. The negative-going transition of the square wave corresponds to the beginning of the negative slope of the triangular wave. The signal input into the interface contains both transients occurring at the turnaround points of the triangular waveform and sinusoidal waveforms generated on the upswing and the downswing of the modulation containing range and range-rate information. The greater the range, the larger the number of periods between the transients available for measurement will be. The amplitude of the input signal is a function of the multipath nulls, range, and type of target.

The 1-kHz input signal is applied to a network that generates a 20- $\mu$ s pulse at each transition of the incoming square wave. The pulses are called the "reset" pulses. The reset pulses, in turn, are applied to a variable-period one-shot multivibrator which generates the blanking pulses. The blanking pulses occur at the transitions of the 1-kHz square wave which corresponds in time to the transient period from the turnaround.

The total signal input consisting of transient pulses and information-carrying sinusoidal waveforms is applied to the threshold circuit. The timing relationships between the triangular wave, blanking, and sinusoidal input from the radar are shown in Figure 32. The function of the threshold circuit is to shut off any input that falls below a preset value either initially or during the time of measurement between the transient pulses. If the input falls below the preset value at any time, the circuit shuts off and is reset by the reset

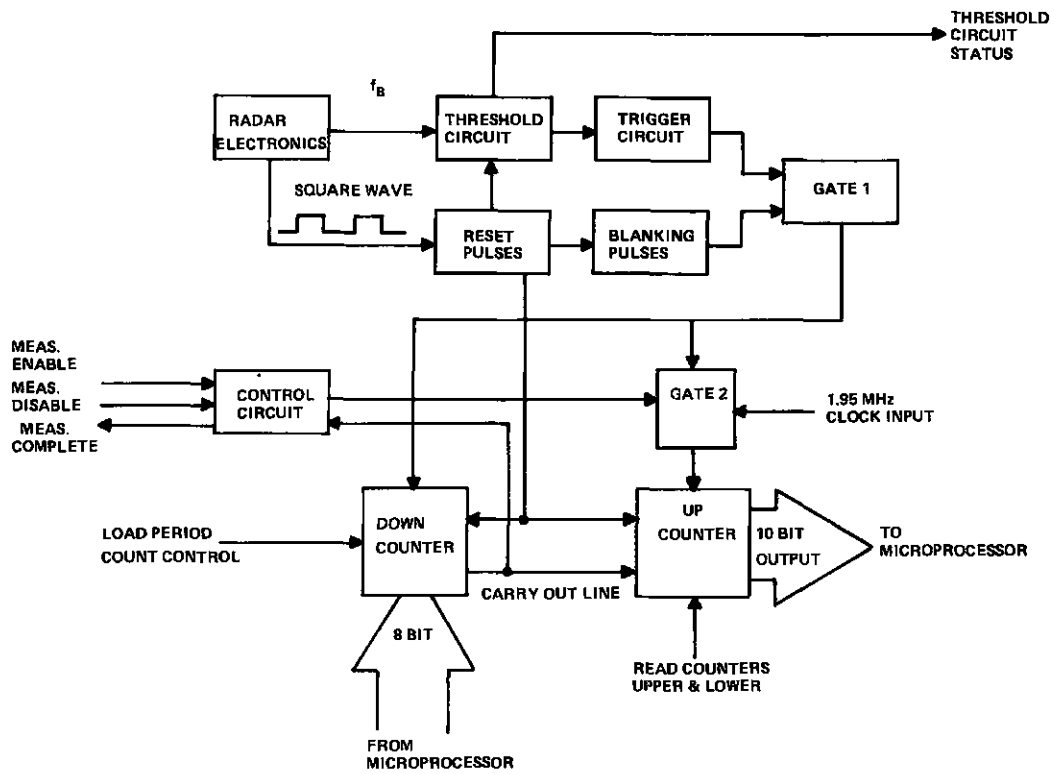


FIGURE 30. BLOCK DIAGRAM OF PHASE II CMS CARD.

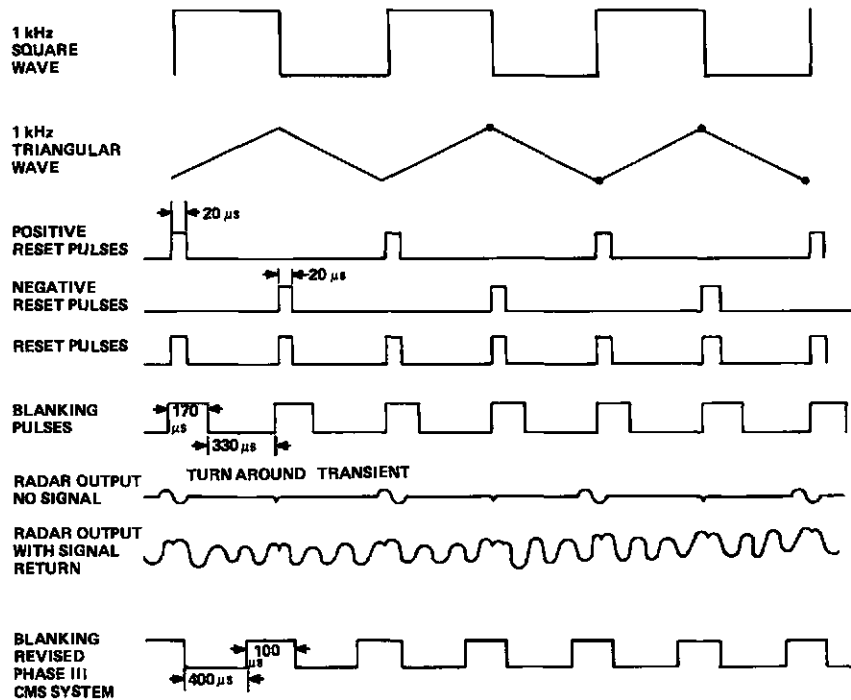


FIGURE 31. WAVEFORMS ON RADAR INTERFACE CARD.

pulse at the beginning of the next modulation cycle. The transient pulse is filtered out and the only pulses passing through to the counter are trigger pulses whose spacing is a function of range.

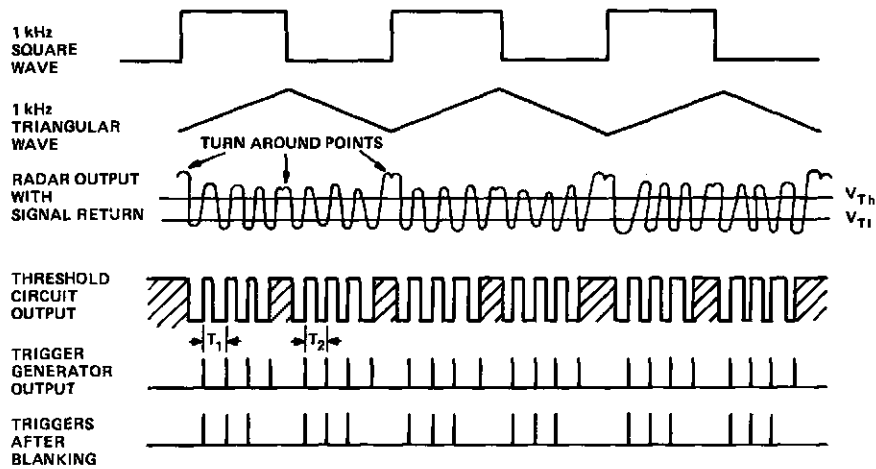


FIGURE 32. SIGNAL-PROCESSING TIME RELATIONS.

Two counters are used in the circuit, a "down" counter and an "up" counter. The down counter is loaded by the microprocessor with the number of periods that would be desirable to measure. When the down counter counts to "0," it generates a "carry out" pulse. The up counter is a high-speed counter which uses 1.95-MHz clock pulses as drivers. The counter is turned on by the first trigger pulse from the input signal and then turned off when the desired number of periods is measured. The reset pulses, which occur during the blanking time, are used to load the down counter with the number of periods to be measured and to reset the up counter to a zero count. Also available at the up counter transmission gate is information as to whether the threshold circuit shuts down during a measurement interval. The blanking pulse is also available at the up counter transmission gate to define the allowed measurement interval. The interface card runs asynchronously with the microprocessor. The control circuit allows the microprocessor to call for a measurement. A flag line is used to indicate that the measurement is complete. Another control line disables the "measurement ready" line.

One of the major problems associated with the use of this particular radar interface card was the possible loss of significant data during consecutive measurements. The Phase II CMS system measured either 1, 2, 3, 4, or 5 periods within a measurement interval. Eight full modulation cycles with the same "set" number of periods must be obtained for a successful measurement. However, during the actual radar measurement process, complex returns from the target cause dropouts during measurement intervals. The dropouts that occurred during the measurement interval would cause the system software to reject readings

until eight consecutive full modulation cycles could be read with the same set period count. This rejection of data during dropouts in the measurement interval makes the overall system seem insensitive to a variety of target situations that should be detected.

Two other problems were associated with the Phase II CMS system. First, selecting the proper period count to be measured within a measurement interval required auto-ranging software which required additional run time for the overall software. The second problem associated with the Phase II CMS system was that at the higher ranges, it is possible to have more than five periods within the measurement interval. An inherent one count error is usually averaged by dividing by the total number of periods; if the number of periods is limited to five, the one count error has a greater effect on the accuracy of the system since one count is a large percentage of the total period count.

### 3. Phase III Radar Card

A new radar interface card, shown in block diagram form in Figure 33, was constructed for Phase III. A square wave to provide the triangular wave modulation for the radar is generated by dividing down the 2-MHz clock frequency of the CPU to obtain 977 Hz. The square wave is passed on to the radar system, so that the triangular wave can be generated, and to the radar interface card. The 977-Hz square wave, 1 kHz nominal, is used to trigger blanking pulses and it is also used as a system reference for the software by means of the status latch. The blanking pulse output from the blanking pulse generator goes to a gate and the system status latch. If we refer to Figure 31 we see that the square-wave level appearing at the status latch during the blanking interval indicates whether the measurement is on the upswing or downswing of the measurement interval.

The beat frequency output,  $f_B$ , of the radar system after passing through the threshold circuit becomes a 5-V pulse train which contains range and range-rate and the turnaround phase discontinuity. A trigger generator generates narrow pulses at the positive transitions of each of the pulses coming from the threshold circuit. The blanking pulse is used to filter out unwanted data for approximately 170  $\mu$ s after the turnaround point.

A high-speed clock of 2 MHz from the microprocessor is used to drive a 12-bit T<sup>2</sup>L counter. The triggers, corresponding to the positive transitions of the beat frequency, are passed to three locations in the radar interface card.

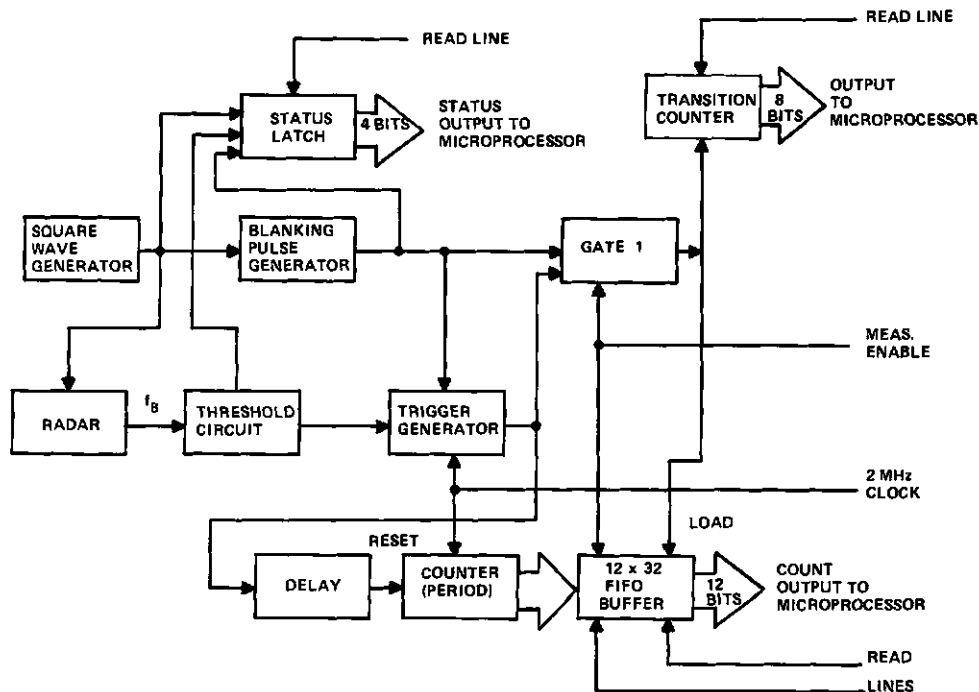


FIGURE 33. BLOCK DIAGRAM OF PHASE III CMS CARD.

When the measurement is enabled by software, the trigger output is passed through the "gate 1" circuit to the transition counter and the buffer. In addition, the first trigger pulse which corresponds to the first positive transition of the beat frequency is fed through a delay to the period counter. This trigger pulse is delayed always by two counts for the reset mode. The reset line initializes the high-speed counter to the count of two. Before the counter is reset, the data from the counter is read into a 12-bit wide x 32-bit deep first-in first-out buffer (FIFO). The measurement enable strobe which allows the measurement also resets the FIFO. The second positive transition of the beat frequency corresponds to the first period. The count corresponding to one period is loaded into the FIFO, and two clock periods later by virtue of a hardware delay, the high-speed clock is reset to a count of two. The two-count delay eliminates the one error usually associated with a high-speed clock measuring technique.

The number of periods in a measurement interval is stored in the FIFO. The square wave and blanking pulse relationship indicates either an up- or downswing of the triangular wave. A dropout that occurs during the measurement interval is noted by reading the threshold circuit condition from the status latch. Software can, therefore, select to accept readings up to the dropout since individual periods are measured and average the partial set of acquired data

in the measurement interval. The new Phase III CMS radar card can, therefore, measure up to 32 periods within a measurement interval. The card will also acquire and use the data up to a dropout in the measurement interval. This particular radar interface card was demonstrated and is used presently with the headway-control system.

#### 4. Revised Phase III Radar Card

Early experiments had shown that the accuracy of the doppler information was not sufficient for proper CMS operation. The problem was traced to the asymmetrical blanking pulse. Since the tuning curve of the TEO in general is not perfectly linear, it is important to operate over the same tuning range of the TEO, both on the upswing of the triangular wave and on the downswing. Referring to Figures 31 and 32, we see that if the blanking starts at the turnaround point, an asymmetric tuning curve results. The beat frequency is read 170  $\mu$ s after the beginning of the positive slope of the triangular wave up to the peak or turnaround point. Then, 170  $\mu$ s later, the beat frequency is read back from the peak to the turnaround point or valley of the triangular wave. A nonlinearity of the TEO tuning curve under the described conditions causes only minor range measurement problems because the range readings average. However, an offset in doppler frequency will occur because of the nonlinearities creating a difference in frequencies of the periods on the upswing and downswing.

The revised Phase III radar interface card, which overcomes this difficulty, is shown in Figure 34. Once again, the square-wave generator divides down the 2-MHz microprocessor clock to obtain the 977-Hz square wave. A status latch is used to monitor the level of the square wave with respect to a blanking pulse which originates at the turnaround point. The blanking pulse generator also generates a blanking pulse that overlaps the turnaround points 50  $\mu$ s on each side, as shown in Figure 31. The symmetrical blanking pulse causes the same part of the TEO tuning curve to be swept through on the upswing and downswing of the triangular wave. The status latch monitors the threshold condition line and a data out ready line from the FIFO. The threshold condition line goes high when the data drops below  $V_{Th}$  (Figure 32) anytime during the measurement interval. The data out ready line indicates the FIFO has at least one set of useful data.

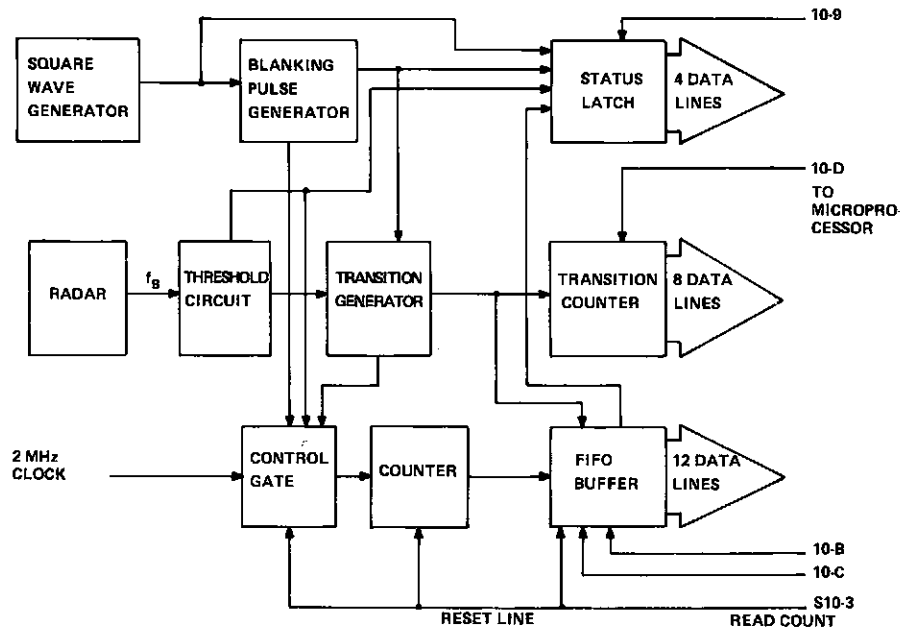


FIGURE 34. REVISED PHASE III CMS CARD.

In order to simplify the hardware, it was decided to accumulate a count across the entire measurement interval and divide out the inherent one count error by averaging the large number of periods. The output of the threshold circuit once again is used to generate narrow trigger pulses within the transition generator. The positive transitions of the beat frequency are counted by a transition counter. The first transition pulse or trigger after blanking turns on the high-speed counter. Each successive transition loads the accumulated count to that respective time in the FIFO. If a dropout occurs during the measurement interval, the count accumulated up to that point is used for the signal processing. The control gate that allows the counter to be initially started is disabled by the blanking pulse or the threshold circuit. A reset line is used to zero the counter initially and to enable the control gate. The data from the status lines, 4 bits, a nibble, is read by a IO-9 pulse. The 12-bit-wide FIFO is read twice. An IO-B pulse is used to read the lower eight bits. An IO-C pulse reads the upper four bits (nibble). The revised Phase III card is now used in the CMS algorithm.

## 5. Threshold Circuit

Figure 35 shows two versions of the threshold circuit used with the radar interface cards of the CMS and headway-control system. The threshold circuits

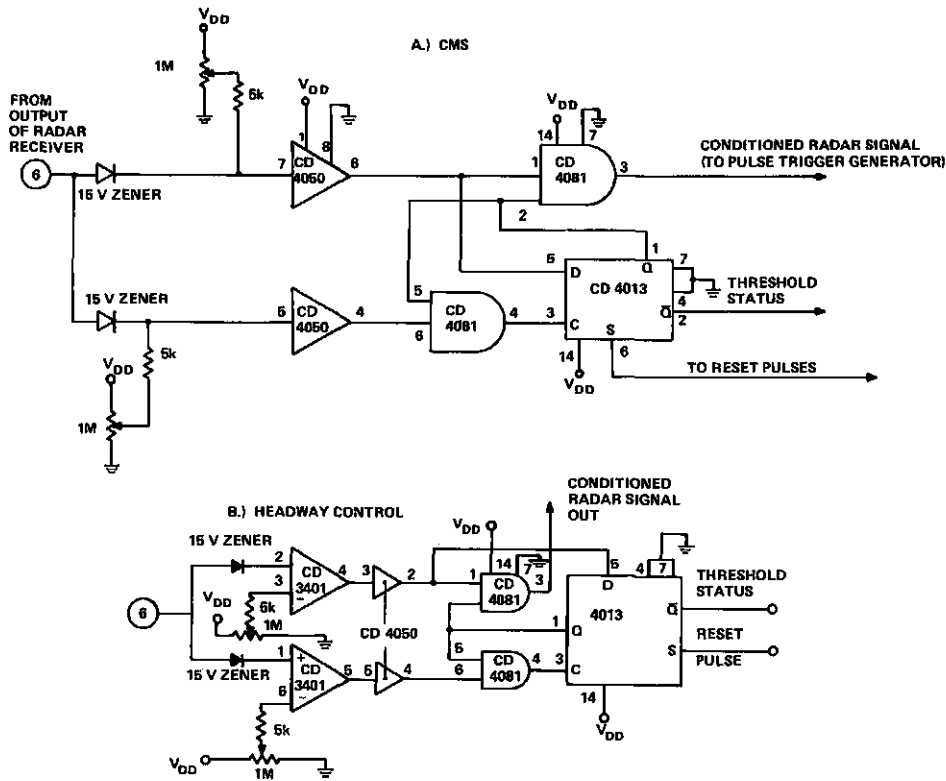


FIGURE 35. THRESHOLD DETECTION CIRCUITS.

differ from each other in the manner in which the analog input,  $f_B$ , is converted to a digital pulse train. The threshold circuit used with the CMS biases the inputs of two buffers to provide a low and high threshold value that must be exceeded for the circuit to perform properly. The threshold circuit used with the headway-control system uses two comparators instead of two digital buffers at the input. After passing through the buffers or comparators, both threshold circuits are the same. The two different input circuits were tried to determine if there were any operational differences between the standard comparator using an OP-AMP and reference voltage, and the voltage-biased digital buffer. At this point, no conclusive data indicates that one comparator circuit is better than the other.

Basically, the threshold circuit consists of two buffers or comparators, two AND gates, and a flip-flop. The input signal is split into two paths to their respective buffers or comparators. A diode in the series leg of each of the paths limits the bipolar signal to a positive-going signal only. (A negative-going signal greater than  $-0.75$  V would cause the buffer to clamp a large signal at this level and create problems in setting threshold levels.)

The threshold level of each buffer with  $V_{dd} = 5 \text{ V}$  is 2.5 V; therefore, a DC level is applied to each buffer or comparator to provide an upper- and lower-threshold level. The lower-threshold level setting has a significant voltage applied to the input so that a small signal of only a few tenths of a volt generates an output from the buffer or comparator. The upper-threshold level provides a low-level bias at the input of the second buffer or comparator and a large signal of the order of 2 V is required to generate an output from this stage. The circuit uses an AND gate to control the signal from the threshold circuit into the rest of the doubler circuit. The other AND gate controls the clocking of the flip-flop used to turn the circuit on or off.

Initially, the CD4013 flip-flop is set by the reset pulse of the radar interface. A high level appears at both AND gates, enabling both circuits. The low-level signal threshold generates a pulse out of the buffer or comparator which is used to clock the flip-flop. If the high-level threshold allows a pulse output from the buffer or comparator, then a pulse will be appearing at the "D" or data input to the flip-flop. Since the clock input is delayed by propagation time through the AND gate, the high-logic level at the "D" input corresponding to the signal will be present when the CD4013 is clocked. Clocking it with a high level keeps Q high and maintains the enabled state of both AND gates; therefore, the threshold circuit is "on."

If at any time the upper-level threshold is not exceeded while the lower-level threshold is generating a pulse from the buffer or comparator, the net result is a clock signal to the CD4013 which sees a zero at the "D" input, and, therefore, Q goes low, shutting off both AND gates. No signal is allowed to pass to the doubler, and additional clock pulses are not allowed to pass to the flip-flop. The Q output of the flip-flop goes high, signaling the microprocessor that the threshold circuit is shut down. The reset pulses of the radar interface are then needed to turn the threshold circuit on again.

## B. CPU AND MEMORY

### 1. Introduction

During the initial stages of hardware and software development a flexible microcomputer system for prototyping purposes is required. The RCA COSMAC development system (CDS) has the necessary memory size required for a prototype system in the form of RAM space so that software can be easily loaded

from another storage area or host computer. To aid in this storage and re-writing function, some type of ROM chip containing a "utility" routine is also included. The utility software enters and retrieves data from the RAM space and, if necessary, can be used to modify the data and then restore the data to any selected location or address.

During Phase II we used exclusively the COSMAC development system for prototyping both hardware and software. The CDS consisted of a card nest, control panel, and a basic set of plug-in modules. The card nest provided user space for the development of interface hardware between external hardware and the control processing unit (CPU) system. A large variety of interface cards was developed for the radar, display, and various sensors on the RSV. Two major problems were, however, noted for the CDS. The plug-in modules that formed the basic microcomputer system were interconnected at the backplane by a printed circuit (PC) structure that connected each card of the module to other modules within the card rack. The continuous insertion and removal of cards during the development period and vibrations from the test vehicle caused the printed circuit connections eventually to deteriorate and some open- and short-circuit conditions on the backplane of the CDS occurred. A second problem was the difficulty in using the system to debug the hardware. A hardware failure in an interface card usually caused one of the plug-in modules of the microcomputer system to fail.

During Phase III, therefore, we switched to the newly released RCA evaluation board, single PC card (24 x 36 cm) that contains all of the necessary components for prototyping. The evaluation board was finally replaced by another standard PC board that fit within the normal card cage to form a compact single-enclosure computing system.

## 2. Phase III Evaluation-Board System

The evaluation board uses an RCA CDP 1802 one-chip microprocessor with a 2-MHz crystal to provide the system clock frequency. Control chips are provided for resetting and starting either a previously loaded program in RAM space or the utility routine located on a ROM chip on the card. Additional chips are provided for addressing the 4K of RAM space on the board and for I/O decoding. Three transistors on the card provide a RS-232 interface which allows communication between the evaluation board, an "execuport" terminal, and the host computer system. A set of LEDs on the card provides a visual

indication of the data address status lines of the microcomputer system. The evaluation board with RAM and ROM operates from a single 5-V supply.

During Phase II, a large number of interface cards had been developed for the radar, display, and sensors of the RSV, using the COSMAC development system. To avoid redesigning the hardware of the interface cards, we designed another card that made the evaluation board look like the CDS to the existing interface hardware; this new card was called the CPU interface card. A card cage was constructed that would hold five standard 11.5 x 16.5 cm cards capable of mating with a 44-pin connector. A picture of the evaluation-board card cage system is shown in Figure 36. The card cage and evaluation board are powered by a single 5-V supply. Connections are made between the card cage via the CPU interface card and the evaluation board by two 16-lead flat ribbon connector cables which mate to standard DIP sockets. Also shown in the photograph is a self-scan display which was found useful for visual readout during testing and debugging.

A typical card cage assembly for CMS testing included the CPU interface card, the radar interface card, and a display interface card. The display was used during testing to indicate range and range-rate data. Early tests of the electronic dashboard display microcomputer also made use of the evaluation-board card cage system. For testing the dashboard display, the card cage assembly contained a CPU interface card, A/D-trip odometer card, clock-fuel economy-tachometer card, and the card which contained the display-binary switches and velocity interface. Both card cage systems were able to use a standard CPU interface card and the evaluation board. As mentioned above, the main purpose of the CPU interface card was to make the evaluation board look like the CDS with regard to I/O functions such as input and output data lines and input and output strobes.

Closer examination of the evaluation board later in the program indicated that the elimination of the circuitry for the utility ROM, two CD 1852 I/O ports, the LEDs with their associated drivers, and the three-transistor RS-232 interface would produce a compact design for a CPU card that could fit within the standard card cage. If the output lines from the CPU card were made the same as the output lines (ribbon cable) from the evaluation board, it would create a system that could be used for initial prototyping and then, with the addition of a CPU card, become a stand-alone microcomputer. This concept is illustrated in Figure 37. The CPU card, CPU interface card, and evaluation board are common to all card cage systems.

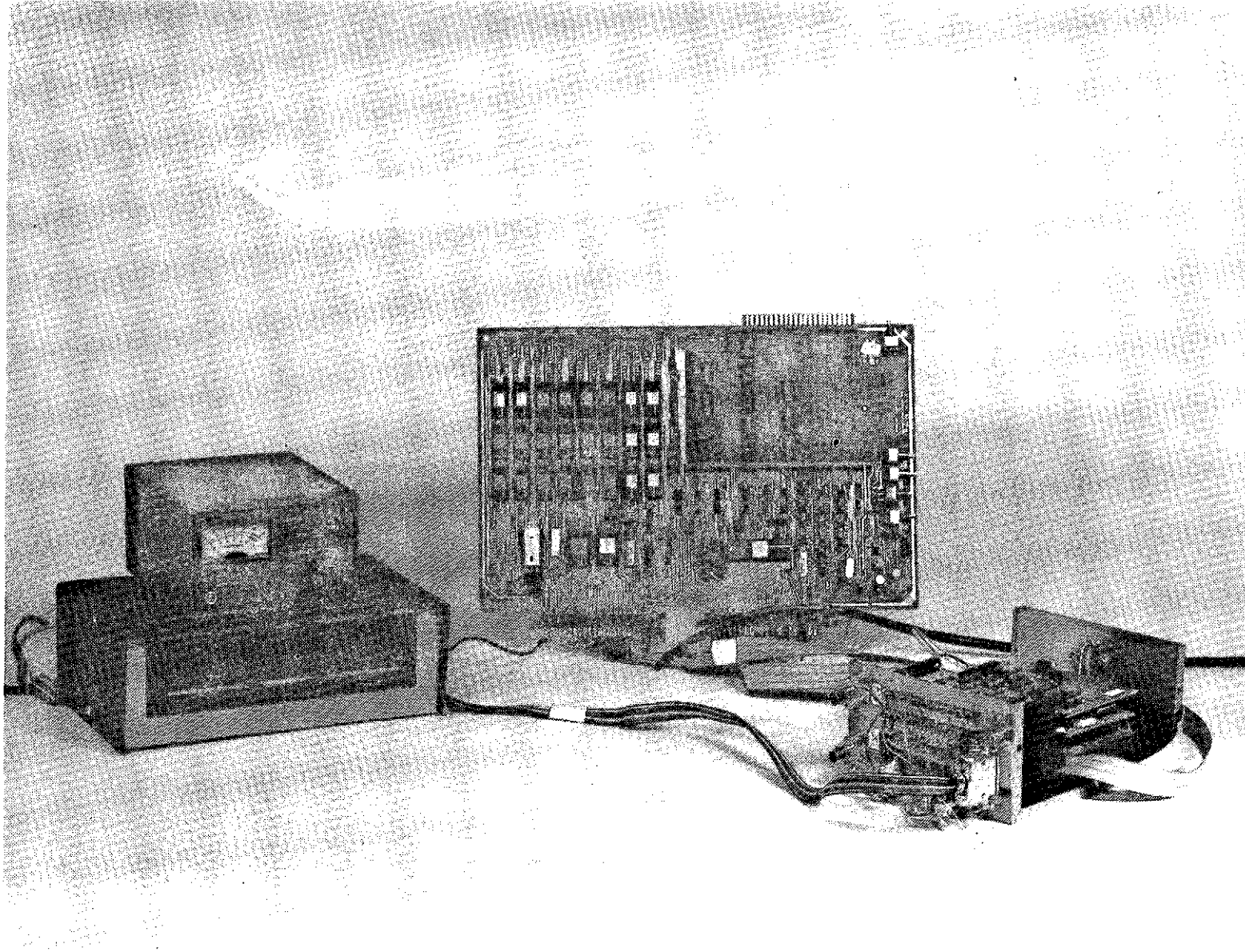


FIGURE 36. EVALUATION BOARD WITH CARD CAGE AND DISPLAY.

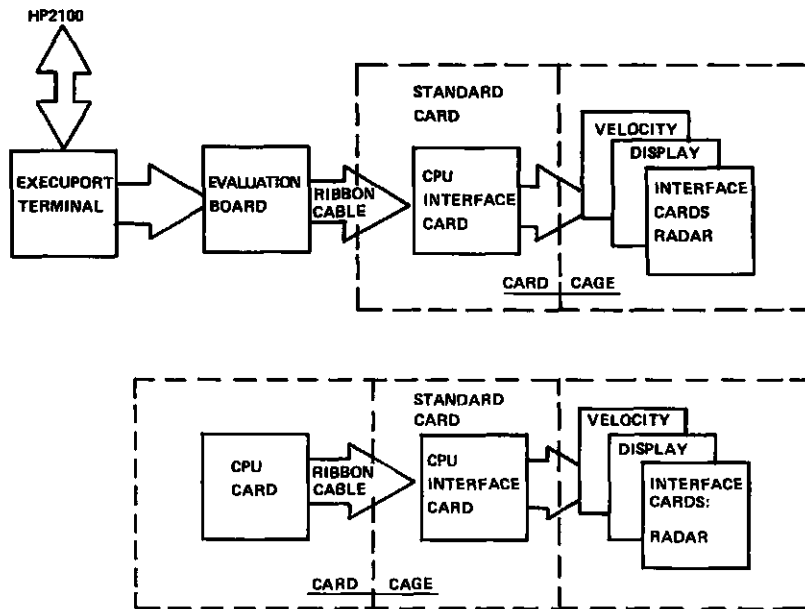


FIGURE 37. EVOLUTION FROM DEVELOPMENT BOARD TO FULL CARD CAGE SYSTEM.

### 3. CPU and Memory Card Cage for RSV Installation

A block diagram of the final CPU card is shown in Figure 38. The card consists of a CDP 1802 microprocessor with a 2-MHz crystal for the system clock. Two CDP 1822 RAM chips provide  $\frac{1}{2}$ K of memory space for available storage. Either 2758 or 2716 EPROMs can be used with the CPU card. The 2758 is a 1K EPROM, and the 2716 is a 2K EPROM. From 1K to 8K of EPROM space is available on the CPU board. Both types of EPROMs are convenient to program and erase, and both operate from a single 5-V supply. An 1852 chip is used as an address latch and a 4555 chip is used for address decoding. A CD4028 is used for I/O decoding. A photograph of the CPU card is shown in Figure 39.

When the EPROM programming is complete, the CPU card, CPU interface card, and hardware interface cards form a stand-alone microcomputer system. A photograph of the complete CMS microcomputer system is shown in Figure 40. Another photograph, Figure 41, shows the CMS with the cover removed. Figure 42 gives a size comparison between the microcomputer system and the CDS. The CMS card cage contains two additional cards intended for the headway-control system in the RSV. The CMS card and headway-control card share the same CPU interface card by means of transmission gates at the connections between the CPU and CPU interface cards. An interrupt throttle controller card is backplane wired to the headway CPU card. A switch is used to select between either the CMS or headway-control system.

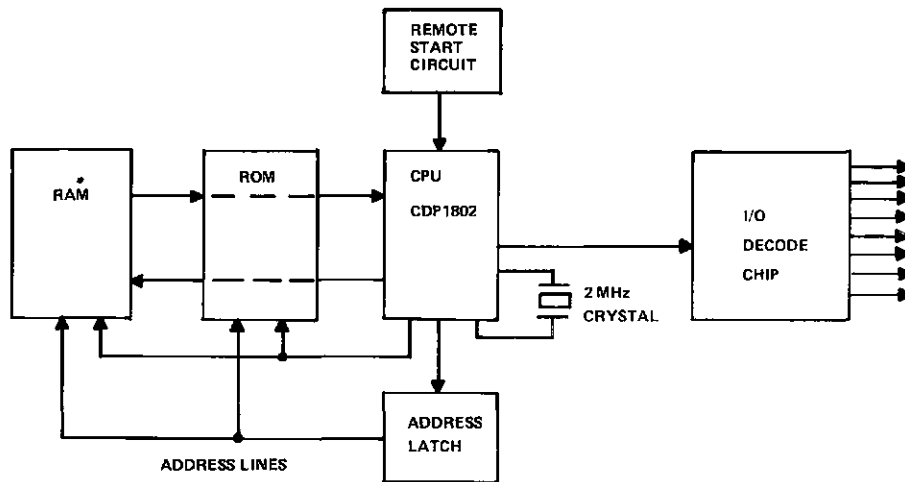


FIGURE 38. BLOCK DIAGRAM OF CPU CARD.

The electronic dashboard microcomputer is the same size as the CMS micro-computer. It consists of a CPU card, CPU interface card, and three additional cards which interface to the hardware and sensors of the RSV. Thus two card cages, each measuring approximately 9 cm x 15 cm x 26 cm contain all computer circuitry for CMS, headway control, and display functions.

#### 4. Remote-Start Circuit for CPU

Both CPU cards contain a special start-up circuit to reset the CPU card and to start the software running at the proper location when the ignition is turned on. A low level on the  $\overline{\text{WAIT}}$  line of the CDP 1802 microprocessor will reset all registers of the microprocessor and start the software running at location 00. The  $\overline{\text{WAIT}}$  line has to be held low until the crystal oscillator stabilizes after turn on (approximately 50 ms).

Figure 43 shows the remote-start circuit of the CPU card. An R-C network is used as input to an inverter. The transient response when the power is applied to the circuit from  $t=0$  is shown at different points (A, B, C, D) on the figure. The capacitor charges as a function of the R-C time constant. The inverter output B remains high until the charging capacitor exceeds the CMOS threshold level of the inverter. At  $t_1$ , the inverter output at B goes low. Examination of diagram (B) shows that when the power is turned on a spike is generated that can be used for initializing hardware. This particular pulse is used to reset the CD4047 one-shot circuit so that  $\overline{\text{Q}}$  is high.

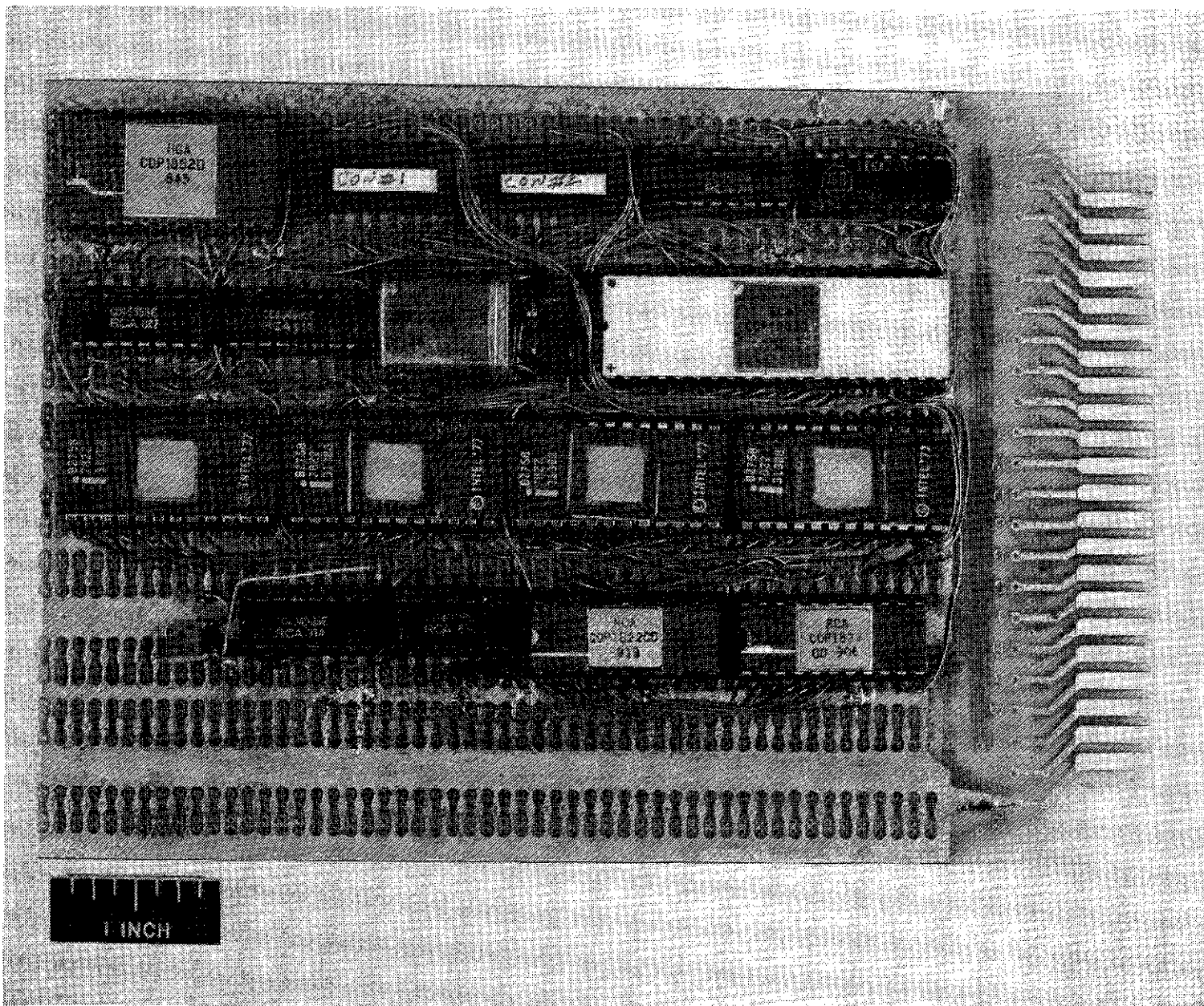


FIGURE 39. PHOTOGRAPH OF CPU CARD.

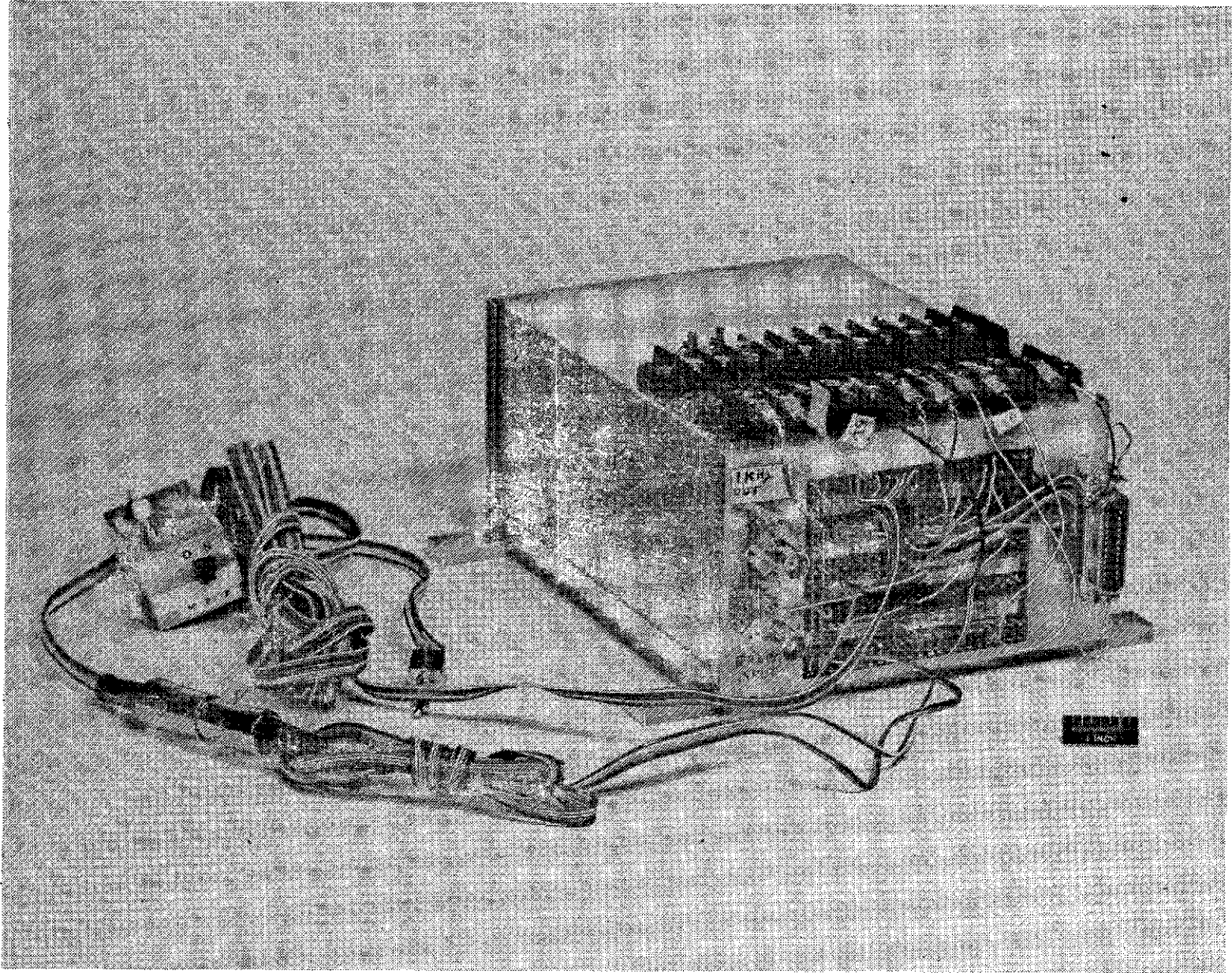


FIGURE 40. COMPLETE CMS CARD CAGE.

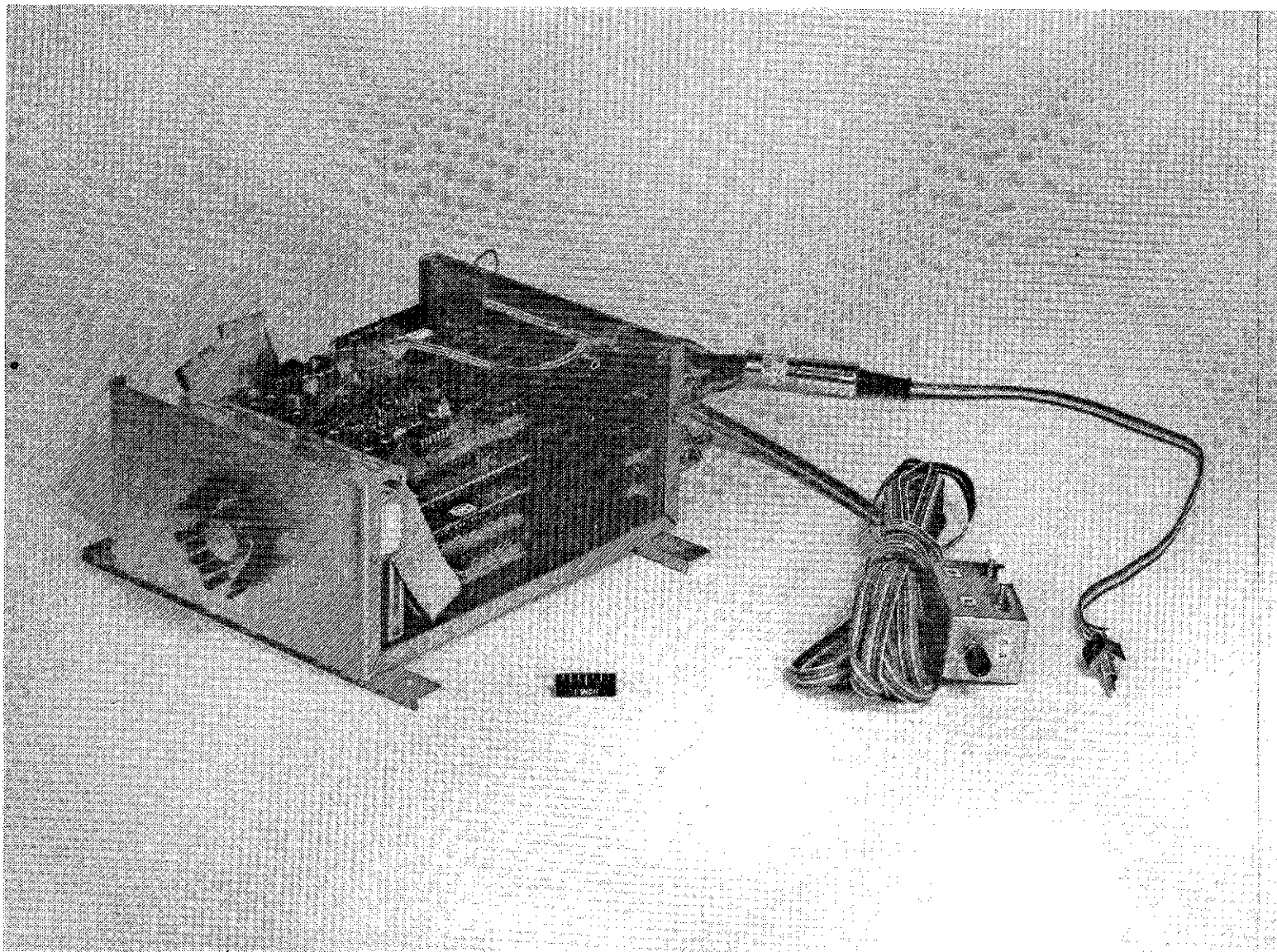


FIGURE 41. CMS CARD CAGE WITH COVER REMOVED.

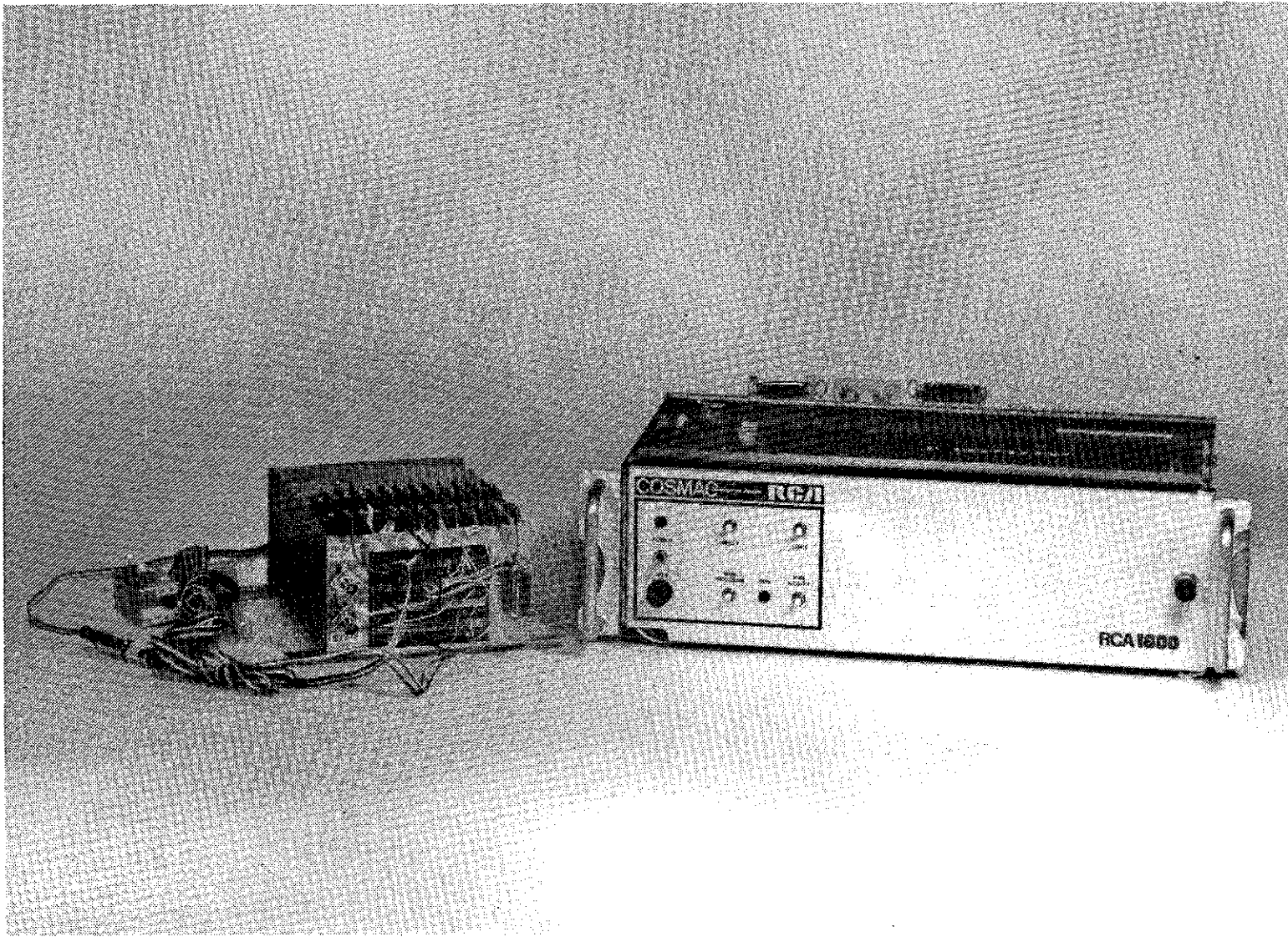


FIGURE 42. SIZE COMPARISON - MICROCOMPUTER AND CDS.

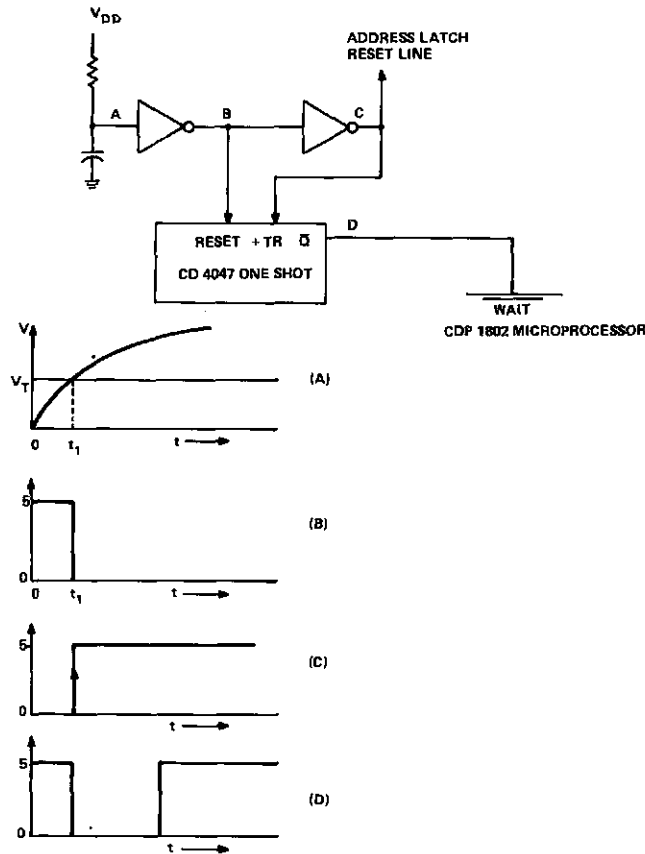


FIGURE 43. REMOTE-START CIRCUIT.

Since point B is high until  $t_1$  and is also the input to another inverter, point C, the output of the second inverter is low until  $t_1$ . This low level is used to reset the address latch to zero. The positive transition shown in diagram (C) is used to generate the pulse to reset and start the microcomputer.

The  $\overline{\text{WAIT}}$  pulse is low in diagram (D) for a time determined by an R-C network associated with the CD4047 one-shot. The output of the second inverter (C) cannot be used to restart the microprocessor because of a conflict in timing between resetting the address latch and restarting the microprocessor. The remote-start circuit for the dashboard display microcomputer is the same except for an additional circuit which is used to inhibit interrupt pulses until the microprocessor is running.

### C. DISPLAY AND SENSOR INTERFACES

The display and sensor interface hardware that originally had been developed for the COSMAC development system during Phase II was consolidated to fit on three standard cards within the card cage system. The three interface cards,

the CPU interface card and the CPU card, form the electronic dashboard display microcomputer.

The top of the dashboard display card cage has the 8-input analog-to-digital conversion circuit and a trip odometer circuit. The A/D circuit uses three of its inputs to monitor fuel level, water temperature, and oil pressure. A voltage divider is formed between 5 V and ground by a series resistance and the resistance of the respective sensor. The voltage developed across the sensor is converted by the A/D system.

The 8-input analog-to-digital circuit is shown in Figure 44. The heart of the circuit is a Burr-Brown\* ADC80AG-10 A/D converter that has a 17- $\mu$ s conversion time for an 9-bit output. The A/D has a 0- to 10-V input voltage range. The  $\pm 15$  V necessary to operate the A/D chip is provided by a Datel\*\* DC-DC converter. A CD4051 multiplex chip has 8-channel capability. The 9, 10, 11 pins of the chip are internally decoded to select a channel and connect it to the A/D converter. The multiplex chip is tied to the  $\pm 15$  V of the DC-DC converter through a voltage-dropping resistor, so that only 10 V actually appears across the chip. The 10 V at the multiplex chip allows 10-V-level signals to be present at the input of the multiplex chip, which can still be switched by 5-V logic levels applied to the channel select pins.

The selection of one of eight channels to be connected to the A/D is accomplished by setting a level at the three binary-coded select pins 9, 10, 11. This level is placed there by the presence or absence of OTD-0, OTD-1, OTD-2 pulses at the "D" input of a CD4013 flip-flop, and is clocked through to the Q outputs (1, 13, 1) by an SIO-4 pulse.

The A/D converter is enabled by an SIO-3 pulse. The completion of the conversion cycle is indicated by the status of the EF-1 flag line. The 8-bit output of the A/D converter is applied to the data bus lines by pulsing a pair of CD4016 transmission gates with a IO-C pulse.

The second circuit located on the top card with the A/D circuit is the trip odometer, shown in Figure 45. The trip odometer must have the capability of retaining distance data when the vehicle is not operating. A connection is made directly to the vehicle battery, and the battery voltage is dropped to the

---

\*Burr-Brown Research Corp., Tucson, AZ.

\*\*Datel Systems, Inc., Canton, MA.

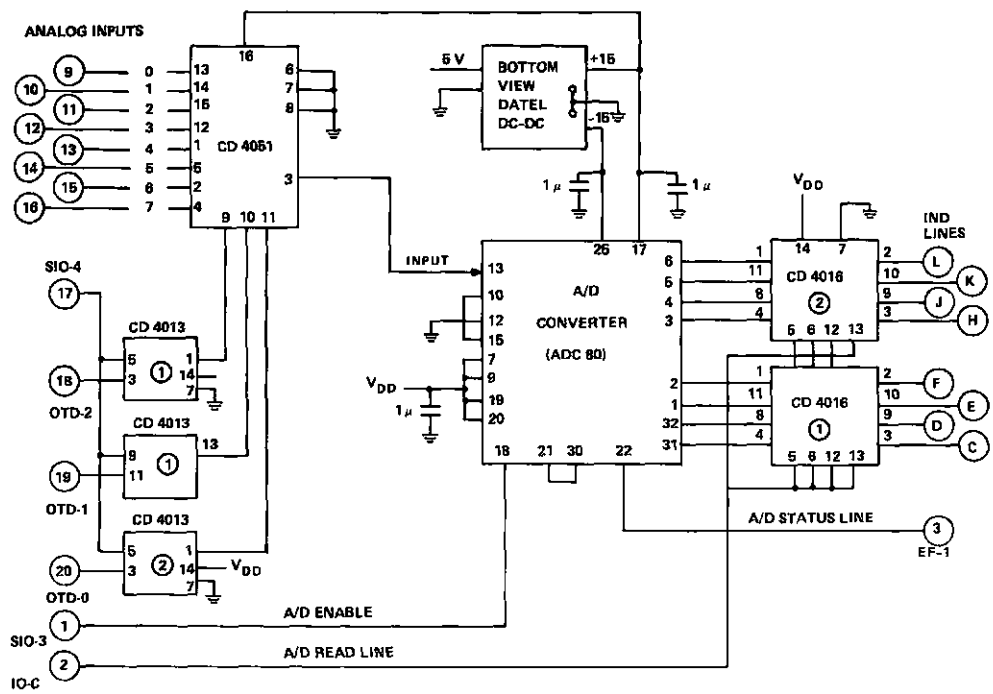


FIGURE 44. 8-INPUT ANALOG/DIGITAL CIRCUIT.

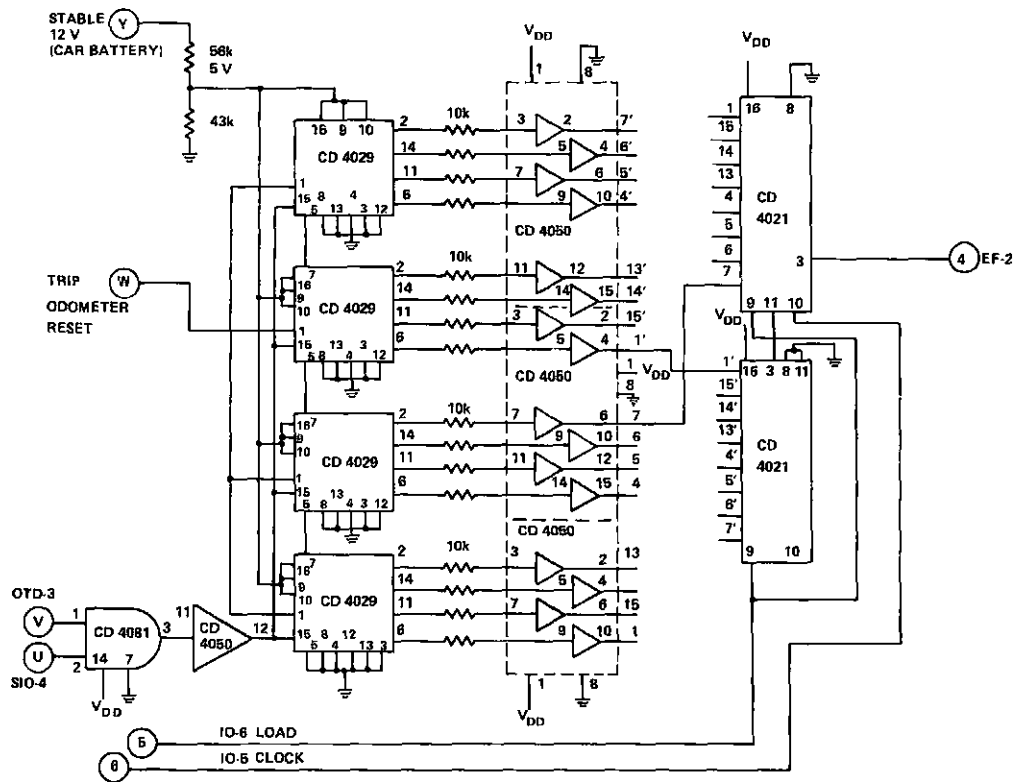


FIGURE 45. TRIP ODOMETER CIRCUIT.

5-V level for operating the CMOS counter by use of a voltage divider. Four CD4029s are used for the trip odometer counters. The counter is updated by a level generated by the simultaneous application of a SIO-4 pulse and an OTD-3 pulse. The 16-bit output of the four counters is connected to 16 buffers through individual 10-k $\Omega$  resistors.

The purpose of the 10-k $\Omega$  resistors in series with each input to the buffer is to provide protection to the buffer when the computer is in the "off" position. The counters will retain the logic level at their respective outputs because of the stable 12-V supply. During normal operation, the 16-bit output of the buffer is loaded by a IO-6 pulse into two shift registers (CD4021) and the 16 bits are then read serially by the application of a IO-5 clocking pulse onto a flag line EF-2. The trip odometer can be reset by applying a level to reset pin 1 of each of the CD4029 counters. The trip odometer is reset by a debounced switch which provides 5 V for this function.

The second card from the top of the dashboard display card cage is the clock, fuel-economy, tachometer interface. The automobile clock is designed to keep accurate time whether the car's ignition is on or off. The automobile clock circuit is shown in Figure 46. A stable 12 V is applied to the counting circuits by the vehicle battery. The voltage to the respective CMOS chips is reduced to 5 V by a 10-k $\Omega$  voltage-dropping resistor connected in series. An inverter (CD4007) is used for isolation between the oscillator and the four CD4029 counters. The four CD4024 counters are used as dividers, dividing down successively from 32768 to 2048 to 128 to 8 and, finally, to 1 Hz. The 8 Hz is applied to the interrupt circuit section of the remote start. The 1-Hz pulse is applied through a buffer to two CD4017 decade counters which count to 60 and generate a pulse per minute.

Figure 47 shows the pulse-per-minute input applied to two CD4029s, whose function is to count to 59 and then at the next minute reset to 0. The CD4082 at the output lines of the CD4029s provides the logic necessary for the "reset after 59" function. The reset pulse 1 minute after 59 is the hour pulse, which is applied to a single CD4029. This counter counts to 12 and then the next hour resets by jam loading to 1. The CD4073 is used for the "reset to 1" logic function.

The manual minute advance is accomplished by the use of a level derived from a debounced switch and applied to the clock line of the two CD4029s. The incrementing or decrementing of the minute counter is accomplished by use of a CD4049 inverter. A "0" at the input results in a high applied to the up/down



count pin, which causes the counter to count up. A high level at the input of the inverter makes the inverter output go low, and the counter decrements when a level is applied to the clock line. The hour advance uses a voltage-level from another debounced switch to advance the hour function. The buffer outputs are loaded into two shift registers by a IO-6 pulse and then clocked out serially by IO-5 clock pulses. Note that the load and clock pulses are the same for both the trip odometer and the clock. However, the automobile clock output is read out on flag line EF-3, while the trip odometer is read out on flag line EF-2.

The tachometer interface and the fuel economy interface are also located on the card with the automobile clock. The circuits are shown in Figures 48 and 49. The tachometer interface obtains its input from the point side of the coil. The input is applied through a buffer to a one-shot multivibrator (CD4047). The one-shot multivibrator generates a pulse that is noise-free and free from ringing effects and therefore can be used to drive a counter. The pulse output is applied to a CD4029 counter whose 4-bit output is read by pulsing a transmission gate (CD4016) with a IO-D pulse. The counters are set to "0" initially by the CLEAR-P line.

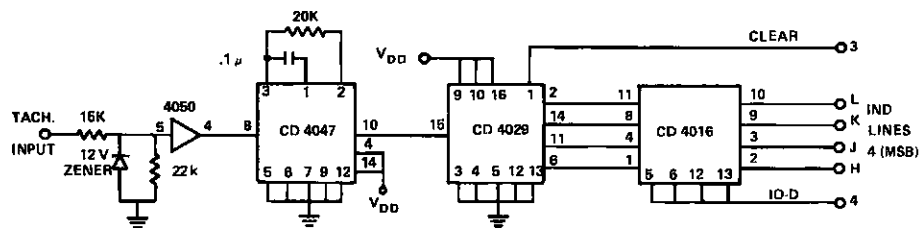


FIGURE 48. TACHOMETER INTERFACE CIRCUIT.

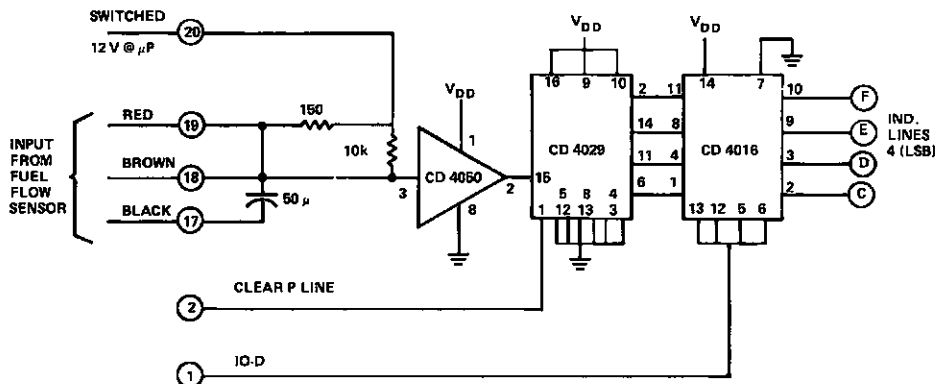


FIGURE 49. FUEL ECONOMY SENSOR CIRCUIT.

The circuitry necessary to operate the Model 261PB-15 flow transducer\* is connected at the input to the fuel-economy sensor interface card. The pulse output of the sensor is applied to a CD4050 buffer for logic level conversion from 12 to 5 V. The pulses clock a CD4029 counter which, in turn, is gated on to the transmission bus by the application of an IO-D pulse to a transmission gate. The CLEAR-P line is used to initialize the counter. Note that the IO-D pulse gates simultaneously the tachometer and fuel economy interfaces by gating the upper 4 bits onto the bus for the fuel economy data and the lower 4 bits for the tachometer data.

The third card from the top of the dashboard display card cage contains the display interface, the binary interface, the velocity interface, and a circuit used to check the condition of the restraint system. The display interface circuitry is shown in Figure 50. Eight bits of data are read from the CPU card interface bus lines and stored in CD4042 latches by use of a stretched SIO-1 pulse. Six bits of data are applied to the self-scan unit by use of CD4049 inverters. A "data present" pulse from the latch coincident with the SIO-1 pulse applied to a CD4023 NAND gate provides a logical 0 which causes the "Data Present" line of the self-scan to go low, thereby permitting the data on the line to enter the memory of the self-scan unit.

Another pulse from the latch is used to clear memory by use of a second CD4023 NAND gate. Pin 14 of the latch is the control bit for "Data Present" or "Clear." Pins 1 and 15 are the latched outputs of the pin 14 input, pin 15 is the complement of pin 1. The two CD4011 NAND gates, the CD4050 buffer, and 1N461 diode and the RC network comprise the pulse stretching network for the SIO-1 pulse. The blank disable line is always tied low so that it is inoperative.

The control function provided by the computer is the same for both the "high brightness" and conventional self-scan display. The conventional self-scan unit makes use of 7 latched data outputs to obtain the 128-character repertoire. The switch located on the clear line of the display is used to stabilize the display from update flicker. If the overall system voltage supply is free from noise, the switch can be left open and the display will not flicker. However, if noise spikes are present on the vehicle's 12-V system,

---

\*Flo Scan Instrument Co., Seattle, WA.

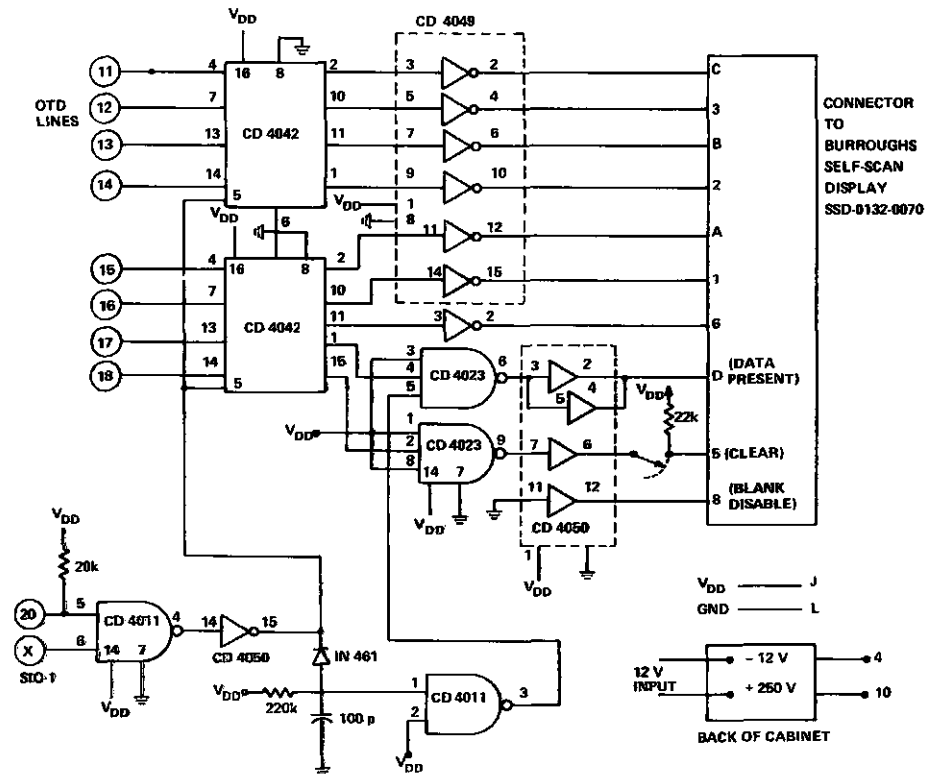


FIGURE 50. SCHEMATIC OF DISPLAY INTERFACE.

the display data will offset because the  $T^2L$  circuitry of the self-scan unit is affected by noise. Closing of the clear switch will eliminate the data shift on the display but will cause some minor update flicker.

The binary input card of the display microcomputer is shown in Figure 51. It makes use of 9 buffers and 3 transmission gates (CD4050 and CD4016, respectively). The card is broken down into families of buffers and quad-latches. The input of each of the buffers is tied to ground through a 22-k $\Omega$  resistor. A 12-V input at the input of any buffer is converted by the buffer to a 5-V logic level at the output. The 12-V inputs are derived from switch sensors. The output of the buffer is read onto the 8-bit data line by gating the proper pair of quad-latches. The quad-latches are selected by IO-9 or IO-A pulses in the display card cage. The binary inputs monitor door switches, service brake switches, brake fluid level switches, battery indication, the selection of the display format, and the airbag or restraint system status.

The circuit used to monitor the voltage from the top of the airbag squib to ground is shown in Figure 52. Two comparator circuits monitor the squib voltage. The voltage from the squib to ground is considered in tolerance if

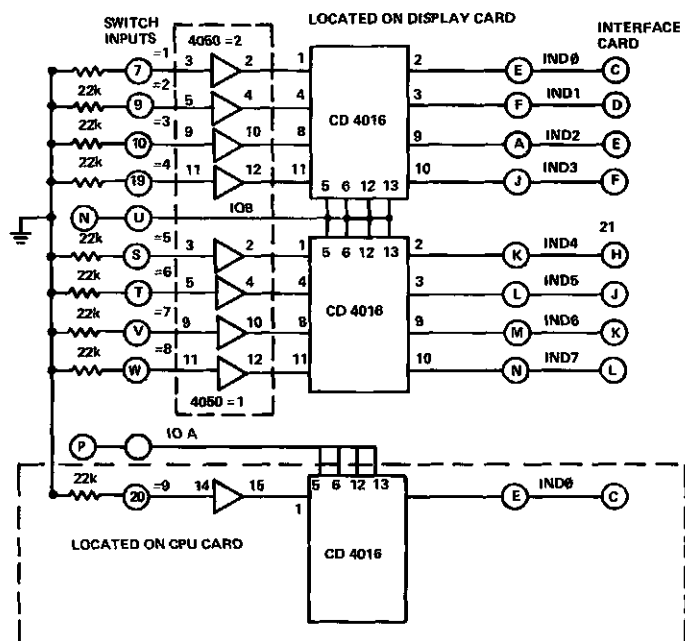


FIGURE 51. BINARY INPUT CARD FOR SWITCHES.

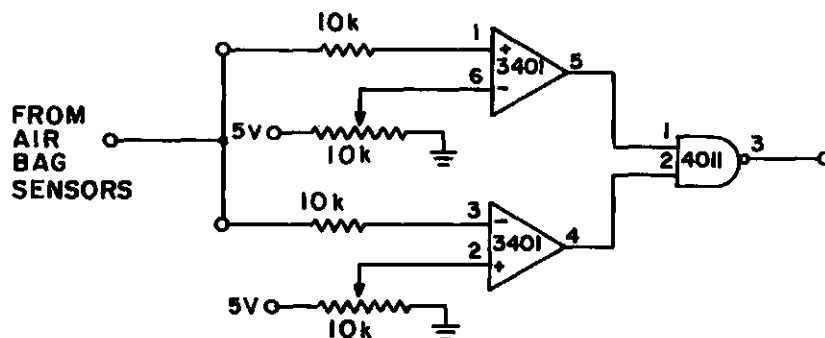


FIGURE 52. SCHEMATIC OF AIRBAG INDICATOR.

it is between 6 and 10 V. Under this condition, the comparator outputs are both high; therefore, the output of the NAND gate is low which in turn is connected to one of the binary input parts. If the voltage from the squib-to-ground should go to 0 or 12 V, one of the comparators will go low; therefore, the NAND gate output will go high thereby causing a 5-V level to appear at a binary input port to trigger the "Restraint System Out" message.

The final circuit on the third card is the velocity sensor interface, shown in Figure 53. A pulse train input is received at the input of the circuit. The pulse frequency is directly proportional to velocity. This pulse

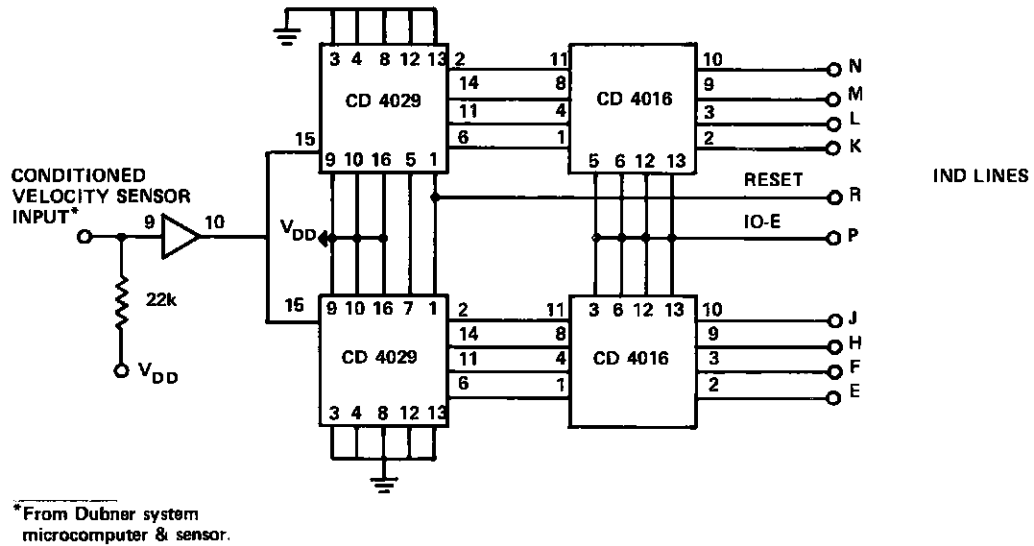


FIGURE 53. SCHEMATIC OF VELOCITY INDICATOR.

train is read by a sensor located on the RSV drive train, buffered by the Dubner system automatic transmission microcomputer, and then passed on via cable to the RCA electronic dashboard display microcomputer. The input circuit is also buffered. The output of the buffer drives a counter which is read through the transmission gates by an IO-E strobe.

## SECTION V

### CONTROL FUNCTIONS AND SOFTWARE IMPLEMENTATION

#### A. COLLISION-MITIGATION BRAKING CONSIDERATIONS

The two key features of the collision-mitigation system are (1) the automatic application of antiskid brakes in case a high-speed collision is definitely unavoidable and (2) the complete elimination of false alarms (i.e., no application of brakes in cases where no real collision is imminent or where the driver could have avoided the collision by himself). For a better understanding of the boundaries that guide automatic braking, a simplified summary of braking dynamics is presented.

The general case of two vehicles moving toward each other, with one being braked, is illustrated by the time-distance relationship shown in Figure 54. The following assumptions are made:

- $v_1$  is the initial velocity of the radar-equipped car
- $v_2$  is the initial velocity of the target vehicle ( $v_2 < 0$ )
- $v_I$  is the impact velocity of the radar-equipped car
- $v_{It}$  is the total impact velocity ( $v_{It} = v_I - v_2$ )
- $\mu g$  is the maximum braking deceleration (0.9 g for dry road, antiskid brakes)
- $R_t$  is the radar detection range
- $\Delta t$  is the reaction delay (0.1 s for the radar processor and algorithm and 0.1 s for the brake system to reach full braking action)

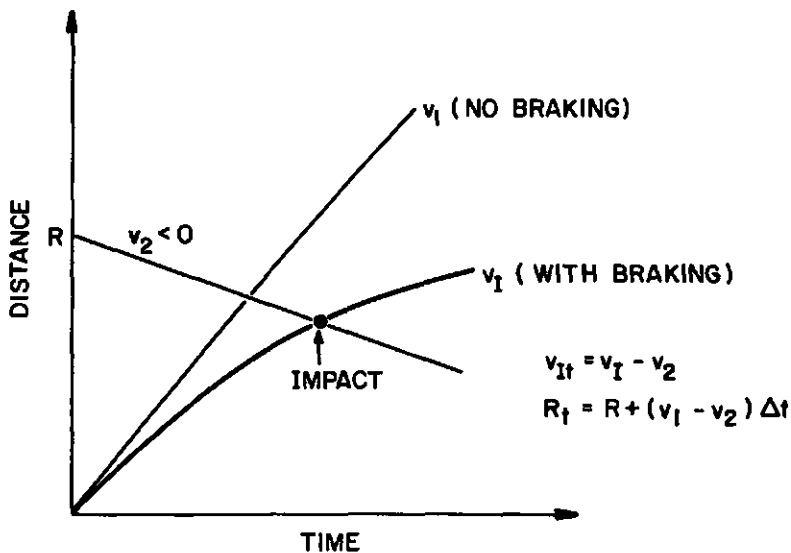


FIGURE 54. DISTANCE/TIME RELATION BETWEEN TWO VEHICLES, ONE OF WHICH IS BEING BRAKED.

The relation between impact velocity,  $v_{It}$ , and the radar detection range,  $R_t$ , can be expressed as

$$R_t = \frac{1}{2\mu g} \left\{ (v_1 - v_2)^2 - v_{It}^2 \right\} + (v_1 - v_2) \Delta t \quad (32)$$

This equation applies, of course, also for the case of impact with a fixed object by setting  $v_2 = 0$ . Since  $v_1 - v_2$  can be replaced by the measured range-rate,  $\dot{R}$ , we obtain the more general relation

$$v_{It} = \sqrt{\dot{R}^2 - (R_t - \dot{R}\Delta t) 2\mu g} \quad (33)$$

The impact velocity as a function of different radar detection ranges,  $R_t$ , and initial closing rates,  $\dot{R}$ , is shown in Figure 55. For a collision with a fixed object, for example, the impact velocity  $v_{It}$  is reduced from an initial speed of 25 m/s (55 mph) to 13.7 m/s (30 mph) if a detection distance of 30 m is maintained. This corresponds to a reduction in impact energy by 70%.

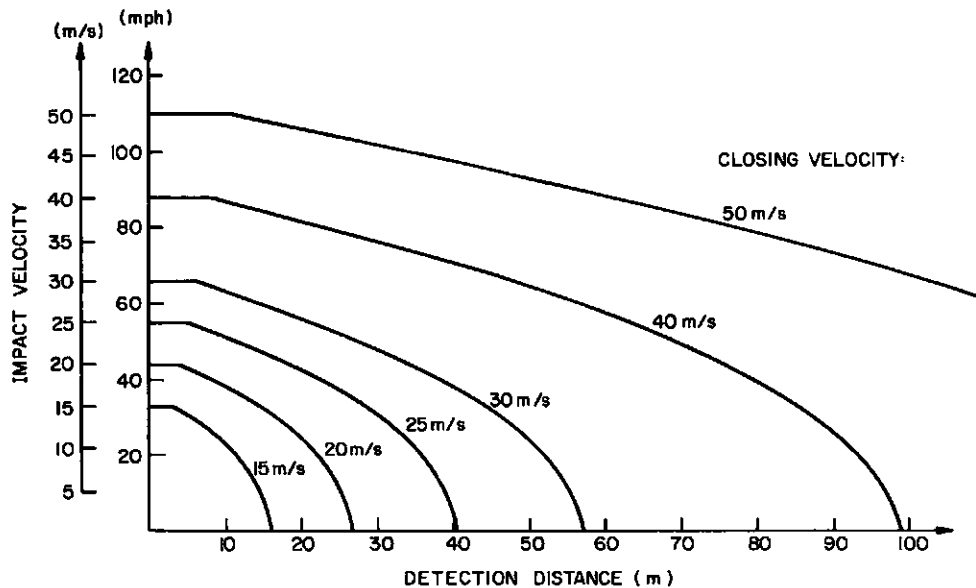


FIGURE 55. IMPACT VELOCITY AS FUNCTION OF DISTANCE BETWEEN RADAR CAR AND COLLISION OBJECT (SYSTEM DELAY 0.2 s; BRAKING COEFFICIENT  $\mu = 0.9$ ).

For head-on collisions where both vehicles are going at a speed of 25 m/s (55 mph), the impact velocity is being reduced by 8.8 m/s (17 mph), provided both cars have CMS braking with a detection range of 30 m. The impact energy

is correspondingly reduced by 30%. Here the energy reduction is not so pronounced, but still significant enough to make a substantial difference in the severity of the injury sustained by the driver. Figure 56 shows the resulting impact velocity,  $v_{It}$ , as a function of closing rate,  $\dot{R}$ , for different detection ranges. Also indicated are lines of constant energy reduction.

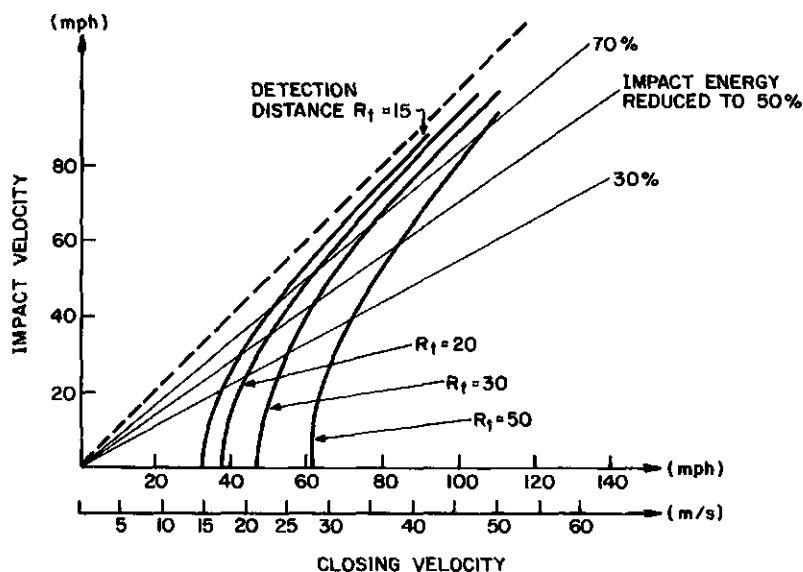


FIGURE 56. ENERGY REDUCTION AS FUNCTION OF DETECTION DISTANCE AND CLOSING RATE.

The above calculations clearly indicate the importance of having a large detection range,  $R_t$ , for the radar and a fast reaction time for the overall system. These requirements are counteracted by the need for keeping all false alarms at an absolute minimum and, equally important, for ensuring that a driver remains in control of the car as long as there is any possibility of avoiding an accident by skillful driving maneuver.

Based on a typical maximum lateral acceleration of 0.3 g (which is rarely exceeded by the average driver), a minimum distance of 32 m is required [11] to avoid an obstacle straight in line with a vehicle driven at 25 m/s (55 mph). We, therefore, selected a maximum detection distance,  $R_t$ , of 30 m for a car driven at 25 m/s. If a driver at this speed approaches an obstacle without

11. R. Limpert, Motor Vehicle Accident Reconstruction and Course Analysis, Michie Company, Charlesville, VA, December 1978.

steering wheel or brake pedal activation, the automatic antiskid braking should take over. At lower speeds, this distance should obviously be reduced further.

## B. COLLISION-MITIGATION SYSTEM

The inputs to the CMS algorithm consist of range, range-rate, steering angle  $\phi$ , brake pedal status indicator, and car velocity. The range-rate is derived directly from the beat counts during the up- and downswing of the frequency modulation cycle, and is not generated by differentiating range with time. Range-rate can, therefore, be used to independently check the validity of range data obtained at different time points.

The entire CMS algorithm (a complete program listing is included in Appendix B) is conveniently subdivided into two parts. The first part includes the acquisition of radar data, calculation of range, range-rate, car velocity, and a check of steering wheel angle and brake pedal position. The second part contains the actual decision subroutine which activates the antiskid brakes if all conditions for two sets of data separated by a time interval,  $\Delta t$ , are fulfilled. Two flags and a status bit, DF, keep track of the decisions made at various points within the algorithm.

GETRAN is the data acquisition part of the algorithm and is shown in flow chart form in Figure 57. First, the number of transitions within a measurement interval are counted. From the number of transitions within the measurement interval, we can determine the number of periods within the measured interval. If we do not have at least one period within either the upswing or downswing measurement interval, we repeat the entire measurement process. The accumulated count is read for both the upswing and downswing modulation interval. The count in each case is averaged by dividing by the number of periods within the respective measurement interval. A deviation check is performed on each period measurement of the up- and downswing. A failure of the deviation check restarts the entire measurement process. If only one period was measured on the up- and downswing of the modulation cycle because of a close target or dropouts, the periods are compared to each other and, if they exceed a set tolerance, the measurement process is restarted.

If after passing the transition counter check, deviation check, and if necessary the single period check, the data is considered acceptable, range and range-rate values are determined from a table using the up and down count

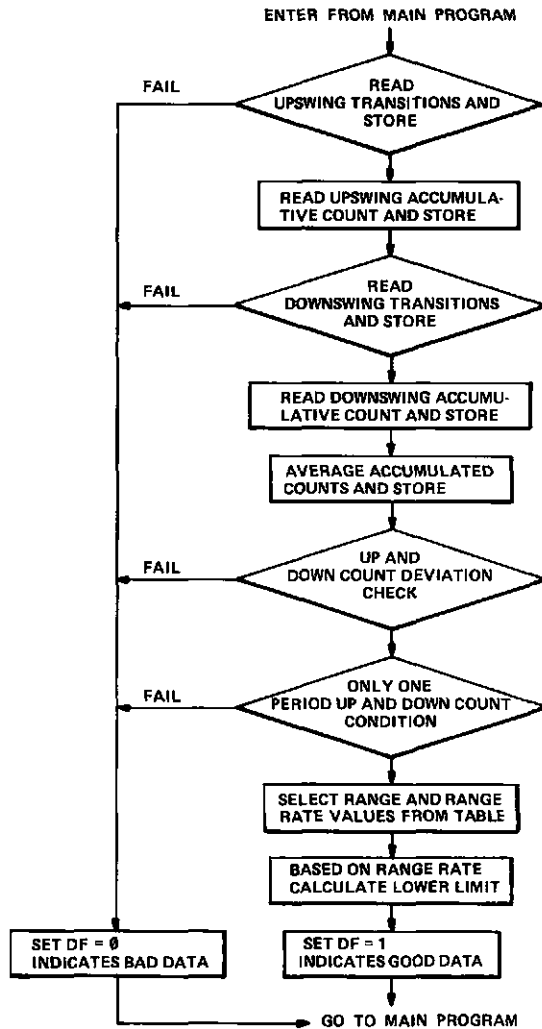


FIGURE 57. FLOW CHART OF GETRAN (DATA ACQUISITION).

readings as a parameter. A 1-bit status indication, DF, is set to indicate good data readings after a lower limit value has been calculated from range-rate data. The good data readings are either taken over a full measurement interval during the full modulation upswing and downswing or over part of a cycle, from the beginning of the interval up to the point of a dropout.

Once range and range-rate data have been computed, the primary purpose of microprocessor software is to sort out real emergency situations from false alarms. This is performed in the main CMS algorithm, shown in Figure 58. A target moving toward a radar-equipped car does not always require automatic braking, as for example in tight turns or parking maneuvers. The speed cutoff eliminates the possibility of emergency braking if the car velocity is less

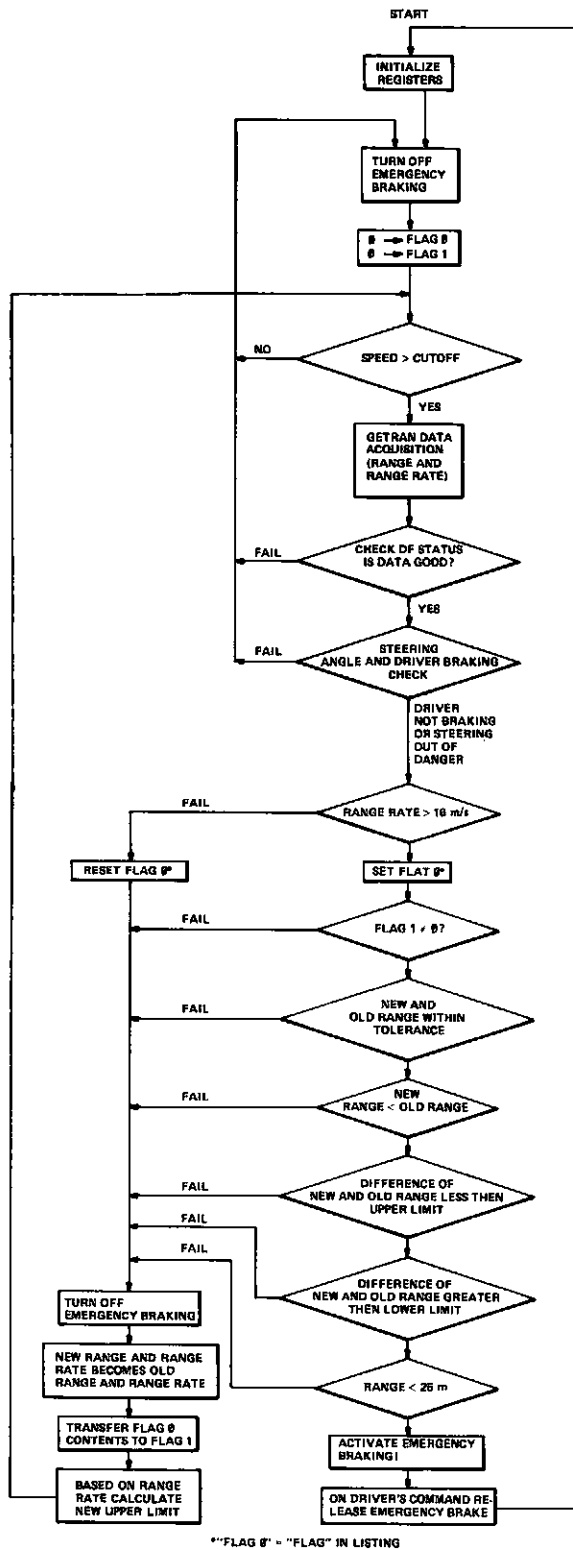


FIGURE 58. FLOW CHART OF MAIN CMS PROGRAM.

than 10 m/s. The velocity cutoff computation is done in the electronic dashboard display software. If the cutoff velocity is exceeded, a flag is set by the dashboard display microcomputer and is read by the CMS algorithm. An indication of bad data acquired by GETRAN is signaled by the status bit DF = 0 and the software restarts the overall measurement process. An indication that a driver is taking action by steering or braking also causes the software to begin again.

If we have reached a point where the vehicle is operating above a set speed and has acquired a target and there is no reaction in the form of braking or steering by the driver, further analysis is then made of the potential threat. If the closing rate between the target and the radar-equipped RSV is less than 16 m/s, the target is not considered a severe threat, emergency braking is prohibited, and the range and range-rate data are stored as a reference. Based on range-rate a new value of range difference is calculated for an upper limit, which is later used in the algorithm. In case the driver is not reacting and the closing rate or range-rate is greater than 16 m/s, a flag is set. Another flag (called flag 1) is checked to see whether this is the first or second test of acquired data. If flag 1 is 0, which corresponds to the first test of acquired data, the range and range-rate data are stored as a reference or "old data" and a new upper limit is computed. The contents of flag 0 which has been set previously are then transferred to flag 1.

Now the process starts again; once data is acquired a second time, the set speed is exceeded, and there is no reaction by the driver, and the closing rate is above 16 m/s, additional checks are performed by software to verify the presence of a real target. Checks are also made to determine if the difference between the newly acquired range-rate and the old range-rate is within a certain tolerance. The newly acquired range must be less than the first range reading. The difference between the new range reading and the previous one must fall between a lower and upper limit value that is a function of range-rate. Finally, the range measured has to be less than the cutoff range of 25 m. Only if all of these conditions are met is the emergency braking activated.

The automatic activation of the antiskid brakes will be disabled if the driver takes over the braking maneuver. This is considered an indication that the driver is in control. Also, if any of the conditions for range comparison are rejected, automatic emergency braking is prohibited. The newly acquired data then becomes the reference or old data, and a new value is calculated for

the range difference upper limit. A target threat is still considered because a flag is set to indicate the successful acquisition of one set of data. Another consecutive set of data is therefore needed which, if it passes all of the test conditions, will enable the automatic emergency braking condition that applies the antiskid brakes.

The computation and decision making time for the CMS algorithm during Phase II was approximately 160 ms. For the new CMS algorithm, which includes more sophisticated decision making, this time is only approximately 80 ms. The reduction in software processing time can be attributed to two reasons. First, the new RCA CDP 1802 microprocessor has a larger instruction set than the 1801 unit used during Phase II. Secondly, the software is greatly improved together with the use of look-up tables and faster multiplying chips.

### C. HEADWAY/CRUISE CONTROL

#### 1. Introduction

A car equipped with a collision-mitigation system has limited sales appeal because under normal conditions, a driver would be totally unaware of the system's presence. As discussed before, emergency braking is to take place only when a severe collision is unavoidable, and a good driver should, hopefully, never find it activated. Public acceptance of the radar could be greatly increased if it were also to provide improvements in convenience and traffic flow. Automatic headway control that governs the safe spacing of successive cars on limited-access highways is such an application.

The difference between regular cruise control and radar headway control is illustrated in Figure 59. In the normal cruise control, a fairly popular option in American cars, the driver can select a particular cruising speed,  $v_{set}$ , and the car will maintain this speed ( $v_1 = v_{set}$ ) until a new speed is set or the brake pedal is tapped. This convenience feature is, unfortunately, not very useful when traffic density increases. Cars ahead, going at only slightly lower speeds, force the temporary disablement of the cruise control or lead to rather dangerous weaving in and out of traffic lanes to avoid having to reset the cruise control.

Under radar headway control, the radar senses the distance and closing rate with respect to the vehicle ahead and controls the throttle to match the speed of the first car ( $v_2 = v_1$ ) and keep a safe headway. If there is no other vehicle ahead, cruise control takes over and the car resumes the preset speed. In the present implementation, only the throttle is interfaced with the radar;

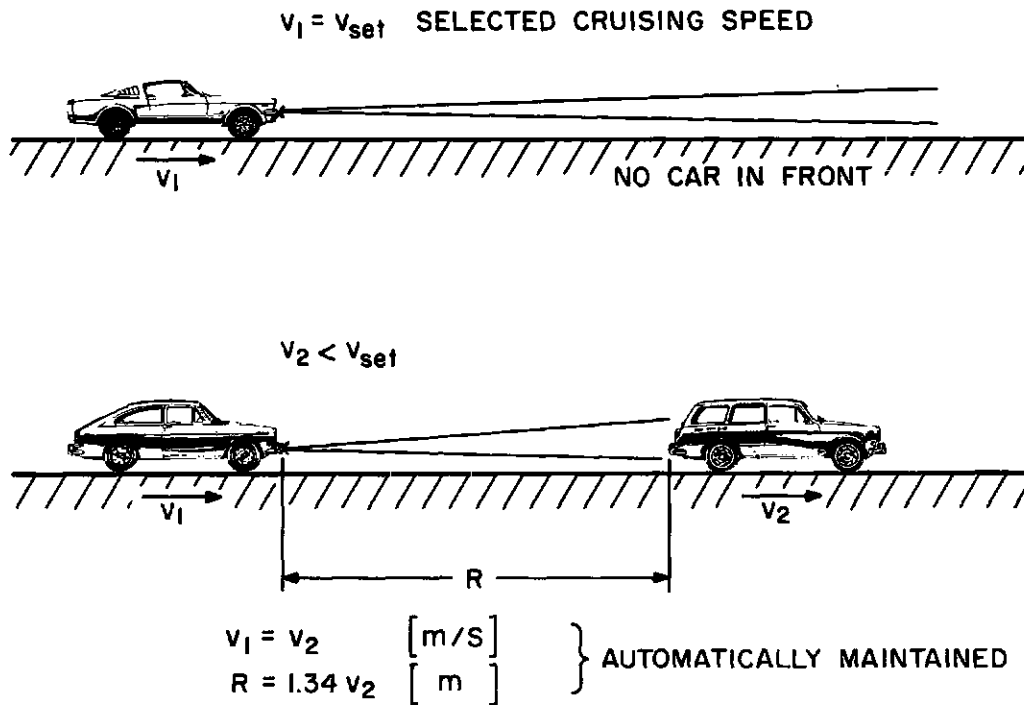


FIGURE 59. COMPARISON BETWEEN CRUISE CONTROL AND RADAR HEADWAY CONTROL.

if the closing rate becomes too high, a warning signal is given on the electronic display and the driver has to take over.

## 2. Design Considerations

A block diagram of RCA's headway-control system is shown in Figure 60. The driver makes his inputs through switches located on the turn signal stalk. An RCA 1802 based microcomputer monitors ground speed and interprets signals from the radar. Throttle control signals are computed and delivered in the form of variable width pulses to a linear DC motor which is connected to the car's throttle by a chain. The computer has control of the full travel of the throttle, but cannot at present initiate brake activation. Limited deceleration due to air friction and engine drag is achieved when the throttle is fully released. When more rapid deceleration is required the driver must intervene by personally applying the brakes. Whenever the computer senses driver application of the brakes, it responds by fully releasing the throttle and relinquishing control back to the driver until instructed by the driver to resume control.

For diagnostic and demonstration purposes we have interfaced a Burroughs\* self-scan single-line display to the computer. Although it is not required for

\*Burroughs Corp., Plainfield, NJ.

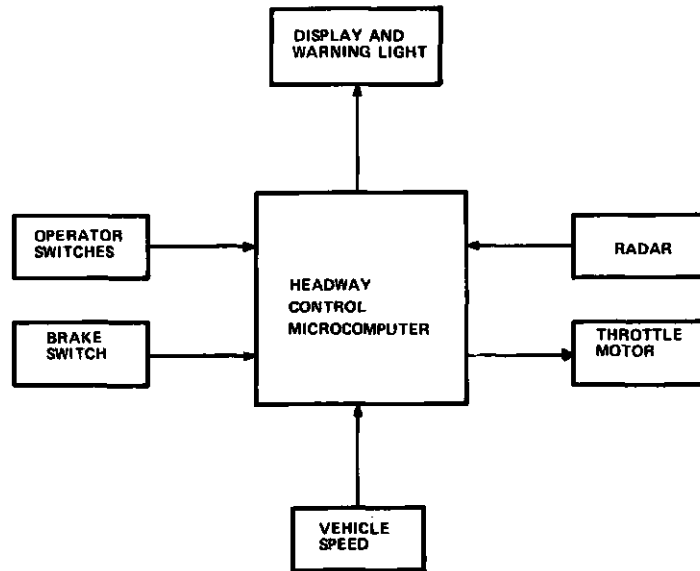


FIGURE 60. BLOCK DIAGRAM OF HEADWAY-CONTROL SYSTEM.

operation of the system, the display is useful for indicating radar-measured range, range-rate, vehicle speed, and other system state information. A yellow warning light on the display is turned on when the closing rate is too high (over 3 m/s) or the following distance is dangerously close (less than 10 m).

Control for the throttle is implemented entirely within microprocessor software as a sequence of discrete-time computations. A diagrammatic representation of these computations is shown in Figure 61. Computed expressions are shown by their z transform equivalents, while events external to the computer are shown as continuous time LaPlace transforms. The fundamental inputs to the computer are range,  $R$ , and velocity,  $v$ . Range-rate,  $\dot{R}$ , is computed as

$$\dot{R} = \frac{R_1 - R_0}{t_s} \quad (34)$$

where  $R_1$  is present range,  $R_0$  is previous range, and  $t_s$  is the sampling time of 0.5 s.

There is some inherent "noise" in range data in headway control because the radar beam looks at different positions on the irregular surface of the target car. Road bounce of the radar and target aggravate the noise. There is also quantization noise of range due to the way the radar signal is processed and to the finite precision of the microprocessor computations. Range measurements are quantized in steps of 5 cm. Velocity is quantized in steps of 0.1 m/s. Input noise is propagated to the throttle control causing annoying jerky motions which can be sensed by passengers.

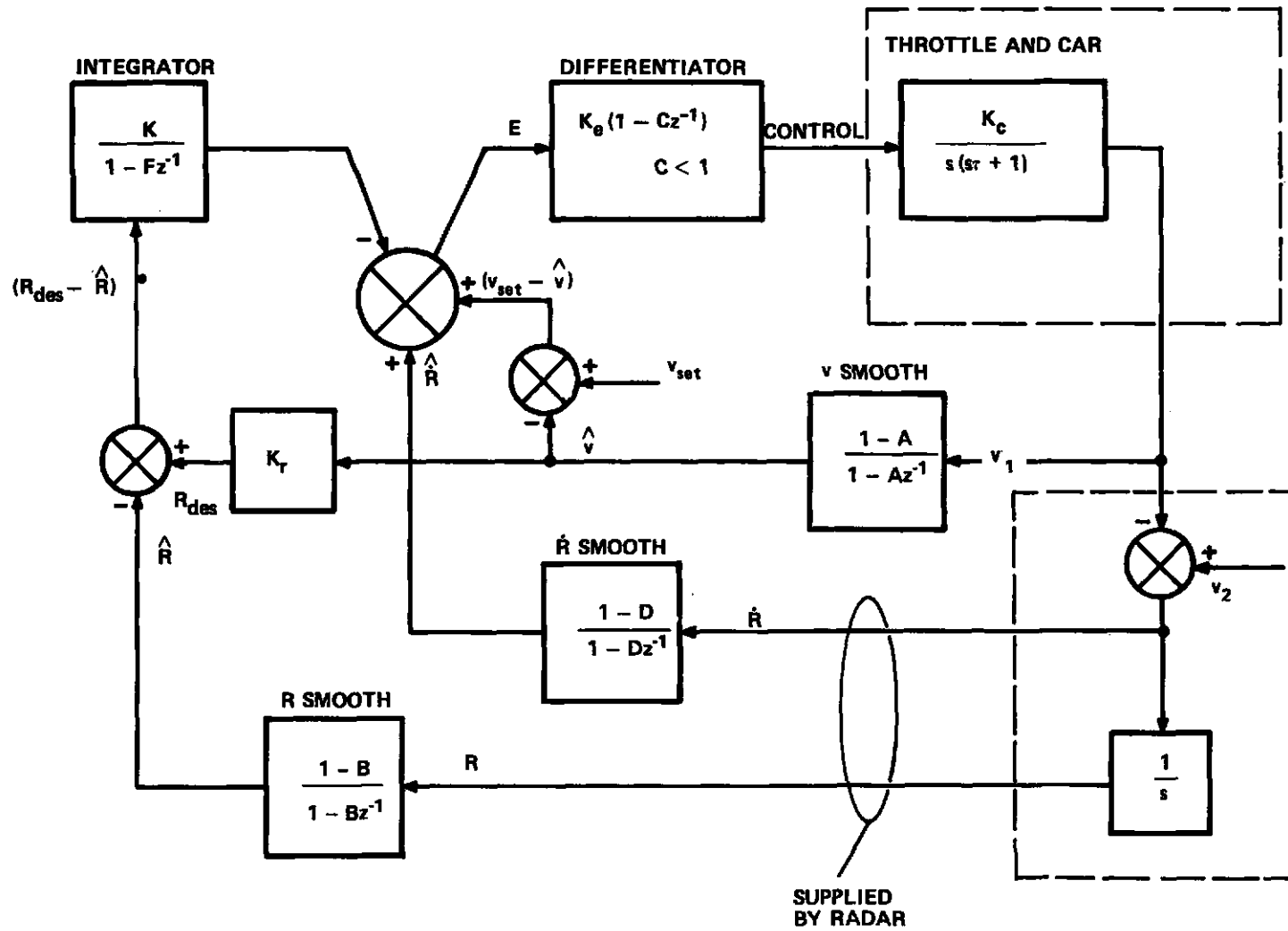


FIGURE 61. AUTOMATIC CRUISE/HEADWAY-CONTROL ALGORITHM.

In an effort to reduce the effects of noise, smoothing functions are used on  $R$ ,  $\dot{R}$ , and  $v$  to generate  $\hat{R}$ ,  $\hat{\dot{R}}$ , and  $\hat{v}$ . Heavy smoothing provides the quietest outputs, but there is a decline in responsiveness as smoothing is increased. Since  $\dot{R}$  is a time derivation of range it is potentially quite noisy and therefore has heavy smoothing. Care must be taken in choosing the  $\dot{R}$  smoothing constant  $D$  so that sudden changes in closing rate are reflected quickly enough in  $\dot{R}$ .

The desired headway distance is computed as

$$R_{\text{des}} = K_r v \quad (35)$$

This headway distance increases linearly with road speed. Constant  $K_r$  is presently 1.5 m per m/s; for example, the desired distance at 25 m/s (55 mph) is 38 m. The difference between  $R_{\text{des}}$  and  $\hat{R}$  constitutes a range error which we attempt to minimize. Similarly, the difference between  $v_{\text{set}}$ , the cruise control set speed, and  $v$  constitutes a velocity error which is minimized in a conventional cruise control. Referring again to Figure 61 we see that velocity difference between the two vehicle,  $\hat{R}$ , and a term representing an integrated range error are fed into the main summing junction to produce error  $E$ . This error is compensated by a differentiating expression  $K_e (1-Cz^{-1})$ ,  $C < 1$ , to generate throttle control. The feedback compensation is designed to force  $E$  toward zero at all times.

In general, increasing  $E$  will produce more throttle acceleration and decreasing  $E$  will cause throttle release. If the radar car is moving at less than  $v_{\text{set}}$ , a positive velocity error is present at the summing junction. The range error integrator permits the velocity error to be canceled out at the junction, even as the range error is reduced toward zero. In the present system we were so far not able to implement a perfect integrator ( $F = 0.9$  instead of 1.0 is being used) because of some instability problems. The remaining residual error has the same polarity as the velocity error and has a magnitude of about 1.45 m for each 1 m/s of velocity error.

The residual error results in a headway distance which is smaller than desired, an effect that becomes more pronounced when the set cruising speed is much higher than the actual speed. We believe that this deficiency can definitely be eliminated by properly adjusting the integrator term. However, since any changes also affect other constants of the loop, work priorities and available time restrictions did not permit us to fully optimize these

counter dependent system parameters. In practice, the deviation from the correct headway distance does otherwise not affect the proper operation of the headway control.

As indicated earlier the control output is in the form of a signed number which is converted by digital circuitry to a pulse, the width of which is proportional to the magnitude of the number. The throttle motor is turned on for the duration of the pulse. Thus the microcomputer generates relative position control for the throttle, rather than absolute or direct positioning. For this reason the throttle is modeled as an integral controller (1/s). The car has a response time  $\tau$ , and the combination of throttle and car are modeled in the diagram as  $K_c/[s(s\tau+1)]$ .

In an ordinary driving situation the radar is constantly acquiring targets and losing them again as they go out of range. At any instant the system can be considered to be in any of the five states, as shown in Figure 62. In addition to "Cruise" and "Resume" found in conventional cruise controls, we also have "Headway," "Capture," and "Lost Targets." The arrows in the diagram show permitted state transitions. "Resume" permits the car to go from present speed to previous set speed after "Cruise" has been disengaged by the brake. "Resume" is implemented as a special form of "Cruise" in which the reference speed to be obtained is gradually raised from present speed to set speed at the rate of 3.3 m/s per second. Thus if set speed were 25 m/s and "Resume" is engaged at

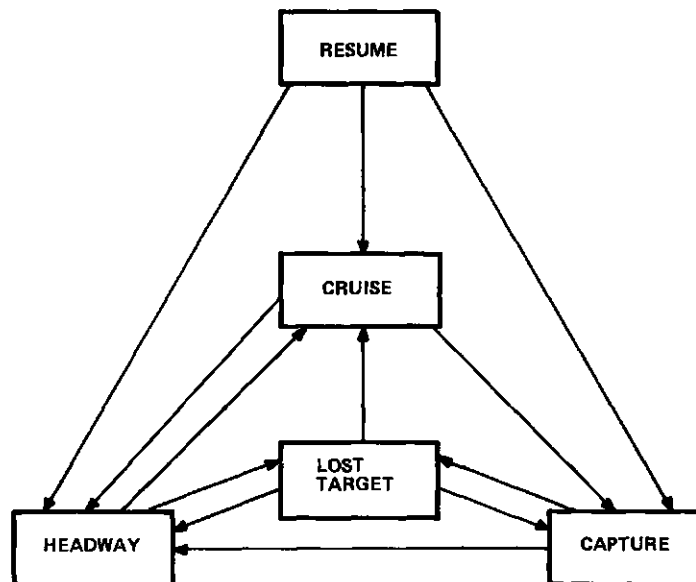


FIGURE 62. STATE TRANSITION DIAGRAM.

15 m/s, the resume state will last approximately 3 seconds. Without a "Resume" state, the car would accelerate very rapidly and overshoot the set speed considerably.

When a target is acquired the system will go from "Resume" or "Cruise" to "Headway" or "Capture." "Capture" is intended as a transition state from "Cruise" to "Headway." "Capture" is implemented as the opposite of "Resume" with "Cruise" reference speed reduced from set speed at the rate of 1.8 m/s. Figure 63 shows how "Capture" begins at range  $R_D$  and terminates when range is  $1.1 R_{des}$ . "Capture" range is computed as

$$R_D = K \dot{R}^2 + R_{des} + 3 \text{ m} \quad (36)$$

Increasing the closing rate increases  $R_D$ , lengthening the capture distance. If a target is acquired at a range of less than  $1.1 R_{des}$ , or if the closing rate is very low, the "Capture" state is bypassed and we go directly to "Headway."

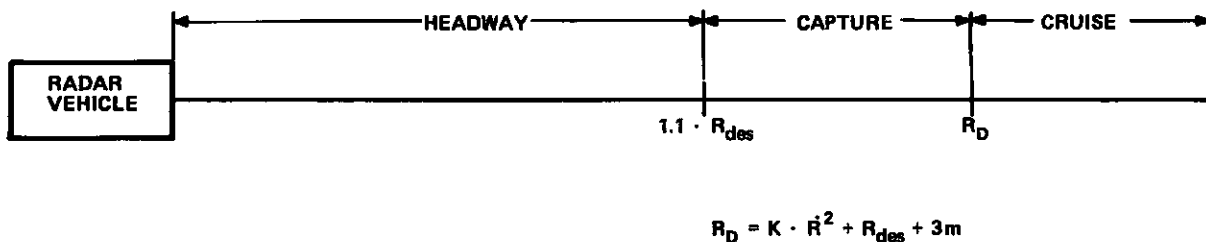


FIGURE 63. CAPTURE MODE.

The "Lost Target" state is needed because a target may appear to drop out occasionally, due to signal multipath or multiple target detection. It is undesirable to return immediately to "Cruise" because of a momentary signal loss. In the "Lost Target" state, the throttle is held steady for up to 1.5 seconds while the radar tries to reacquire the target. If at the end of this time there is still no target, the system transits from "Lost Target" to "Cruise."

The important transition rules are summarized below:

- (1) From "Resume" or "Cruise" to "Capture" -- Target is acquired and  $1.1 \cdot R_{des} < \hat{R} < R_D$
- (2) From "Resume" or "Cruise" to "Headway" -- Target is acquired and  $\hat{R} < R_D$  and  $R < 1.1 \cdot R_{des}$

- (3) From "Capture" to "Headway" --  $\hat{R} < 1.1 \cdot R_{des}$   
 (4) From "Headway" to "Cruise" --  $(v - 1.4 \text{ m/s}) > v_{set}$  or  $\hat{R} > 2.3 \text{ m/s}$

Rule 4 inhibits the target car from "towing" the radar car.

### 3. Algorithm Flow Diagram

The headway-control software is written in RCA Level II Assembly language and is stored in 3K bytes of EPROM. It consists of an interrupt service routine which executes whenever the driver presses a switch or the timer interrupts, and a main program loop, which runs continuously. The interrupt service routine has the following functions:

When a switch is pressed on the driver's stalk, a status bit is set in a microprocessor register, provided the current velocity is above 9 m/s (20 mph). The main program later tests this status bit to determine if the switch has been pressed. For the SET SPEED or SET 55 switches, the interrupt routine will store  $v_{set}$  as present speed or 55 mph (90 km/h), respectively. When the foot brake is depressed, the interrupt routine will release the throttle completely, giving the fastest possible response. When the timer interrupts, the velocity sensor is read and  $v$  is computed. In addition, timer status is used to synchronize the main program so that range measurements are taken at precise intervals.

The main program loop is shown in flowchart form in Figure 64. A description of the basic algorithm using block numbers from the flow chart is given below.

- I Initialize microprocessor registers and memory locations.
- II Release throttle completely (normally not engaged) and erase start-up message from display. This step requires about 2 seconds.
- III Wait for driver to press SET SPEED or SET 55.
- IV Loop synchronization. Wait for timer interrupt indication. Time interrupt occurs every 0.5 second.
- V Input data from radar card. Determine validity of data using deviation check.
- VI, VII If data valid, compute range,  $R$ .
- VII-X If target has been lost for 1.5 seconds, leave headway state; otherwise hold throttle.

- XI-XIII Warning light management. If  $R < 10$  m or there are two consecutive measurements with  $R < -3$  m/s, warning light is turned on; otherwise it is turned off.
- XIV-XVI If this is first valid range measurement, variables must be initialized. Two consecutive valid range measurements are required to compute radar control.
- XVII Compute smoothed range, range-rate, smoothed range-rate, and summing junction error.
- XVII-XXI If not in HEADWAY state, transition rules are used to see if we should go to CAPTURE.
- XXI If in CAPTURE state, capture processing is done.
- XXIII If  $\hat{v} > v_{set}$  or  $\hat{R} > 2.3$  m/s transition to RESUME or NORMAL is made.
- XXIV Control is computed using headway control compensation equation.
- XXV-XXVIII If RESUME switch has been pressed, do RESUME state processing until  $v_{ref} > v_{set}$ ; otherwise  $v_{ref} = v_{set}$ .
- XXIX Control is computed using normal cruise compensation equations.
- XXX-XXXII If brake has been pressed, we want to avoid sending further control outputs to the throttle since it has been disengaged by the interrupt service routine. Wait until driver releases brake and presses a switch before continuing.
- XXXIII Control is sent to the throttle pulsing circuitry.
- XXXIV Self-scan display is formatted according to current state. This is not essential to system operation.

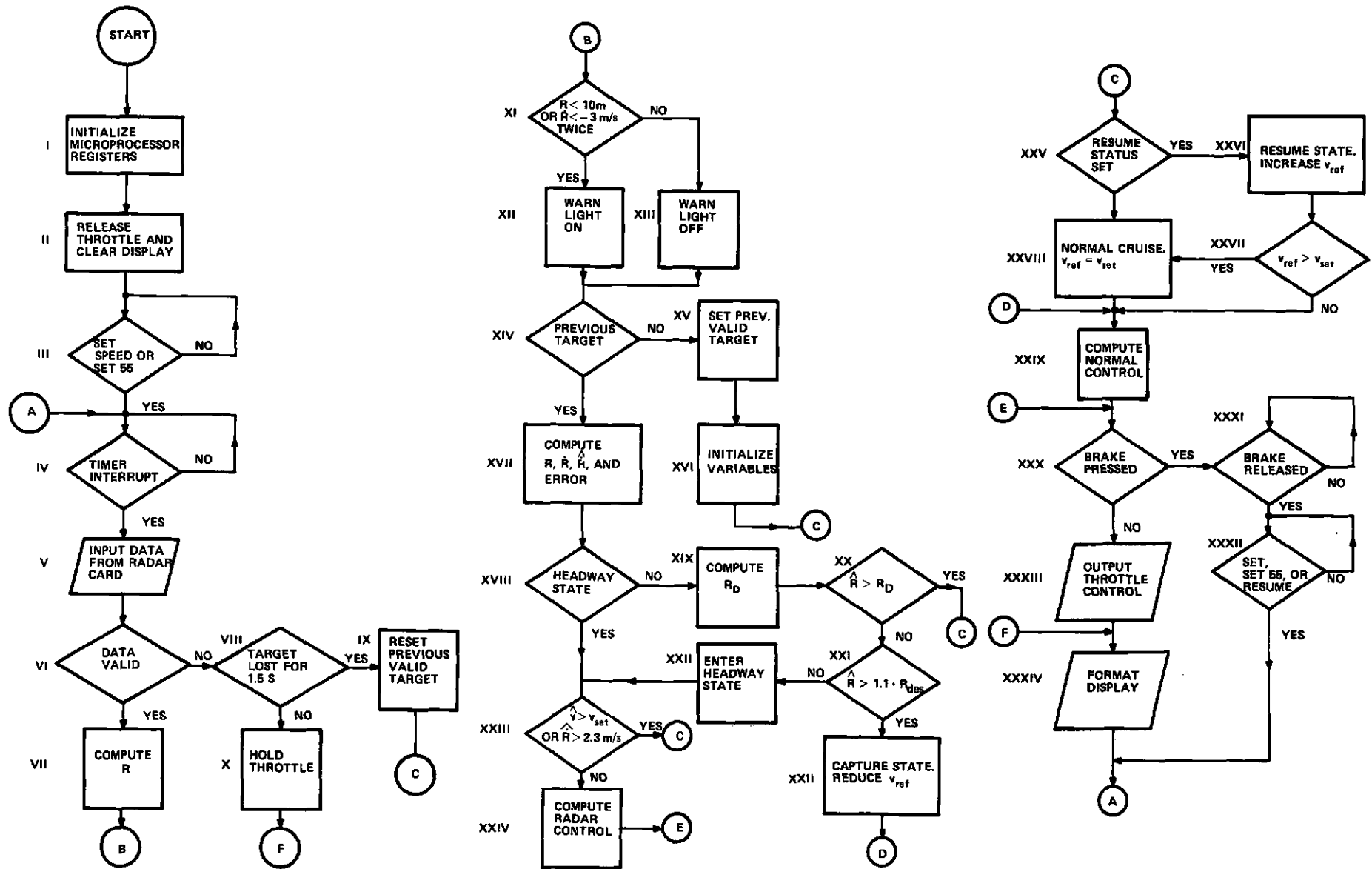


FIGURE 64. HEADWAY-CONTROL FLOW CHART.

SECTION VI  
PERFORMANCE TESTS

A. TEST VAN INSTRUMENTATION

A special test vehicle was equipped to permit the recording of radar and video data for optimization of the radar hardware and software. Aside from providing a test platform for the radar, the vehicle is also fully instrumented with recording equipment and other test gear for evaluating the performance of various components of the radar system. A Ford "Econoline" van, shown in Figure 65 houses all of the test equipment and acts as a mobile laboratory. The front of the van is fitted with a support structure that accommodates different antenna configurations. Figure 65 also shows the Ku-band bistatic system radar without radome assembly mounted on the van. The metal plate underneath the radar antenna assembly is covered with an RF absorber material and shaped to simulate the front of the RSV. By use of the absorber material and metal plate, the near-field effects of the nose assembly of the RSV were studied as a function of the positioning of the absorber material relative to the plate and antenna.

The interior of the van is fitted with instrument benches and a seat for the equipment operator. Figure 66 shows the video camera in front and the radar recorder in back of the van with its supporting equipment. The camera is fitted with a wide-angle lens to give a panoramic view of road conditions. It is mounted next to the driver, strapped down on the motor housing. A view of the scene presented to the camera through the windshield is shown in Figure 67.

In addition to the camera, the test van is also equipped with a velocity sensor and steering wheel indicator. The velocity sensor is a generator-type unit attached to the speedometer cable whose output is a frequency directly proportional to velocity. The steering wheel sensor is a potentiometer attached to the front wheel linkage. The resistance of the potentiometer is part of an R-C network of an astable multivibrator whose frequency therefore varies as a function of steering wheel angle. Information from the three sensors, camera, steering wheel, and velocity sensor is recorded by the Panasonic\* video tape recorder.

\*Panasonic Co., Secaucus, NJ.



FIGURE 65. TEST VAN FOR RECORDING OF VIDEO AND RADAR INFORMATION.

A block diagram of power sources for instrumentation and environmental control is shown in Figure 68. AC power for the instrumentation, especially the video equipment, is provided by a Deltec\* static inverter. This unit provides a sinusoidal output of 110 VAC at 60 Hz  $\pm 0.15\%$ . The inverter has a power capacity of 1.2 kW. The power input to the inverter is provided by an additional heavy duty 135-A Leece-Neville\*\* alternator with a 250-A/hour battery backup. The AC power for the environmental control and the less frequency-sensitive instruments is provided by a 4-kW Onan<sup>†</sup> motor generator mounted in a separate compartment at the rear of the vehicle. The environmental control for the mobile lab is provided by an Intertherm<sup>††</sup> RV roof-mount airconditioner. The unit provides 12,600 BTUH of cooling and 5400 BTUH

\*Deltec Corp., San Diego, CA.

\*\*Sheller Globe Corp., Leece Neville Div., Cleveland, OH.

†Onan, Huntsville, AL.

††Intertherm, St. Louis, MO.

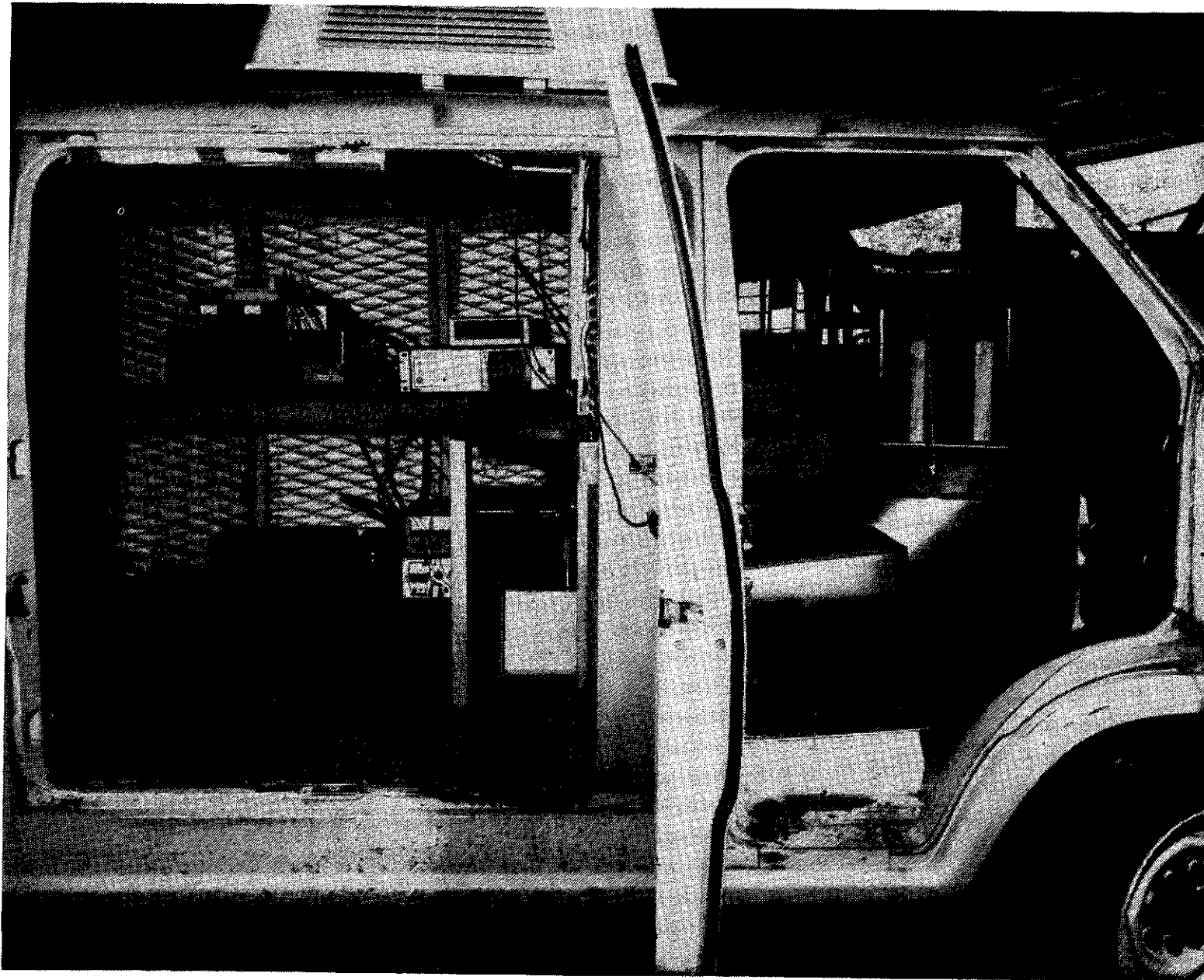


FIGURE 66. INTERIOR OF TEST VAN.

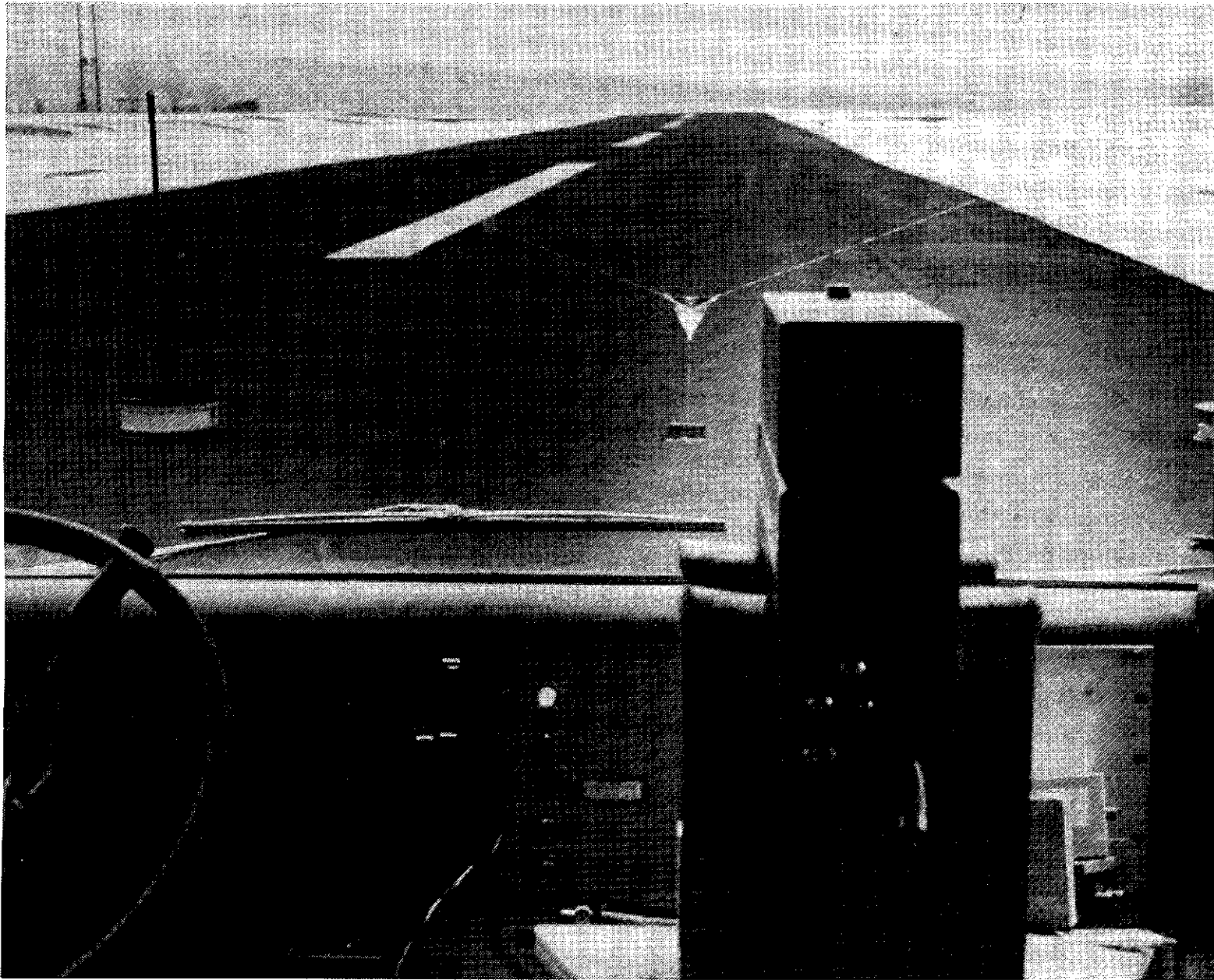


FIGURE 67. VIEW FROM TEST VAN DURING CMS TESTS ON AIRPORT RUNWAY.

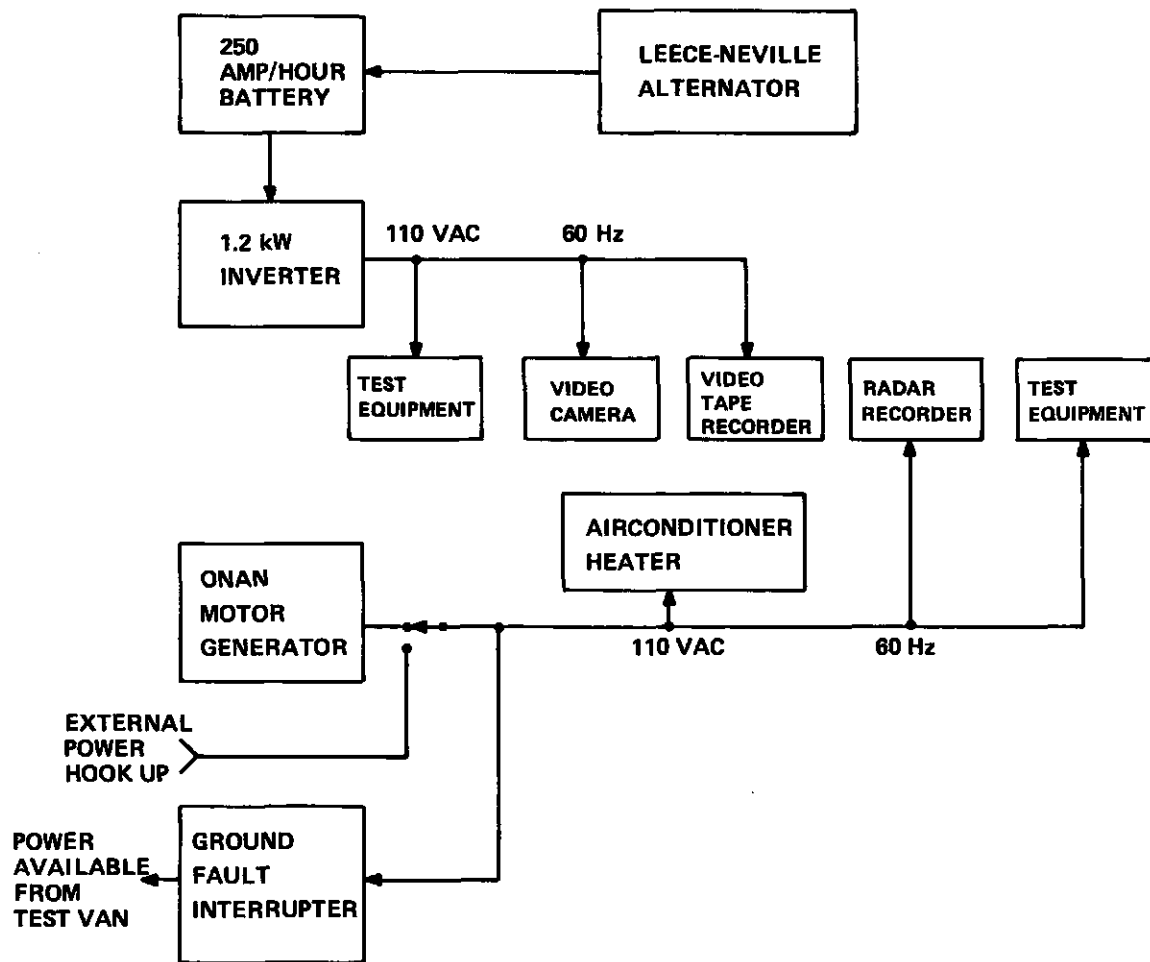


FIGURE 68. BLOCK DIAGRAM OF POWER DISTRIBUTION IN TEST VAN.

of heat. The Intertherm unit has been rewired to operate in a bucking mode to alternately heat and cool so that a relative humidity of 40% maximum could be maintained. The low humidity is necessary for the tape used with the recorders. A switching arrangement is available to power all equipment in the van from an external AC line voltage. In the field, AC voltage is available from the van through a ground fault interrupter protected circuit.

The test van has proved itself extremely valuable in the testing of all X- and Ku-band monostatic and bistatic radar systems. It was also used in simulated crash tests with disposable 1- and 10-m<sup>2</sup> targets at various speeds, on a runway at a nearby airport, as shown in Figure 69. The most extensive use of the vehicle was for recording radar returns and video representations



FIGURE 69. TEST VAN DURING CMS TEST WITH EXPENDABLE TARGET.

of actual traffic situations. These radar recordings, which were used for the optimization of the CMS algorithm, were performed during different weather conditions and with a variety of road and traffic scenarios.

#### B. COLLISION-MITIGATION SYSTEM TESTS

One of the problems encountered during Phase II was the testing and evaluation of hard- and software for the mitigation system. Rather than repeatedly drive a fixed route and possibly tailor a system to operate only for that peculiar case, we found that a better, more true-to-life approach is to drive as much as possible in many different scenarios. However, following the random driving procedure still made system evaluation subjective. For example, an event that occurred in a particular location on a road with a particular traffic pattern and under unique weather conditions might cause a false alarm during testing. Corrective software and/or hardware changes would therefore be made to the system. Returning to the same location where the original false alarm occurred would possibly indicate that we no longer receive a false alarm. The question is, have we really accomplished anything? The answer can only be perhaps. Returning to the same location only partially ensures a repeat of road condition. The traffic pattern and weather condition during the initial test that may have given a false alarm can not easily be repeated.

During Phase III, we resorted, therefore, to a more rigorous approach for testing and algorithm optimization. A system was developed that recorded both the beat frequency return from the radar and the video information from the scene that the radar was illuminating. In addition to the radar and video recording, the audio track of the video recorder was used to read both speed and steering information. By use of this recording system a tape library of a variety of traffic situations was acquired. Playback of the recording system through the microprocessor would thus give perfect repetition of events. Hard- and software changes could be made and the effect of these changes could reproducibly be observed when the tapes were played back.

A block diagram of the recording system is shown in Figure 70. The video output from the camera, trace (a) of Figure 70, shows the video format. The camera generates horizontal sync pulses every 63  $\mu$ s. Between the 10- $\mu$ s-long sync pulses, the video information is contained which represents a single line (horizontal) on a video monitor. The video system uses random interlace which means a vertical sync pulse moves through the horizontal sync pulse every 1/16 of a second. The horizontal line frequency of the camera was chosen as the system clock.

The video output from the camera feeds into a video tape recorder (VTR), a switch, and a sync stripper circuit. The sync stripper circuit picks up the sync pulses from the video. To eliminate the effect of the vertical sync pulse moving through the horizontal sync pulses, the horizontal sync pulses are fed to a digital phase lock loop (DPLL) which operates at the horizontal line frequency. The output of the DPLL is divided down to give 977 Hz, which corresponds to the repetition frequency of the radar modulation. To further smooth the square wave generated from the horizontal line frequency, the divided-down signal is fed to a DPLL operating at 977 Hz. The output of this circuit, a 977-Hz square wave, goes to three locations. First, the 977-Hz square wave is used to generate the triangular wave to modulate the radar system TEO. The 977-Hz square wave is also used to provide external sync for a radar recorder, thereby electrically synchronizing the video and radar recorder, and finally the 977-Hz square wave goes to the sync pulse generator and combining circuit. The positive and negative transitions of the square wave trigger one-shot circuits.

The relationships between the sync pulse generator and the incoming square wave are shown in diagrams (b) and (c) of Figure 70. The wider sync pulse

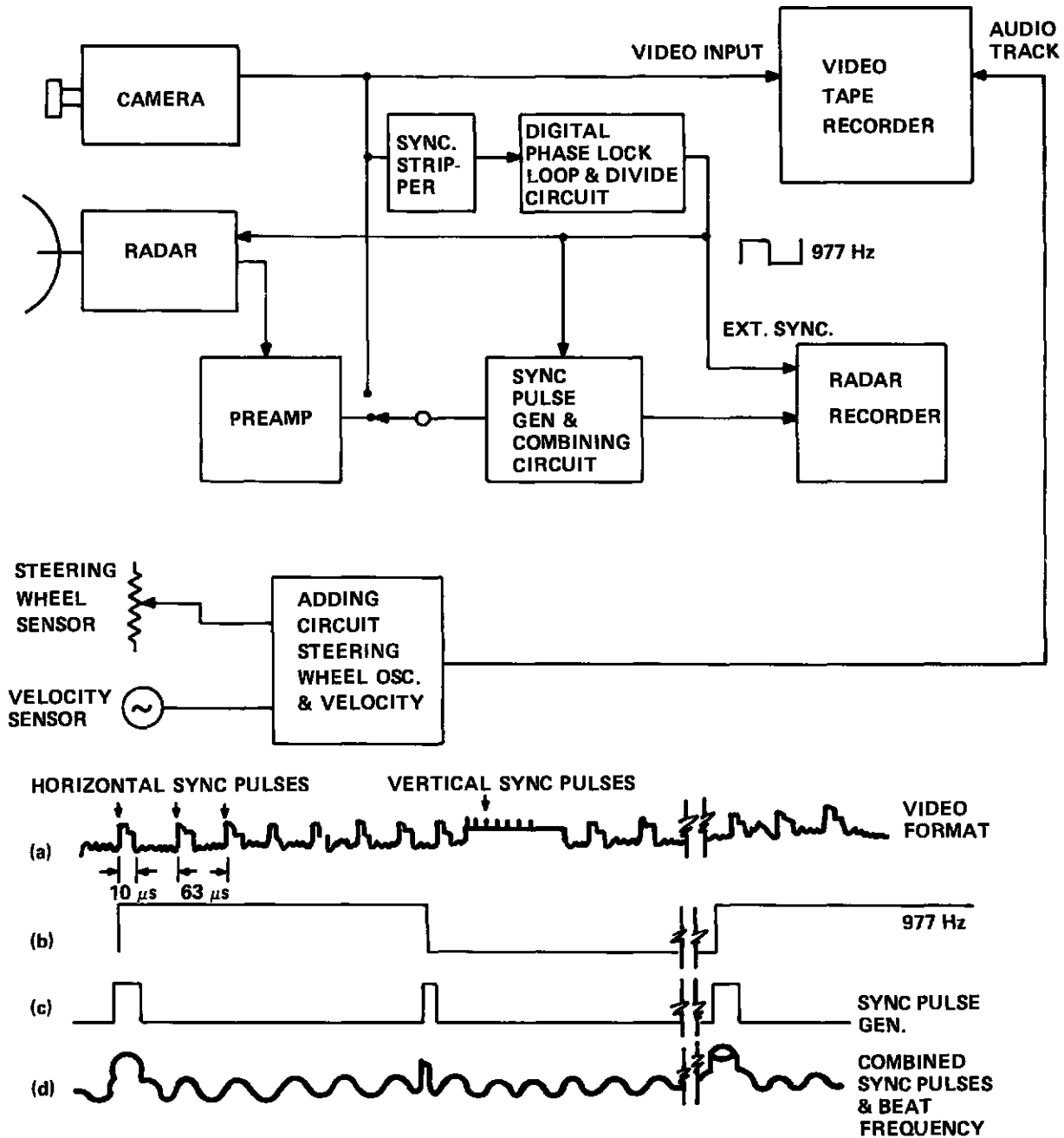


FIGURE 70. BLOCK DIAGRAM AND WAVEFORMS OF RECORDING SYSTEM.

corresponds to the positive transient of the square wave. The sync pulses generated from the square wave are combined with the beat frequency return from the radar preamplifier and recorded. The reason for the simultaneous recording of the sync pulse and the beat frequency is to maintain the proper phase relationship between the beat frequency waveform and the square wave that is used to modulate the TEO.

Two additional sensors on the test van are used to record velocity and steering angle. The pulse train from the steering-wheel angle sensor and the velocity information are combined and both recorded on the audio track of the VTR. The recording system therefore records the beat frequency return from the radar postamplifier in correct phase relationship with respect to the modulating square wave.

The video tape recorder used with the system is a Panasonic NV-5120, a standard consumer type cartridge unit with a recording time of 30 minutes. The radar recorder is a flight test "Star" manufactured by RCA in Camden, NJ for military use. This unit has a 3-MHz bandwidth (modified) and is capable of being synched to an external source (977-Hz square wave). The "Star" recorder uses standard video tape and can record about 20 minutes.

The block diagram of the playback system is shown in Figure 71. The output of the VTR is fed to the TV monitor. The video recorded on the tape recorder is also passed on to a sync stripper circuit and DPLL divider circuit that generates a 977-Hz square wave from the horizontal line frequency of the recorded video. The 977-Hz square wave is used to externally sync the radar recorder. The output from the radar recorder goes to another sync stripper circuit which strips off the pulses corresponding to the transitions of the original waveform. The output of this circuit goes to two locations. The first location is a DPLL and square-wave reconstruction circuit which restores the original modulating square wave. A switch is used to determine the positive transition by referring to the wider sync pulse that had been recorded. The second location that receives the stripped sync pulse is a sync canceling circuit. Another input to this particular circuit is the beat frequency which includes the sync pulses from the radar recorder. The sync canceling circuit subtracts the stripped sync pulse from the beat frequency, which then goes through a radar postamplifier to the microprocessor.

The audio track of the VTR is separated by filtering, and velocity information and speed information are fed separately to the microprocessor. The microprocessor thus receives the beat frequency input, a 977-Hz square wave, and the sensor inputs. The microprocessor response is indicated by a self-scan unit or by reading out memory locations from the evaluation board using an execuport terminal. A photograph of the system set up in the playback mode is shown in Figure 72. At the left is the "Star" recorder; next to the "Star" recorder is the Panasonic recorder. The monitors and self-scan display are visible in the photograph as well.

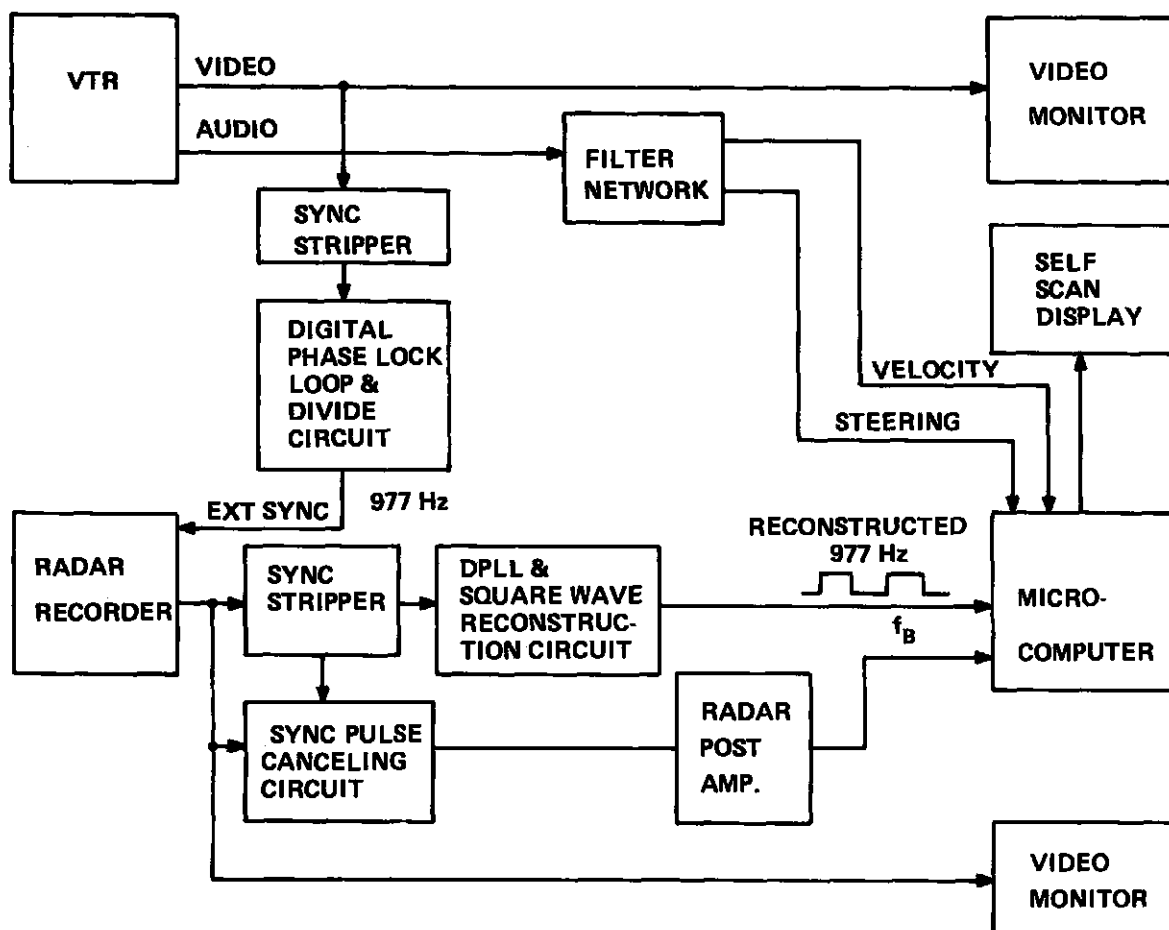


FIGURE 71. BLOCK DIAGRAM OF PLAYBACK SYSTEM.

The purpose for using two video monitors is to synchronize the data recorded by both recorders. The two recorders are always electrically synchronized, but only in multiples of the sync pulses. To sync the two recorders in time, video information is simultaneously recorded on both recorders for a short period of time. During playback, the video recorder is started first, advanced to an easily identifiable scene, and frozen. (The Panasonic VTR has stop-action capability.) The radar recorder then is started and when the video scenes of both monitors match, the Panasonic unit is restarted and both recorders are in time synchronization.

With the recording system loaded in the test van, a large variety of scenarios were taped. Several runs were made on Route 1, a four-lane divided highway with moderate-to-heavy traffic. These runs were made with both the X-band and Ku-band bistatic radar systems. Two tapes were made during light

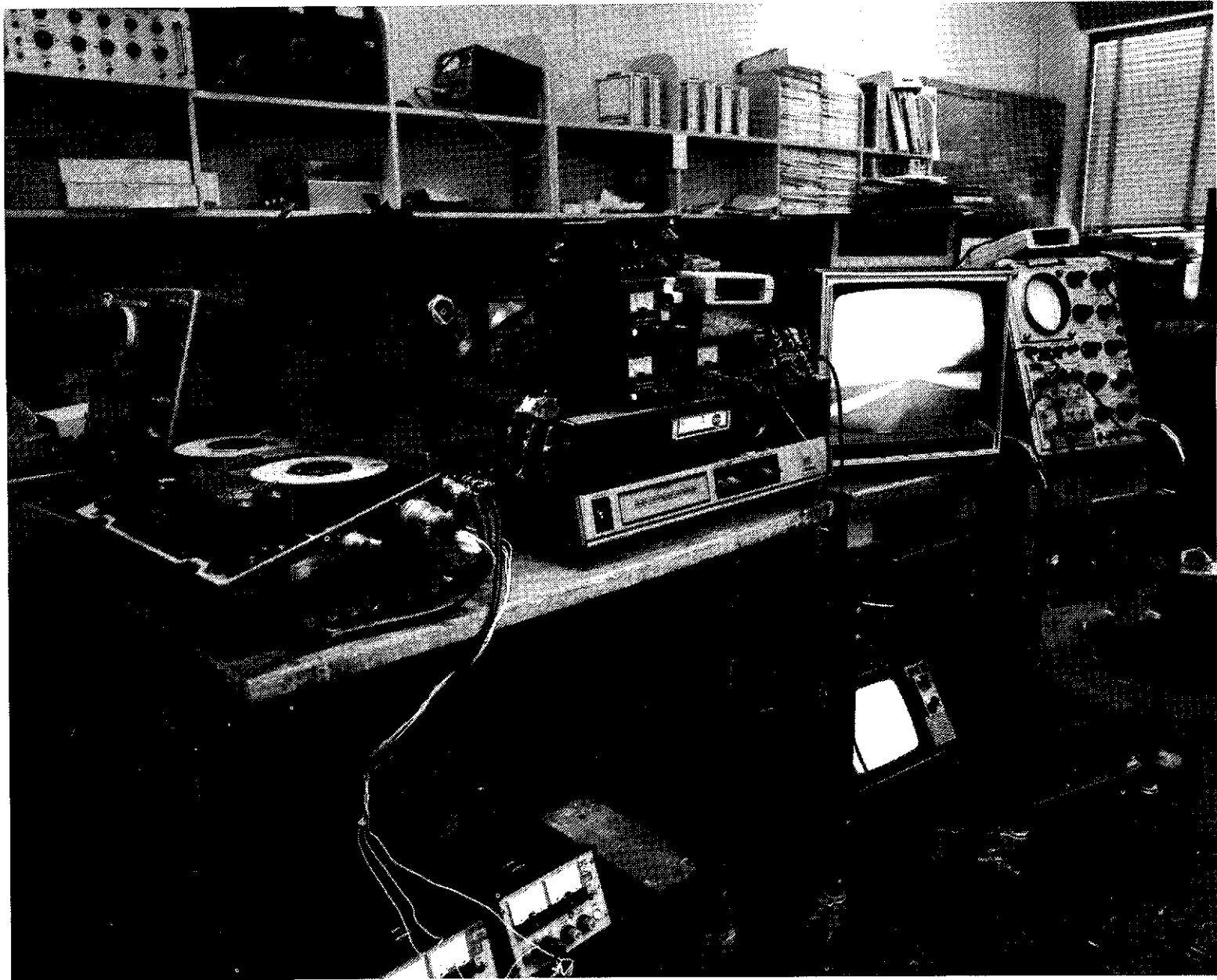


FIGURE 72. SYSTEM FOR SIMULTANEOUS PLAYBACK OF RADAR AND VIDEO INFORMATION.

and moderate snow conditions on Route 1. An attempt to record data during a severe blizzard failed because only video data was inadvertently recorded on both recorders. Recording runs were also made on Route 206, a heavily travelled two-lane road with a variety of curves. The effect of very hilly terrain was recorded northwest of Princeton.

In order to investigate the effects of bridges and tunnels, several recording runs were made to New York City. A recording run was also made on the NJ Turnpike, a six-lane divided highway with limited access. When it became clear that the Ku-band bistatic system was definitely superior to the X-band system, several of the X-band tapes were erased and recorded over with Ku-band data. Runs through a disposable target at a nearby airport were also recorded. The airport runs were made for  $1\text{-m}^2$  and  $10\text{-m}^2$  targets at 20, 30, 40, 50 and 60 mph.

The use of this recording system greatly helped in the systematic evaluation and optimization of the radar system. By playing back the tapes, the early version Phase III CMS radar interface hardware could clearly be identified as more sensitive to a variety of target conditions than the Phase II CMS radar interface card. This was demonstrated to DOT and Minicars personnel in September 1978. Another recorded tape during playback through the microprocessor indicated a constant offset in the range-rate readings. While the tapes were rerun, the microprocessor was halted and memory locations that contained the up and down counts were examined. An analysis of this data showed that the range-rate offset was caused by a nonlinear FM deviation in the TEO of the radar system.

The majority of the tapes had been recorded in situations that had a high probability of giving a false alarm with the CMS system. Two examples of tapes that initially gave us false alarm indications were the bridge and tunnel runs to NYC and the curve-rich part of the Route 206 run. False alarms were generated by one of the towers that supports the suspension cables of the Verrazano Narrows Bridge. Modification of the CMS software, specifically the deviation check constant, eliminated this problem. Once this correction was made to the software, the tapes were rerun to ensure that the correction did not destroy the sensitivity of the system. The deviation check tolerance tightening that eliminated the bridge tower false alarm in the first tape also eliminated the problem in the second tape.

The most informative tapes about the operation of the CMS were the airport tapes. These tapes of runs through the disposable target were considered the standard by which any changes in hardware or software were measured. The runway tapes were particularly useful to determine when a brake signal is given. The reaction time of the braking system was measured by putting a stop in the CMS software when the braking command is given. The memory contents of the evaluation-board card cage system can then be used to measure reaction time. For a given run through a target, the velocity of the vehicle is known. From the data in memory we can determine when the target was acquired (range), and the range-rate when the braking signal was given is also available. From these data the reaction time of the CMS can accurately be determined. The brake signal appeared reproducibly at a distance of at least 23 m from the target for all targets and speeds. Based on a car speed of 25 m/s (55 mph) and a brake system delay of 0.1 s, the automatic application of antiskid brakes with the above system would result in a 45% reduction in crash energy.

### C. HEADWAY-CONTROL TESTS

#### 1. System Optimization

The main requirements on a radar headway-control system are safety, driver convenience (smooth control, with minimum action required from driver), and fuel economy. Whereas false alarms are totally unacceptable in the collision-mitigation mode, which limits the active range to below 30 m, the headway control requires range information up to at least 45 m, but permits some false alarms, provided they do not lead to jerky movement of the car. Satisfactory headway control under actual traffic conditions is difficult to realize because it requires low-fluctuation, high-accuracy range and range-rate data that constantly act upon the car's throttle and thus are continuously perceived by the driver.

Since it is very difficult to separate problems caused by the control loops from radar processing problems, the initial optimization and program development for the headway control was performed with a cooperative radar system. An existing X-band FM/CW radar was modified to accept only return signals from tagged targets, as discussed in subsection III.B. By use of the cooperative system, problems with false alarms, signal dropouts, target scintillation, etc., are greatly reduced or totally eliminated. The headway-

control algorithm can thus be investigated and optimized under idealized conditions; this is important for separating the possible causes of erratic or jerky performance and helped greatly in the initial phases of the headway algorithm development.

The tagged target car provided a clean reliable return signal which could be processed to give stable, highly accurate range readings. Tests with two tagged cars simultaneously pointed to the possibility of false alarms, even with the cooperative system. For example, in gradual curves and at great distances, a tagged vehicle in the outer lane may easily be mistaken for a vehicle in the radar car's lane. Thus, although the cooperative system was very instrumental in the headway-control development, it does not represent the complete solution to the false alarm problem when there are many tagged vehicles on the road.

The initial headway-control system optimization was performed using RCA-owned station wagons for the radar car and as tagged target vehicles. The radar-controlled car was equipped, aside from the cooperative X-band radar and its associated computer, with a strip chart recorder and an inverter to permit the use of an executive terminal in the car for on-the-road program changes of algorithm constants. The strip chart recorder provided accurate readouts of vehicle velocity, range, throttle position, and throttle control voltage as a function of time. For later fuel economy runs the car was also equipped with a highly accurate fuel metering device. A photograph of the experimental computer and recorder installation is shown in Figure 73. The system was mounted in place of one of the front seats which was removed for the testing period. The throttle of one car was activated through a chain by a linear DC motor, which in turn was controlled by the computer. This arrangement is shown in Figure 74. The potentiometer attached to the throttle axis was used only for monitoring and diagnostic purposes.

## 2. Road Tests

The flow chart algorithm of the headway control shown in Figure 61 is the outgrowth of a series of other algorithms that were tried and step-by-step improved to arrive at a workable control system. Initial tests with a simple vacuum-based throttle controller proved unsatisfactory until a more reproducible and linear DC motor was installed as control element. Single-loop control laws originally tried had to be abandoned in favor of more complex ones to obtain suitable, stable operation under a variety of operating conditions.

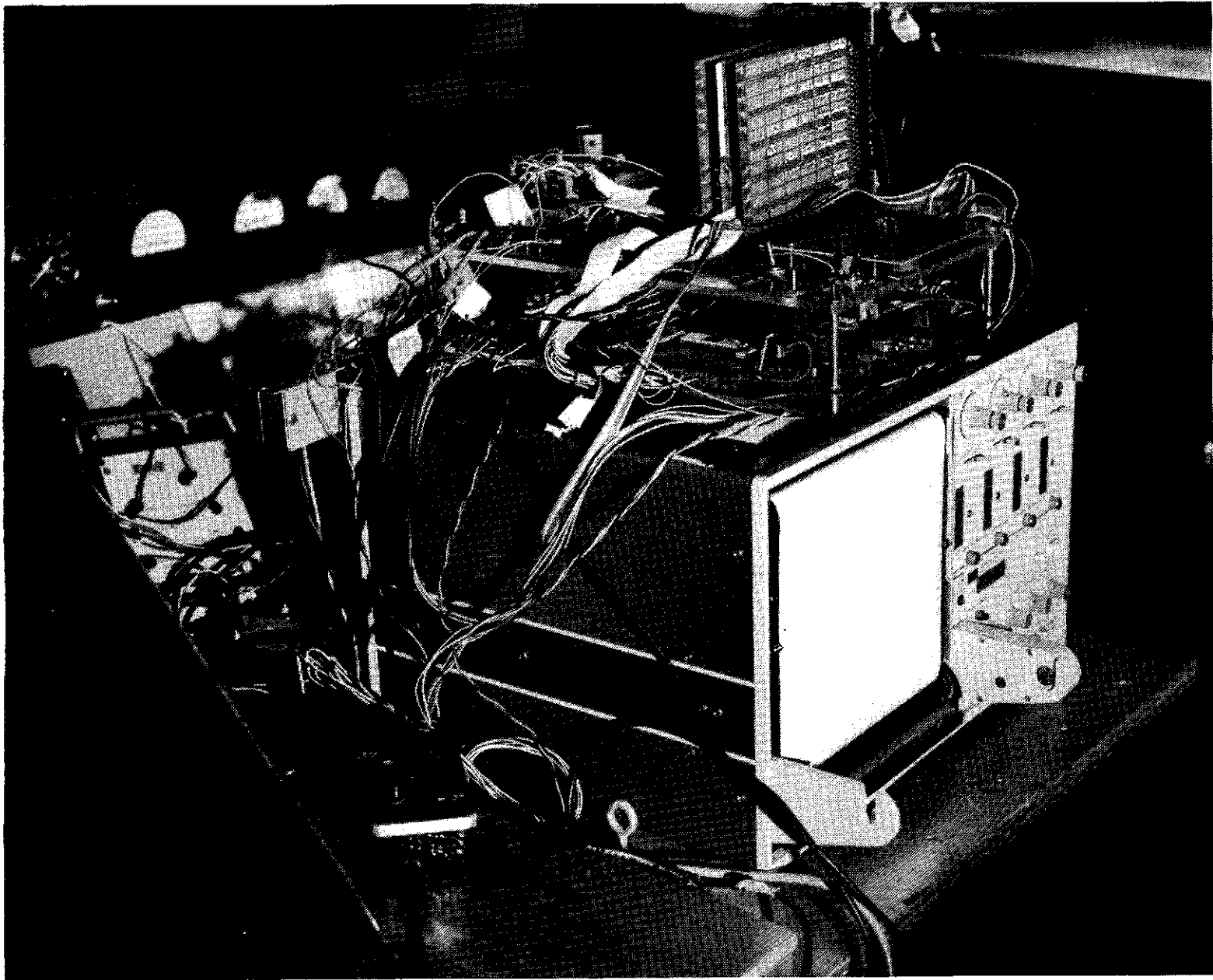


FIGURE 73. HEADWAY-CONTROL COMPUTER AND STRIP CHART RECORDER MOUNTED IN FRONT OF RCA STATION WAGON.

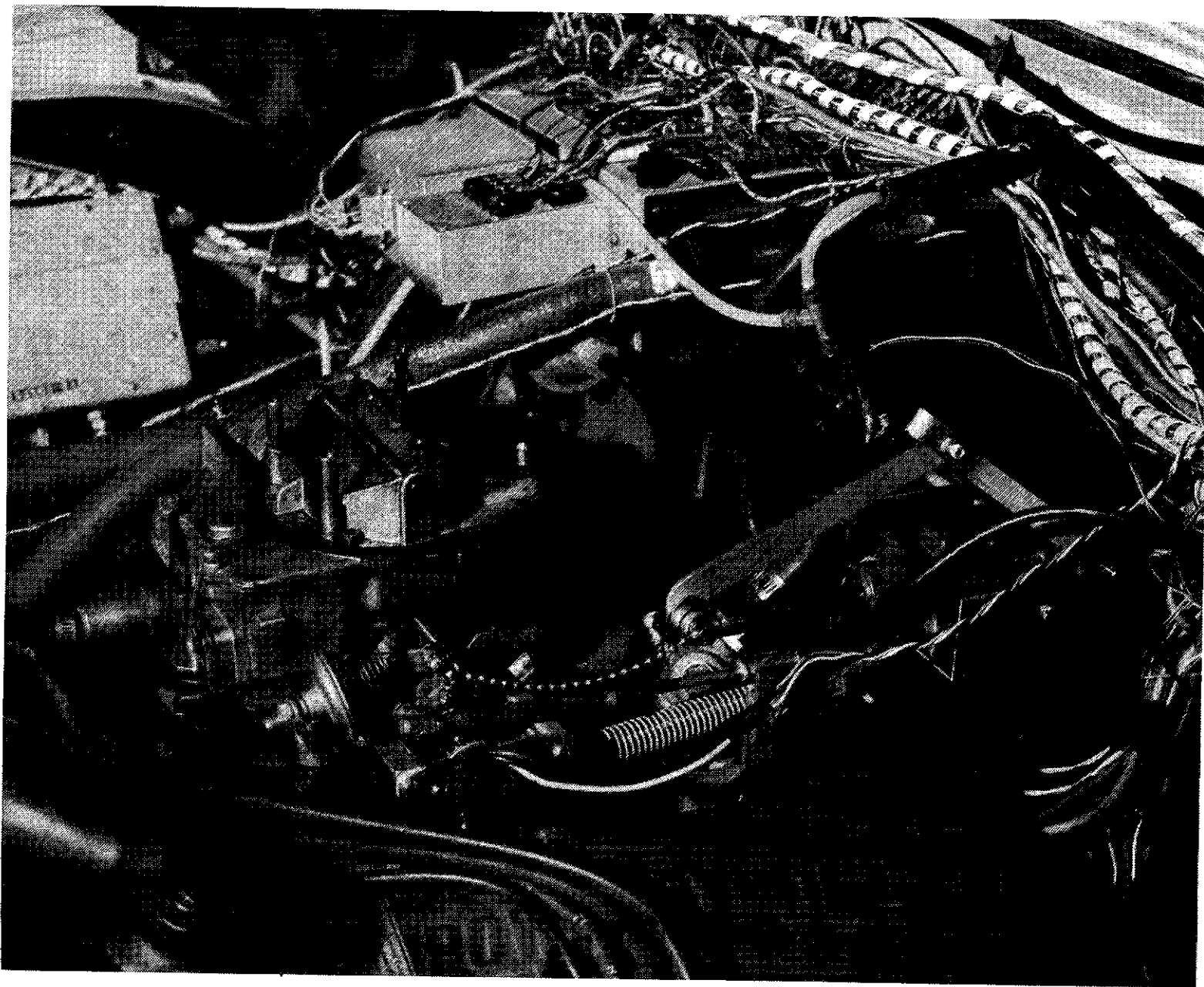


FIGURE 74. LINEAR THROTTLE ACTIVATOR.

Initial values for the constants in the final algorithm shown in Figure 61 were derived from dynamic tests performed on the car with a dynamometer and from certain driving tests. The optimization of these constants was then performed experimentally with the help of the strip chart recorder and by driving with the cooperative radar system over the same stretches of road to ensure reproducibility. The final fine tuning of the algorithm was performed with the noncooperative Ku-band radar in open traffic driving.

Figure 75 shows a typical strip chart recording from early tests. The tick marks on the uppermost line represent 1-minute intervals. The next trace represents the radar car velocity ranging from 13.6 to 25 m/s (30 to 55 mph). The next lower trace shows the range to the tagged target car ahead which in this case was operating under cruise control at 45 mph. The two lowest traces are the actual throttle position,  $\theta_{Th}$ , and the control voltage,  $V_{Th}$ , to the throttle. This particular run represents early results on the cooperative system. Although the range and the velocity are kept reasonably constant (range deviations remain within  $\pm 1.5$  m), the throttle control voltage fluctuates widely causing a very jerky and erratic driving behavior.

For comparison, Figure 76 shows a run obtained with the noncooperative Ku-band radar following a standard passenger car at the final stages of algorithm optimization. Here, in spite of the fact that the radar faces the full road environment in the noncooperative mode, velocity and range variations remain acceptably small while short-term throttle angle fluctuations have decreased to approximately 1 degree, providing a smooth ride free from perceptible jerks.

Aside from headway control, the system is also capable of providing regular cruise control operation and includes special programs for the transition modes of target capture, lost target, and resume speed. All of these functions were finally optimized under actual traffic conditions found on typical high-speed, limited-access freeways.

A series of controlled test runs were performed toward the end of the program to investigate the possibility of cruise and headway control having a beneficial effect on fuel consumption. Contrary to some earlier, not well documented tests which showed a superiority of cruise/headway control, no significant differences could be established within the bounds of run-to-run fluctuations ( $\pm 2\%$ ) between cruise/headway control and average "sensible" driving behavior. Some drivers indeed had the habit of using a "heavy" foot on the gas pedal and, consequently, ended up with poor fuel economy. However, anybody aware

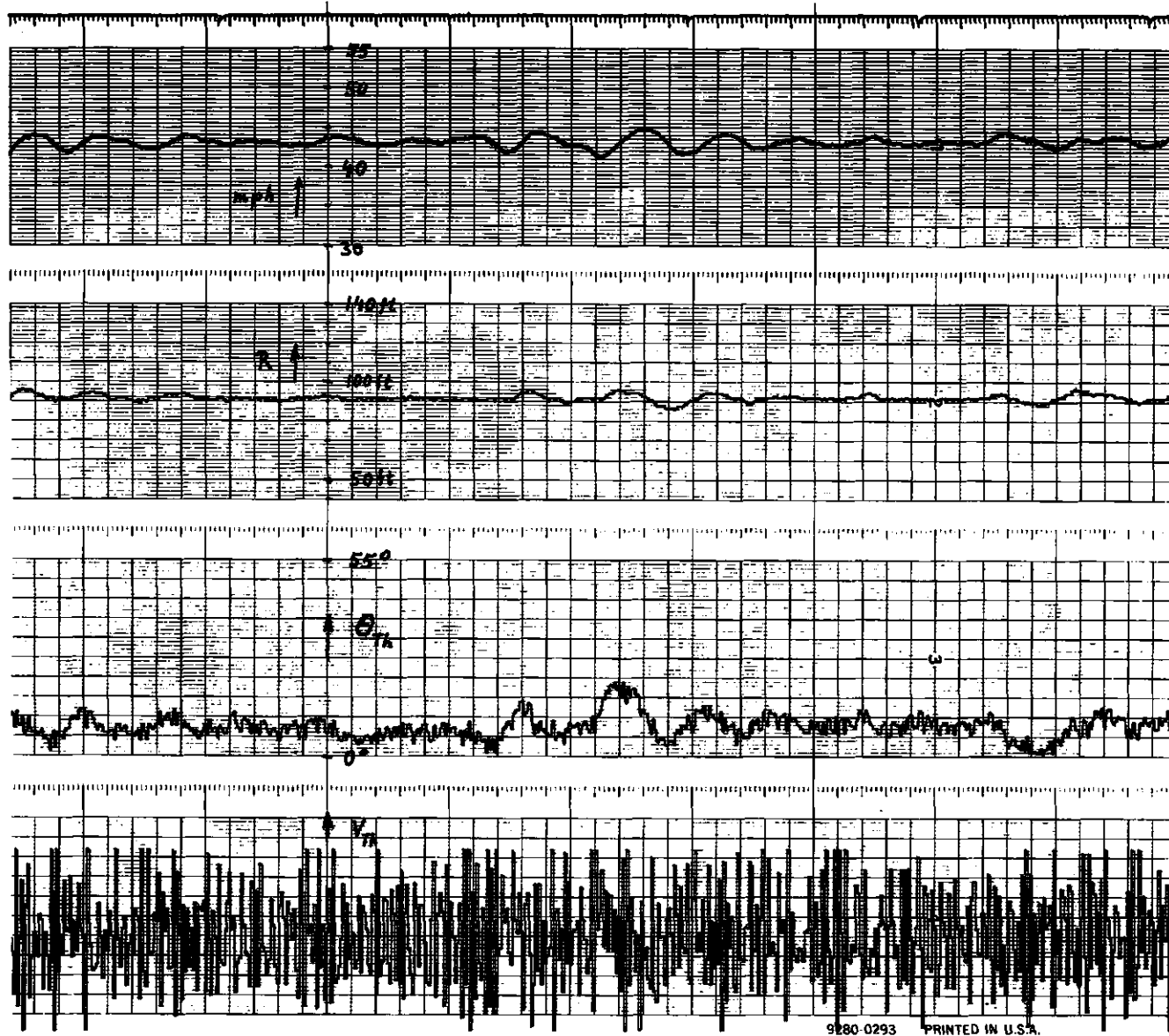
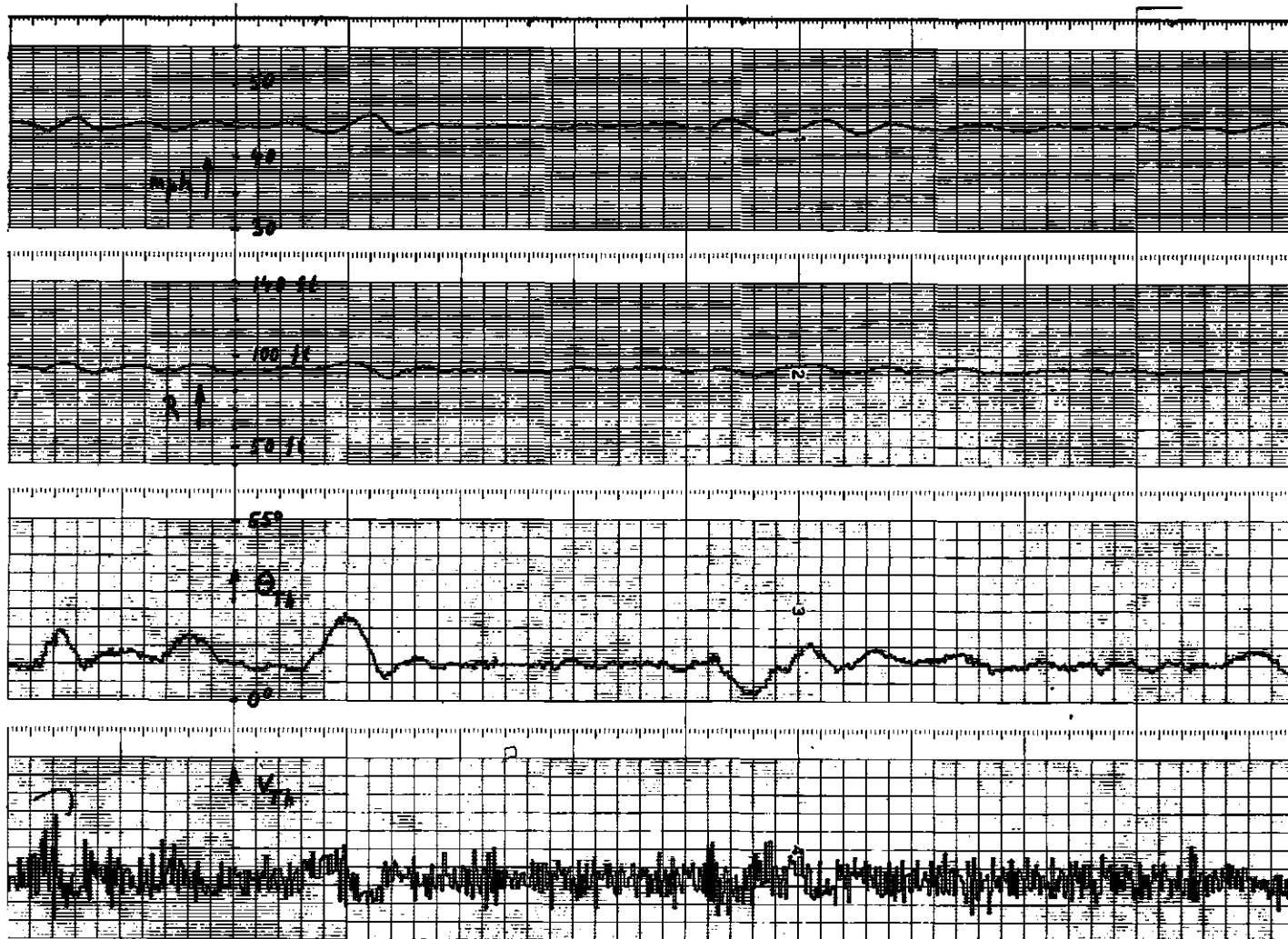


FIGURE 75. EARLY RECORDING OF COOPERATIVE RADAR CAR FOLLOWING A TARGET CAR OPERATING IN CRUISE CONTROL AT 45 mph.



9280-0293 PRINTED IN U.S.A.

FIGURE 76. NONCOOPERATIVE Ku-BAND RADAR CAR FOLLOWING STANDARD PASSENGER CAR (PINTO) USING OPTIMIZED ALGORITHM.

of what causes poor fuel economy could, without difficulty, duplicate the fuel economy of the cruise control. The tests were performed over a 26-mile stretch of highway in both directions to average wind loading; each type of test consisted of several runs. The fuel consumption was measured by a Fluidyne\* fuel flow meter.

The following test runs were taken:

- (a) Driver only (asked to keep reasonably constant speed)
- (b) Cruise control
- (c) Radar car following cruise control car
- (d) Driver asked to keep constant distance after cruise control car
- (e) Driver asked to intentionally accelerate and slow down while keeping average speed equal to cruise-control car ahead.

Tests a, b, and c did not show any significant differences in fuel consumption. Only test e showed clearly poorer performance whereas test d, while demonstrating much poorer performance in keeping a constant distance to the car ahead ( $\pm 5$  m versus  $\pm 1.5$  m for the radar headway control), showed only a slight ( $\sim 10\%$ ) increase in fuel consumption.

Based on these admittedly limited tests, we concluded that no significant claims to better fuel economy could be made. The headway-control system, however, did perform equally to a cruise-control system or the average conscientious driver and is capable of keeping the spacing between cars to much closer values than average drivers can. The latter effect may be quite beneficial in establishing better column stability and higher throughput for high-density "safe" traffic flow. However, these factors require considerably more theoretical and practical studies.

### 3. Headway-Control Demonstration Vehicle

The unavailability of a suitable RSV for headway-control development made it necessary to use an RCA station wagon for algorithm optimization. For demonstration purposes the car was finally stripped of all the excessive electronic attachments and prepared as a demonstration vehicle. Figure 77 shows the RCA headway/cruise control car with a Ku-band bistatic radar attached to the front.

\*Fluidyne Instrumentation, Oakland, CA.

A-112



FIGURE 77. HEADWAY-CONTROL RADAR MOUNTED ON RCA STATION WAGON.

The car is also equipped with a display which provides range, range-rate, distance error, and vehicle speed information. This display is used for demonstration purposes only and would not be present in a regular headway-control-equipped car.

Operation of the headway-control system is similar to operation of a conventional cruise control, since the computer makes all decisions concerning how the radar information is to be used. The directional signal control stalk has three momentary contact switches added for "Set," "Set 55 mph," and "Resume." None of the momentary switches can be activated below a speed of 9 m/s (20 mph). The "Set 55 mph" switch is a convenience feature not found on conventional cruise controls, but is easily implemented in software. An on/off toggle switch is used to inhibit control of the throttle, but in the present system the display will be actively updated even in the off position. This is useful for checking the operation of the radar.

In general, drivers adapt quickly to the headway-control system, learning to use it within a few minutes. The major difficulty is learning which circumstances require driver braking, and which can be handled adequately by computer release of the throttle. As a rule the computer can handle closing rates on the order of 2.3 to 4.5 m/s (5 to 10 mph), depending on where the target is acquired. The system has been driven extensively in real traffic, following cars and trucks of various sizes and shapes, and found to perform smoothly in most situations.

Figure 78 shows the format of the Burroughs display when the system is in the headway control state. The values  $\hat{R}$ ,  $\dot{\hat{R}}$ ,  $(R_{des} - \hat{R})$  and  $\hat{v}$  are displayed. The warning light requires two consecutive range-rates smaller than -3 m/s for activation. Nonsmoothed range-rate is used for rapid response. The light goes out when  $\dot{\hat{R}} > -3$  m/s. The light is also activated if range is less than 10 m. If the driver activates the brake, the throttle immediately returns to the closed position and the display information disappears. The car is then fully under the control of the driver.

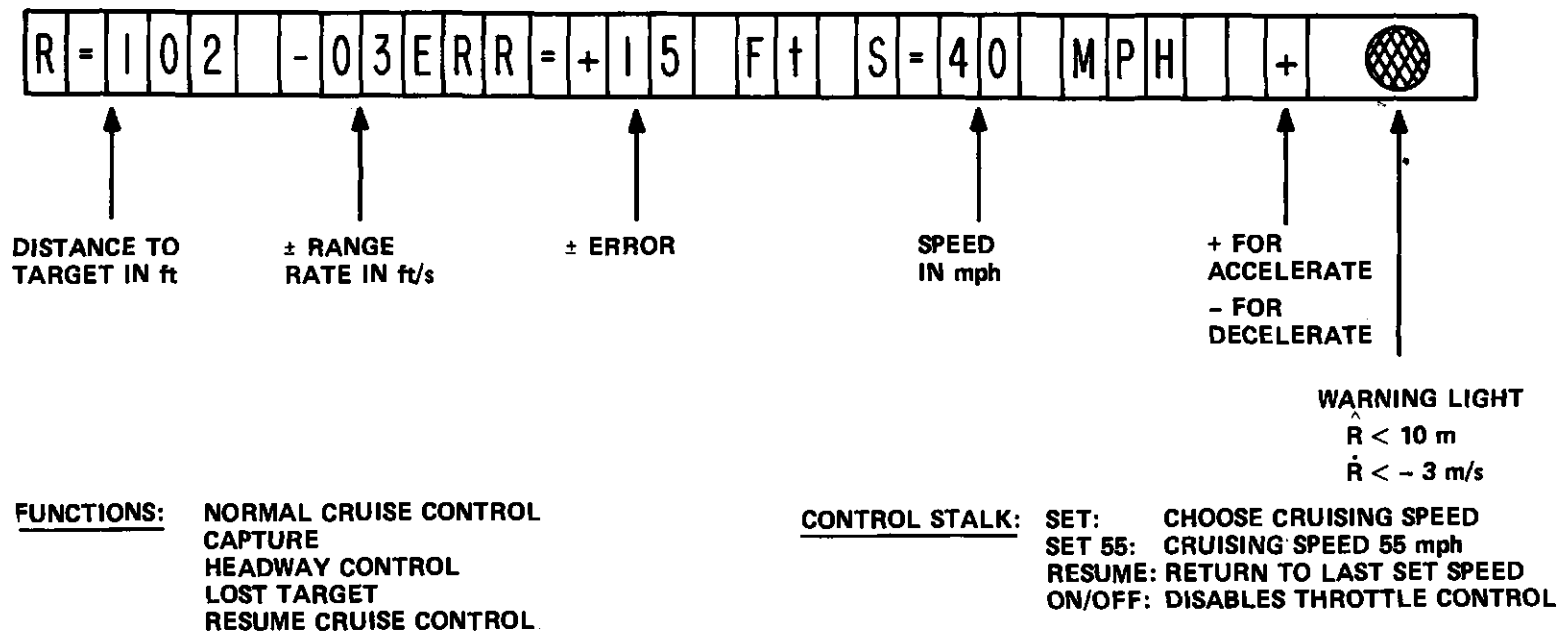


FIGURE 78. DISPLAY FORMAT FOR HEADWAY-CONTROL DEMONSTRATION.

## SECTION VII

### INSTALLATION OF EQUIPMENT INTO THE RSV

#### A. GENERAL

The original program plan called for the integration of all electronic systems into a high-technology version of the RVS. This includes, aside from the RCA-developed components, an antiskid system, an airbag deployment system and a computer-controlled automatic transmission. Due to delays in getting the RSV to RCA Laboratories for installation of our systems and difficulties with the operation of the automatic transmission, the final integration of the CMS and headway control into the RSV had to be postponed to mid-1980 at which time the car should return to RCA Labs and be equipped with all other electronic systems and be completely operational. In the meantime, the RSV was instrumented with the alphanumeric display and associated microcomputer and sensors. The CMS computer was installed and interconnected for tryouts of the basic functions and then removed again. Also the fitting of the antenna radome into the nose section of the RSV was completed; it awaits final installation after all other body work on the RSV is finished. The performance of the CMS and headway-control system has been demonstrated so far only on RCA-owned vehicles.

#### B. MICROCOMPUTER AND SENSOR INSTALLATION

The dashboard display and CMS/headway-control microcomputers were installed in the luggage compartment of the RSV. Proper sensor connections to both microcomputers were made with conventional twisted wire pairs. Only the radar was connected via two coaxial lines to avoid spurious pickups on the modulation and IF return lines. A dedicated 12-V and ground line was run from the battery to a terminal strip mounted on the side wall of the front compartment near the two RCA microcomputers. The purpose of running dedicated lines to the microcomputers and radar was to minimize the effects of possible ground loops or excess voltage drops between the battery and the respective systems.

The following sensors were interfaced, calibrated where necessary, and checked for proper operation: hand-brake switch, brake fluid level switch, door switch, water temperature sensor, oil pressure sensor, velocity sensor, fuel flow sensor, fuel level sensor, tachometer, battery status indicator, restraint system status, and brake and steering wheel position switches. All

sensor wires were connected to a terminal strip mounted on the top of the dashboard display microcomputer. In this way, if necessary, each sensor could be tested individually for proper operation. A set of instrument gauges that came with the RSV was used as reference to calibrate the dashboard display microcomputer with respect to water temperature and oil pressure. The sensors that monitored these functions were connected by dashboard mounted switches to either the gauges or the dashboard microcomputer.

Two intra-microcomputer connections were also made. The first connection was between the Dubner system microcomputer and the RCA dashboard display microcomputer. This connection, after buffering, is used to pass on the velocity pulse train monitored by the Dubner microcomputer system. A connection between the dashboard display microcomputer and the CMS microcomputer passes on information when the calculated velocity is above the set speed in the CMS algorithm by setting an appropriate level.

The steering angle microswitch and associated hardware were mounted in an enclosed area adjacent to the luggage compartment that afforded protection from harsh automotive environmental conditions. An illustration of the electro-mechanical arrangement used to determine when the preset steering wheel angle cutoff is exceeded is shown in Figure 79. The cams and microswitches are adjusted to allow 1-1/2 degrees of steering on either side of center. Exceeding this limit on either side provides a 5-V level to a flag line on the CMS microcomputer. A calibration of the wheel's center alignment was made by following a 40-m-long line on the test range and noting the steering wheel position. Using alignment plates marked in degrees with the front wheels, the microswitches and cams were set to allow 1-1/2 degrees steering on either side of the center position before triggering the flag level. The lock-to-lock steering for the RSV is approximately 30 degrees on either side of the center position. The 1-1/2-degree steering angle was chosen as a compromise between having a good margin against false alarms on one hand, and not being too sensitive on the other hand. The steering wheel angle tolerance can be adjusted independently to have a greater or smaller cutoff angle on either side of the wheel's center line.

The airbag sensor circuit consists of resistances associated with the three impact sensors in series with the two paralleled airbag squibs. The airbag sensor interface (see Figure 52) monitors the voltage drop from the squib to ground. Thus, should any one of the six sensor switches (each impact sensor includes two sensor switches) have accidentally shorted out or more than two

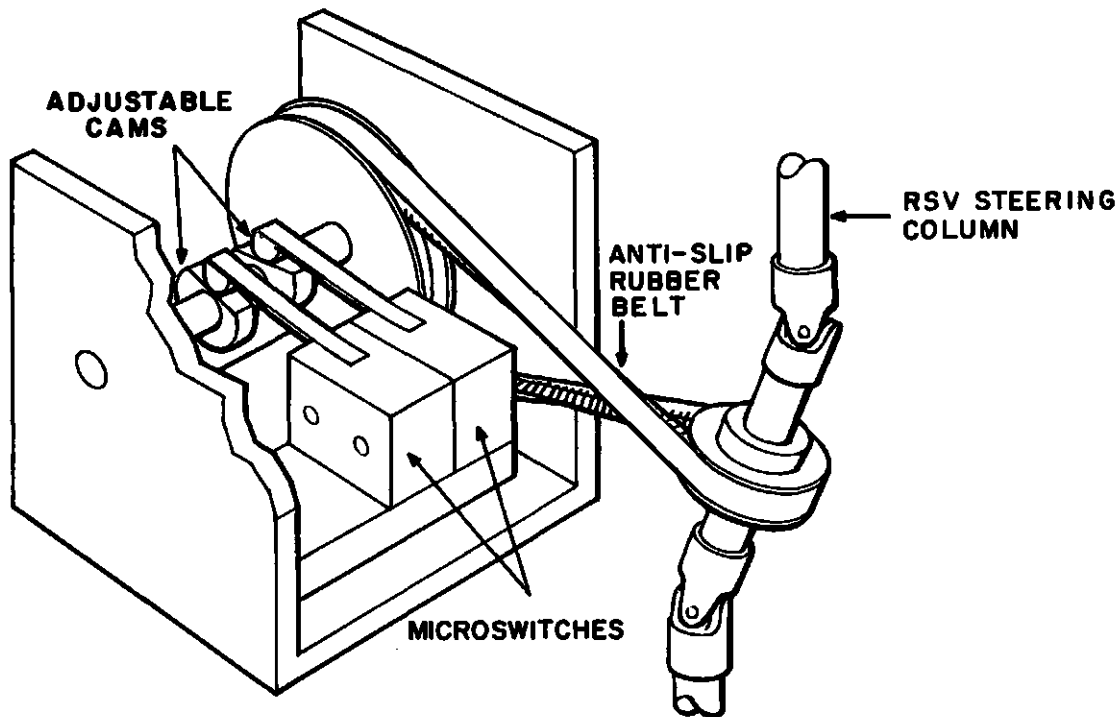


FIGURE 79. ELECTROMECHANICAL ARRANGEMENT FOR STEERING ANGLE DETERMINATIONS.

be open-circuited, the sensor interface will provide a warning message on the display. The problem of determining whether the squibs themselves are possibly either open or short circuited is being addressed separately by Minicars.

A Burroughs high brightness display with two bezels and edge lighting was mounted in the display housing that was delivered with the RSV. The assembly was temporarily mounted by a bracket to the RSV dashboard and interfaced with the dashboard display microcomputer through a set of connectors for ease in installation and servicing. A switch was installed on the dashboard to select either the upper or lower bezel with the corresponding proper display format. A potentiometer permits variation of the intensity of edge lighting of the bezels. The final installation of the display in the proper dashboard location will be made after Minicars replaces the present experimental dashboard with the final version.

### C. RADAR SAFETY CONSIDERATIONS

In view of the growing concern on part of the public and the government with nonionizing radiation effects, the microwave power typically radiated from a collision-mitigation/headway-control radar was investigated theoretically as well as practically.

Our present Ku-band radar emits nominally a power of 10 mW from an antenna with a gain of  $\sim 30$  dB. In the far field of the antenna, the power density decreases as  $\frac{1}{R^2}$  with R, the distance from the antenna. Closer to the antenna this law does not hold since we are in the near field or Fresnel region of the antenna. By normalizing the field in the far-field region, we can recalculate the field intensities closer to the antenna, as shown in Figure 80. The field pattern undergoes various spatial maxima and minima due to interference in the near field. Based on a radiation of 10 mW from a 30-dB antenna, the maximum power density is  $20 \mu\text{W}/\text{cm}^2$  at a distance of 0.6 m.

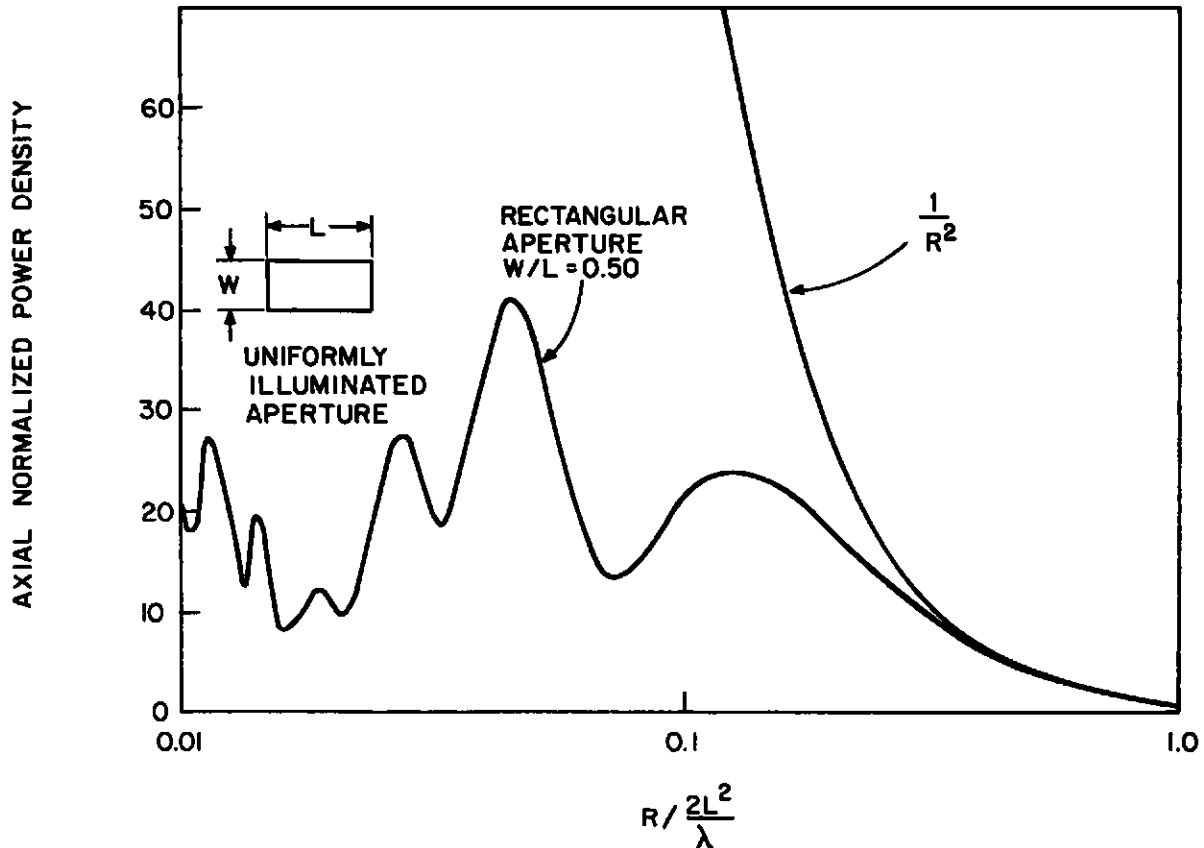


FIGURE 80. ANTENNA FIELD INTENSITIES.

Actual measurements performed with a small waveguide antenna in the near-field area of the antenna showed a maximum power density of  $15 \mu\text{W}/\text{cm}^2$  at a distance of approximately 1 m from the antenna. These measurements are not to be considered very accurate since the presence of the waveguide distorts the existing field pattern; however, the measured values give a good order-of-magnitude indication of what fields can be expected in front of the antenna.

At present, the United States microwave radiation limit is  $10 \text{ mW}/\text{cm}^2$ , which is based on the onset of thermal effects in the human body. The Soviet Union, on the other extreme, maintains a limit for continuous exposure as low as  $10 \mu\text{W}/\text{cm}^2$  to avoid possible neurological and physiological effects. Substantial controversy exists as to where a realistic safe limit should be drawn. In any case, the amount of nonionizing radiation to which humans may be exposed from CMS/headway radars is very low, and for distances above a few meters is even below Russia's very stringent standards. In addition, the radar could be easily equipped with a solid-state switch that prohibits radiation below a certain critical speed, which would further reduce the radiation exposure of humans in actual traffic.

SECTION VIII  
COST ESTIMATES

A production cost analysis of the CMS and headway-control system was prepared using RCA's PRICE program [12]. The system analysed consists of an FM/CW Ku-band bistatic radar and a three-chip microprocessor controller set (since large production quantities are assumed, VLSI would be implemented) in a metallized weather-tight plastic box. The cost of the velocity and steering wheel position sensor, the throttle controller for the cruise control system, integration, and testings are included in the overall production cost figure. The complete CMS and radar cruise control system is estimated to have a production cost figure of \$177. This production cost figure is based on 100,000 units, 1979 dollars and 1985 technology.

The PRICE program gives a range of production costs for each item. The upper value is the worst-case prediction. The actual production cost of an item will be somewhere between the high and low extremes. The cost breakdowns are as follows:

The electronics for the radar and processor are assumed to be contained within a metallized weather-tight plastic box. The box also contains the bistatic radar system consisting of two antennas and associated electronics. The purpose of metallizing the box is to provide a ground plane for the printed circuit antennas. The predicted production cost range of the metallized weather-tight plastic box varies between \$12.92 to \$18.77, with \$15.07 the average cost. The microprocessor system that will provide the CMS and cruise control functions is assumed to require a total of three VLSI chips. The production cost for the three-chip system including the PC board on which the ICs would be mounted ranges from \$7.99 to \$12.98. The average cost of the three-chip microprocessor controller including the necessary ROM and RAM is \$9.58.

The cost evaluation of the radar system, antennas, transmitter and receiver is based on the use of microwave IC technology. The bistatic antennas are fabricated in PC form. The modulating and analog processing circuitry is assumed to be in IC form. The computed cost range low is \$92.67; the maximum cost computed for the Ku-band radar production system is \$144.95 with an average of

---

12. R. F. Freiman, "PRICE - A Parametric Cost Modeling Methodology," RCA Government and Commercial Systems, Cherry Hill, NJ, May 1978.

\$112.50. An electromechanical solenoid that is used to control the throttle was also estimated by a description of the size and complexity of the device. The PRICE system predicts a cost range between \$18.48 and \$28.31.

The steering and speed sensor were the final components of the CMS/headway-control system that were cost evaluated. The speed sensor is described as a device that outputs a pulse train at logic voltage levels whose frequency is a function of velocity. The steering wheel sensor is a geared potentiometer attached to a steering arm on the front wheel. Based on a description of the function of both sensors and the approximate size of each unit, the sensors have a predicted production cost of \$7.06 to \$10.89. The assembling of the overall systems and testing is computed by PRICE to be \$10.00 per unit.

The production cost of the complete CMS/headway-control system (excluding braking system) ranges from \$147.26 to \$228.51. The average \$177.00 figure is based on a production run of 100,000 units.

## SECTION IX

### CONCLUSIONS AND RECOMMENDATIONS

The present effort under DOT sponsorship has contributed greatly to establishing the viability of the radar concept for automotive applications. Truly promising results have been obtained with a radar-controlled collision-mitigation system. With the help of tape recordings of a large number of traffic, road, and weather conditions, a systematic approach to the optimization of the hardware and software of the radar-controlled safety system has been made possible. The importance of these tests lies in the recording of raw radar data that permit a thorough comparative study of how different signal-processing techniques affect the false alarm rate while, at the same time, giving valuable information about the minimum detection distance and the speed with which a proper alarm (output to initiate antiskid braking) is being generated from experimental targets of various cross sections.

With the present system adjusted for practically no false alarms, a target as small as  $1 \text{ m}^2$  is recognized at a distance of at least 23 m, and braking is initiated if the closing rate is high enough to make a severe collision unavoidable. In a car traveling 25 m/s (55 mph) against a fixed object, this action results in a reduction of crash energy by ~45%, an amount that can be very significant with respect to the injuries sustained by the car's occupants. Obviously such a system does not provide the full solution to crash survivability but, if combined with other means such as car structures with higher impact tolerance and use of airbags, a substantial societal savings can be achieved.

It also has to be realized that the system discussed here represents only a feasibility demonstration of the present state-of-the-art; further work in radar processing certainly could still increase the minimum detection range to around 30 m while keeping false alarms in check. Some of the desirable improvements that are considered feasible, but were not implemented during this program, are a further reduction in size of the antenna by using higher frequencies and the introduction of range gate processing to reduce weather interference and multiple-target problems. Also, it can be assumed that further progress in signal processing can be made to increase the safety margin against false alarms.

Aside from the collision-mitigation safety aspects, the present DOT program also addressed two other important areas, an electronic display as driver

aid and automatic cruise/headway control. The final high-technology version of the RSV was equipped with an alphanumeric display which presents driving-related data as well as a series of warning messages if a vital part of the car malfunctions. The display system corresponds closely to the one developed originally during Phase II of the program and includes some refinements and additions, among others a conversion to metric readouts of all measured parameters.

The final version of the high-technology RSV was also to have an automatic cruise/headway control using the existing radar. Since a suitable RSV test vehicle was not available in time, the development of this system was carried out exclusively with RCA-owned station wagons. An experimental system was successfully developed and the algorithm optimized for operation on typical limited access highways using a noncooperative Ku-band FM/CW radar identical in design to the one used in the RSV for collision mitigation.

The cruise/headway control operates either in standard cruise control or automatically switches to a safe headway spacing mode when a vehicle in front is driving at a slower speed than the chosen cruising speed. Since the spacing between cars by the radar system can be maintained considerably more accurately than can be achieved by average drivers, such a system holds promise to provide a better throughput on highways while reducing the common safety hazards of bunching and tailgating. In addition, such a system can be expected to add greatly to the overall sales appeal of the radar and enhance the driver's convenience.

Duplicates of the hard- and software of the cruise/headway-control system were prepared for the RSV but could not be included and fully optimized because of time and certain compatibility problems. A proposal is presently being submitted for a subsequent joint effort between Minicars, Dubner Computer Systems, and RCA to solve the compatibility problems and include the headway control in the final RSV. The high-technology RSV will be returned to RCA at a future time after installation of an antiskid brake system, a new dashboard, and an improved electronically controlled transmission for the final incorporation of the radar and the above-mentioned joint effort.

While substantial progress has been made during this program to show the basic feasibility of cruise/headway control under real, every day traffic conditions, it must be realized that a large amount of work still remains to be done before such a system can be implemented in passenger cars. First, low-g

proportional braking should be included to handle most of the frequently occurring situations where a slightly faster deceleration is needed than can be obtained from engine braking alone; second, radar improvements such as recommended above for the collision-mitigation system (smaller antenna and multiple target resolution) would further enhance the system's versatility; and third, the question of the stability of long columns of cars (under study for some time with the driver as part of the feedback loop) will have to be looked at under the special conditions and restrictions of radar headway control.

Finally, we want to suggest that the time has come to take a serious look at the benefits that radar can add to the automotive environment. Plans for fabrication of a limited number of systems should be initiated to permit a more detailed and thorough testing of the concepts discussed here under actual road conditions by average drivers. Extensive road tests on many cars for a prolonged period of time would certainly be required before a radar-based system could be considered by the rule-making body of the government.

**APPENDICES**

## APPENDIX A

### COVERAGE PATTERN CALCULATIONS

#### A. BISTATIC Ku-BAND RADAR

##### 1. Statement of the Problem

To determine the detection area of the Ku-band radar, contours of constant power were calculated. An ideal bistatic radar above a ground plane was assumed. The target was assumed to be an isotropic point source. Based on the above assumptions, the power,  $P_r$ , returned to the radar becomes

$$P_r = \frac{P_T G_\phi(\phi_1) G_\phi(\phi_2) \lambda \sigma P_m}{(4\pi)^3 R_1^2 R_2^2} \quad (\text{A-1})$$

where,

- $\phi_1$  = Azimuth angle between transmit antenna and target
- $\phi_2$  = Azimuth angle between receive antenna and target
- $G_\phi$  = Antenna azimuth gain function
- $\lambda$  = Wavelength in free space
- $P_m$  = Multipath factor
- $R_1$  = Distance from transmit antenna to target
- $R_2$  = Distance from receive antenna to target

A typical configuration defining the coordinate system is shown in Figure 10 in the main body of the report. The transmit and receive antennas are located at  $(S_o/2, 0)$  and  $(-S_o/2, 0)$ , respectively, and the target is located at  $(x, y)$ . The radar and target are at the same height above ground. From Figure 10,  $R_1$  and  $R_2$  are given by

$$R_1 = \sqrt{\left(x - \frac{S_o}{2}\right)^2 + y^2}$$

$$R_2 = \sqrt{\left(x + \frac{S_o}{2}\right)^2 + y^2} \quad (\text{A-2a})$$

$$\phi_1 = \tan^{-1} \frac{\frac{S_o}{2} - x}{y} \quad (\text{A-2b})$$

$$\phi_2 = \tan^{-1} \frac{\frac{S_o}{2} + x}{y} \quad (\text{A-2c})$$

The multipath factor,  $P_m$ , is given by [6]

$$P_m = \left\{ (1-P)^2 + 4P \sin^2 \frac{2\pi h_1 h_2}{\lambda R} \right\}^2 \quad (\text{A-3a})$$

where  $R = \text{mean range, } (\frac{1}{2} (R_1 + R_2))$

$$P^2 = \frac{G_\theta(\theta_2)}{G_\theta(\theta)} |\Gamma|^2 \quad (\text{A-3b})$$

$|\Gamma| = \text{reflection coefficient of the road } \approx 0.5$

$h_1 = \text{radar height above ground}$

$h_2 = \text{target height above ground}$

$$\frac{G_\theta(\theta_2)}{G_\theta(\theta)} = \text{relative gain of multipath component}$$

$G_\theta = \text{antenna elevation gain function}$

$\theta = \text{elevation angle between antenna and target (0 degrees)}$

$\theta_2 = \text{elevation angle between antenna and ground}$

Assuming the mixer to be linear, the output of the mixer  $P_r'$  is proportional to  $P_r$ . Since only the relative variations in power level are significant and not the absolute power levels,  $P_r'$  can be written as

$$P_r' = \frac{G(\phi_1) G(\phi_2) P_m}{R_1^2 R_2^2} \quad (\text{A-4})$$

Similarly, the output,  $P_r''$  of the preamplifier is

$$P_r'' = P_r' |H_{HP}(f)|^2 \quad (\text{A-5})$$

and the output of the postamplifier  $P_r'''$  is

$$P_r''' = P_r'' |H_{LP}(f)|^2 \quad (\text{A-6})$$

where  $|H_{HP}(f)|^2$  = preamplifier gain function  
 $|H_{LP}(f)|^2$  = postamplifier gain function  
 $f$  = IF frequency

## 2. Mathematical Models

### a. Multipath

The mathematical model of the multipath is given in equations (A-3a) and (A-3b). Since the target and radar are at the same height ( $h = 0.67$  m),  $\theta$  is zero and  $\theta_2$  is

$$\theta_2 = \tan^{-1} \frac{2h}{R} \quad (A-7)$$

Experimentally,  $|\Gamma|$  has been found to be approximately 0.5. Knowing the gain function,  $G_\theta$ , the multipath is also known as a function of distance.

### b. Antenna

The gain function of the antenna is modeled as

$$G = G_H(\phi, \theta) G_V(\phi, \theta) \quad (A-8)$$

with  $G_H$  = gain function corresponding to a horizontal 32-element linear array of dipoles with a Chebyshev illumination function to realize -30-dB side lobes.

$G_V$  = gain function corresponding to a vertical 16-element linear array of dipoles with a Chebyshev illumination function to realize -20-dB side lobes.

The array function  $\psi_H(x_H)$  or  $\psi_V(x_V)$  for a Chebyshev distribution can be written as [7]

$$\psi_H(x_H) = \frac{T_{nH}^2(a_H x_H)}{T_{nH}^2(a_H)} \quad (A-9)$$

$$\begin{aligned} T_n(\mu) &= \cos(n \cos^{-1}\mu) \quad \mu \leq 1 \\ T_n(\mu) &= \cosh(n \cosh^{-1}\mu) \quad \mu \geq 1 \end{aligned} \tag{A-10a}$$

$$x_H = \cos\left(\frac{\pi S_H}{\lambda} \sin\phi \cos\theta\right) \tag{A-10b}$$

$S_H$  = horizontal dipole spacing

$$a_H = \cosh \frac{1}{n_H} \cosh^{-1} r_H \tag{A-10c}$$

$r_H$  = ratio of peak field to side-lobe field for horizontal array (e.g., for 30-dB side lobes  $r = 31.62$ ).

$n_H$  = number of elements in horizontal array -1

$\psi_V$  is derived from a parallel development with H replaced by V

$$\text{and } X_V = \cos\left[\frac{\pi S_V}{\lambda} \sin\theta\right]$$

The effect of the ground plane is taken into account by the method of images; the ground plane is replaced by a dipole of negative polarity and spaced a half-wavelength from the given dipole. In effect one has a two element array of out-of-phase current elements  $\lambda/2$  apart.

$$G_H = D \psi_H$$

$$G_V = D \psi_V$$

where D is the element directivity function with ground plane

$$D = \cos \theta \sin [90^\circ \cos\theta \sin\phi] \tag{A-11}$$

Equations (A-10) and (A-11) are sufficient to calculate the azimuth and elevation gain functions.

### c. Preamplifier

Since only normalized values of the return power are significant, the magnitude of the gain will be unity and only the shaping will be specified.

A maximally flat high pass filter response,  $\left|H_{HP}(f)\right|^2$ , was used to represent the shaping. That is,

$$\left|H_{HP}(f)\right|^2 = 1 + \left(\frac{f_c}{f}\right)^{2N} \quad (A-12)$$

where  $f_c$  = cut-off frequency

$f$  = frequency at which response is measured

$N$  = number of filter sections

For a stationary target, the range is proportional to frequency, so that equation (A-12) can be written as

$$\left|H_{HP}(R)\right|^2 = \left(1 + \frac{R_c}{R}\right)^{2N} \quad (A-13)$$

where  $R = \frac{f}{1.302} m$  (A-14)

#### d. Postamplifier

The gain of the postamplifier  $\left|H_{LP}(f)\right|^2$  will also be represented by the shaping; a low pass maximally flat response

$$\left|H_{LP}(f)\right|^2 = \left(1 + \frac{f}{f_c}\right)^{2N} \quad (A-15a)$$

As in the preamplifier, the frequency can be expressed in terms of range and equation (A-14) becomes

$$\left|H_{LP}(R)\right|^2 = \left(1 + \frac{R}{R_c}\right)^{2N}$$

### 3. Calculated Results

Power contours at the output of the mixer  $P_r'$ , at the output of the preamplifier  $P_r''$ , and at the output of the postamplifier  $P_r'''$  were computed using the above models. The results are shown in Figures A-1 through A-3. Because of reflection symmetry about the y axis, only the results for the positive x axis were computed.



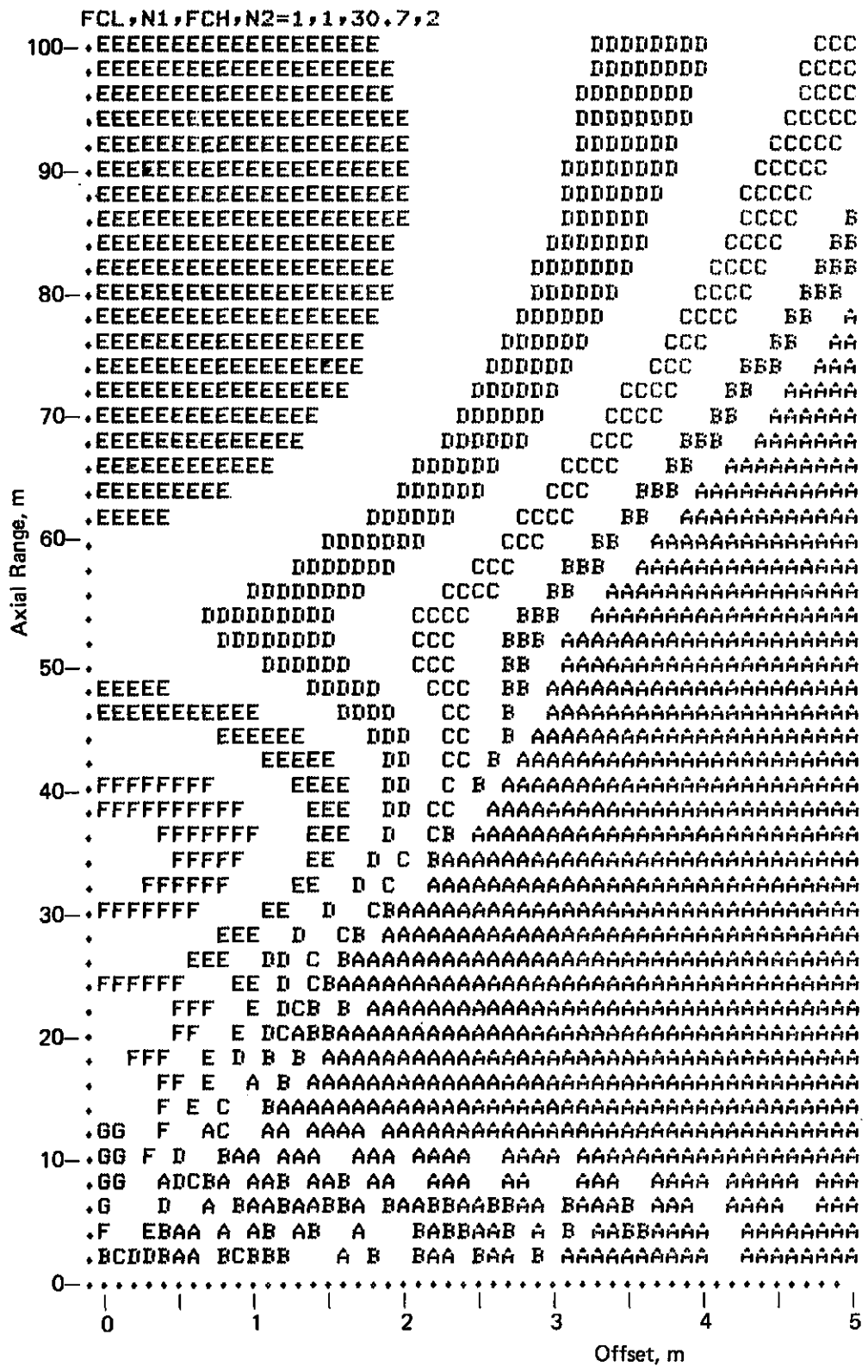


FIGURE A-2. CALCULATED DETECTION PATTERN (HIGH-PASS: 1 SECTION, CUTOFF AT 30.7 m).



The target location varied from 2 to 100 m in the axial direction and 0 to 5 m in the x direction. Letters ranging from A to H are used to represent the relative power received from a target located at that letter position. The power levels increase from A to H in approximately 10-dB steps, and each letter ranges in value about 5 dB.

For the calculation  $P_r''$ , the cutoff range was specified as 30.7 m and the slope was 6 dB/octave. For the calculation of  $P_r'''$ , the high and low pass filter cutoff frequencies (ranges) were taken from the measured composite preamplifier and postamplifier characteristics. From Figure 15, the high pass filter was modeled as a single-section filter with cutoff at 15.4 m. Similarly, the low pass filter was modeled, as a four-section filter with cutoff at 32.2 m. Using the composite filter characteristic takes into account the interaction when the preamplifier is integrated with the postamplifier.

Comparisons between the calculated and measured contours of  $P_r''$  show good agreement if letter E of Figure A-2 is the -40 dB level, shown in Figure 11. Similarly for  $P_r'''$ , when letter F of Figure A-3 is the -15 dB level shown in Figure 12, Figure A-3 demonstrates the range containment that can be achieved by shaping the postamplifier.

## B. MONOSTATIC COOPERATIVE X-BAND RADAR

### 1. Tagged Channel Operation

The detection area of the cooperative X-band radar was also determined from contours of constant power. The power returned to the radar is calculated in a two-step process. First the power received by the tag is formulated and then this power is considered to be reradiated back to the radar. That is

$$P_{TAG} = \frac{P_T G_R G_T \lambda^2}{(4 \pi R)^2} \sqrt{P_m} \quad (A-16)$$

$$P_R = \frac{L P_{TAG} G_R G_T \lambda^2}{(4 \pi R)^2} \sqrt{P_m} \quad (A-17)$$

From equations (A-16) and (A-17)

$$P_R = \frac{L P_T G_R^2 G_T^2 \lambda^4}{(4 \pi R)^4} P_m \quad (\text{A-18})$$

where  $L$  = loss in modulator  
 $G_R$  = antenna gain of radar  
 $G_T$  = antenna gain of tag

When  $G_R = G_T = G$

$$P_r = K \left( \frac{G}{R} \right)^4 P_m \quad (\text{A-19})$$

$$K = \frac{L P_T \lambda^4}{(4\pi)^4} \quad (\text{A-20})$$

The factor  $K$  is normalized to unity for the calculation of the power contours as before and  $P_m$  is given by equation (A-3). The geometry of the radar and tag for a typical power calculation is shown in Figure A-4. From the figure, the distance to the tag  $R$ , is given by

$$R = \sqrt{x^2 + y^2 + (h_1 - h_2)^2} \quad (\text{A-21a})$$

The azimuth angle  $\phi$  is given by

$$\phi = \tan^{-1} \frac{x}{y} \quad (\text{A-21b})$$

and the elevation angle  $\theta$

$$\theta = \sin^{-1} \frac{h_1 - h_2}{\sqrt{x^2 + y^2 + (h_1 - h_2)^2}} \quad (\text{A-21c})$$

The multipath angle  $\theta_2$  is

$$\theta_2 = \tan^{-1} \frac{h_1 + h_2}{\sqrt{x^2 + y^2}} \quad (\text{A-22})$$

$h_1$  = height of radar above ground = 0.675 m

$h_2$  = height of tag above ground = 0.385 m

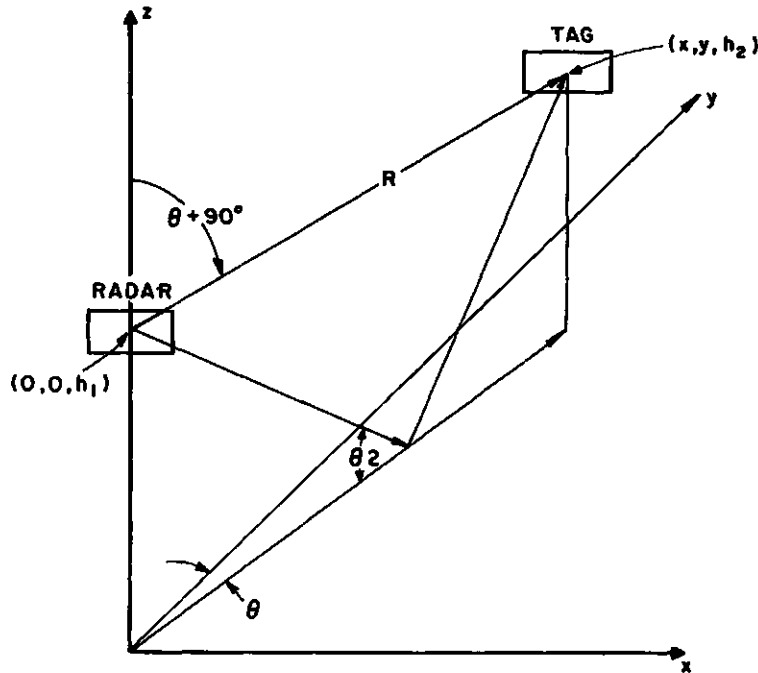


FIGURE A-4. COOPERATIVE RADAR-TAG GEOMETRY FOR COVERAGE PATTERN MEASUREMENTS.

The power contours are calculated at the output of the detector  $P_r''$  and at the output of the postamplifier,  $P_r'''$ . (See Figure 16.) The output of the detector  $P_r''$  is given by

$$P_r'' = \left(\frac{G}{R}\right)^4 P_m \quad (A-23)$$

Equation (A-23) assumes a linear detector and a flat response from the preamplifier at the tag modulation frequency. The output of the postamplifier  $P_r'''$  is given by

$$P_r''' = \left(\frac{G}{R}\right)^4 P_m |H_{LP}(f)|^2 \quad (A-24)$$

where  $|H_{LP}(f)|^2$  = gain function of the postamplifier.

The amplitude of the gain is normalized to unity and the shape is given by a maximally flat filter response as in subsection A.2.c above.

## 2. Mathematical Models

### a. Multipath

The same model is used as in subsection A.2 above with the following changes: θ is given by equation (A-21c) and θ<sub>2</sub> by equation (A-22).

b. Antenna

The gain function of the antenna is modeled as  $G = G_H(\phi, \theta) G_V(\phi, \theta)$  as before. However, the side lobe-level is only -20 dB in azimuth and elevation, and the number of elements is reduced from 32 x 16 to 16 x 8 to approximate the antenna used at X-band.

The elevation gain  $G_V(\theta)$ , is taken into account, with  $\theta$  given by equation (A-21c).

c. Preamplifier

The preamplifier is modeled as a high pass filter of unit gain. At the tag modulation frequency and over the signal bandwidth, the preamplifier is assumed to be operating in its passband so that  $|H_{HP}(f)|^2 = 1$ .

d. Postamplifier

The postamplifier is modelled as a single-section, low-pass filter with range frequency cutoff at 50 m. For example,

$$\left| H_{LP}(R) \right|^2 = \left( 1 + \frac{R}{R_c} \right)^2 \quad (A-25)$$
$$R_c = 50 \text{ m}$$

3. Calculated Results

Figure A-5 shows contours of constant power as measured at the output of the detector of the tagged channel; no shaping was used. These results are in good agreement with the measured results shown in Figure 18, when letter E of Figure A-5 is compared with the -50 dB contour of Figure 18.

Figure A-6 shows the beam confinement when a postamplifier with a shape factor corresponding to a single-section, low-pass filter is used. The cutoff range is 50 m. The output is taken at the postamplifier. Even with the simple filter, the maximum range associated with the letter E is reduced from 68 m to 58 m. Measurements were not taken at the output of the postamplifier so that comparisons cannot be made.

A fortunate departure between the measured and calculated results is the extent and depth of the multipath null. The measured results indicate that the null is not as broad or as deep as the calculated results. This may be due to the nonideal nature of the tag; i.e., it is not a perfect reflector

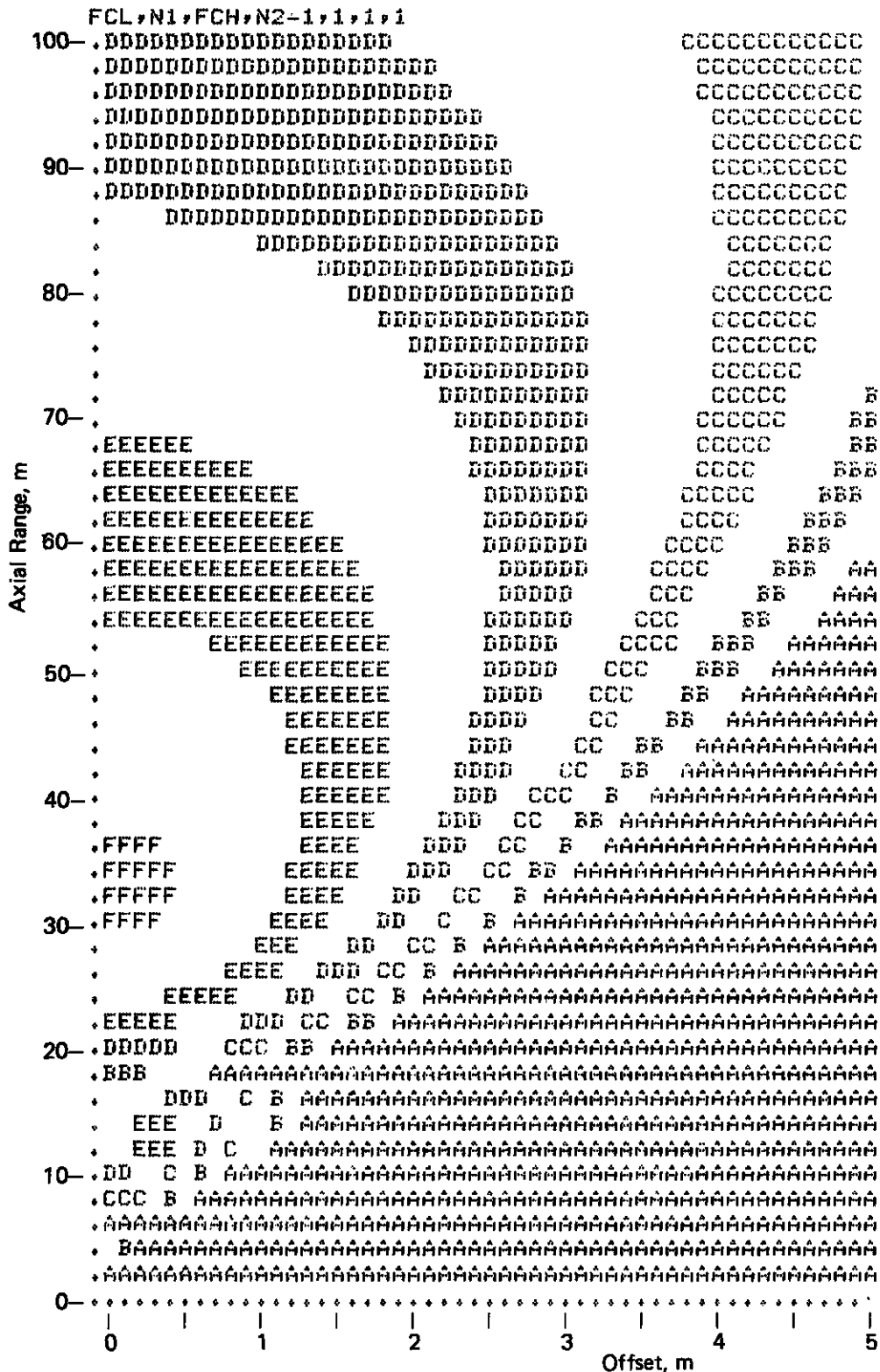


FIGURE A-5. DETECTION PATTERN FOR COOPERATIVE RADAR (OUTPUT OF DETECTOR).

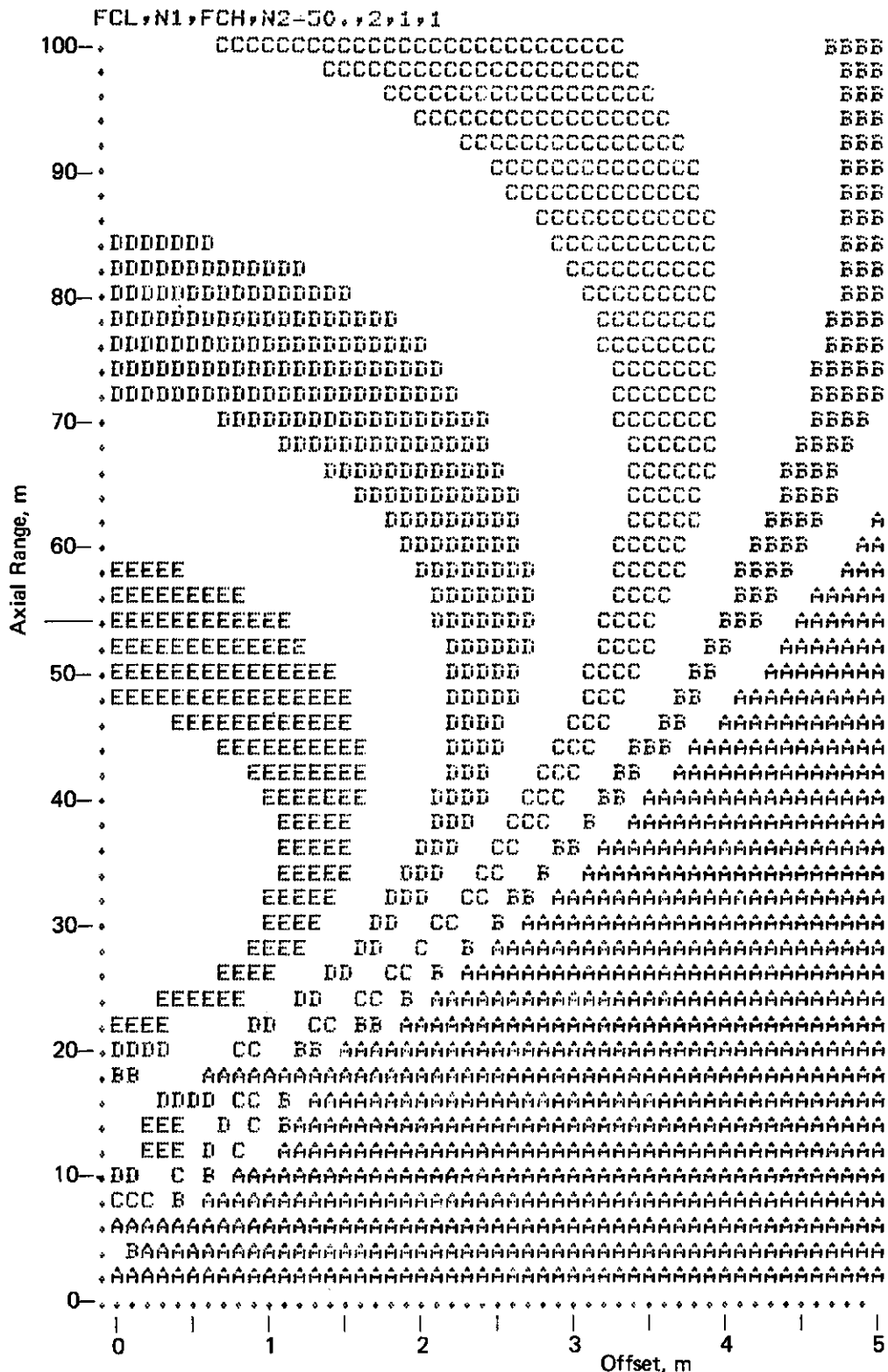


FIGURE A-6. DETECTION PATTERN OF COOPERATIVE RADAR  
(OUTPUT OF POSTAMPLIFIER).

whose radiation pattern is unaltered by the modulator as a termination. Also, the nonideal nature of the road surface contributes to a flattening of the null.

### C. MONOSTATIC NONCOOPERATIVE X-BAND (BASEBAND OPERATION)

The baseband channel of the X-band radar can be treated as a special case of the bistatic radar discussed in Section A, with  $S_0=0$ . The only other changes required are in the physical constants such as the number of antenna elements and side lobes and the amplifier cutoff ranges. From equation (A-4)

$$P_r' = \frac{G^2(\phi) P_m}{R^4} \quad (\text{A-25})$$

where  $\phi = \tan^{-1} \frac{x}{y}$

$R$  = distance from radar to target

Similarly,  $P_r'' = P_r' |H_{HP}(f)|^2$

and  $P_r''' = P_r'' |H_{LP}(f)|^2$

where  $|H_{HP}(f)|^2$  is modeled by equations (A-12) and (A-13). The conversion from frequency to range is different at X-band due to the different modulation parameters so that equation (A-14) becomes

$$R = \frac{f}{0.667} \text{ m} \quad (\text{A-26})$$

with  $f$  expressed in kHz. Similarly, the postamplifier is given by equations (A-15a) and (A-15b).

Contours of the power out of the preamplifier are shown in Figure A-7. The preamplifier was modeled as a single-section high-pass filter, with cutoff at 50 m. The antenna was modeled as a 20-dB side-lobe Chebyshev array with 16 x 8 elements. The contour represented by the letter E has a maximum range of 80 m and an axial offset of 2.7 m. The multipath null extends from 30 to 36 m. This contour approximates the -60 dB contour shown in Figure 11. The measured results show the maximum range to be about 90 m and the axial offset to be about 3 m. The measured multipath null extends from 31 to 41 m.

If one keeps in mind the large number of approximations and simplifying assumptions that have to be taken in the calculation of these antenna patterns,



the agreement between theory and measured results is quite good. The computer solution presented here thus can be used to predict with reasonable accuracy other situations not treated here.

•

•

•

•

## APPENDIX B

### SOFTWARE LISTING FOR CMS ALGORITHM

```

0000      1 ..
0000      2 ..      >CMS3   M. I.   RCA LABS 10:16:79
0000      3 ..      CDP1802 MICROPROCESSOR VERSION
0000      4 ..      FOR RSV CAR
0000      5 ..      DEVIATION, SPEED, STEERING WHEEL ANGLE
0000      6 ..      CHECK
0000      7 ..
0000      8 ..      THIS VERSION IS EQUIVALENT TO CMS1
0000      9 ..      NO SWITCHES ARE USED
0000     10 ...
0000     11 ..      STACK=#10FF
0000     12 ..      UPBUF=#1000
0000     13 ..      DNBUF=#1030
0000     14 ...
0000     15 ...
0000     16 ...
0000     17 ..      VAR=#1060
0000     18 ..      V=VAR
0000     19 ..      UCOUNT=VAR+2
0000     20 ..      DCOUNT=VAR+4
0000     21 ..      NUP=VAR+6
0000     22 ..      NDN=VAR+8
0000     23 ..      TEMP1=VAR+10
0000     24 ..      TEMP2=VAR+12
0000     25 ..      TEMP3=VAR+14
0000     26 ..      DOPRR=VAR+16
0000     27 ..      DOPRR1=VAR+18
0000     28 ..      DOPRR0=VAR+20
0000     29 ..      RRDV2=VAR+22
0000     30 ..      RANGE=VAR+24
0000     31 ..      RANGE0=VAR+26
0000     32 ..      TVAL=VAR+28
0000     33 ..      AVGUCT=VAR+30
0000     34 ..      AVGDCT=VAR+32
0000     35 ..      FLAC=VAR+34
0000     36 ..      FLAG1=VAR+35
0000     37 ..      FLAG2=VAR+37
0000     38 ..      FLAG3=VAR+39
0000     39 ..      LOLIM=VAR+41
0000     40 ..      UPLIM=VAR+43
0000     41 ...
0000     42 ...
0000     43 ...
0000     44 ...
0000     45 ..      ORC 0
0000     46 ..
F 0000 F800B3     47 ..      A.1(NEWPC)->R3.1
F 0003 F800A3     48 ..      A.0(NEWPC)->R3.0
0006 D3          49 ..      GO STATE R3      .R3 IS PC
0007 F810B2     50 NEWPC: A.1(STACK)->SP.1
000A F8FFA2     51 ..      A.0(STACK)->SP.0
000D E2         52 ..      SEX SP
000E F80FB4     53 ..      A.1(CALLS)->R4.1

```

	0011	F85EA4	54	A.0(CALLS)->R4.0
	0014	F80FB5	55	A.1(RETR)->R5.1
	0017	F86EA5	56	A.0(RETR)->R5.0
	001A	6522	57	OUT 5; DEC SP ..TURN OFF MEAS. CIRCUIT
	001C		58	...
F	001C	F800BA	59	START: A.1(SYSAC)->AR.1
F	001F	F800AA	60	A.0(SYSAC)->AR.0
F	0022	D40000	61	CALL DISP ..DISPLAY "SYSTEM ACTIVE"
	0025	D40F8CFFFF	62	CALL DELAY; ,#FFFF
	002A	D40F8CFFFF	63	CALL DELAY; ,#FFFF ..ABOUT 3 SECS
	002F	F810BA	64	CLEAN: A.1(FLAG3)->AR.1
	0032	F887AA	65	A.0(FLAG3)->AR.0
	0035	4A	66	LDA AR
F	0036	3200	67	BZ CLEN
	0038	F88052	68	#80->@SP
	003B	6122	69	OUT 1;DEC SP ..CLEAR DISPLAY
	003D	F80052	70	CLEN: 0->@SP
	0040	6622	71	OUT 6;DEC SP ..TURN OFF WARNING
	0042	F810BA	72	A.1(FLAG)->RA.1
	0045	F882AA	73	A.0(FLAG)->RA.0
	0048	F800	74	LDI 0
	004A	5A	75	STRA ...FLAG=0
	004B	1A5A	76	INC AR;STRA ...FLAG1=0
	004D		77	.....
	004D	D40F8C0001	78	FIRST: CALL DELAY; ,0,1
	0052	F810BA	79	A.1(FLAG3)->AR.1
	0055	F887AA	80	A.0(FLAG3)->AR.0
	0058	F8005A	81	#0->@AR
	005B	3C2F	82	BN1 CLEAN ..EF1=1 SPEED<SPEED CUTOFF
	005D	7B	83	SEQ
F	005E	D40000	84	LOOK: CALL GETRAN ...ACQ. DATA,DEVIATION CHECK
	0061	3B2F	85	RNF CLEAN
	0063	3D2F	86	BN2 CLEAN...EF2=1 S.W. ANGLE>NUM.NC
	0065	7A	87	REQ
	0066		88	...
	0066		89	...
	0066	D40E491070	90	CAON: CALL LOADOP; ,A(DOPRR)
F	006B	D40C2D0000	91	CALL SMOP; ,A(RRTHR) ...RR>RRTHR
F	0070	9FFA80CA0000	92	AC.1.AND.#80;LBZ NOALAR1
	0076	F810BA	93	A.1(FLAG)->AR.1
	0079	F882AA	94	A.0(FLAG)->AR.0
	007C	F8805A	95	LDI #80;STR AR ...FLAG=80
F	007F	1A4AC20000	96	INC AR;LDA AR;LBZ NOALAR ...FLAG1=0->N
	0084	D40E491070	97	CALL LOADOP; ,A(DOPRR)
	0089	D40C2D1072	98	CALL SMOP; ,A(DOPRR1)
F	008E	D40000	99	CALL ABSAC ..(DOPRR-DOPRR1)
F	0091	D40C2D0000	100	CALL SMOP; ,A(DELRR) ...-DELRR
F	0096	9FFA80C20000	101	AC.1.AND.#80; LBZ NOALAR ...DIFF. RR>DE
	009C	D40E49107A	102	CALL LOADOP; ,A(RANGE0)
	00A1	D40C2D107B	103	CALL SMOP; ,A(RANGE) ...PRESENT R<PREVIO
F	00A6	9FFA80CA0000	104	AC.1.AND.#80;LBZ NOALAR
	00AC	9FB0BFA0	105	AC.1->R0.1;AC.0->R0.0
	00B0	D40C2D108B	106	CALL SMOP; ,A(UPLIM) ...DIFF. RANGE<UPLI
F	00B5	9FFA80C20000	107	AC.1.AND.#80;LBZ NOALAR

	00BB	90BF80AF	108	R0.1->AC.1;R0.0->AC.0
	00BF	D40C2D1089	109	CALL SMOP; ,A(LOLIN) ...DIFF. RANGE>LOLI
F	00C4	9FFA80CA0000	110	AC.1.AND.#80;LBNZ NOALAR
	00CA	D40E491078	111	CALL LOADOP; ,A(RANGE)
F	00CF	D40C2D0000	112	CALL SMOP; ,A(RCUTOF) ..RANGE<RCUTOF
F	00D4	9FFA80C20000	113	AC.1.AND.#80;LBZ NOALAR
	00DA	F801526622	114	ALARM:1->@SP;OUT 6;DEC SP ...TURN ON ALARM
	00DF	D40E491078	115	CALL LOADOP; ,A(RANGE)
	00E4	D40E57107A	116	CALL STOROP; ,A(RANGE0) ...RANGE->RANGE
	00E9	D40E491070	117	CALL LOADOP; ,A(DOPRR)
	00EE	D40E571072	118	CALL STOROP; ,A(DOPRR1) ...DOPRR->DOPRR
	00F3	F810BA	119	A.1(FLAG)->AR.1
	00F6	F882AA	120	A.0(FLAG)->AR.0
	00F9	4A5A	121	LDA AR; STR AR ...FLAG->FLAG1
F	00FB	D40000	122	CALL RANUP ...CALCULATE UPLIM
	00FE	D40E57108B	123	CALL STOROP; ,A(UPLIM) ...UPLIM=.078*DOP
	0103		124	..... DISPLAY SUBROUTINE
F	0103	D40F7A0000000020	125	FORMAT:CALL MOVB,A(MESOUT),A(OUTBF),32
F	010B	F800BA	126	A.1(OUTBF)->AR.1
F	010E	F802AA	127	A.0(OUTBF+2)->AR.0
	0111	D40E491078	128	CALL LOADOP; ,A(RANGE)
	0116	D40FA20401	129	CALL CVT; ,4,1
	011B	D40E491070	130	CALL LOADOP; ,A(DOPRR)
F	0120	F80AAA	131	A.0(OUTBF+10)->AR.0
	0123	F82B5A	132	T'+'->@AR
F	0126	9FFA803200	133	AC.1.AND.#80; BZ CHSIGN
	012B	F82D5A	134	T'-'->@AR
F	012E	D40000	135	CALL ABSAC
	0131	1A	136	CHSIGN: INC AR
	0132	D40FA20401	137	CALL CVT; ,4,1
	0137	D40E491060	138	CALL LOADOP; ,A(V)
F	013C	F813AA	139	A.0(OUTBF+19)->AR.0
	013F	D40FA20200	140	CALL CVT; ,2,0
	0144	D40E491066	141	CALL LOADOP; ,A(NUP)
F	0149	F81AAA	142	A.0(OUTBF+26)->AR.0
	014C	D40FA20300	143	CALL CVT; ,3,0
F	0151	F800AA	144	A.0(OUTBF)->AR.0
F	0154	D40000	145	CALL DISP
	0157	C0004D	146	LBR FIRST .... TO STORE R,RR PUT 3 NOP
	015A	D40E491083	147	CALL LOADOP; ,A(FLAG1)
	015F	9FFB80	148	AC.1.XOR.#80
F	0162	C20000	149	LBZ CTD
	0165	C0004D	150	LBR FIRST
	0168	00	151	CTD: IDLE .... TO STORE R,RR PUT NOP (C4)
	0169		152	..... STORE R,RR SUBROUTINE
	0169	D40E491078	153	CALL LOADOP; ,A(RANGE)
	016E	8FFD40	154	GLO AC;SDI #40
F	0171	C30000	155	LBDF ZIP
	0174	8FB0	156	GLO AC;PHI R0
	0176	D40E491070	157	CALL LOADOP; ,A(DOPRR)
	017B	8FA0	158	GLO AC;PLO R0
	017D	D40E491085	159	CALL LOADOP; ,A(FLAG2)
	0182	905F1F	160	CHI R0;STR AC;INC AC
	0185	805F1F	161	GLO R0;STR AC;INC AC

0188	D40E571085	162	CALL STOROP; ,A(FLAG2)
018D	C0004D	163	LBR FIRST
0190	00	164	ZIP: IDL
0191		165	....
0191		166	.... TURN OFF ALARM SUBROUTINE
0191		167	....
0191	F810BA	168	NOALR1: A.1(FLAG)->AR.1
0194	F832AA	169	A.0(FLAC)->AR.0
0197	F8003A	170	LDI #0;STR AR ... FLAG=0
019A	F800526622	171	NOALAR: 0->@SP;OUT 6;DEC SP ...TURN OFF ALA
019F	D40E491078	172	CALL LOADOP; ,A(RANGE)
01A4	D40E57107A	173	CALL STOROP; ,A(RANGE0) .. RANGE->RANGE0
01A9	D40E491070	174	CALL LOADOP; ,A(DOPRR)
01AE	D40E571072	175	CALL STOROP; ,A(DOPRR1) ... DOPRR->DOPRR
01B3	F810BA	176	A.1(FLAG)->AR.1
01B6	F832AA	177	A.0(FLAC)->AR.0
01B9	4A5A	178	LDA AR;STR AR ... FLAG->FLAG1
F 01BB	D40000	179	CALL RANUP ... CALCULATE UPLIM
01BE	D40E57108B	180	CALL STOROP; ,A(UPLIM) .. UPLIM=.078*DO
01C3	C00103	181	LBR FORMAT ... BRANCH TO DISPLAY
01C6		182	...
01C6		183	...
01C6		184	...RANGE DIFFERENCE UPER LIMIT CALCULATION
01C6		185	... UPLIM=.078*DOPRR
01C6		186	...
01C6	D40E491070	187	RANUP: CALL LOADOP; ,A(DOPRR)
F 01CB	D40C4F0000	188	CALL MPYOP; ,A(DEC5)
F 01D0	F800BD	189	A.1(DEC40)->MA.1
F 01D3	F800AD	190	A.0(DEC40)->MA.0
01D6	D40D5F	191	CALL DIVQ .. UPLIM=1.25*DOPRR
01D9	D5	192	EXIT
01DA		193	.. >ABSAC J.M.C. RCA LABS
01DA		194	..
01DA		195	.... COMPUTE ABS VALUE OF AC
01DA		196	..
F 01DA	9FFA80C20000	197	ABSAC: AC.1.AND.#80; LBZ ABSEX
01E0	8FFBFFFC01AF	198	AC.0.XOR.#FF+1->AC.0 .. WAS NEG
01E6	9FFBFF	199	AC.1.XOR.#FF .. COMPLEMENT IT
01E9	3BEDFC01	200	BNF *+4; +1
01ED	BF	201	->AC.1
01EE	D5	202	ABSEX: EXIT
01EF		203	...
01EF		204	...
01EF		205	...FAST VERSION-- OBTAIN VEHICLE SPEED
01EF		206	...
01EF		207	...
01EF		208	...
01EF	F88052	209	DISP:#80->@SP
01F2	6122	210	OUT 1; DEC SP ... CLEAR MEMORY
01F4	F808AC	211	8->CR.0
01F7	2C8C3AF7	212	CLP: DEC CR; CR.0; BNZ CLP
01FB	F820AC	213	32->CR.0
01FE	EAEAEA	214	DGO: SEX AR;SEX AR;SEX AR .. MORE SEX
0201	4A2A	215	LDA AR;DEC AR ..STALL A WHILE

0203	61	216	OUT 1	..ZING IT
0204	8CFF01AC	217	CR.0-1->CR.0	..SLOW DECREMENT
0208	CA01FEE2	218	LBNZ DGO; SEX SP	
020C	FB0152	219	1->@SP	
020F	6222	220	OUT 2; DEC SP	..MAKE SURE IT IS ON
0211	D5	221	EXIT	
0212		222	...	
0212		223	...	
0212		224	...	
0212		225	W=1; X=3; Y=4; Z=5	
0212		226	..	
0212	69FA03FB03	227	GETRAN: INP W; .AND.3.XOR.3	
0217	CA0212	228	LBNZ GETRAN	
021A	6322	229	OUT 3; DEC SP	..PRESET STROBE
021C	69FA03FB01	230	GET1: INP W; .AND.3.XOR.1	
F 0221	CA0000	231	LBNZ GET11	
0224	6DFBFFFF02AF	232	INP Z; .XOR.#FF-2->AC.0	
F 022A	FC00C20000	233	CLRU: ADI 0; LBZ GETX	
022F	BFFA80	234	AC.0; .AND.#80	
F 0232	CA0000	235	LBNZ GETX	
0235	FB00BF	236	0->AC.1	
0238	D40E571066	237	CALL STOROP; ,A(NUP)	
F 023D	C00000	238	LBR PKUP	
0240	FC0069FA04	239	GET 11: ADI #0; INP W; .AND.4	
0245	76	240	RSHR	
0246	CA021C	241	LBNZ GET1	
0249	6DFBFFFF02AF	242	INP Z; .XOR.#FF-2->AC.0	
024F	C0022A	243	LBR CLRU	
0252	F810B0	244	PKUP: A.1(UPBUF)->R0.1	
0255	FB00A0	245	A.0(UPBUF)->R0.0	
0258	1F	246	INC AC	
0259	6B50	247	GET2: INP Y; ->@R0	..READ FIFO
025B	10	248	INC Y	
025C	6C50	249	INP Y; ->@R0	
025E	10	250	INC R0	
025F	2F8FCA0259	251	DEC AC; AC.0; LBNZ GET2	
0264		252	..	
0264		253	...	
0264		254	..	
0264	69FA03FB01	255	GET3: INP W; .AND.3.XOR.1	
0269	3A64	256	BNZ GET3	
026B	6322	257	OUT 3; DEC SP	..PRESET STROBE
026D	69FA03FB03	258	GET4: INP W; .AND.3.XOR.3	
F 0272	CA0000	259	LBNZ GET 44	
0275	6DFBFFFF02AF	260	INP Z; .XOR.#FF-2->AC.0	
F 027B	FC00C20000	261	CLRD: ADI 0; LBZ GETX	
0280	BFFA80	262	AC.0; .AND.#80	
F 0283	CA0000	263	LBNZ GETX	
0286	FB00BF	264	0->AC.1	
0289	D40E571068	265	CALL STOROP; ,A(NDN)	
F 028E	C00000	266	LBR PKDN	
0291	FC0069FA04	267	GET 44: ADI #0; INP W; .AND.4	
0296	76	268	RSHR	
0297	CA026D	269	LBNZ GET4	

029A	6DFBFFFF02AF	270	INP Z; .XOR. #FF-2->AC.0
02A0	C0027B	271	LBR CLRD
02A3	F810B0	272	PKDN: A.1(DNBUF)->R0.1
02A6	F830A0	273	A.0(DNBUF)->R0.0
02A9	1F	274	INC AC
02AA	6B50	275	GET5: INP X;->@R0 ..READ FIFO
02AC	10	276	INC R0
02AD	6C50	277	INP Y;->@R0
02AF	10	278	INC R0
02B0	2F8F3AAA	279	DEC AC; AC.0; BNZ GET5
02B4	F810B0	280	A.1(UPBUF)->R0.1
02B7	F800A0	281	A.0(UPBUF)->R0.0
02BA	D40E491066	282	CALL LOADOP; ,A(NUP)
02BF	2F	283	DEC AC
F 02C0	D40000	284	CALL AUPDN
02C3	D40E571062	285	CALL STOROP; ,A(UCOUNT)
02C8	F800AEBE	286	0->NQ.0, NQ.1
02CC	D40CA11066	287	CALL DIVOP; ,A(NUP)
02D1	D40E57107E	288	CALL STOROP; ,A(AVGUCT)
02D6	F810B0	289	A.1(DNBUF)->R0.1
02D9	F830A0	290	A.0(DNBUF)->R0.0
02DC	D40E491068	291	CALL LOADOP; ,A(NDN)
02E1	2F	292	DEC AC
F 02E2	D40000	293	CALL AUPDN
02E5	D40E571064	294	CALL STOROP; ,A(DCOUNT)
02EA	F800AEBE	295	0->NQ.0, NQ.1
02EE	D40CA11068	296	CALL DIVOP; ,A(NDN)
02F3	D40E571080	297	CALL STOROP; ,A(AVGUCT)
02F8	F800BC	298	0->CR.1
02FB	D40E491066	299	CALL LOADOP; ,A(NUP)
0300	8FAC	300	AC.0->CR.0
F 0302	D40E490000	301	CALL LOADOP; ,A(DELRAN)
0307	9F73	302	GHI AC;STXD
0309	8F73	303	GLO AC;STXD
030B	D40E49107E	304	CALL LOADOP; ,A(AVGUCT)
0310	9F73	305	GHI AC;STXD
0312	8F73	306	GLO AC;STXD
0314	F810B0	307	A.1(UPBUF)->R0.1
0317	F800A0	308	A.0(UPBUF)->R0.0
031A	40AF	309	@R0!->AC.0
031C	40FA0F73	310	@R0!.AND.15;STXD
0320	8F7312	311	GLO AC;STXD;INC SP
0323	40AF	312	CHKUP: @R0!->AC.0
0325	F5AA	313	SD;->AR.0
0327	12	314	INC SP
0328	40FA0FBF	315	@R0!.AND.15->AC.1
032C	75BA	316	SDB ;->AR.1
032E	12	317	INC SP
032F	8AF5AA	318	AR.0;SD;->AR.0
0332	12	319	INC SP
0333	9A75BA	320	AR.1;SDB ;->AR.1
F 0336	C30000	321	LBDP AH1
0339	8AFBFFFC01AA	322	AR.0.XOR.#FF+1->AR.0
033F	9AFBFFFA0F	323	AR.1.XOR.#FF.AND.15

	0344	7C00BA	324		ADCI #0;->AR.1
	0347	12	325	AH1:	INC SP
	0348	8AF712	326		AR.0;SM;INC SP
	034B	9A77	327		AR.1;SMB
F	034D	C30000	328		LBDF GEREX
F	0350	2C8CC20000	329		DEC CR;CR.0;LBZ DEVDN
	0355	22222222	330		DEC SP;DEC SP;DEC SP;DEC SP
	0359	9F738F7312	331		AC.1;STXD;AC.0;STXD;INC SP
	035E	C00323	332		LBR CHKUP
	0361	F800BC	333	DEVDN:	0->CR.1
	0364	D40E491068	334		CALL LOADOP; ,A(NDN)
	0369	8FAC	335		AC.0->CR.0
F	036B	D40E490000	336		CALL LOADOP; ,A(DELTRAN)
	0370	9F73	337		GHI AC;STXD
	0372	8F73	338		GLO AC;STXD
	0374	D40E491080	339		CALL LOADOP; ,A(AVGDCT)
	0379	9F73	340		GHI AC;STXD
	037B	8F73	341		GLO AC;STXD
	037D	F810B0	342		A.1(DNBUF)->R0.1
	0380	F830A0	343		A.0(DNBUF)->R0.0
	0383	40AF	344		@R0!->AC.0
	0385	40FA0F73	345		@R0!.AND.15;STXD
	0389	8F7312	346		GLO AC;STXD;INC SP
	038C	40AF	347	CHKDN:	@R0!->AC.0
	038E	F5AA	348		SD;->AR.0
	0390	12	349		INC SP
	0391	40FA0FBF	350		@R0!.AND.15->AC.1
	0395	75BA	351		SDB;->AR.1
	0397	12	352		INC SP
	0398	8AF5AA12	353		AR.0;SD;->AR.0;INC SP
	039C	9A75BA	354		AR.1;SDB;->AR.1
F	039F	C30000	355		LBDF AH2
	03A2	8AFBFFFC01AA	356		AR.0.XOR.#FF+1->AR.0
	03A8	9AFBFFFA0F	357		AR.1.XOR.#FF.AND.15
	03AD	7C00BA	358		ADCI #0;->AR.1
	03B0	12	359	AH2:	INC SP
	03B1	8AF712	360		AR.0;SM;INC SP
	03B4	9A77	361		AR.1;SMB
F	03B6	C30000	362		LBDF GEREX
F	03B9	2C8CC20000	363		DEC CR;CR.0;LBZ DEVON
	03BE	22222222	364		DEC SP;DEC SP;DEC SP;DEC SP
	03C2	9F738F7312	365		AC.1;STXD;AC.0;STXD;INC SP
	03C7	C0038C	366		LBR CHKDN
	03CA	D40E491066	367	DEVON:	CALL LOADOP; ,A(NUP)
F	03CF	8FFF01C20000	368		GLO AC;SMI 1;LBZ CHK1
	03D5	D40E491068	369		CALL LOADOP; ,A(NDN)
F	03DA	8FFF01C20000	370		GLO AC;SMI 1;LBZ CHK1
F	03E0	C00000	371		LBR COMPRA
	03E3	D40E49107E	372		CHK1:CALL LOADOP; ,A(AVGUCT)
	03E8	D40C2D1080	373		CALL SMOP; ,A(AVGDCT)
	03ED	D401DA	374		CALL ABSAC
F	03F0	D40C2D0000	375		CALL SMOP; ,A(DELTRAN)
	03F5	9FFA80FC00	376		AC.1.AND.#80;ADI 0
F	03FA	C20000	377		LBZ GEREX

03FD	D40E491080	378	COMPRA:	CALL LOADOP; , A(AVGDCCT)
0402	8FA0	379		GLO AC;PLO R0
0404	9FFC05B0	380		GHI AC;ADI #5;PHI R0
0408	40AA	381		@R0!->AR.0
040A	D40E49107E	382		CALL LOADOP; , A(AVGUCT)
040F	8FA0	383		GLO AC;PLO R0
0411	9FFC05B0	384		GHI AC;ADI #5;PHI R0
F 0415	40528AF4AF	385		@R0!->@SP;AR.0;ADD;PLO AC
F 041A	CB0000	386		LBNF DAV
F 041D	F801BF	387		1->AC.1
F 0420	C00000	388		LBR DAV1
0423	F800BF	389	DAV:	0->AC.1
0426	D40E57107B	390	DAV1:	CALL STOROP; , A(RANGE)
042B	D40E491080	391		CALL LOADOP; , A(AVGDCCT)
0430	8FFEA0	392		GLO AC;SHL;PLO R0
0433	9F7EFC08B0	393		GHI AC;SHLC;ADI #8;PHI R0
0438	40BF	394	AC3:	@R0!->AC.1
043A	40AF	395		@R0!->AC.0
043C	8FAA9FBA	396		AC.0->AR.0;AC.1->AR.1
0440	D40E49107E	397		CALL LOADOP; , A(AVGUCT)
0445	8FFEAD	398		GLO AC;SHL;PLO MA
0448	9F7EFC08BD	399		GHI AC;SHLC;ADI #8;PHI MA
044D	9ABF8AAF	400	AC1:	AR.1->AC.1;AR.0->AC.0
0451	D40C31	401		CALL SM
0454	D40E571070	402		CALL STOROP; , A(DOPRR)
0459	F800BCF805AC	403		0->CR.1;#5->CR.0
045F	9FFE9F76BF	404	RD2:	GHI AC;SHL;GHI AC;SIIRC;PHI AC
0464	8F76AF	405		GLO AC;SHRC;PLO AC
0467	2CBCCA045F	406		DEC CR;CR.0;LBNZ RD2
046C	D40E571089	407		CALL STOROP; , A(LOLIM)
0471	FF00	408		SMI 0
0473	D5	409	GETRX:	EXIT
0474	FC00D5	410	GEREX:	ADI #0;EXIT
0477	F810BA	411	GETX:	A.1(FLAG3)->AR.1
047A	F887AA	412		A.0(FLAG3)->AR.0
047D	F8015A	413		#1->@AR
0480	FC00D5	414		ADI #0;EXIT
0483		415	...	
0483		416	...	
0483		417	..	AVERAGE UPAND DOWN COUNT
0483	40AA	418	AUPDN:	@R0!->AR.0
0485	4073	419		@R0!;STXD
0487	8A7312	420		AR.0;STXD;INC SP
048A	10102F	421	AVE:	INC R0;INC R0;DEC AC
048D	8FCA048A	422		AC.0;LBNZ AVE
0491	40F5AF12	423		@R0!;SD;->AC.0;INC SP
0495	4075FA0FBF	424		@R0!;SDB;.AND.15->AC.1
049A	D5	425		EXIT
049B		426	...	
049B		427	...	TABLE FOR RANCE CONSTANTS
049B		428	...	>RTAB 8:27:1979
049B		429	...	
051E		430	...	ORG #51E
051E		431	..	

051E	FEF6EFE7E0DAD4CE	432	,254,246,239,231,224,218,212,206,201,196,191
0530	9F9C989593908D8B	433	,159,156,152,149,147,144,141,139,136,134,13
0542	7372706E6D6B6A68	434	,115,114,112,110,109,107,106,104,103,101,1
0556	5857	435	,88,87
0558	5655545453525150	436	,86,85,84,84,83,82,81,80,79,78,78,77,76,75,
056F	4444434342414140	437	,68,68,67,67,66,65,65,64,64,63,63,62,62,61,
0586	3938383737373636	438	,57,56,56,55,55,55,54,54,53,53,53,52,52,52,
059D	3030302F2F2F2E2E	439	,48,48,48,47,47,47,46,46,46,46,45,45,45,44,
05B3	2A2A2A2A29292929	440	,42,42,42,42,41,41,41,41,41,40,40,40,40,40,39,
05CA	2525252525242424	441	,37,37,37,37,37,36,36,36,36,36,36,35,35,35,
05E2	2121212121212020	442	,33,33,33,33,33,33,32,32,32,32,32,32,32,32,
05FA	1E1E1E1E1E1D1D1D	443	,30,30,30,30,30,29,29,29,29,29,29,29,29,29,
0611	1C1B1B1B1B1B1B1B	444	,28,27,27,27,27,27,27,27,27,27,27,26,26,26,
0629	1919191919191919	445	,25,25,25,25,25,25,25,25,25,25,24,24,24,24,
0641	1717171717171717	446	,23,23,23,23,23,23,23,23,23,23,23,23,22,22,
0657	1616161616151515	447	,22,22,22,22,22,21,21,21,21,21,21,21,21,21,
066F	1414141414141414	448	,20,20,20,20,20,20,20,20,20,20,20,20,20,20,
0684	1313131313131313	449	,19,19,19,19,19,19,19,19,19,19,19,19,19,19,
083C		450	ORG #083C
083C	0AE10AB70A3309E4	451	,2785,2695,2611,2532,2457,2387,2321,2258,219
0838	076B0741071806F2	452	,1899,1857,1816,1778,1741,1705,1671,1638,16
0874	05A095880570055A	453	,1440,1416,1392,1370,1347,1326,1305,1285,12
0890	048804780469045A	454	,1160,1144,1129,1114,1099,1085,1071,1057,10
08AC	03CB03C003B503AA	455	,971,960,949,938,928,918,908,898,889,879,87
08CE	032B0323031B0314	456	,811,803,795,788,781,773,766,759,752,746,73
08F0	02B802B202AD02A7	457	,696,690,685,679,673,668,663,658,652,647,64
0912	0262025D02590254	458	,610,605,601,596,592,588,584,580,576,572,56
0936	021B021702140210	459	,539,535,532,528,525,522,519,515,512,509,50
0958	01E501E301E001DD	460	,485,483,480,477,474,472,469,466,464,461,45
097C	01B701B501B301B1	461	,439,437,435,433,430,428,426,424,422,419,41
09A0	0191018F018D018C	462	,401,399,397,396,394,392,390,388,386,385,38
09C4	01710170016E016C	463	,369,368,366,364,363,361,360,358,357,355,35
09E6	0157015601550153	464	,343,342,341,339,338,336,335,334,332,331,33
0A0A	0140013E013D013C	465	,320,318,317,316,315,314,313,311,310,309,30
0A2E	012B012A01290128	466	,299,298,297,296,295,294,293,292,291,290,28
0A52	0119011801170116	467	,281,280,279,278,277,276,275,274,274,273,2
0A76	0109	468	,265
0A78	0108010701060105	469	,264,263,262,261,261,260,259,258,257,257,25
0A96	00FC00FB00FA00FA	470	,0,252,0,251,0,250,0,250,0,249,0,248,0,247,
0AAC	00F400F300F200F2	471	,0,244,0,243,0,242,0,242,0,241,0,240,0,240,
0AC4	00EC00EB00EA00EA	472	,0,236,0,235,0,234,0,234,0,233,0,232,0,232,
0ADC	00E400E300E300E2	473	,0,228,0,227,0,227,0,226,0,225,0,225,0,224,
0AF4	00DD00DC00DB00DB	474	,0,221,0,220,0,219,0,219,0,218,0,218,0,217,
0B0C	00D600D500D500D4	475	,0,214,0,213,0,213,0,212,0,212,0,211,0,211,
0B24	00CF00CF00CE00CE	476	,0,207,0,207,0,206,0,206,0,205,0,205,0,204,
0B3C	00C900C900C800C8	477	,0,201,0,201,0,200,0,200,0,199,0,199,0,198,
0B54	00C400C300C300C2	478	,0,196,0,195,0,195,0,194,0,194,0,193,0,193,
0B6C	00BE00BE00BD00BD	479	,0,190,0,190,0,189,0,189,0,189,0,188,0,188,
0B84	00B900B900B800B8	480	,0,185,0,185,0,184,0,184,0,184,0,183,0,183,
0B9C	00B400B400B400B3	481	,0,180,0,180,0,180,0,179,0,179,0,178,0,178,
0BB4	00B000AF00AF00AF	482	,0,176,0,175,0,175,0,175,0,174,0,174,0,174,
0BCC	00AB00AB00AB00AA	483	,0,171,0,171,0,171,0,170,0,170,0,170,0,169,
0BE4	00A700A700A700A6	484	,0,167,0,167,0,167,0,166,0,166,0,166,0,165,
0BFC	00A300A3	485	,0,163,0,163

0C00		486	...
0C00		487	...
0C00		488	...
0C00		489	...
0C00		490	OUTBF=#1090
0C00		491	...
0700		492	ORG #0700
0700	2020202020	493	SYSAC: ,32,32,32,32,32
0705	20202020	494	,32,32,32,32
0709	53595354454D20	495	,T'SYSTEM',32
0710	414354495645	496	,T'ACTIVE'
0716	2020202020	497	,32,32,32,32,32
071B	2020202020	498	,32,32,32,32,32
0720		499	...
0720		500	...
0720	523D58582E5820	501	MESOUT: ,T'R=XX.X',32
0727	52523D2D58582E58	502	,T'RR=+XX.X',32,32
0731	533D58582020	503	,T'S=XX',32,32
0737	4E55503D585858	504	,T'NUP=XXX'
073E	202020	505	,32,32,32
0741		506	...
0741	00A0	507	RRTHR: ,0,160
0743	003C	508	DELRR: ,0,60
0745	000A	509	SCUTOF: ,0,10
0747	00FA	510	RCUTOF: ,0,250
0749	0010	511	DELCNT: ,0,16
074B	000D	512	DELRRAN: ,0,13
074D	0005	513	DEC5: ,0,5
074F	002B	514	DEC40: ,0,40
0751		515	PEND:END

## APPENDIX C

### SOFTWARE LISTING FOR ARITHMETIC SUBROUTINE GETRAN

FL LOC	COSMAC CODE	LNNO	SOURCE LINE
	0000	1	..COPYRIGHT 1976 RCA CORPORATION
	0000	2	.. COSMAC ARITHMETIC SUBROUTINE PACKAGE
	0C00	3	ORG #C00       ..**FOR RADAR CRUISE CONTROL
	0C00	4	..
	0C00	5	.. VERSION 1.1 FOR CDP1802
	0C00	6	..
	0C00	7	.. EXTRACTED FOR BINARY ARITHMETIC
	0C00	8	.. AND CONVERSIONS FOR DECIMAL
	0C00	9	.. OCCUPIES 1K BYTES
	0C00	10	..
	0C00	11	..
	0C00	12	.. DESIGNED FOR STANDARD CSDP SUBROUTINE CA
	0C00	13	..
	0C00	14	.. FOR STANDARD LINKAGE,
	0C00	15	SP= #02 ...IT SHOULD BE THE STACK POINTER.
	0C00	16	PC= #03 ...IT IS THE PROGRAM COUNTER
	0C00	17	.. USED BY THESE SUBROUTINES.
	0C00	18	CALL= #04 ...IT SHOULD POINT TO THE ROUTINE
	0C00	19	.. WHICH EFFECTS SUBROUTINE CALLS.
	0C00	20	RETN= #05 ...IT SHOULD POINT TO THE ROUTINE
	0C00	21	.. WHICH EFFECTS SUBROUTINE RETURN.
	0C00	22	LINK= #06 ...IT SHOULD POINT TO CALL PARAM
	0C00	23	.. .. (USUALLY OPERAND ADDRESSES AND/OR CON
	0C00	24	..THE FOLLOWING REGISTERS MUST BE ASSIGNED
	0C00	25	AR= #0A ..(USED FOR RESULT ADDRESS)
	0C00	26	NR= #0B ..(USED FOR RESULT DIGIT COUNT)
	0C00	27	.. 16-BIT BINARY ARITHMETIC ROUTINES
	0C00	28	.. THE FOLLOWING REGISTERS MUST BE ASSIGNED
	0C00	29	AC =#0F ..16-BIT ACCUMULATOR=RF
	0C00	30	MQ =#0E ..16-BIT ACCUMULATOR=RE EXTENSION
	0C00	31	MA =#0D ..(TEMPORARY) OPERAND MEMORY ADDRESS.
	0C00	32	CR =#0C .. (TEMPORARY) SCRATCHPAD AND COUNTER.
	0C00	33	..
	0C00	34	..
	0C00	35	.. SWAP AC WITH MQ REGISTERS
	0C00 9E	36	SWAPAQ: CHI MQ .. SAVE MQ.1
	0C01 AC	37	PLO CR .. IN CR.0 (COULD HAVE PUSHED ON STA
	0C02 9F	38	CHI AC .. NOW AC.1 TO MQ.1
	0C03 BE	39	PHI MQ
	0C04 BE	40	GLO MQ .. SAVE MQ.0
	0C05 BF	41	PHI AC .. IN AC.1
	0C06 BF	42	GLO AC .. THEN AC.0 TO MQ.0
	0C07 AE	43	PLO MQ
	0C08 9F	44	CHI AC .. NOW SAVED MQ.0 TO AC.0
	0C09 AF	45	PLO AC
	0C0A BC	46	GLO CR .. FINALLY SAVED MQ.1
	0C0B BF	47	PHI AC .. TO AC.1
	0C0C P5	48	SEP RETN
	0C0D	49	.. 16-BIT SUBTRACT AC FROM CONSTANT
	0C0D	50	.. *****AC= CONSTANT-AC
	0C0D	51	.. ***** (TO CALL, WRITE) *****
	0C0D	52	.. *****CALL SDCON ; ,CONSTANT
	0C0D 86	53	SDCON: GLO LINK .. (ESSENTIALLY SAME AS ADCON)

	0C0F AD	54	PLO MA
	0C0F 96	55	GHI LINK
	0C10 BD	56	PHI MA
	0C11 16	57	INC LINK
	0C12 16	58	INC LINK
F	0C13 3000	59	BR SD
	0C15	60	..
	0C15	61	.. 16-BIT SUBTRACT AC FROM OPERAND
	0C15	62	.. ****AC=OPRN-AC
	0C15	63	.. ***** (TO CALL, WRITE) *****
	0C15	64	.. *****CALL SDOP ; ,A(OPRN)
	0C15	65	..
	0C15 46	66	SDOP: LDA LINK .. FETCH OPERAND ADDRESS
	0C16 BD	67	PHI MA .. TO MA REGISTER
	0C17 46	68	LDA LINK
	0C18 AD	69	PLO MA .. FALL INTO SD
	0C19	70	.. 16-BIT SUBTRACT AC FROM OPERAND.
	0C19	71	.. CALL HERE IF OPERAND
	0C19	72	.. ADDRESS IN REGISTER MA
	0C19	73	.. ****AC=M(R(MA))-AC
	0C19	74	.. ***** (TO CALL, WRITE) *****
	0C19	75	.. *****CALL SD
	0C19	76	..
	0C19 ED	77	SD: SFX MA .. SET X PTR TO MA
	0C1A 9F	78	GHI AC ..CHECK SIGN BIT OF AC
	0C1B F3	79	XOR ..AND OPERAND @MA
	0C1C 52	80	STR SP ..AND STORE ON STACK
	0C1D 1D	81	INC MA ..POINT TO LOW 8
	0C1E 8F	82	GLO AC .. FETCH AC LOW 8
	0C1F F5	83	SD .. SUBTRACT FROM LOW 8 IN MEMORY
	0C20 AF	84	PLO AC .. PUT IT BACK
	0C21 2D	95	DEC MA .. NOW HIGH 8
	0C22 9F	86	GHI AC
	0C23 75	87	SDNB: SDB .. SUBTRACT HIGH 8
	0C24 EF	88	PHI AC .. PUT IT BACK
	0C25 02	89	LDN SP ..LOAD STORED COMPARING BIT OF OPE
	0C26 FE	90	SHL ..CHECK STORED SIGN COMPARISION BIT
F	0C27 3B00	91	BNF SDFF ..IF OPERAND'S SIGNS ARE SAME
	0C29 9F	92	GHI AC ..NO OVERFLOW POSSIBLE
	0C2A F3	93	XOR ..OTHER WISE CHECK RESULT
	0C2B FE	94	SHL ..SET DF=0 IF OK
	0C2C D5	95	SDFF: SEP RETN ..RETURN
	0C2D	96	.. 16-BIT SUBTRACT FROM AC (ADDRESS IN CALL
	0C2D	97	.. ****AC=AC-OPRN
	0C2D	98	.. ***** (TO CALL, WRITE) *****
	0C2D	99	.. *****CALL SMOP ; ,A(OPRN)
	0C2D	100	..
	0C2D 46	101	SMOP: LDA LINK
	0C2E BD	102	PHI MA
	0C2F 46	103	LDA LINK
	0C30 AD	104	PLO MA
	0C31	105	.. 16-BIT SUBTRACT FROM AC (ADDRESS IN MA)
	0C31	106	.. CALL HERE IF OPERAND
	0C31	107	.. ADDRESS IN REGISTER MA

0C31		108	.. ****AC=AC-M(R(MA))
0C31		109	.. ***** (TO CALL, WRITE) *****
0C31		110	.. ****CALL SM
0C31		111	..
0C31 ED		112	SM: SEX MA ..SET X PTR
0C32 9F		113	GHI AC ..GET SIGN OF AC AND
0C33 F6		114	SHR ..AND STORE IN 7TH BIT OF CR
0C34 52		115	STR SP ..BUT PUT IN (SP) FIRST
0C35 9F		116	GHI AC ..AND SEE IF OPERANDS SIGNS ARE THE
0C36 F3		117	XOR
0C37 FA80		118	ANI #80 ..TAKE OUT COMPARING SIGN BIT
0C39 E2		119	SEX SP ..NOW STORE THAT BIT IN 8TH OF CR
0C3A F4		120	ADD ..BY ADDING TO IT
0C3B 52		121	STR SP ..AND STORE THESE TWO BITS ON STACK
0C3C 1D		122	INC MA ..POINT TO LOW 8
0C3D ED		123	SEX MA ..REMEMBER TO SET X TO OPERANDS
0C3E 8F		124	GLO AC .. FETCH AC LOW 8
0C3F F7		125	SM .. SUBTRACT MEMORY FROM IT
0C40 AF		126	PLO AC .. PUT IT BACK.
0C41 2D		127	DEC MA .. NOW HIGH 8
0C42 9F		128	GHI AC
0C43 77		129	SMNB: SHB .. HIGH 8 SUBTRACT, NO BORROW ACROSS
0C44 BF		130	PHI AC .. PUT HIGH 8 BACK
0C45 E2		131	SEX SP ..NOW CHECK IF UNDERFLOWED
0C46 F0		132	LDX ..LOAD THE STORED TWO BITS
0C47 FE		133	SHL ..AND TAKE OUT THE COMPARING SIGN BIT
F 0C48 3B00		134	BNF SMRT ..THE SAME, UNDERFLOW NOT POSSIBLE
0C4A 52		135	STR SP ..PUT IT BACK TO STACK
0C4B 9F		136	GHI AC ..OTHERWISE HAVE TO COMPARE SIGN 0
0C4C F3		137	XOR ..SIGN BIT OF AC WAS STORED ON STACK
0C4D FE		138	SHL ..TAKE OUT THAT 7TH BIT
0C4E D5		139	SMRT: SEP RETN ..DF=0 IF SUBTRACTION OK
0C4F		140	..
0C4F		141	..
0C4F		142	..16X16 BIT SIGNED MULTIPLY(2'S COMPLEMENT)
0C4F		143	..****AC=AC*OPRN
0C4F		144	..***** (TO CALL, WRITE)*****
0C4F		145	..****CALL MPYOP ; ,A(OPRN)
0C4F		146	..
0C4F 46		147	MPYOP: LDA LINK ..FETCH MULTIPLICAND ADDR
0C50 BD		148	PHI MA ..INTO REGISTER A
0C51 46		149	LDA LINK
0C52 AD		150	PLO MA ..FALL INTO MPY
0C53		151	.. 16X16 BIT SIGNED MULTIPLY (2'S COMPLEMEN
0C53		152	.. CALL HERE IF OPERAND ADDRESS
0C53		153	.. IN REGISTER MA
0C53		154	.. ****AC=AC*M(R(MA))
0C53		155	.. ***** (TO CALL, WRITE) *****
0C53		156	.. ****CALL MPY
0C53		157	..
0C53 ED		158	MPY: SEX MA .. SET X NOW
0C54 9F		159	GHI AC ..CHECK IS THE SIGN OF MULTICAND
0C55 F3		160	XOR ..THE SAME AS THE SIGN OF MULTIPR
0C56 FA00		161	ANI #80 ..AND STORE THAT BIT

0C58	BC	162	PHI CR	.. INTO CR.1
0C59	F810	163	LDI #10	.. SET COUNTER TO 16
0C5B	AC	164	PLO CR	
0C5C	F800	165	LDI #00	.. INITIALIZE MQ TO 0
0C5E	BE	166	PHI MQ	... TO HOLD PRODUCT.
0C5F	AE	167	PLO MQ	
0C60	2C	168	MPL: DEC CR	.. IF NOT, DECREMENT IT.
0C61	9F	169	CHI AC	.. SHIFT AC (=MULTIPLIER) RIGHT
0C62	F6	170	SHR	
0C63	BF	171	PHI AC	
0C64	8F	172	GLO AC	
0C65	76	173	SHRC	.. SHIFT 0 ACCROSS BYTES ..
0C66	AF	174	PLO AC	
0C67	9E	175	CHI MQ	
F 0C68	3B00	176	BNF MPB	.. IF NO BIT OUT, DON'T ADD.
0C6A	1D	177	INC MA	.. POINT TO LOW 8 OF MULTIPLICAND
0C6B	8C	178	GLO CR	.. IF NOT LAST ITERATION,
F 0C6C	3A00	179	BNZ MPA	.. GO ADD.
0C6E	8E	180	GLO MQ	.. LOAD MQ.0 INTO D
0C6F	F7	181	SM	.. MQ.0-(MA.0)
0C70	AE	182	PLO MQ	.. AND STORE BACK INTO MQ.0
0C71	2D	183	DEC MA	.. NOW DO THE HIGH BYTE
0C72	6E	184	CHI MQ	..
0C73	77	185	SMB	.. REMEMBER THE BORROW BIT
0C74	BE	186	PHI MQ	.. AND PUT BACK INTO MQ.1
0C75	9C	187	CHI CR	.. NOW ARE THE SIGNS OF OPERANDS THE
0C76	FE	188	MPB: SHL	.. TEST FOR SIGN BIT
F 0C77	3003	189	BR MPS+#03	.. IF NEGATIVE, SIGN EXTEND
0C79	8E	190	MPA: GLO MQ	.. DO MQ+(MA)
0C7A	F4	191	ADD	.. MQ.0+(MA.0)
0C7B	AE	192	PLO MQ	.. AND PUT BACK INTO MQ.0
0C7C	2D	193	DEC MA	.. SAME FOR HIGH BYTE
0C7D	9E	194	CHI MQ	..
0C7E	74	195	ADC	.. ADD WITH CARRY
0C7F	BE	196	PHI MQ	..
0C80	CF	197	MPS: LSDF	
0C81	F0	198	LDX	
0C82	FE	199	SHL	.. IF OPERAND IS NEGATIVE, THEN
0C83	9E	200	CHI MQ	.. PUT MQ.1 INTO D
0C84	76	201	SHRC	.. SHIFT IN CARRY
0C85	BE	202	PHI MQ	
0C86	8E	203	GLO MQ	.. CONTINUE TO LOW 8 OF MQ
0C87	76	204	SHRC	
0C88	AE	205	PLO MQ	
F 0C89	3B00	206	BNF MT	.. IF NO CARRY OUT, ITERATE.
0C8B	9F	207	CHI AC	.. ADD CARRY OUT INTO AC MSB.
0C8C	F980	208	ORI #80	
0C8E	BF	209	PHI AC	
0C8F	8C	210	MT: GLO CR	.. CHECK COUNTER
0C90	3A60	211	BNZ MPL	.. IF COUNTER IS NOT 0, GO BACK FOR
0C92	9F	212	MPX: CHI AC	.. FINISHED;
0C93	FE	213	SHL	.. CHECK FOR PRODUCT > 15 BITS.
0C94	8E	214	GLO MQ	
0C95	C7	215	LSNF	.. THAT'S HIGH 17 BITS

0C96	FBFF	216	XRI #FF .. ALL 00 OR FF.
0C98	3A9E	217	BNZ *+#06 .. NAW.
0C9A	9E	218	CHI MQ
0C9B	C7	219	LSNF
0C9C	FNFF	220	XRI #FF
0C9E	FCFF	221	ADI #FF .. SET DF IF PRODUCT > 15 BITS
0CA0	D5	222	SEP RETN .. RETURN.
0CA1		223	.. 32/16 BIT SIGNED DIVIDE (2'S COMPLEMENT)
0CA1		224	.. AC=MQ, AC/OPRN
0CA1		225	.. QUOTIENT IN AC , REMAINDER IN MQ
0CA1		226	.. ***** (TO CALL, WRITE) *****
0CA1		227	.. CALL DIVOP ; ,A(OPRN)
0CA1		228	..
0CA1	46	229	DIVOP: LDA LINK .. FETCH OPERAND ADDRESS
0CA2	BD	230	PHI MA .. TO REGISTER MA
0CA3	46	231	LDA LINK
0CA4	AD	232	PLO MA .. FALL INTO DIVO/DIV/DIVQ.
0CA5		233	.. 32/16 BIT SIGNED DIVIDE (2'S COMPLEMENT)
0CA5		234	... OPTION #1: CLEAR MQ AND CHECK FOR ZERO
0CA5		235	.. ****AC=MQ, AC/M(R(MA))
0CA5		236	.. ***** (TO CALL, WRITE) *****
0CA5		237	.. ****CALL DIVO
0CA5	E0	238	DIVO: SEX MA .. SET X TO POINT TO DIVISOR (0)
0CA6	9F	239	CHI AC .. LOOK AT AC SIGN (0)
0CA7	FE	240	SHL .. COPY IT TO DF (0)
0CA8	F000	241	LDI #00 .. EXTEND #00 IF POSITIVE, (0)
0CAA	C7	242	LSNF .. (0)
0CAE	F0FF	243	LDI #FF .. #FF IF NEGATIVE. (0)
0CAD	BE	244	PHI MQ .. GIVING +0 OR -0 IN MQ (0)
0CAE	AE	245	PLO MQ .. (0)
0CAF	4D	246	LDA MA .. CHECK FOR ZERO DIVISOR (0)
0CB0	F1	247	OR .. (0)
0CB1	ED	248	DEC MA .. (DON'T FORGET TO FIX POINTER)(0)
0CB2	FD00	249	SDI #00 .. IF ZERO, CALL IT DIVIDE CHECK(0)
F 0CB4	3B00	250	BNF DIV ..GO ON IF NO DIVIDE CHECK ERR
0CB6	D5	251	SEP RETN ..AND RETURN WITH DF=1 (0)
0CB7		252	... OPTION #2: PERMIT 32-BIT DIVIDEND; (/)
0CB7		253	..
0CB7		254	..MAKE SURE QUOTIENT DOES NOT EXCEED 16 BIT
0CB7		255	.. ***** (TO CALL, WRITE) *****(/)
0CB7		256	.. ***** CALL DIV *****(/)
0CB7	9E	257	DIV: CHI MQ ..SAVE PARTIAL DIVIDEND(/)
0CB8	BC	258	PHI CR ..INTO CR.1(/)
0CB9	8E	259	GLO MQ ..(/)
0CBA	AC	260	PLO CR ..AND CR.0(/)
0CBB	FE	261	SHL ..(/)
0CBC	AE	262	PLO MQ ..(/)
0CBD	9E	263	CHI MQ ..DO THE SAME FOR HIGH BYTE(/)
0CBE	7E	264	SHLC ..REMEMBER CARRY(/)
0CBF	BE	265	PHI MQ ..(/)
0CC0	9F	266	CHI AC ..ALSO SHIFT IN AC HIGH(/)
0CC1	FE	267	SHL ..(/)
F 0CC2	33FF	268	BDF D2-#01 ..(/)
0CC4	8C	269	GLO CR ..SEE IF MQ.0 =0(/)

F	0CC5	3A00	270	BNZ D2	..IF NOT GO THROUGH CHECKING STEPS
	0CC7	9C	271	CHI CR	..SEE IF MQ.1 IS #40(/)
	0CC8	FB40	272	XRI #40	..WHICH SHOULD RESULT 0 IF TRUE(/)
F	0CCA	3200	273	BZ D4	..IF TRUE,SKIP NORMAL CHECKING(/)
	0CCC	38	274	,#38	
	0CCD	1E	275	INC MQ	..IF 1, SHIFT INTO MQ(/)
	0CCE	9C	276	D2: CHI CR	..CHECK IF HIGH 2 BITS OF MQ AR
	0CCF	FAC0	277	ANI #C0	..TAKE OUT 2 HIGH BITS(/)
	0CD1	FD00	278	SDI #00	..SEE IF THEY ARE THE SAME(/)
	0CD3	FE	279	SHL	..SHIFT OUT COMPARISON (/)
F	0CD4	C30000	280	LDDF DVXX	..SET DF AND RETURN(/)
	0CD7	9C	281	D4: CHI CR	..LOOK AT THE SIGNS OF DIVND AND D
	0CD8	ED	282	SEX MA	..POINT X TO DIVISOR(/)
	0CD9	F3	283	XOR	..(/)
	0CDA	FE	284	SHL	..SET DF IF THE SAME(/)
	0CDB	1D	285	INC MA	..MQ.0-(MA)(/)
	0CDC	8E	286	GLO MQ	..MQ.0 TO D(/)
F	0CDD	3300	287	BDF DVA	..IF FLAG ,MQ.0+(MA)(/)
	0CDF	F7	288	SM	..MQ.0-(MA.0)(/)
	0CE0	AE	289	PLO MQ	..AND STORE BACK INTO MQ.0(/)
	0CE1	2D	290	DEC MA	..DO THE SAME FOR HIGH BYTE(/)
	0CE2	9E	291	CHI MQ	..LOAD MQ.1 INTO D(/)
	0CE3	77	292	SMB	..MQ.1-(MA.1) WITH CARRY(/)
F	0CE4	3C00	293	BR DVB	..SKIP OVER ADD STEP(/)
	0CE6	F4	294	DVA: ADD	..MQ+(MA)(/)
	0CE7	AE	295	PLO MQ	..STORE BACK TO MQ.0(/)
	0CE8	2D	296	DEC MA	..SAME FOR HIGH BYTE(/)
	0CE9	9E	297	CHI MQ	..MQ.1+(MA.1)(/)
	0CEA	74	298	ADC	..ADD MQ.1 AND (MA.1) WITH CARRY(/)
	0CEB	8E	299	DVB: PHI MQ	..AND STORE BACK INTO MQ.1(/)
	0CEC	9C	300	CHI CR	..LOOK AT THE SIGN OF DIVND(/)
	0CED	FE	301	SHL	..SET DF IF DIVND IS NEG@ATIVE
F	0CEE	CB0000	302	LBNF DV2	..IF NOT, DON'T COMPLEMENT DIFF(/)
	0CF1	9E	303	CHI MQ	..COMPLEMENT MQ(/)
	0CF2	FBFF	304	XRI #FF	..BY XOR TO #FF(/)
	0CF4	BE	305	PHI MQ	..(/)
	0CF5	8E	306	GLO MQ	..(DO THE SAME FOR LOW BYTE)(/)
	0CF6	FBFF	307	XRI #FF	..(/)
	0CF8	AE	308	PLO MQ	..(/)
	0CF9	1E	309	INC MQ	..REMEMBER TO ADD 1 (/)
	0CFA	9E	310	DV2: CHI MQ	..NOW LOOK AT THE DIFF OF MQ&M
F	0CFB	C20000	311	LBZ D10	..IF 0,CHECK MQ=0(/)
	0CFE	FE	312	SHL	..CHECK IF MQ IS NEGATIVE(/)
F	0CFF	3300	313	BDF DDQ	..IF YES, NO PROBLEM(/)
F	0D01	3000	314	BR D9	..IF NOT 0 NOR NEG, DIVND IS TOO LARG
	0D03	8E	315	D10: GLO MQ	..HERE WE CHECK DIFF=0 CASES(/)
	0D04	FCFE	316	ADI #FE	..IF MQ.0 IS NOT EITHER 0 OR 1(/)
F	0D06	3300	317	BDF DVXX	..THEN DIVND IS STILL TOO LARGE(/)
	0D08	FBFF	318	XRI #FF	..RESULT 0 IF MQ.0 WAS 1(/)
F	0D0A	3A00	319	BNZ DVH	..IF NOT, MUST BE 0, GO TO DVH(/)
	0D0C	9C	320	CHI CR	..SEE IF DIVND IS NEGATIVE(/)
	0D0D	FA80	321	ANI #80	..RESULT 80 IF YES(/)
F	0D0F	3200	322	BZ D9	..IF DIVND POSITIVE, IT CANNOT DIV
	0D11	F4	323	ADD	..SEE IF DIVISOR IS POSITIVE(/)

F	0D12	3300	324	BDF DVXX	..IF NEGATIVE, DIVND CANNOT DIVI
	0D14	1D	325	INC MA	..AC+(MA) TO MQ(/)
	0D15	8F	326	GLO AC	..DO AC LOW FIRST(/)
	0D16	F4	327	ADD	..(/)
	0D17	AE	328	PLO MQ	..STORE BACK TO LOW MQ(/)@
	0D18	2D	329	DEC MA	..DO THE SAME FOR HIGH BYTE(/)
	0D19	9F	330	GHI AC	..(/)
	0D1A	74	331	ADC	..ADD WITH CARRY(/)
	0D1B	BE	332	PHI MQ	..(/)
	0D1C	ID	333	INC MA	..LEAVE MA POINTING TO LOW DIVISOR(/
	0D1D	F0	334	LDX	..NOW HECK LOW BIT (MA) IS 0 OR 1(/)
	0D1E	F6	335	SHR	..SHIFT THAT LOW BIT OUT(/)
	0D1F	2D	336	DEC MA	..REMEMBER TO RESET MA(/)
	0D20	9E	337	GHI MQ	..READY TO ADD #80(/)
	0D21	C7	338	LSNF	..IF LOW BIT OF AC IS 1(/)
	0D22	FC80	339	ADI #80	..TO MQ.1(/)
	0D24	BE	340	PHI MQ	..STORE STATUS(/)
	0D25	FE	341	SHL	..SEE IF MQ >0(/)
	0D26	9C	342	GHI CR	..SEE IF DIVND POSTIVE(/)
	0D27	FA80	343	ANI #80	..BY TAKE OUT SIGN(/)
	0D29	3A2F	344	BNZ *+#06	..(/)
F	0D2B	3B00	345	BNF D9	..EXIT WITH DF=1(/)
F	0D2D	3000	346	BR DDQ	..OK(/)
F	0D2F	3300	347	BDF DVXX	..IF NEGATIVE, THEN OUT(/)
	0D31	9E	348	GHI MQ	..SEE IF MQ=0?(/)
F	0D32	3A00	349	BNZ DDQ	..IF NOT, THEN NO PROBLEM(/)
	0D34	BE	350	GLO MQ	..MAKE SURE MQ.0 IS 0 TOO(/)
F	0D35	3200	351	BZ D9	..IF YES, THEN RETURN WITH DF=1(/)
F	0D37	3000	352	BR DDQ	..OR ELSE GO TO DIVIDE(/)
	0D39	9C	353	DVH: GHI CR	..SEE IF THE OPERANDS SIGNS DIF
	0D3A	F3	354	XOR	..BY COMPARING SIGN BITS(/)
	0D3B	FE	355	SHL	..AND TAKE OUT THAT BIT(/)
	0D3C	3314	356	BDF D10+#11	..IF SINGS DIFF, IT'S OK(/)
	0D3E	9C	357	GHI CR	..OTHERWISE TEST SIGN OF DIVND(/)
	0D3F	FE	358	SHL	..IF POSITIVE, RETURN WITH DF=1(/)
F	0D40	3B00	359	BNF D9	..RETURN WITH DF=1(/)
	0D42	1D	360	INC MA	..SEE IF LOW BIT OF AC IS 0 OR 1(/
	0D43	10	361	LDX	..LOAD THAT IN D(/)
	0D44	2D	362	DEC MA	..REMEMBER TO RESET MA(/)
	0D45	F6	363	SHR	..SHIFT THAT BIT OUT(/)
	0D46	8F	364	GLO AC	..IF AC IS NOT 0 ,NOT PROBLEM(/)
F	0D47	3A00	365	BNZ DDQ	..GO TO DIVIDE(/)
	0D49	9F	366	GHI AC	..READY TO CHECK #80 IF LOW BIT AC
	0D4A	3350	367	BDF *+#06	..(/)
F	0D4C	3200	368	BZ D9	..NO GOOD, RETURN WITH DF=1(/)
F	0D4E	3000	369	BR DDQ	..ANY THING ELSE IS OK(/)
	0D50	FB80	370	XRI #80	..IF AC.1 IS'NT #80(/)
F	0D52	3A00	371	BNZ DDQ	..IT'S OK(/)
	0D54	FF00	372	D9: SMI #00	..DF IS SET TO 1(/)
	0D56	9C	373	DVXX: GHI CR	..PUT ORGINAL DIVND(/)
	0D57	BE	374	PHI MQ	..INTO MQ(/)
	0D58	8C	375	GLO CR	..(/)
	0D59	AE	376	PLO MQ	..(/)
	0D5A	D5	377	SEP RETN	..AND RETURN WITH DF=1(/)

0D5B	9C	378	DDQ:	CHI CR	...PUT ORIGINAL DIVND(/)
0D5C	BE	379		PHI MQ	..BACK INTO MQ(/)
0D5D	8C	380		GLO CR	..(/)
0D5E	AE	381		PLO MQ	..(/)
0D5F		382			... OPTION #3: ASSUME BENIGN PROGRAM; NOCHE
0D5F		383			.. ***** (TO CALL, WRITED) *****
0D5F		384			.. ****CALL DIVQ
0D5F	9E	385	DIVQ:	CHI MQ	..LOOK AT DIVIDEND SIGN
0D60	FE	386		SHL	.. IF POSITIVE,
0D61	F890	387		LDI #90	.. PLAN TO BEGIN WITH SUBTRACT,
0D63	C7	388		LSNF	.. (ALSO SAVE SIGN OF DIVIDEND)
0D64	F850	389		LDI #50	.. OTHER WISE BEGIN WITH ADD.
0D66	AC	390		PLO CR	.. SET ITERATION COUNT IN CR.0
0D67	8E	391	DVL:	GLO MQ	..SHIFT MQ LEFT 1 BIT
0D68	FE	392		SHL	..SHIFT LEFT MQ.0
0D69	AE	393		PLO MQ	..
0D6A	9E	394		CHI MQ	..SAME FOR HIGH BYTE
0D6B	7E	395		SHLC	..SHIFT LEFT WITH CARRY
0D6C	BE	396		PHI MQ	..
0D6D	8F	397		GLO AC	..SHIFT AC LEFT 1 BIT
0D6E	FE	398		SHL	..SHIFT AC.0
0D6F	AF	399		PLO AC	..
0D70	9F	400		GHI AC	..
0D71	7E	401		SHLC	..SHIFT WITH CARRY
0D72	BF	402		PHI AC	..
0D73	3B76	403		BNF **03	.. BIT SHIFTED OUT OF AC.1,
0D75	1E	404		INC MQ	.. GOES INTO MQ.0
0D76	ED	405		SEX MA	..
0D77	8C	406		GLO CR	.. NOW, WAS THAT ADD, OR SUBTRACT?
0D78	F3	407		XOR	.. IT DEPENDS ON SAVED FLAG,
0D79	FE	408		SHL	..AND SIGN OF DIVISOR
0D7A	1D	409		INC MA	..MQ.0-(MA.0)
0D7B	8E	410		GLO MQ	..
F 0D7C	3B00	411		BNF DSA	.. IF NO FLAG, MQ.0+(MA.0)
0D7E	F7	412		SM	..
0D7F	AE	413		PLO MQ	..
0D80	2D	414		DEC MA	..FIX X PTR
0D81	9E	415		CHI MQ	..DO THE SAME FOR HIGH BYTE
0D82	77	416		SMB	..REMEMBER THAT BORROW BIT
F 0D83	3000	417		BR DSM	..SKIP OVER ADD STEPS
0D85	F4	418	DSA:	ADD	..MQ+(MA)
0D86	AE	419		PLO MQ	..
0D87	2D	420		DEC MA	..DO THE SAME FOR HIGH BYTE
0D88	9E	421		CHI MQ	..
0D89	74	422		ADC	..ADD WITH CARRY
0D8A	BE	423	DSM:	PHI MQ	..STORE BACK TO MQ.1
0D8B	2C	424		DEC CR	.. COUNT DOWN ITERATION COUNTER
0D8C	8C	425		GLO CR	..
0D8D	FA7F	426		ANI #7F	..
0D8F	3B94	427		BNF **05	.. TEST CARRY OUT OF ADD/SUBTRACT
0D91	1F	428		INC AC	.. IF 1, SHIFT INTO QUOTIENT,
0D92	F980	429		ORI #80	.. AND FLAG NEXT OP AS SUBTRACT.
0D94	AC	430		PLO CR	.. OTHERWISE IT'S ADD.
0D95	FA3F	431		ANI #3F	.. LOOK AT COUNTER:

	0D97 3A67	432	BNZ DVL .. IF NOT 0, LOOP BACK;
F	0D99 3300	433	BDF DVR .. AT END, CHECK REMAINDER ADJUST.
	0B9B 38	434	,#38
	0D9C 1F	435	DVC: INC AC .. (FINAL DIVIDE STEP)
	0D9D F3	436	XOR .. BE SURE TO GET POLARITY
	0D9E FE	437	SHL .. OF ADJUSTMENT RIGHT...
	0D9F 1D	438	INC MA .. YES, ADD DIVISOR BACK ON.
	0DA0 9E	439	GLO MQ .. TO CORRECT FOR FINAL SUBTRACT,
F	0DA1 3300	440	BDF DVM .. (ADDING NEGATIVE IS SUBT.)
	0DA3 F4	441	ADD .. WHICH SHOULDN'T HAVE.
	0DA4 AE	442	PLO MQ
	0DA5 2D	443	DEC MA
	0DA6 9E	444	CHI MQ
	0DA7 74	445	ADC ..ADD WITH CARRY
F	0DA8 30FF	446	BR DVR=#01
	0DAA F7	447	DVM: SM .. SAME THING,
	0DAB AE	448	PLO MQ .. EXCEPT, FOR NEGATIVE DIVISOR.
	0DAC 2D	449	DEC MA
	0DAD 9E	450	CHI MQ
	0DAE 77	451	SMB
	0DAF BE	452	PHI MQ
	0DE0 9E	453	DVR: CHI MQ .. IF REMAINDER IS NOT ZERO,
	0DB1 3AB6	454	BNZ **#05
	0DB3 8E	455	GLO MQ
F	0DB4 3200	456	BZ DVM .. BUT IT IS; NO PROBLEM.
	0DE6 3C	457	GLO CR .. IF NOT ZERO,
	0DB7 FE	458	SHL .. IT SHOULD BE SAME SIGN
	0DB8 FE	459	SHL .. AS ORIGINAL DIVIDEND.
	0DB9 9E	460	CHI MQ
	0DBA CF	461	LSDF
	0DBB FB80	462	XRI #29
	0DBD FC60	463	ADI #80 .. IF NOT, WE NEED
	0DEF 3B9C	464	BDF DVC .. ONE MORE DIVIDE ITERATION.
	0DC1 F0	465	DVN: LDX .. FINALLY, IF DIVISOR NEGATIVE,
	0DC2 FE	466	SHL
F	0DC3 3B00	467	BDF DVX .. (IT'S NOT; WE ARE DONE)
	0DC5 8F	468	GLO AC .. COMPLEMENT QUOTIENT,
	0DC6 FBFF	469	XRI #FF .. BY INVERTING IT,
	0DC8 AF	470	PLO AC
	0DC9 9F	471	CHI AC
	0DCA FBFF	472	XRI #FF
	0DCC BF	473	PHI AC
	0DCD 1F	474	INC AC .. THEN INCREMENTING
	0DCE FC00	475	ADI #00 .. ALSO CLEAR DF.
	0DD0 D5	476	DVX: SEP RETN .. DF=0 IF DIVIDE SUCCESSFUL.
	0DD1	477	..
	0DD1	478	.. 16-BIT ADD TO AC, OPERAND ADDRESS IN CAL
	0DD1	479	.. ****AC=AC+OPRN .. OPRN=2 BYTE OPERAND
	0DD1	480	.. ***** (TO CALL, WRITE) *****
	0DD1	481	.. ****CALL ADDOP ; ,A(OPRN)
	0DD1	482	..
	0DD1	483	..
	0DD1 46	484	ADDOP: LDA LINK .. FETCH OPERAND ADDRESS
	0DD2 FD	485	PHI MA .. TO REGISTER MA

0DD3	46	486	LDA LINK
0DD4	AD	487	PLO MA .. FALL INTO ADD
0DD5		488	.. 16-BIT ADD TO AC, OPERAND ADDRESS IN REG
0DD5		489	.. CALL HERE IF OPRN ADDRESS
0DD5		490	.. IS IN REGISTER MA
0DD5		491	.. *****AC=AC+M(R(MA))
0DD5		492	.. ***** (TO CALL, WRITE) *****
0DD5		493	.. *****CALL ADD
0DD5		494	..
0DD5	LD	495	ADD: SEX MA ..CHECK SIGN BIT OF AC
0DD6	9F	496	GHI AC ..GET THE OPERAND
0DD7	F3	497	XOR ..AND OPERAND @MA
0DD8	F80	498	XRI #80 ..RESULT A 1 IF DIFF
0DDA	52	499	STR SP ..STORE ON STACK
0DDE	1D	500	INC MA ..POINT TO LOW 8 BITS
0DDC	2F	501	GLO AC .. FETCH AC LOW 8
0DDD	F4	502	ADD .. ADD LOW 8 FROM MEMORY
0DDE	AF	503	PLO AC .. PUT IT BACK
0DDF	2D	504	DEC MA .. POINT TO HIGH 8 MEMORY LOCATION
0DE0	9F	505	GHI AC
0DE1	74	506	ADC ..ADD HIGH BYTE WITH CARRY
0DE2	BF	507	PHI AC .. PUT IN AC.
0DE3	62	508	LDN SP ..LOAD THE STORED COMPARING SIGN BI
0DE4	FE	509	SHL ..RESET STACK PTR
F 0DE5	3B01	510	BNF ADDR+*01 ..NOT POSSIBLE
0DE7	9F	511	GHI AC ..OTHERWISE SEE IF SUM IS RIGHT
0DE8	F3	512	XOR ..BY COMPARING SIGN BITS
0DE9	FE	513	ADDRT: SHL ..SHIFT OUT 0 INTO DF
0DEA	D5	514	SEP RETN ..RETURN TO MAIN
0DEB		515	..
0DEB		516	.. 16-BIT CONSTANT ADD TO AC.
0DEB		517	.. CALL HERE FOR ADD CONSTANT TO AC
0DEB		518	.. *****AC=AC+CONSTANT
0DEB		519	.. ***** (TO CALL, WRITE) *****
0DEB		520	.. *****CALL ADDCON ; ,CONSTANT
0DEB		521	..
0DEB	86	522	ADDCON: GLO LINK .. COPY LINK TO MA
0DEC	AD	523	PLO MA
0DED	96	524	GHI LINK
0DEE	BD	525	PHI MA
0DEF	16	526	INC LINK .. INCREMENT PAST DATUM
0DF0	16	527	INC LINK
0DF1	30D5	528	BR ADD .. GO ADD.
0DF3		529	..
0DF3		530	.. 16-BIT ADD FROM TOP OF STACK
0DF3	92	531	ADDST: CHI SP .. COPY STACK POINTER
0DF4	DD	532	PHI MA .. TO MA REGISTER
0DF5	82	533	GLO SP
0DF6	AD	534	PLO MA
0DF7	1D	535	INC MA .. ADVANCE TO SUB-TOP (@)
0DF8	1D	536	INC MA .. (@)
0DF9	1D	537	INC MA .. (@)
0DFA	30D5	538	BR ADD .. GO DO IT
0DFC		539	

0DFC	540	..
0DFC	541	..
0DFC	542	.. PUSH AC INTO STACK
0DFC	543	.. STACK POINTER = SP
0DFC	544	.. ***** (TO CALL, WRITE) *****
0DFC	545	.. *****CALL PUSHAC
0DFC	546	.. PUSH AC (UNDER TOP OF STACK)
0DFC 92	547	PUSHAC: CHI SP .. COPY STACK POINTER TO MA
0DFD BD	548	PHI MA
0DFE 82	549	GLO SP
0DFE AD	550	PLO MA
0E00 1D	551	INC MA .. NOW SLICE OFF TOP 2 BYTES,
0E01 1D	552	INC MA
0E02 E2	553	SEX SP
0E03 0D	554	LDN MA .. TO MAKE A 2-BYTE HOLE.
0E04 73	555	STXD
0E05 2D	556	DEC MA
0E06 0D	557	LDN MA
0E07 73	558	STXD
0E08 9F	559	CHI AC .. NOW STUFF AC INTO THE HOLE.
0E09 5D	560	STR MA
0E0A 8F	561	GLO AC
0E0B 1D	562	INC MA
0E0C 5D	563	STR MA
0E0D 2D	564	DEC MA .. LEAVE MA POINTING TO IT.
0E0E D5	565	SEP RETN .. (AC UNCHANGED)
0E0F	566	.. PUSH CR, MA, MQ (UNDER TOP OF STACK)
0E0F 6D	567	PUSHCQ: GLO MA .. FIRST PUSH MA ONTO TOP
0E10 E2	568	SEX SP
0E11 73	569	STXD
0E12 9D	570	CHI MA
0E13 52	571	STR SP
0E14 92	572	CHI SP .. NOW COPY SP TO MA
0E15 BD	573	PHI MA
0E16 62	574	GLO SP
0E17 AD	575	PLO MA
0E18 22	576	DEC SP
0E19 1D	577	INC MA .. THEN ADJUST IT
0E1A 1D	578	INC MA
0E1B 1D	579	INC MA .. TO POINT INTO OLD TOP
0E1C EE	580	GLO MQ .. CONTINUE PUSHING, MQ
0E1D 73	581	STXD
0E1E 9E	582	CHI MQ
0E1F 73	583	STXD
0E20 0D	584	LDN MA
0E21 73	585	STXD
0E22 2D	586	DEC MA
0E23 0D	587	LDN MA
0E24 73	588	STXD
0E25 9C	589	CHI CR .. FINALLY INSERT CR IN HOLE
0E26 5D	590	STR MA
0E27 1D	591	INC MA
0E28 8C	592	GLO CR
0E29 5D	593	STR MA

0E2A	D5	594	SEP RETN .. (MA IS GARBAGE OUT)
0E2B		595	.. POP STACK INTO MQ, MA, CR (UNDER TOP OF
0E2B		596	POPCQ: INC SP
0E2B	12	597	CHI SP .. COPY STACK POINTER TO MA
0E2C	92	598	PHI MA
0E2D	BD	599	GLO SP
0E2E	82	600	PLO MA
0E2F	AD	601	INC MA .. ADJUST POINTER TO CR DATUM
0E30	1D	602	INC MA
0E31	1D	603	INC MA
0E32	1D	604	INC MA
0E33	1D	605	INC MA
0E34	1D	606	INC MA
0E35	1D	607	INC MA
0E36	4D	608	LDA MA .. FETCH IT
0E37	BC	609	PHI CR
0E38	0D	610	LDN MA
0E39	AC	611	PLO CR
0E3A	2D	612	DEC MA .. COPY TOP OF STACK INTO GAP
0E3B	42	613	LDA SP
0E3C	5D	614	STR MA
0E3D	1D	615	INC MA
0E3E	42	616	LDA SP
0E3F	5D	617	STR MA
0E40	42	618	LDA SP .. THEN POP MQ
0E41	BE	619	PHI MQ
0E42	42	620	LDA SP
0E43	AE	621	PLO MQ
0E44	42	622	LDA SP .. FINALLY POP MA
0E45	BD	623	PHI MA
0E46	02	624	LDN SP
0E47	AD	625	PLO MA
0E48	D5	626	SEP RETN
0E49		627	.. 16-BIT ACCUMULATOR LOAD (ADDRESS IN CALL
0E49		628	.. ****AC=OPRN
0E49		629	.. ***** (TO CALL, WRITE) *****
0E49		630	.. *****CALL LOADOP ; ,A(OPRN)
0E49		631	..
0E49	46	632	LOADOP: LDA LINK .. FETCH ADDRESS
0E4A	BD	633	PHI MA .. TO MA REGISTER
0E4B	46	634	LDA LINK
0E4C	AD	635	PLO MA .. FALL INTO LOAD
0E4D		636	.. 16-BIT ACCUMULATOR LOAD (ADDRESS IN MA)
0E4D		637	.. CALL HERE IF OPERAND
0E4D		638	.. ADDRESS IN REGISTER MA
0E4D		639	.. ****AC=M(R(MA))
0E4D		640	.. ***** (TO CALL, WRITE) *****
0E4D		641	.. *****CALL LOAD
0E4D		642	..
0E4D	4D	643	LOAD: LDA MA .. FETCH HIGH 8
0E4E	BF	644	PHI AC
0E4F	4D	645	LDA MA .. NOW LOW 8
0E50	AF	646	PLO AC .. LEAVE MA AT NEXT DOUBLE-BYTE
0E51	D5	647	SEP RETN .. GEE, THAT WAS QUICK.

0E52		648	..
0E52		649	.. 16-BIT ACCUMULATOR LOAD FROM CONSTANT IN
0E52		650	.. ****AC=CONSTANT
0E52		651	.. ***** (TO CALL, WRITE) *****
0E52		652	.. ****CALL LODCON ; ,CONSTANT
0E52		653	..
0E52	46	654	LODCON: LDA LINK .. FETCH HIGH 8
0E53	BF	655	PHI AC
0E54	46	656	LDA LINK .. THEN LOW 8
0E55	AF	657	PLO AC
0E56	D5	658	SEP RETN
0E57		659	..
0E57		660	.. 16-BIT ACCUMULATOR STORE (ADDRESS IN CAL
0E57		661	.. ****OPRN=AC
0E57		662	.. ***** (TO CALL, WRITE) *****
0E57		663	.. ****CALL STOROP ; ,A(OPRN)
0E57		664	..
0E57	46	665	STOROP: LDA LINK .. FETCH ADDRESS INTO MA
0E58	BD	666	PHI MA
0E59	46	667	LDA LINK
0E5A	AD	668	PLO MA .. THEN FALL INTO STORE
0E5B		669	.. 16-BIT ACCUMULATOR STORE (ADDRESS IN MA)
0E5B		670	.. ****M(R(MA))=AC
0E5B		671	.. ***** (TO CALL, WRITE) *****
0E5B		672	.. ****CALL STORE
0E5B		673	..
0E5B	9F	674	STORE: PHI AC .. FIRST HIGH 8
0E5C	5D	675	STR MA
0E5D	1D	676	INC MA .. INCREMENT MA, SINCE STR DOESN'T
0E5E	8F	677	GLO AC .. NOW LOW 8
0E5F	5D	678	STR MA
0E60	1D	679	INC MA .. LEAVE MA POINTING TO NEXT WORD
0E61	D5	680	SEP RETN .. QUIT
0E62		681	..
0E62		682	..
0E62		683	.. 16-BIT COMPARE, OPERAND ADDRESS IN CALL
0E62		684	.. ****AC-OPRN (DF SET IF 0 OR +)
0E62		685	.. ***** (TO CALL, WRITE) *****
0E62		686	.. ****CALL COMOP ; ,A(OPRN)
0E62		687	..
0E62	46	688	COMOP: LDA LINK .. FETCH ADDRESS
0E63	BD	689	PHI MA .. TO MA REGISTER
0E64	46	690	LDA LINK
0E65	AD	691	PLO MA
0E66		692	.. 16-BIT COMPARE, OPERAND ADDRESS IN REGIS
0E66		693	.. CALL HERE IF OPERAND
0E66		694	.. ADDRESS IN REGISTER MA
0E66		695	.. ****AC-M(R(MA)) (DF SET IF 0 OR +)
0E66		696	.. ***** (TO CALL, WRITE) *****
0E66		697	.. ****CALL COMP
0E66		698	..
0E66	ED	699	COMP: SEX MA .. COMPARE HIGH 8 FRST
0E67	9F	700	PHI AC .. CHECK IF SIGN OF OPERANDS ARE SA
0E68	F3	701	XOR .. BY LOOKING AT THE HIGHEST SIGN BIT

0E69	FA30	702	ANI #80 ..RESULT A '1' IF NEGATIVE
F 0E6B	3A00	703	BNZ CNE ..IF NOT, THEN GO TO CNE
0E6D	9F	704	GHI AC
0E6E	F7	705	SM
F 0E6F	3A00	706	BNZ CMPX .. NOT EQUAL QUILTS
0E71	1D	707	INC MA .. TRY LOW 8
0E72	8F	708	GLO AC
0E73	F7	709	SM
0E74	2D	710	DEC MA .. LEAVE MA POINTING TO IT
0E75	38	711	,#30
0E76	F4	712	CNE: ADD ..SEE IF OPERAND IS NEGATIVE
0E77	D6	713	CMPX: SEP RETN ..DF=1 IF AC>=(MA)
0E78		714	..
0E78		715	..
0E78		716	..
0E78		717	..
0E78		718	..TEST 16-BIT ACCUMULATOR SIGN/ZERO .....
0E78	16	719	INC LINK ..SKIP OVER NON ZERO RETURN
0E79	16	720	INC LINK ..
0E7A	D5	721	SEP RETN
0E7B	9F	722	TEST: GHI AC .. FIRST LOOK AT SIGN
0E7C	FE	723	SHL ..SET DF IF MINUS
0E7D	9F	724	GHI AC .. NOW CHECK FOR 0
0E7E	3A78	725	BNZ TEST-#03 .. NO.
0E80	3F	726	GLO AC
0E81	327A	727	BZ TEST-#01 .. GO TAKE ZERO EXIT.
0E83	3078	728	BR TEST-#03 .. GO TAKE NON-ZERO EXIT.
0E85		729	.. POP STACK (INTO AC) (UNDER TOP)
0E85		730	.. POPS 2 BYTES FROM STACK INTO AC
0E85		731	.. ***** (TO CALL, WRITE) *****
0E85		732	.. *****CALL POPAC
0E85	FF00	733	POPAC: SMI #00 .. SET DF TO REMEMBER THIS ENTRY
0E87	C3	734	LSKP
0E88	1C00	735	POP: ADI #00 .. CLEAR DF FOR THIS ENTRY
0E8A	12	736	INC SP
0E8D	92	737	GHI SP .. COPY SP TO MA
0E8C	BD	738	PHI MA
0E8D	B2	739	GLO SP
0E8E	AD	740	PLO MA
0E8F	1D	741	INC MA .. ADJUST TO SUB-TOP OF STACK
0E90	1D	742	INC MA
0E91	3B98	743	BNF **#07
0E93	4D	744	LDA MA .. POPPING INTO AC. GET DATUM
0E94	BF	745	PHI AC
0E95	0D	746	LDN MA
0E96	AF	747	PLO AC
0E97	2D	748	DEC MA
0E98	42	749	LDA SP .. NOW CLOSE UP THE GAP
0E99	5D	750	STR MA
0E9A	1D	751	INC MA
0E9B	02	752	LDN SP
0E9C	5D	753	STR MA
0E9D	1D	754	INC MA
0E9E	D5	755	SEP RETN .. MA POINTS TO NEW SUB-TOP

OE9F	756	..	DECIMAL TO BINARY CONVERSION
OE9F	757	..	***** AC=DECIMAL NUMBER OF N BYTES
OE9F	758	..	DECIMAL NUMBER = SIGN, NN, . . . . ., N1, N0
OE9F	759	..	SIGN=#0B +
OE9F	760	..	SIGN=#0D -
OE9F	761	..	N0=10**0 DIGIT
OE9F	762	..	N1=10**1 DIGIT
OE9F	763	..	***** (TO CALL, WRITE) *****
OE9F	764	..	**** CALL CDB; ,A(NUMBER); ,LENGTH
OE9F	765		
OE9F 46	766	CDB:	LDA LINK ..GET NUM ADDRESS
OEAO BA	767		PHI AR ..AND STORE IN RA.
OEAI 46	768		LDA LINK
OEAA AA	769		PLO AR
OEAS 46	770		LDA LINK ..GET LENGTH
OEAA4 FF01	771		SNI #01 ..MINUS SIGN BYTE
OEAA6 AB	772		PLO NR ..AND STORE IN RB.
OEAA7 F300	773		LDI #00 ..CLEAR RF
OEAA9 AF	774		PLO AC
OEAAA BF	775		PHI AC
OEAA8 CA	776		LDR AR ..CHECK SIGN BYTE
OEAAE EB0D	777		XRI #0D ..MINUS?
OEAAE EB	778		PHI NR ..INTO NR.1
OEAAE JA	779	LOOP:	INC AR ..GRAB THE FIRST DIGIT
OEAB0 E2	780		SEX SP ..FIX X PTR
OEAB1 CA	781		LDR AR ..CLEAR HIGH BYTE (FOR ASCII)
OEAB2 FA0F	782		ANI #0F
OEAB4 52	783		STR SP ..PUT IT BACK
OEAB5 8F	784		GLO AC ..ADD THAT DIGIT TO ACCUM
OEAB6 F4	785		ADD
OEAB7 AF	786		PLO AC
OEAB8 9F	787		GHI AC
OEAB9 7C00	788		ADCI #00 ..REMEMBER CARRY OVER
OEABB BF	789		PHI AC
F OEADC 3300	790		BDF OVFLW ..EXCEEDS ACCUM LIMIT?
OEABE EB	791		DEC NR ..DEC DIGIT COUNTER
OEABF 8B	792		GLO NR ..SEE IF IT IS 0?
F OECC0 3200	793		BZ FINAL ..YES, THEN DONE
OECC2 8F	794		GLO AC ..OTHERWISE MULTIPLY THE ACC BY 10
OECC3 FE	795		SHL
OECC4 73	796		STXD
OECC5 9F	797		GHI AC
OECC6 7E	798		SHLC ..CARRY OVER
OECC7 73	799		STXD
F OECC8 33FE	800		BDF OVFLW-#02 ..EXCEEDED ACC LIMIT
OECA F802	801		LDI #02
OECC 52	802	MPY3:	STR SP ..LOOP COUNT
OECD 8F	803		GLO AC
OECE FE	804		SHL ..NOW SHIFT AC OVER 4 TIMES MORE
OECE AF	805		PLO AC
OEED0 9F	806		GHI AC ..SAME FOR AC.1
OEED1 7E	807		SHLC
OEED2 BF	808		PHI AC
F OEED3 33FE	809		BDF OVFLW-#02 ..IF OVFLOW, RESET STACK

0ED5 02	810	LDN SP ..CHECK LOOP COUNT
F 0ED6 3200	811	BZ MPY10 ..AFTER MULPLY BY 8
0ED8 FF01	812	SMI #01 ..OR ELSE DEC LOOP COUNT
0EDA 30CC	813	BR MPY3 ..BACK FOR MORE ADDITION
0EDC 12	814	MPY10: INC SP ..RECOVER LOOP COUNT
0EDD 9F	815	GHI AC ..ADD HIGH BYTE
0EDE F4	816	ADD ..ADD 8ACC TO 2ACC
0EDF BF	817	PHI AC
F 0EE0 33FF	818	BDF OVFLW-#01 ..RESULT DF IF OVFLOW
0EE2 12	819	INC SP ..RESET STACK PNTR
0EE3 5F	820	GLO AC ..SAME FOR AC.0
0EE4 F4	821	ADD
0EE5 AF	822	PLO AC
0EE6 9F	823	GHI AC ..FOR CARRY OUT
0EE7 7C00	824	ADCI #00
0EE9 BF	825	PHI AC
0EEA 3BAF	826	BNF LOOP ..IF NOT OVFLW, GO BACK FOR MORE
0EEC C8	827	LSKP ..SKIP STACK RESET
0EED 12	828	INC SP ..RESET STACK PTR
0EEE 12	829	INC SP
0EEF D5	830	OVFLW: SEP RETN ..DF=1
0EF0 9F	831	FINAL: GHI AC ..CHECK IF EXCEED MAX POS NUM L
0EF1 FC80	832	ADI #80
F 0EF3 3A00	833	BNZ CP ..IF NOT POSSIBLE, SKIP
0EF5 BF	834	GLO AC
F 0EF6 3A00	835	BNZ CP ..IF NOT, GO TO COMP
0EF8 9B	836	GHI NR ..SEE IF IT IS POSITIVE
0EF9 FCFF	837	ADI #FF ..SET DF ACCORDINGLY
0EFB D5	838	SEP RETN
0EFC 33FB	839	CP: BDF *-#01 ..OVERFLOWED!
0EFE 9B	840	GHI NR ..TEST FOR SIGN
F 0EFF 3A00	841	BNZ EXIT ..IF POS, DONE
0F01 BF	842	GLO AC ..IF NEG, SUBTRACT FROM 0
0F02 FD00	843	SDI #00
0F04 AF	844	PLO AC
0F05 9F	845	GHI AC
0F06 7D00	846	SDBI #00
0F08 BF	847	PHI AC
0F09	848	..
0F09	849	.. BINARY TO DECIMAL CONVERSION
0F09	850	.. ****DECIMAL NUMBER = AC
0F09	851	.. DECIMAL NUMBER = SIGN,NN,.....,N1,N0
0F09	852	.. SIGN=#0B +
0F09	853	.. SIGN=#0D -
0F09	854	.. N0=10**0 DIGIT
0F09	855	.. N1=10**1 DIGIT, ETC
0F09	856	.. ***** (TO CALL, WRITE) *****
0F09	857	.. ***** CALL CBD; ,A(NUMBER); ,LENGTH
0F09 D5	858	EXIT: SEP RETN
0F0A 46	859	CBD: LDA LINK ..GET THE ADDRESS
0F0B BA	860	PHI AR ..AND STORE IN RA
0F0C 46	861	LDA LINK ..SAME FOR LOW BYTE
0F0D 4A	862	PLO AR
0F0E 46	863	LDA LINK ..GET LENGTH

	0F0F	FF01	864	SMI #01	..SUBTRAC FOR SIGN BYTE
	0F11	AE	865	PLO NR	..STORE IN NR.0
	0F12	BB	866	PHI NR	..AND NR.1
	0F13	F80F	867	LDI #0F	..NUM OF ITERATIONS
	0F15	AD	868	PLO MA	..STORE IN MA.0
	0F16	9F	869	GHI AC	..TEST FOR SIGN
	0F17	FE	870	SHL	
	0F18	F80B	871	LDI #0B	.. IF DF=0, IT IS POS
F	0F1A	3B00	872	BNF POS	..
	0F1C	8F	873	GLO AC	..OTHERWISE CONVERT IT TO POS
	0F1D	FD00	874	SDI #00	
	0F1F	AF	875	PLO AC	
	0F20	9F	876	GHI AC	
	0F21	7D00	877	SDBI #00	
	0F23	BF	878	PHI AC	
	0F24	F80D	879	LDI #0D	..MINUS SIGN
	0F26	C8	880	LSKP ..	
	0F27	F800	881	LDI #00	
	0F29	5A	882	POS: STR AR	..PUT IT IN SIGN BYT
	0F2A	8B	883	GLO NR	..CHECK DIGIT COUNTER
F	0F2B	32FE	884	BZ LOOP1-#02	..GO BACK FOR MORE ITERATION
	0F2D	1A	885	INC AR	..GO TO NEXT DIGIT
	0F2E	2B	886	DEC NR	..DEC DIGIT CNTR
	0F2F	3027	887	BR POS-#02	..GO BACK FOR MORE CLEAR
	0F31	E2	888	SEX SP	
	0F32	9B	889	GHI NR	..RESET DIGIT CNTR
	0F33	AB	890	PLO NR	..
	0F34	8F	891	LOOP1: GLO AC	..SHIFT BIT OF AC OUT
	0F35	FE	892	SHL ..	
	0F36	AF	893	PLO AC	
	0F37	9F	894	GHI AC	
	0F38	7E	895	SHLC ..	SAME FOR AC.1
	0F39	BF	896	PHI AC	
	0F3A	0A	897	LDN AR	
	0F3B	7C00	898	ADCI #00	..ADD TO LOWEST DIGIT
	0F3D	5A	899	STR AR	
	0F3E	8D	900	GLO MA	..FOR MORE ITERATION?
	0F3F	3A42	901	BNZ **#03	..CONTINUE IF MORE ITERATION
	0F41	D5	902	END: SEP RETN	
	0F42	0A	903	NEXT: LDN AR	..LOAD DIGIT
	0F43	7E	904	SHLC ..	SHIFT LEFT OVER ONCE
	0F44	5A	905	STR AR	..PUT IT BACK
	0F45	FF0A	906	SMI #0A	..NEED TO INC NEXT DIGIT?
	0F47	3B4A	907	BNF **#03	..SKIP IF NOT>10
	0F49	5A	908	STR AR	..ELSE UPDATE DIGIT
	0F4A	2A	909	DEC AR	..GO TO NEXT DIGIT
	0F4B	2B	910	DEC NR	..DEC DIGIT COUNT
	0F4C	8B	911	GLO NR	..CHECK IF 0?
	0F4D	3A42	912	BNZ NEXT	..IF NOT, DO THE SAME FOR NEXT DI
	0F4F	3341	913	BDF END	..OVERFLOWED
	0F51	2D	914	DEC MA	..DEC NO OF SHIFTS
	0F52	9B	915	GHI NR	..RESET ADDRESS PTR
	0F53	52	916	STR SP	..PUT DIGIT ON STACK
	0F54	8A	917	GLO AR	

0F55	F4	918	ADD
0F56	AA	919	PLO AR
0F57	9A	920	GHI AR
0F58	7C00	921	ADCI #00
0F5A	BA	922	PHI AR
0F5B	3032	923	BR LOOP1-#02 ...
0F5D		924	::
0F5D		925	:: *****SUBROUTINE CALL (CDP1802 VERSION)***
0F5D		926	::
0F5D	D3	927	CALLR: SEP PC ..TO SUBROUTINE...
0F5E	E2	928	CALLS: SEX SP ..POINT TO STACK
0F5F	96	929	GHI LINK ..SAVE LINK ON STACK.
0F60	73	930	STXB
0F61	86	931	GLO LINK
0F62	73	932	STXB
0F63	93	933	GHI PC
0F64	D6	934	PHI LINK
0F65	83	935	GLO PC
0F66	A6	936	PLO LINK
0F67	46	937	LDA LINK
0F68	B3	938	PHI PC
0F69	46	939	LDA LINK
0F6A	A3	940	PLO PC
0F6B	305D	941	BR CALLR ..JUMP TO SUBROUTINE.
0F6D		942	::
0F6D		943	:: *****SUBROUTINE RETURN (CDP1802 VERSION)*
0F6D		944	::
0F6D	D3	945	RETR: SEP PC ..RETURN TO MAIN ...
0F6E	96	946	RETR: GHI LINK ..RESTORE RETURN ADDRESS
0F6F	B3	947	PHI PC ..INTO PC.
0F70	86	948	GLO LINK
0F71	A3	949	PLO PC
0F72	E2	950	SEX SP
0F73	12	951	INC SP ..ON STACK INTO LINK.
0F74	72	952	LDXA
0F75	A6	953	PLO LINK
0F76	F0	954	LDX
0F77	B6	955	PHI LINK
0F78	306D	956	BR RETNR ..RETURN.
0F7A		957	...
0F7A		958	...ADDITIONS BY J.M.C.
0F7A		959	...NOT SUPPORTED!!!!
0F7A		960	...
0F7A		961	.. MOVN -- ROUTINE TO MOVE N BYTES
0F7A		962	.. OF MEMORY FROM ONE LOCATION TO ANOTHER
0F7A		963	..CALLING SEQUENCE:
0F7A		964	.. CALL MOVN; ,A(SOURCE), A(DEST), NBYTES
0F7A		965	..
0F7A	46BD	966	MOVN: @R6!->MA.1
0F7C	46AD	967	@R6!->MA.0
0F7E	46BA	968	@R6!->AR.1
0F80	46AA	969	@R6!->AR.0
0F82	46AB	970	@R6!->NR.0
0F84	4D5A1A	971	MOVN01: @MA!->@AR; INC AR

0F87	2B8B3A84	972	DEC NR; NR.0; BNZ MOVBO1
0F8B	D5	973	EXIT ..DONE
0F8C		974	...
0F8C		975	...
0F8C		976	...
0F8C		977	.. CALLING SEQ.: CALL DELAY; ,DCON
0F8C		978	.. WHERE DCON IS A 2 BYTE CONSTANT.
0F8C		979	.. DCON=(TIME-400)/24
0F8C		980	.. TIME IN MICROSECONDS
0F8C		981	...
0F8C	8C5222	982	DELAY: CR.0->@SP; DEC SP
0F8F	9C52	983	CR.1->@SP ..COPY CR TO STACK
0F91	46BC	984	@R6!->CR.1
0F93	46AC	985	@R6!->CR.0
0F95	38	986	SKIP
0F96	2C8C3A96	987	DEL1: DEC CR; CR.0; BNZ DEL1
0F9A	9C3A96	988	CR.1; BNZ DEL1
0F9D	42BC	989	@SP!->CR.1
0F9F	F0AC	990	@->CR.0 ..RESTORE CR
0FA1	D5	991	EXIT
0FA2		992	...
0FA2		993	... >CVT CONVERT BINARY (16 BIT) TO ASCII
0FA2		994	...CALL CVT; ,(NO. CHARS) ,(CHARS AFTER ". ")
0FA2		995	...
0FA2	46BC52	996	CVT: @LINK!->CR.1,@SP
0FA5	46AC	997	@LINK!->CR.0
0FA7	8AF4AA	998	AR.0+@->AR.0
0FAA	3BB0	999	BNF *+6
0FAC	9AFC01BA	1000	AR.1+1->AR.1 ..ADJUST AR
0FB0	2A	1001	DEC AR
0FB1	F300BEAE	1002	DIV10: 0->M0.1,MQ.0
0FB5	3FFF0AAF	1003	DLOOP: AC.0-10->AC.0
0FB9	1E	1004	INC MQ ..BUMP QUOTIENT COUNTER
0FBA	33B5	1005	BDF DLOOP
0FBC	9FFF01BF	1006	AC.1-1->AC.1 ..PROCESS HI BYTE BORROW
0FC0	33B5	1007	BDF DLOOP
0FC2	2E	1008	DEC MQ ..AR HAS ROLLED OVER NEG
0FC3	8FFC3A5A	1009	AC.0+*3A->@AR ..CONVERT REMAIN TO ASCII
0FC7	2A	1010	DEC AR
0FC8	9EBF	1011	MQ.1->AC.1 ..COPY MQ TO AC
0FCA	9EAF	1012	MQ.0->AC.0
0FCC	8CFF01AC	1013	CR.0-1->CR.0
F	0FD0 3A00	1014	IF >0 GOTO CVT01
	0FD2 F82E5A	1015	T.'->@AR ..OUTPUT DEC POINT
	0FD5 2A	1016	DEC AR
	0FD6 9CFF01BC	1017	CR.1-1->CR.1
F	0FDA 3A00	1018	IF >0 GOTO CVT01
F	0FDC 3000	1019	GOTO CVT03
	0FDE 9CFF01BC	1020	CVT01: CR.1-1->CR.1
	0FE2 3AB1	1021	IF >0 GOTO DIV10
	0FE4 1A	1022	CVT03: INC AR
	0FE5 D5	1023	EXIT ..DONE
	0FE6	1024	...
		1025	END

## APPENDIX D

### SOFTWARE LISTING FOR ELECTRONIC DASHBOARD DISPLAY

```

0000      1 ..   >DASH      J.M.C. RCA LABS  9:3:76
0000      2 ...
0000      3 ..
0000      4 ..   REGISTER ALLOCATION
0000      5 ...
0000      6 ..   SP =R2 ... IT SHOULD BE THE STACK POINTER.
0000      7 ..   PC =R3 ... IT IS THE PROGRAM COUNTER
0000      8 ..   .. USED BY THESE SUBROUTINES.
0000      9 ..   CALL =R4 ... IT SHOULD POINT TO THE ROUTINE
0000     10 ..   .. WHICH EFFECTS SUBROUTINE CALLS.
0000     11 ..   RETN =R5 ... IT SHOULD POINT TO THE ROUTINE
0000     12 ..   .. WHICH EFFECTS SUBROUTINE RETURN.
0000     13 ..   LINK=R6      .. USED FOR SUBROUTINE PARAM
0000     14 ..
0000     15 ..   MS=R9      .. (MESSAGE POINTER/COUNTER)
0000     16 ..   AR=RA      .. (USED FOR RESULT ADDRESS)
0000     17 ..   AC=RF      .. 16-BIT ACCUMULATOR=RF.
0000     18 ..   MQ=RE      .. 16-BIT ACCUMULATOR=RE EXTENSION.
0000     19 ..   MA=RD      .. (TEMPORARY) OPERAND MEMORY ADDRESS.
0000     20 ..   CR=RC      .. (TEMPORARY) SCRATCHPAD AND COUNTER.
0000     21 ..
0000     22 ..   MESSL=#10FE; STACK=#1000
0000     23 ..
0000     24 ..   INPUT--OUTPUT INSTRUCTION ALLOCATION
0000     25 ..   OUT 1  ENTER DATA IN DISPLAY MEMORY
0000     26 ..   OUT 2  TURN DISPLAY ON OR OFF
0000     27 ..   OUT 3  STROBE FOR A TO D CONVERSION
0000     28 ..   OUT 4  GROUP SELECT FOR A TO D CONVERSION
0000     29 ..   OUT 5  CLOCK SHIFT REGISTERS
0000     30 ..   OUT 6  SHIFT REGISTER LOAD (STROBE)
0000     31 ..   OUT 7  FREE
0000     32 ..
0000     33 ..   INP 1  READ BINARY DEVICES (CHANNEL 1)
0000     34 ..   INP 2  READ BINARY DEVICES (CHANNEL 2)
0000     35 ..   INP 3  READ BINARY DEVICES (CHANNEL 3)
0000     36 ..   INP 4  READ 8 BIT A TO D CONVERTED DATA
0000     37 ..   INP 5  READ TACH(4-7)/FUEL(0-3) COUNTERS
0000     38 ..   INP 6  READ SPEED COUNTER
0000     39 ..   INP 7  FREE
0000     40 ..
0000     41 ..   EF1   A TO D CONVERSION COMPLETE
0000     42 ..   EF2   ODOMETER SERIAL INPUT
0000     43 ..   EF3   CLOCK SERIAL INPUT
0000     44 ..   EF4   READ TELEPRINTER (UT2 UTILITY)
0000     45 ..
0000     46 ..   IMMEDIATE BYTE DATA VALUES
0000     47 ..
0000     48 ..   ACT1=#7F; ACT2=0 ; ACT3=0
0000     49 ..   INV1=#FE; INV2=#FF; INV3=#FF .. 12V -> DANGER!
0000     50 ..   OV2=237; OV3=217; OV4=196 .. OIL PRESSURE DATA
0000     51 ..   OV5=176; OV6=156; OV7=135
0000     52 ..
0000     53 ...

```

0000	54	ORC 0
0000 F0	55	SEX 0
0001 F0	56	SEX 0
0002 7100	57	DISABLE; ,0 ..TURN INTERRUPTS OFF!
F 0004 F800B3	58	A.1(PC3)->R3.1
F 0007 F800A3	59	A.0(PC3)->R3.0
000A D3	60	GO STATE R3 ..FREE R0
000B F810B2F880A2	61	PC3: A.1(STACK)->SP.1; A.0(STACK)->SP.0
0011 F810BDF8FEADB9	62	A.1(MESSL)->MA.1; A.0(MESSL)->MA.0,MS.1
0018 F8F05D2DF8FF5D	63	#F0->@MA; DEC MA; #FF->@MA ..SET MESS ARE
001F F8F0A9	64	240->MS.0 ..MESSAGE COUNTER
0022 F800A0	65	0->R0.0 ..INTERRUPT COUNTER
0025 F80EAC	66	14->CR.0 ..ZERO RAM CONSTANT AREA
F 0028 F800BDF800AD	67	A.1(RAM)->MA.1; A.0(RAM)->MA.0
002E F8005D1D	68	ZLOOP: 0->@MA; INC MA
0032 2C8C3A2E	69	DEC CR; CR.0; BNZ ZLOOP
F 0036 F800B4F800A4	70	A.1(CALLS)->R4.1; A.0(CALLS)->R4.0
F 003C F800B5F800A5	71	A.1(RET)->R5.1; A.0(RET)->R5.0
F 0042 F800B1	72	A.1(INTCD)->R1.1 ..PREPARE FOR INTERRUPTS
F 0045 F800A1	73	A.0(INTCD)->R1.0
0048 E37023	74	SEX R3; RETURN; ,#23 ..ENABLE INTERRUPTS
004B	75	...
004B	76	...
004B	77	... WAIT FOR INTERRUPT
004B	78	...
004B 304B	79	INTWT: GO TO INTWT
004D	80	...
004D F800B3F84BA3	81	EXIT: A.1(INTWT)->R3.1; A.0(INTWT)->R3.0
0053 70	82	RETURN
0054	83	...
0054	84	... INTERRUPT SERVICE STARTS HERE
0054	85	...
0054 2278	86	INTCD: DEC SP; SAVE
0056 22	87	DEC SP ..POINT TO FREE
F 0057 F800B3	88	A.1(NEWPC)->R3.1
F 005A F800A3	89	A.0(NEWPC)->R3.0
005D D3	90	GO STATE R3 ..R3 IS PC
005E 1080FB08	91	NEWPC: INC R0; R0.0.XOR.8 ..CHECK FOR RESET
0062 3A65A0	92	BNZ *+3; ->R0.0
0065 F820AC	93	32->CR.0
F 0068 F800BA	94	A.1(OUTBF+#400)->AR.1
F 006B F800AA	95	A.0(OUTBF+#400)->AR.0
006E F8203A1A	96	CLEAN: 32->@AR; INC AR ..PUT SPACES IN
0072 2C8C3A6E	97	DEC CR; CR.0; BNZ CLEAN ..DISPLAY BUFFER
0076	98	...
0076	99	... UPDATE ECONOMY/TACH RAW VALUES
0076	100	...
0076 6D22	101	ECOTAC: INP 5; DEC SP
0078 6DF012F3	102	INP 5; LDX; INC SP; XOR ..READ AND COMPAR
007C 3A76	103	BNZ ECOTAC ..SHOULD BE SAME OR REPEAT
007E F0FBFA7	104	@.XOR.#FF->R7.0
0082	105	...
0082	106	... UPDATE FUEL COUNTER
0082	107	...

F	0082	D400000400	108	CALL LOADOP; ,A(FCNT+#400)
	0087	8752	109	R7.0->@SP
	0089	9BF5FA0FA852	110	RB.1-+@.AND.#F->RB.0,@SP ..NEW MINUS OLD
	008F	8FF4AF3B98	111	AC.0+@->AC.0; BNF *+6
	0094	9FFC01BF	112	AC.1+1->AC.1 ..ADD WITH CARRY
F	0098	D400000400	113	CALL STOROP; ,A(FCNT+#400)
	009D		114	...
	009D		115	..
	009D		116	... UPDATE TACH COUNTER
F	009D	F800BDF800AD	117	A.1(TCNT+#400)->MA.1; A.0(TCNT+#400)->MA.0
	00A3	4DAF2D	118	@MA!->AC.0; DEC MA
	00A6	87FAF052	119	R7.0.AND.#F0->@SP
	00AA	9BFAF0F5FAF0B8	120	RB.1.AND.#F0-+@.AND.#F0->RB.1 ..NEW-OLD
	00B1	F6F6F6F652	121	/2/2/2/2->@SP
	00B6	8FF45D	122	AC.0+@->@MA ..CUMULATIVE TCNT
	00B9	87BB	123	R7.0->RB.1 .. NEW PREVIOUS VALUE
	00BB	80FA07	124	R0.0.AND.7 ..LOOK FOR 3 LSB=0
F	00BE	3A00	125	BNZ EPAG1 ..=>POWER OF 8 (EVERY SECOND)
	00C0	F800BFAFBEAE	126	0->AC.1,AC.0,MQ.1,MQ.0
	00C6	F806ACED	127	6->CR.0; SEX MA ..COMPUTE R.P.M.
	00CA	8FF4AF3BD3	128	MPY6: AC.0+@->AC.0; BNF *+6
	00CF	9FFC01BF	129	AC.1+1->AC.1
	00D3	2C8C3ACA	130	DEC CR; CR.0; BNZ MPY6
	00D7	E2F8005D	131	SEX SP; 0->@MA ..ZERO TCNT
	00DB	8FFF13AF	132	DIVTEN:AC.0-19->AC.0
	00DF	1E33DB	133	INC MQ; BDF DIVTEN
	00E2	9FFF01BF	134	AC.1-1->AC.1 ..SUBTRACT WITH BORROW
	00E6	33DB2E	135	BDF DIVTEN; DEC MQ
F	00E9	F800BDF800AD	136	A.1(RPM+#400)->MA.1; A.0(RPM+#400)->MA.0
	00EF	8E5D	137	MQ.0->@MA ..SAVE RPM
F	00F1	D400000000	138	EPAG1: CALL JUMP; ,A(PAGE1)
	00F6		139	...
	0100		140	PAGE
	0100		141	...
	0100		142	...
	0100		143	.. READ VELOCITY --CONVERT TO KM/H.
	0100		144	...
F	0100	80F63300	145	PAGE1:R0.0/2; BDF SPEED ..EVERY OTHER TIME
F	0104	D400000000	146	CALL JUMP; ,A(PML)
	0109		147	...
	0109	6E22	148	SPEED: INP 6; DEC SP ..READ A BYTE
	010B	6EF012F3	149	INP 6; LDX; INC SP; XOR ..READ AND COMPARE
	010F	3A09	150	BNZ SPEED ..SHOULD BE SAME OR REPEAT
	0111	F0FBFF52	151	@.XOR.#FF->@SP
	0115	8BF5A7	152	RB.0-+@->R7.0..NEW MINUS OLD
	0118	FOAB	153	@->RB.0 ..NEW BECOMES OLD
F	011A	F800BDF800AD	154	A.1(KPH+#400)->MA.1; A.0(KPH+#400)->MA.0
	0120	875D	155	R7.0->@MA
	0122		156	...
	0122		157	..
	0122		158	... UPDATE ODOMETER COUNT AND REGISTER
F	0122	D400000400	159	CALL LOADOP; ,A(OCNT+#400)
	0127	8752	160	R7.0->@SP ..SPEED DIFFERENCE
	0129	8FF4AF3B32	161	AC.0+@->AC.0; BNF *+6

```

012E 9FFC01BF 162 AC.1+1->AC.1 ..ADD WITH CARRY
F 0132 D400000400 163 CALL STOROP; ,A(OCNT+#400)
F 0137 D400000000 164 CALL SMOP; ,A(TENTH)
F 013C 9FFA803200 165 AC.1.AND.#80; BZ ODO2
F 0141 D400000000 166 CALL JUMP; ,A(PML)
F 0146 F800BFAF 167 ODO2: 0->AC.1,AC.0
F 014A D400000400 168 CALL STOROP; ,A(OCNT+#400)
014F F808FBFF52 169 8.XOR.#FF->@SP ..HAVE CONE 0.1 KM.
0154 6422 170 OUT 4; DEC SP ..STROBE ODOMETER REGISTER
0156 171 ...
0156 172 .. COMPUTE FUEL ECONOMY EVERY 0.1 KM.
0156 173 ...
0156 F800AF 174 0->MQ.0
F 0159 D400000400 175 CALL LOADOP; ,A(FCNT+#400) ..DIVIDE BY ZER
F 015E 8F3A009F3A00 176 AC.0; BNZ KP; AC.1; BNZ KP ..FCNT=0?
F 0164 F800BDF800AD 177 A.1(KMPL+#400)->MA.1; A.0(KMPL+#400)->MA.0
016A 8F5D 178 AC.0->@MA ..KMPL=0
F 016C 3000 179 GO TO KPLEX
F 016E D400000000 180 KP: CALL LOADOP; ,A(KPLCON)
F 0173 D400000400 181 KPLDIV: CALL SMOP,A(FCNT+#400)
0178 1E 182 INC MQ
0179 9FFA803273 183 AC.1.AND.#80; BZ KPLDIV
017E 2E 184 DEC MQ ..ROLLED NEGATIVE
F 017F F800BDF800AD 185 A.1(KMPL+#400)->MA.1; A.0(KMPL+#400)->MA.0
0185 8E5D 186 MQ.0->@MA
0187 F800BFAF 187 0->AC.1,AC.0
F 018B D400000400 188 KPLEX: CALL STOROP; ,A(OCNT+#400) ..ZERO ODOMETER
F 0190 D400000400 189 CALL STOROP; ,A(FCNT+#400) ..FUEL COUNTERS
F 0195 D400000000 190 CALL JUMP; ,A(PML)
019A 191 ...
019A 192 ...
019A 193 ...
019A 194 .. PROCESS MESSAGE LIST
019A 195 ...
019A 196 ...MESSAGE PROCESSING STATUS IS MAINTAINED
019A 197 ...LIST AREA OF MEMORY WHICH HAS THE
019A 198 ...FOLLOWING FORMAT:
019A 199 ...
019A 200 ... #FF ..END OF LIST MARKER
019A 201 ... (MESSAGE #) ..2ND MESSAGE OUTPUT
019A 202 ... (MESSAGE #) ..1ST MESSAGE OUTPUT
019A 203 ...MESSL: #F0 ...DOING A 30 SECOND WAIT
019A 204 ...
019A 99ADF810BD 205 PML: MS.1->MA.0; A.1(MESSL)->MA.1 ..LIST POINT
019F 2989 206 DEC MS; MS.0 ..DECREMENT MESSAGE COUNTER
F 01A1 3A00 207 BNZ MSTAT ..COUNTER AT ZERO?
01A3 2D99FF01B9 208 DEC MA; R9.1-1->R9.1 ..DECR LIST POINTER
01AB 4D522DFBFF 209 @MA!->@SP; DEC MA; .XOR.#FF ..END OF LIST?
F 01AD 3A00 210 BNZ NOTEOL
01AF F8FEADB9 211 A.0(MESSL)->MA.0,MS.1 ..MESS ALL OUTPUT
01B3 F8F0A9 212 240->MS.0 ..SET UP 30 SEC WAIT
F 01B6 3000 213 GO TO MSTAT
01B8 F800BAF805ACF0AA 214 NOTEOL:0->AR.1; 5->CR.0; @->AR.0 ..NEXT MESSAGE
01C0 9A52F4BA 215 SHL5: AR.1->@SP; 8+@->AR.1 ..COMPUTE MESS ADDR

```

	01CB	3BCF	217	BNF *+6 ..16 BIT SHIFT LEFT
	01CA	9AFC01BA	218	AR.1+1->AR.1 ..PROCESS CARRY
	01CE	2C8C3AC0	219	DEC CR; CR.0; BNZ SHL5
	01D2	9AFC07BA	220	AR.1+A.1(MES0)->AR.1 ..ADD OFFSET
F	01D6	D40000	221	CALL DISP ..OUTPUT THE MESSAGE
	01D9	F81BA9	222	24->MS.0 ..SET UP 3 SEC WAIT
F	01DC	4DFBF03200	223	MSTAT: @MA!.XOR.*F0; BZ BIP ..NOW ON DISPLAY?
F	01E1	D400000000	224	CALL JUMP; ,A(INTEX)
	01E6		225	...
	01E6		226	..
	01E6		227	.. LOOK FOR NEW BINARY PROBLEMS
F	01E6	80F63B00	228	BIP: R0.0/2; BNF BEZEL ..ODD COUNTS ONLY
F	01EA	D40000	229	CALL BSCAN
	01ED		230	...
	01ED		231	..
	01ED		232	.. UPPER OR LOWER BEZEL ACTIVE?
F	01ED	69F0FAB03200	233	BEZEL: INP 1; @.AND.#80; BZ LOBEZ
F	01F3	D400000000	234	CALL JUMP; ,A(UPBEZ)
	01F8		235	...
	01F8		236	..
	01F8		237	.. LOWER BEZEL PROCESSING:
	01F8	80FA03	238	LOBEZ: R0.0.AND.3 ..LOOK FOR 2 LSB=0
F	01FB	C20000	239	LBZ TANK .. =>POWER OF 4(EVERY 0.5 SEC)
F	01FE	D400000000	240	CALL JUMP; ,A(INTEX) ..SKIP DISPLAY
	0203		241	...
	0203		242	..
	0203		243	.. FORMAT DISPLAY IN 1/6 TANK INCREMENTS
	0203	F801FBFF52	244	TANK: 1.XOR.*FF->@SP
	020B	6422	245	OUT 4; DEC SP ..GROUP SELECT
	020A	6322	246	OUT 3; DEC SP ..CONVERT
	020C	3C0C	247	BN1 * ..WAIT FOR CONVERSION
	020E	6CF0FF05AF	248	INP 4; @-5->AC.0 ..ACCOUNT FOR OFFSET
F	0213	F800BAF800AA	249	A.1(OUTBF+#400)->AR.1; A.0(OUTBF+#400)->AR
	0219		250	...
	0219	F807AC	251	7->CR.0 ..MAX 6 BARS ON FUEL DISPLAY
	021C	8FFF10AF	252	FUEL: AC.0-16->AC.0
	0220	F8405A1A	253	T'@'->@AR; INC AR ..FILL IN FUEL BAR
F	0224	2C8C3200	254	DEC CR; CR.0; BZ FUEL1
	0228	331C	255	BDF FUEL
	022A	2AF8205A	256	FUEL1: DEC AR; 32->@AR ..BLANK ROLLOVER
	022E		257	...
	022E		258	..
	022E		259	.. FORMAT DISPLAY IN TACH REVS (TWO DIGITS)
F	022E	F800BDF800AD	260	TACH: A.1(RPM+#400)->MA.1; A.0(RPM+#400)->MA.0
	0234	4DAF	261	@MA!->AC.0
F	0236	D400000407	262	CALL FMT2; ,A(OUTBF+#400+7)
	023B	4AFB303A44	263	@AR!.XOR.*30; BNZ *+6 ..LEADING ZERO?
	0240	2AF8205A	264	DEC AR; 32->@AR ..BLANK IT
	0244		265	...
	0244		266	..
	0244		267	.. FORMAT DISPLAY IN KM/H (SPEED)
	0244	F800A7B7	268	0->R7.0,R7.1
F	0248	F800BDF800AD	269	A.1(KPH+#400)->MA.1; A.0(KPH+#400)->MA.0

	024E 4DAF	270	@MA!->AC.0
F	0250 F80AAA	271	A.0(OUTBF+#400+10)->AR.0
	0253 8FFF07AF	272	DIV11:AC.0-7->AC.0 ..DIVIDE BY 7
	0257 FB405A1A	273	T'@'->@AR; INC AR ..AND FILL IN SPEED BAR
	025B 178752	274	INC R7;R7.0->@SP
	025E 3353	275	BDF DIV11 ..POSITIVE REMAINDER?
	0260 2AF8205A	276	DEC AR; 32->@AR ..BLANK IT
F	0264 F809F53300	277	9;SD;BDF RESQL
	0269 7B38	278	SEQ;SKP
	026B 7A	279	RESQL:REQ
F	026C D400000000	280	CALL JUMP; ,A(DISALL)
	0271	281	...
	0300	282	PAGE
	0300	283	...
	0300	284	...
	0300	285	.. UPPER BEZEL PROCESSING:
	0300	286	...
F	0300 803200	287	UPBEZ: R0.0; BZ TIME ..ONCE A SEC
F	0303 D400000000	288	CALL JUMP; ,A(INTEX) ..ELSE WE ARE DONE.
	0308 F800A7B7BF	289	TIME:0->R7.0,R7.1,AC.1
F	030D F800BDF800AD	290	A.1(KPH+#400)->MA.1;A.0(KPH+#400)->MA.0
	0313 4DAF	291	@MA!->AC.0
	0315 8FFF07AF	292	DIV8:AC.0-7->AC.0
	0319 178752	293	INC R7;R7.0->@SP
	031C 3315	294	BDF DIV8
F	031E F809F53300	295	9;SD;BDF RESQ1
	0323 7B38	296	SEQ;SKP
	0325 7A	297	RESQ1:REQ
	0326	298	...
	0326	299	.. READ IN SERIAL TIME AND CONVERT
	0326	300	...
	0326 F800B7A7F810AC	301	0->R7.1,R7.0;16->CR.0
	032D 6622	302	OUT 6; DEC SP ..LOAD SHIFT REGISTER
	032F 87F6A7	303	CLOSH: R7.0/2->R7.0 ..SHIFT LO BYTE
	0332 97F63638F980B7	304	R7.1/2; B3*+4; .OR.#80->R7.1
	0339 3B3F87F980A7	305	BNF *+6; R7.0.OR.#80->R7.0
	033F 6522	306	OUT 5; DEC SP ..CLOCK SHIFT REGISTER
	0341 2C8C3A2F	307	DEC CR; CR.0; BNZ CLOSH
	0345	308	...
	0345	309	... BIT 15 IS MSB. BIT 0 IS LSB.
	0345	310	... BITS 15-8 CONTAIN MINUTES
	0345	311	... BITS 7-4 CONTAIN HOURS
	0345	312	...
	0345 F800BF	313	0->AC.1
	0348 87F6F6F6F6AF	314	R7.0/2/2/2/2->AC.0 ..SHIFT RIGHT 4
F	034E D400000400	315	CALL FMT2; ,A(OUTBF+#400) ..FORMAT HOURS
	0353 4A2AFB303A5C	316	@AR!; DEC AR; .XOR.T'0'; BNZ *+5
	0359 F8205A	317	32->@AR ..SUPPRESS LEADING ZERO
F	035C F802AA	318	A.0(OUTBF+#400+2)->AR.0
	035F F83A5A	319	T':'->@AR ..PUT OUT A COLON
	0362 97AF	320	R7.1->AC.0 ..GET MINUTES
F	0364 D400000403	321	CALL FMT2; ,A(OUTBF+#400+3)
	0369	322	...
	0369	323	...

0369		324	..	READ IN SERIAL ODOMETER AND CONVERT
0369		325	...	
0369	F800BFAFF810AC	326		0->AC.1, AC.0; 16->CR.0
0370	6622	327		OUT 6; DEC SP ..LOAD SHIFT REGISTER
0372	8FF6AF	328	ODOSH:	AC.0/2->AC.0 ..SHIFT LO BYTE
0375	9FF6357BF980BF	329		AC.1/2; B2*+4; .OR.#80->AC.1
037C	3B828FF980AF	330		BNF*+6; AC.0.OR.#80->AC.0
0382	6522	331		OUT 5; DEC SP..CLOCK SHIFT REGISTER
0384	2C8C3A72	332		DEC CR; CR.0; BNZ ODOSH
0388		333	...	
0388		334	..	ODOMETER RANGE IS 0 TO 999.9 KM.
0388		335	..	REGISTER AC CONTAINS 4 BCD DIGITS.
0388		336	...	
F 0388	F806AA	337		A.0(OUTBF+#400+6)->AR.0
038B	9FF6F6F6F6FC305A	338		AC.1/2/2/2/2+#30->@AR; INC AR ..1ST DIGIT
0394	9FFA0FFC305A1A	339		AC.1.AND.#F+#30->@AR; INC AR ..2ND DIGIT
039B	8FF6F6F6F6FC305A	340		AC.0/2/2/2/2+#30->@AR; INC AR ..3RD DIGIT
03A4	F82E5A1A	341		T.'->@AR; INC AR ..DECIMAL POINT
03AB	8FFA0FFC305A	342		AC.0.AND.#F+#30->@AR ..4TH DIGIT
03AE		343	...	
03AE		344	..	SUPPRESS LEADING ZEROES
03AE		345	...	
F 03AE	F806AAEA	346		A.0(OUTBF+#400+6)->AR.0; SEX AR
F 03B2	F0FB303A00	347		@.XOR.#30; BNZ ESUP
03B7	F8205A1A	348		#20->@AR; INC AR
F 03DB	F0FB303A00	349		@.XOR.#30; BNZ ESUP
03C0	F8205A1A	350		#20->@AR; INC AR
F 03C4	F0FB303A00	351		@.XOR.#30; BNZ ESUP
03C9	F8205A	352		#20->@AR
03CC	E2	353	ESUP:	SEX SP
03CD		354	...	
03CD		355	..	DO A TO D ON WATER TEMPERATURE. FORMAT.
03CD		356	...	
03CD	F802FBFF52	357		2.XOR.#FF->@SP
03D2	6422	358		OUT 4; DEC SP ..GROUP SELECT
03D4	6322	359		OUT 3; DEC SP ..CONVERT
03D6	3CD6	360		BN1 * ..WAIT FOR CONVERSION
03DB	6CF0AF	361		INP 4; @->AC.0
F 03DB	D400000000	362		CALL JUMP; ,A(SCALW)
03E0		363	...	
0400		364		PAGE
0400		365	...	
0400		366	...	
0400		367	..	SCALE THRU 0-99
0400		368	...	
F 0400	F80FAA	369	SCALW:	A.0(OUTBF+#400+15)->AR.0
0403	F84F5A1A	370		T'O'->@AR; INC AR ..PUT IN OK
0407	F84B5A	371		T'K'->@AR
F 040A	8FFFF43300	372		AC.0-244; BCE FLW ..TEMP < 60?
040F	8FF652	373		AC.0/2->@SP ..USE LINEAR APPROX.
0412	F8B6F7AFA7	374		182-@->AC.0,R7.0 ...TO COMPUTE TEMP
F 0417	E40900040C	375		CALL FMT2; ,A(OUTBF+#400+12) ..NO. FORMAT
F 041C	87FF613B00	376		R7.0-97; IF LESS GO TO FLW
0421	F800BCF807AC	377		0->CR.1; 7->CR.0 ..MESSAGE #7

F	0427	D40000	378	CALL MESADD .. "WATER TEMP HIGH"
F	042A	F80FAA	379	A.0(OUTBF+#400+15)->AR.0
	042D	F84B5A1A	380	T'H'->@AR; INC AR .. IT IS HIGH
	0431	F8495A	381	T'I'->@AR
F	0434	3000	382	GO TO OIL
	0436	F800BCF807AC	383	FLW: 0->CR.1; 7->CR.0 .. MESSAGE #7
F	043C	D40C00	384	CALL MESSUB
	043F		385	...
	043F		386	.. DO A TO D ON OIL PRESSURE. FORMAT.
	043F		387	...
	043F	F803FBFF52	388	OIL: 3.XOR.#FF->@SP
	0444	6422	389	OUT 4; DEC SP .. GROUP SELECT
	0446	6322	390	OUT 3; DEC SP .. CONVERT
	0448	3C48	391	BN1 * .. WAIT FOR CONVERSION
	044A	6CFOAF	392	INP 4; @->AC.0
	044D		393	...
	044D		394	... SCALE 0-7
	044D		395	...
	044D	F802AE	396	2->MQ.0
F	0450	8FFFD3300	397	AC.0-OV2; IF GE GO TO OILEX
F	0455	1E8FFFD93300	398	INC MQ; AC.0-OV3; IF GE GO TO OILEX
F	045B	1E8FFFC43300	399	INC MQ; AC.0-OV4; IF GE GO TO OILEX
F	0461	1E8FFFB03300	400	INC MQ; AC.0-OV5; IF GE GO TO OILEX
F	0467	1E8FFF9C3300	401	INC MQ; AC.0-OV6; IF GE GO TO OILEX
F	046D	1E8FFF873300	402	INC MQ; AC.0-OV7; IF GE GO TO OILEX
	0473	1E	403	INC MQ .. MQ NOW UP TO 7
F	0474	F813AA	404	OILEX:A.0(OUTBF+#400+19)->AR.0
	0477	8EF6AFFC305A	405	MQ.0; SHR;->AC.0;+#30->@AR
	047D	F808BCF800AC	406	8->CR.1; 0->CR.0 .. MESSAGE #8
	0483	1A1A	407	INC AR; INC AR
F	0485	8FFF023300	408	AC.0-2; IF GE GO TO OILOK
	048A	F84C5A1A	409	T'L'->@AR; INC AR
	048E	F84F5A	410	T'O'->@AR
F	0491	D40000	411	CALL MESADD .. "OIL PRESSURE LOW"
F	0494	3000	412	GO TO FUELEC
	0496	F84F5A1A	413	OILOK:T'O'->@AR; INC AR
	049A	F84B5A	414	T'K'->@AR
F	049D	D40000	415	CALL MESSUB
	04A0		416	...
	04A0		417	.. FORMAT FUEL ECONOMY
	04A0		418	...
	04A0		419	...
F	04A0	F800BDF800AD	420	FUELEC: A.1(KMPL+#400)->MA.1; A.0(KMPL+#400)->MA
	04A6	4DAF	421	@MA!->AC.0
F	04AB	8FA73200	422	AC.0->R7.0; BZ AMPS1
F	04AC	D400000418	423	CALL FMT2; ,A(OUTBF+#400+24)
	04B1	4AFB303ABA	424	@AR!.XOR.#30; BNZ *+6 .. LEADING ZERO?
	04B6	2AFB205A	425	DEC AR; 32->@AR .. BLANK IT
	04BA	E7AF	426	R7.0->AC.0
F	04BC	F81BAA	427	A.0(OUTBF+#400+27)->AR.0
F	04BF	8FFF093300	428	AC.0-9; IF GE GO TO TRYOK
	04C4	F84C5A1A	429	T'L'->@AR; INC AR
	04C8	F84F5A	430	T'O'->@AR
F	04CB	3000	431	GO TO AMPS1

F	04CD	FFFF0D3300	432	TRYOK:AC.0-13; IF GE GO TO TRYHI
	04D2	F84F5A1A	433	T'O'->@AR; INC AR
	04D6	F14B5A	434	T'K'->@AR
F	04D9	3000	435	GO TO AMPS1
	04DB	F84B5A1A	436	TRYHI:T'H'->@AR; INC AR
	04DF	F8495A	437	T'I'->@AR
	04E2		438	...
F	04E2	D400000000	439	AMPS1:CALL JUMP; ,A(AMPS)
	0500		440	PAGE
	0500		441	...
	0500		442	...
	0500		443	.. DO "LO" OR "OK" INDICATION FOR AMPS
	0500		444	...
F	0500	F81EAA	445	AMPS: A.0(OUTBF+#400+30)->AR.0
	0503	F84F5A1A	446	T'O'->@AR; INC AR
	0507	F84B5A	447	T'K'->@AR
F	050A	6AF0FA013200	448	INP 2;@.AND.1;BZ DISALL..UNUSED BINARY
	0510	2AF84C5A1A	449	DEC AR; T'L'->@AR; INC AR
	0515	F84F5A	450	T'O'->@AR
	0518		451	...
	0518		452	...
F	0518	F800BAF800AA	453	DISALL: A.1(OUTBF+#400)->AR.1; A.0(OUTBF+#400)->
F	051E	D40000	454	CALL DISP
	0521		455	...
	0521		456	.. EXIT FROM INTERRUPT
	0521		457	...
	0521	12	458	INTEX:INC SP
	0522	F800B1	459	A.1(EXIT)->R1.1
	0525	F84DA1	460	A.0(EXIT)->R1.0
	0528	D1	461	GO STATE R1
	0529		462	...
	0529		463	...
	0529		464	.. SCAN AND PROCESS ALL BINARY INPUTS
	0529		465	...
F	0529	F800BDF800AD	466	BSCAN:A.1(OST1+#400)->MA.1; A.0(OST1+#400)->MA.0
	052F	4DAF	467	@MA!->AC.0
	0531	8F5222	468	AC.0->@SP; DEC SP
	0534	69	469	INP 1 ..LEAST SIGNIF. (DEV 7-0)
	0535	F0FBFEFA7F	470	@.XOR.INV1.AND.ACT1
	053A	52AF	471	->@SP,AC.0
	053C	12F3	472	INC SP; XOR ..XOR OLD,NEW STATUS
	053E	A7	473	->R7.0 ..SAVE FOR LATER
	053F	22	474	DEC SP ..POINT BACK TO NEW STATUS
	0540	F2B7	475	AND;->R7.1 ..DETECT 0->1 TRANSITION
F	0542	F800BDF800AD	476	A.1(OST1+#400)->MA.1; A.0(OST1+#400)->MA.0
	0548	8F5D	477	AC.0->@MA ..STORE IT
	054A	F800BC	478	0->CR.1 ..DEVICE OFFSET
F	054D	D4000012	479	CALL BINDET; INC SP
F	0551	F800BDF800AD	480	A.1(OST2+#400)->MA.1; A.0(OST2+#400)->MA.0
	0557	4DAF	481	@MA!->AC.0
	0559	8F5222	482	AC.0->@SP; DEC SP
	055C	6A	483	INP 2 ..DEVICES 15-8
	055D	F0FBFFFA00	484	@.XOR.INV2.AND.ACT2 ..PROCESS SAME WAY
	0562	52AF	485	->@SP,AC.0

	0564	12F3A7	486	INC SP; XOR; ->R7.0
	0567	22F2B7	487	DEC SP; AND; ->R7.1
F	056A	F800BDF800AD	488	A.1(OST2+#400)->MA.1; A.0(OST2+#400)->MA.0
	0570	8F5D	489	AC.0->@MA
	0572	F808BC	490	8->CR.1 ..DEVICE OFFSET
F	0575	D4000012	491	CALL BINDET; INC SP
F	0579	1800BDF800AD	492	A.1(OST3+#400)->MA.1; A.0(OST3+#400)->MA.0
	057F	*DAF	493	@MA!->AC.0
	0581	8F5222	494	AC.0->@SP; DEC SP
	0584	6D	495	INP 3 ..DEVICES 23-16
	0585	F0FBFFFA00	496	@.XOR. INV3. AND. ACT3
	058A	52AF	497	->@SP, AC.0
	05DC	12F3A7	498	INC SP; XOR; ->R7.0
	05DF	22F2B7	499	DEC SP; AND; ->R7.1
F	0592	F800BDF800AD	500	A.1(OST3+#400)->MA.1; A.0(OST3+#400)->MA.0
	0598	8F5D	501	AC.0->@MA
	059A	F810BC	502	16->CR.1 ..DEVICE OFFSET
F	059D	D4000012	503	CALL BINDET; INC SP
	05A1	D5	504	EXIT ..DONE
	05A2		505	...
	05A2		506	...
	05A2		507	...
	05A2		508	.. DETECT DEVICE TRANSITIONS
	05A2		509	...
	05A2	F800ACAF	510	BINDET: 0->CR.0, AC.0
	05A6	97F6B7	511	BIND01: R7.1/2->R7.1 ..SHIFT OUT LOW BIT
F	05A9	3B00	512	IF NDF GOTO CONT0 ..NO CHANGE DETECTED?
F	05AB	D40000	513	CALL MESADD ..GO ADD DEVICE MESSAGE
	05AE	1C8CFB083AA6	514	CONT0: INC CR; CR.0.XOR.8; BNZ BIND01
	05B4	F800AC	515	0->CR.0 ..RESET
	05B7	121212	516	INC SP; INC SP; INC SP ..POINT TO OLD STAT
	05BA	87F2B7	517	R7.0.AND.@->R7.1 ..1->0 TRANSITION
	05BD	222222	518	DEC SP; DEC SP; DEC SP ..RESTORE STACK
	05C0	97F6B7	519	LOOP1: R7.1/2->R7.1 ..SHIFT OUT LOW BIT
F	05C3	3B00	520	IF NDF GOTO CONT1 ..NO CHANGE DETECTED?
F	05C5	D40000	521	CALL MESSUB ..GO REMOVE DEVICE MESSAGE
	05C8	1C8CFB083AC0	522	CONT1: INC CR; CR.0.XOR.8; BNZ LOOP1
	05CE	D5	523	EXIT ..END OF BINARY DETECT
	05CF		524	...
	0600		525	PAGE
	0600		526	...
	0600		527	...
	0600		528	...
	0600		529	.. ADD MESSAGE TO DISPLAY LIST
	0600		530	...
	0600	9C528CF4A8	531	MESADD: CR.1->@SP; CR.0+@->RB.0 ..DEVICE NUM
	0605	F810BD	532	A.1(MESSL)->MA.1 ..ADD MESSAGE
	0608	F8FEAD	533	A.0(MESSL)->MA.0
	060B	ED	534	SEX MA
	060C	88F3	535	MESA01: RB.0; XOR ..ITEM TO BE ADDED?
	060E	3A00	536	BNZ MESA02
F	0610	3000	537	BR MESA99 ..REJECT
F	0612	F0FBFF	538	MESA02: @; XRI #FF ..EOL MARKER?
	0615	2D	539	DEC MA

0616	3A0C	540	BNZ MESA01
0618	1D885D	541	INC MA; R8.0->@MA ..PUSH ON MESSAGE STAC
061B	2D	542	DEC MA
061C	F8FF5D	543	#FF->@MA ..MARK NEW EOL
061F	F810BD99AD	544	A.1(MESSL)->MA.1; MS.1->MA.0
F 0624	4DFBF03A00	545	@MA!.XOR.#FO; BNZ MESA99 ..MESS ON DISPLAY
0629	F801A9	546	1->MS.0 ..FORCE DISPLAY OF MESSAGES
062C	E2D5	547	MESA99: SEX SP;EXIT ..GOOD RETURN
062E		548	...
062E		549	.. REMOVE MESSAGE FROM DISPLAY LIST
062E		550	...
062E	9C528CF4A8	551	MESSUB: CR.1->@SP; CR.0+@->R8.0 ..DEVICE NUM
0633	F810BDF8FEADED	552	A.1(MESSL)->MA.1; A.0(MESSL)->MA.0; SEX MA
063A	F800B0	553	0->R0.1 ..CLEAR FOUND FLAG
063D	F052	554	MESS01: @->@SP ..PUSH MESSAGE LIST ON SP
063F	88F3	555	R8.0;XOR ..ITEM TO REMOVE?
F 0641	3A00	556	BNZ NOTIT
0643	12F801B0	557	INC SP; 1->R0.1 ..KNOCK IT OFF SP
0647	F0FBFF	558	NOTIT: @.XOR.#FF ..EOL?
064A	2D22	559	DEC MA;DEC SP
064C	3A3D	560	BNZ MESS01
064E	121D	561	INC SP;INC MA
F 0650	903200	562	R0.1; BZ MESS02
0653	1D	563	INC MA ..COMPRESS LIST IF FOUND
0654	425D1D	564	MESS02: @SP!->@MA;INC MA ..PUT BACK MESSAGE LIST
0657	FBFO	565	XRI #FO ..FRAME MARKER?
0659	3A54	566	BNZ MESS02
065B	22E2D5	567	DEC SP;SEX SP;EXIT
065E		568	...
065E	F88052	569	DISP:#80->@SP
0661	6122	570	OUT 1; DEC SP ... CLEAR MEMORY
0663	F808AC	571	8->CR.0
0666	2C8C3A66	572	CLP: DEC CR; CR.0; BNZ CLP
066A	F820AC	573	32->CR.0
066D	EAEA EA	574	DCO: SEX AR;SEX AR;SEX AR ..MORE SEX
0670	4A2A	575	LDA AR;DEC AR ..STALL A WHILE
0672	61	576	OUT 1 ..ZING IT
0673	8CFF01AC	577	CR.0-1->CR.0 ..SLOW DECREMENT
0677	3A6DE2	578	BNZ DCO; SEX SP
067A	F80152	579	1->@SP
067D	6222	580	OUT 2; DEC SP ..MAKE SURE IT IS ON
067F	D5	581	EXIT
0680		582	...
0680	46BA	583	FMT2: @R6!->AR.1 ..FORMAT 2 DIGIT ASCII
0682	46AA	584	@R6!->AR.0 ..GET DESTINATION ADDRESS
0684	F800AE	585	D10: 0->MQ.0
0687	8FFF0AAF	586	DLP: AC.0-10->AC.0
068B	1E3387	587	INC MQ; BDF DLP
068E	2EBEFC305A	588	DEC MQ; MQ.0+#30->@AR
0693	1ABFFC3A5A2A	589	INC AR; AC.0+#3A->@AR; DEC AR
0699	D5	590	EXIT ..REGISTER AR IS UNCHANGED
069A		591	...
069A	E2	592	JUMP: SEX SP ..MAKE SURE
069B	4652	593	@R6!->@SP ..SAVE HIGH BYTE

069D	46A6	594	@R6!->R6.0 ..PUT IN LOW
069F	F0B6	595	@->R6.1 ..PUT IN HIGH
06A1	D5	596	EXIT ..RETURN ADJUSTED
06A2		597	...
06A2	46	598	LOADOP: LDA LINK .. FETCH ADDRESS
06A3	BD	599	PHI MA .. TO MA REGISTER
06A4	46	600	LDA LINK
06A5	AD	601	PLO MA .. FALL INTO LOAD
06A6	4D	602	LOAD: LDA MA .. FETCH HIGH B
06A7	BF	603	PHI AC
06A8	4D	604	LDA MA .. NOW LOW B
06A9	AF	605	PLO AC .. LEAVE MA AT NEXT DOUBLE-BYTE
06AA	D5	606	SEP RETN .. GEE, THAT WAS QUICK.
06AB		607	...
06AB	46	608	STOROP: LDA LINK .. FETCH ADDRESS INTO MA
06AC	BD	609	PHI MA
06AD	46	610	LDA LINK
06AE	AD	611	PLO MA .. THEN FALL INTO STORE
06AF	9F	612	STORE: CHI AC .. FIRST HIGH B
06B0	5D	613	STR MA
06B1	1D	614	INC MA .. INCREMENT MA, SINCE STR DOESN'T
06B2	8F	615	GLO AC .. NOW LOW B
06B3	5D	616	STR MA
06B4	1D	617	INC MA .. LEAVE MA POINTING TO NEXT WORD
06B5	D5	618	SEP RETN .. QUIT
06B6		619	...
06B6	46	620	SMOP: LDA LINK
06B7	BD	621	PHI MA
06B8	46	622	LDA LINK
06B9	AD	623	PLO MA
06BA	1D	624	SM: INC MA .. POINT TO LOW B
06BB	ED	625	SEX MA .. SET X TO MA
06BC	8F	626	GLO AC .. FETCH AC LOW B
06BD	F7	627	SM .. SUBTRACT MEMORY FROM IT
06BE	AF	628	PLO AC .. PUT IT BACK.
06BF	2D	629	DEC MA .. NOW HIGH B
06C0	9F	630	CHI AC
F 06C1	3300	631	BDF SMNB
06C3	FF01	632	SMI #1 .. PROPAGATE BORROW OF LOW B
F 06C5	3300	633	BDF SMNB
06C7	F3	634	XOR .. SECOND BORROW; FORCE BORROW OUT,
06C8	38	635	,#38 .. WHILE SUBTRACTING HIGH B.
06C9	F7	636	SMNB: SM .. HIGH B SUBTRACT, NO BORROW ACCROSS.
06CA	BF	637	PHI AC .. PUT HIGH B BACK
06CB	E2	638	SEX SP
06CC	D5	639	SEP RETN .. RETURN. DF=NO BORROW OUT
06CD		640	...
06CD	D3	641	SEP R3 ... RETURN TO MAIN
06CE	9652	642	CALLS: R6.1->@R2
06D0	22	643	DEC R2 ... STACK LEFT POINTING AT
06D1	8652	644	R6.0->@R2 ... NEXT FREE LOCATION
06D3	22	645	DEC R2
06D4	93B6	646	R3.1->R6.1 ... COPY R3 TO R6
06D6	83A6	647	R3.0->R6.0

```

06DB 46B3      648      @R6!->R3.1
06DA 46A3      649      @R6!->R3.0
06DC 30CD      650      COTO CALLS-1
06DE          651      ...
06DE D3        652      SEP R3          ... RETURN TO MAIN
06DF 96B3      653 RET: R6.1->R3.1 ... COPY R6 TO R3
06E1 86A3      654      R6.0->R3.0
06E3 12        655      INC R2
06E4 42A6      656      @R2!->R6.0     ... POP R6 FROM STACK
06E6 42B6      657      @R2!->R6.1
06E8 22        658      DEC R2
06E9 30DE      659      COTO RET-1
06EB          660      ...
06EB          661      ..          ROM CONSTANTS
06EB          662      ...
06F0          663      ORG #6F0
06F0 0BB8      664      KPLCON: ,3000 ..TO COMPUTE KM/LITER
06F2 0F4E      665      TENTH: ,3918 ..TENTH OF A KILOMETER
06F4          666      ...
06F4          667      ...
06F4          668      ..          RAM STORAGE REQUIRED
06F4          669      ...
0C00          670      ORG #C00
0C00          671      ...
0C00          672 RAM: ..RAM START ADDRESS
0C00 00        673 KPH: .0          ..PROPORTIONAL TO KM. PER HR.
0C01 00        674 RPM: .0
0C02 00        675 OST1: ,0
0C03 00        676 OST2: ,0
0C04 00        677 OST3: ,0
0C05 0000      678 OCNT: ,0,0     ..ODOMETER COUNT
0C07 00        679 TCNT: ,0
0C08 0000      680 FCNT: ,0,0     ..FUEL COUNT
0C0A 00        681 KMPL: ,0       ..CURRENT FUEL ECONOMY
0C0B          682      ...
0C0B          683 OUTBF: ..WORKING RAM BUFFER FOR DISPLAY
0C0B          684      ...
0C0B          685      ...
0C0B          686 END: END

```

FL LOC	COSMAC CODE	LNNO	SOURCE LINE		
FL LOC	COSMAC CODE	LNNO	SOURCE LINE		
0000		1	...	>MESS	J. M. C. RCA LABS 8:16:76
0000		2	...		
0000		3	...	ELECTRONIC DASHBOARD MESSAGES	
0000		4	...		
0700		5	...	ORG #700	
0700		6	...		
0700	20202020202020	7	MES0:	,32,32,32,32,32,32,32,32	
0708	5345325649434520	8		,T'SERVICE',32	
0710	4252414B45204F4E	9		,T'BRAKE',32,T'ON'	
0718	20202020202020	10		,32,32,32,32,32,32,32,32	
0720		11		...	
0720	20202020202020	12	MES1:	,32,32,32,32,32,32,32,32	
0728	202020444F4F5253	13		,32,32,32,T'DOORS'	
0730	204F50454E20	14		,32,T'OPEN',32	
0736	20202020202020	15		,32,32,32,32,32,32,32,32	
073E	2020	16		,32,32	
0740		17		...	
0740	20202020202020	18	MES2:	,32,32,32,32,32,32,32,32	
0748	2020202020	19		,32,32,32,32,32	
074D	48415A415244	20		,T'HAZARD'	
0753	20202020202020	21		,32,32,32,32,32,32,32,32	
075B	2020202020	22		,32,32,32,32,32	
0760		23		...	
0760	20202020202020	24	MES3:	,32,32,32,32,32,32,32,32	
0768	4252414B4520	25		,T'BRAKE',32	
076E	464C55494420	26		,T'FLUID',32	
0774	404F5720	27		,T'LOW',32	
0778	20202020202020	28		,32,32,32,32,32,32,32,32	
0780		29		...	
0780	202020202020	30	MES4:	,32,32,32,32,32,32,32	
0786	2020	31		,32,32	
0788	44414E47465220	32		,T'DANGER',32	
078F	534C4F5720	33		,T'SLOW',32	
0794	444F574E	34		,T'DOWN'	
0798	2020	35		,32,32	
079A	202020202020	36		,32,32,32,32,32,32	
07A0		37		...	
07A0	202020202020	38	MES5:	,32,32,32,32,32,32,32	
07A6	524553545241494E	39		,T'RESTRAIN'	
07AE	542053595354454D	40		,T'T',32,T'SYSTEM'	
07B6	204F5554	41		,32,T'OUT'	
07BA	202020202020	42		,32,32,32,32,32,32	
07C0		43		...	
07C0	20202020202020	44	MES6:	,32,32,32,32,32,32,32,32	
07CB	20414E54492D	45		,32,T'ANTI-	
07CE	534B494420	46		,T'SKID',32	
07D3	4F5554202020	47		,T'OUT',32,32,32	
07D9	20202020202020	48		,32,32,32,32,32,32,32	
07E0		49		...	
07E0		50	...	ANALOG SENSORS	
07E0		51		...	
07E0	2020202020	52	MES7:	,32,32,32,32,32	

07E5	574154455220	53	, T' WATER' , 32
07EB	5445405045524154	54	, T' TEMPERAT'
07F3	5552452048494748	55	, T' URE' , 32, T' HIGH'
07FB	2020202020	56	, 32, 32, 32, 32, 32
0800		57	...
0800	2020202020202020	58	MESS: , 32, 32, 32, 32, 32, 32, 32, 32
0808	4F494C20	59	, T' OIL' , 32
080C	5052455353555245	60	, T' PRESSURE'
0814	204C4F57	61	, 32, T' LOW'
081B	2020202020202020	62	, 32, 32, 32, 32, 32, 32, 32, 32
0820		63	...

## REFERENCES

1. D. Zur Heiden and H. Oehlen, "Radar Anticollision Warning System for Road Vehicles," Electrical Communications 52(2), 141 (1977).
2. G. Hahlganss and L. Hahn, "Headway Radar Using Pulse Techniques," Int. Conf. on Automobile Electronics, London, July 1976, pp. 132-135.
3. E. Dull and H. Peters, "Collision Avoidance System for Automobiles," Society of Automotive Engineers, Publication #780263, March 1978.
4. F. E. Nathanson, Radar Design Principles, (McGraw-Hill Publishing Company, New York, 1969).
5. S. A. Hovanessian, Radar Detection and Tracking Systems, (Artech House, Inc., Massachusetts, 1973).
6. E. F. Belohoubek et al., "Electronic Subsystems for Research Safety Vehicle (RSV)," Final Report, Phase II, 1976.
7. S. Silver, Microwave Antenna Theory and Design, Rad. Lab Series, Vol. 12, Boston Tech. Publications, 1964.
8. J. Shefer et al., "A New Kind of Radar For Collision Avoidance," SAE Automotive Engineering Congress and Exposition, Detroit, Michigan, February 26, 1974.
9. G. S. Kaplan and F. Sterzer, "Dual-Mode Automobile Collision Avoidance Radar," SAE Automotive Engineering Congress and Exposition, Detroit, Michigan, February 24-28, 1975.
10. A. G. Kandoian et al., Reference Data for Radio Engineers, International Telephone & Telegraph Corp., New York, 1964.
11. R. Limpert, Motor Vehicle Accident Reconstruction and Course Analysis, Michie Company, Charlesville, VA, December 1978.
12. R. F. Freiman, "PRICE - A Parametric Cost Modeling Methodology," RCA Government and Commercial Systems, Cherry Hill, NJ, May 1978.

APPENDIX B

VOLVO OF AMERICA CORPORATION FINAL REPORT

LARGE RESEARCH SAFETY VEHICLE (LRSV)  
ENGINE DEVELOPMENT

LARGE RESEARCH SAFETY VEHICLE (LRSV)

ENGINE DEVELOPMENT FINAL REPORT

February, 1981

Minicars, Inc. Subcontract Purchase Order #5185

Prepared by:

Product Planning & Development Department  
Volvo of America Corporation  
Rockleigh, New Jersey 07647

Volvo of America Corporation, Rockleigh, New Jersey 07647

ABSTRACT:

The intent of the Large Research Safety Vehicle (LRSV) program is to research passenger car technology for the purpose of meeting the discussed safety, fuel economy and emission standards for the mid 1980s. It is also the goal of that program to be able to meet these standards while still retaining the comfort and size of an automobile typical to the U. S. motoring public.

Volvo of America Corp., (VAC) under contract to Minicars, Inc. of Goleta, California, and subcontract to the LRSV program, agreed to provide an engine capable of meeting the defined fuel economy, performance and emission goals of that program.

This report describes the procedure and results by which a refined spark ignition engine was developed, constructed, tested and provided for that program.

## TABLE OF CONTENTS

<u>TITLE</u>	<u>PAGE</u>
INTRODUCTION AND SUMMARY	1
PROCEDURE	4
RESULTS	8
APPENDIX	
A. General Specifications and Performance Objectives	20
B. General Description of the Lambda-Sond <sup>®</sup> Air Fuel Control System	23
C. Development Test Equipment Description	28
D. FTP Results	32
E. Task Results	35
F. Observed and Calculated Data Recorded During Dynamometer Study	47
G. Steady State Emission Data	52

## LIST OF FIGURES

<u>FIGURE</u>	<u>TITLE</u>	<u>PAGE</u>
1	Manifold Vacuum vs. Time (1978 FTP)	13
2	Engine Break In Schedule Manifold Vacuum vs. Time	14
3	Engine Break In Schedule Engine Speed vs. Time	14
4	BSFC vs. Rpm B-21 and B-19 at WOT	15
5	BSFC vs. Rpm B-19 at 13" Hg	15
6	Exhaust Emissions B-19 at 13" Hg	16
7	BSFC vs. Rpm with Synthetic Oil at 13" Hg	16
8	BSFC vs. Rpm with Reduced Accessory Drive at 13" Hg	17
9	BSFC vs. Rpm with MSD Ignition at 13" Hg	17
10	Max. Hp Production B-19 and Turbo B-19	18
11	Boost Retard System	18
12	Crankcase Pressure vs. Rpm at 13" Hg	19
13	Engine Performance Measurement System	30
14	Engine Dynamometer Fuel Measurement System	30
15	Engine Dynamometer Exhaust Emission Measurement	31
16	LRSV Engine Performance Turbo, Normally Aspirated	35

17	Predicted LRSV Performance	37
18	Predicted Acceleration Curve	38
19	Actual Acceleration Times LRSV - Volvo - Chassis	44
20	Predicted Emission Levels and Fuel Economy at 50,000 Miles	45
21	Zero Mile Test Data	46

## INTRODUCTION AND SUMMARY:

The need for clean running and fuel efficient vehicles combined with passenger comfort and safety are major concerns for car manufacturers.

Aware of the need to research such technology, the U. S. Government through U.S. DOT/NHTSA implemented the Large Research Safety Vehicle (LRSV) program.

Volvo of America Corp. (VAC), under contract to Minicars, Inc. of Goleta, California, and subcontract to the LRSV program, agreed to supply a refined spark ignition engine capable of meeting the program objectives. The program commenced with Issuance of Subcontract January 20, 1978 and was concluded Summer, 1979.

The program's intentions, as set by NHTSA, specified development of technology which may be translated into a feasible, affordable, mass-produced product for the mid-eighties but did not necessarily require the provided engine to be an actual production engine.

The engine program had the following goals to be met:

### EXHAUST EMISSIONS

<u>Objective</u>	<u>Maximum Acceptable</u>
HC - .41 g/mi	HC - .41 g/mi
CO - 3.4 g/mi	CO - 3.4 g/mi
NOx - .4 g/mi	NOx - 1.0 g/mi

### FUEL ECONOMY

#### Objective

27.5 mi/gal. combined EPA cycle

### ACCELERATION

#### Objective

0-60 mph - 13.5 secs.

#### Maximum Acceptable

0-60 mph - 20.0 secs.

The general specification and performance objectives are further detailed in Appendix A.

To this end, DM Engineering, Inc. of Brookfield, Conn., under VAC direction, was contracted to complete the hardware development and construction of the LRSV engine.

With their assistance, a methodology was developed for considering what technical features would be incorporated and the means by which they

would be tested.

As an overview, technical modifications to be developed would be centered around: improving cycle and thermal efficiency, reducing internal frictional losses and rotational mass, and improving combustion characteristics within established emission levels.

The basic engine selected for the program was the Volvo B-21F 2.1 in-line 4 cylinder engine. To stay within the intent of the program, a serious effort was made to retain as much of the present engine as possible. It was further realized that the Lambda-Sond<sup>®</sup> feedback control system, would form a vital part of the program. A detailed description of the system is presented in Appendix B.

The program for the engine was outlined to follow this course of development: initially candidate technical modifications were to be evaluated with the engine on a dynamometer and run under a predetermined steady state condition. All the modifications which were found to improve either the fuel efficiency or emission characteristics would be explored further with the aim to be incorporated into the final refined engine. Subsequently, the refined engine would be installed in a Volvo 244 DL with over-drive transmission and developed on DM's chassis dynamometer. Once completed, the LRSV-Volvo chassis would undergo final development and fine-tuning at an approved EPA lab. Results would then be verified on the FTP cycle.

During the approved EPA lab testing the dyno horsepower would be set to the PAU (Power Absorption Unit) setting for the actual LRSV chassis, as determined by Minicars. Upon completion of this course of development, a duplicate EPA test cycle would be run to verify the repeatability of the results. The Volvo test chassis would serve the dual purpose of investigating and determining specific gear ratios and proving acceleration times and driveability.

From this work the following refinements were found to be beneficial: reduced engine displacement, elevated coolant temperature, synthetic engine lubricants, reduction of accessory drive speed, multi-spark capacitive discharge system, reduced rotational mass, and matched fuel injectors.

As a result of these technical features and tuning the program goals were met. They account for an approximate 15% increase in fuel economy over the stock production engine while remaining within the emission and acceleration objectives.

\* The name Lambda-Sond is a registered trademark of A.B. Volvo.

It should be noted that the engine, including turbocharger as developed in the program and tested in the Volvo chassis, met the test goals. However, when the engine was fitted to the LRSV the turbo was removed to ease installation. It was found that all the program goals could be met with the engine in its normally aspirated version, and therefore this vehicle configuration was pursued.

Following January, 1980, the initial LRSV program was extended to facilitate replacement of original engine and further fitting and testing. For this, DM Engineering was named as the prime contractor with Volvo of America Corporation, again, named as a subcontractor.

The final results stated below were acquired with DM as the prime contractor.

To clarify and conclude, this is a special research engine that was carefully prepared for the needs of this program. Therefore, it should be realized that application of all the refinements would not necessarily yield the same results in a production car or in a production environment. Rather, it should be concluded that gains in fuel economy can be attained with the utilization of a similar engine development program.

<u>Results:</u>	<u>LRSV</u>
Emissions:	
HC	0.19 gpm
CO	2.38 gpm
NOx	0.57 gpm
MPG:	
EPA City (Est.)	22.8 mpg
EPA Highway	36.5 mpg
EPA Combined	27.43 mpg
Dyno Setting:	10.8 hp @ 50 mph
Inertia Weight:	3250 lbs.

## PROCEDURE:

The goal of the LRSV engine development program was to arrive at a Volvo B-21 based power plant which would meet established emissions and fuel economy levels as measured by the 1978 FTP emission/fuel economy cycle and 0-60 mph acceleration times.

To expedite development, a modeling "tool" was devised to approximate the transient conditions of the FTP test cycle. Therefore, it was desired to find a steady state condition which would, on a "first cut" basis, resemble the driving cycle. In this way, the effect of technical features or modifications could be assessed to determine the contribution to the program. The exact effect of all the technical additions would later be verified by the testing on the FTP cycle.

To determine this steady state condition, a 1978 B-21F Lambda-Sond engine was fitted with a vacuum transducer to monitor intake manifold pressure. The obtained vacuum trace, along with a speed trace of the driving cycle, allowed an average engine load schedule to be developed.

Calculating the N/V ratio (engine RPM in 4th. gear/mph) of the test Volvo led to an rpm range which the engine operated during the EPA cycle. This rpm range was later corrected for the actual LRSV drivetrain N/V ratio. Subsequently, an engine dynamometer testing schedule was structured to record various engine performance and operating conditions under partial and wide-open throttle.

These recorded engine parameters are:

1. Engine RPM
2. Engine Torque
3. Engine Air-inlet Temperature, Dry Bulb
4. Engine Air-inlet Temperature, Wet Bulb
5. Barometric Pressure
6. Engine Oil Pressure
7. Engine Water Temperature

8. Engine Inlet Oil Temperature
9. Engine Fuel Flow Rate, Pounds per Hour
10. Exhaust gas %CO
11. Exhaust gas HC, ppm
12. Exhaust gas NOx, ppm
13. Manifold Vacuum/pressure
14. Ignition Patterns/RPM

For reference, a description of equipment used and its application is presented in Appendix C.

A list of technical modifications were compiled for evaluation and, as stated earlier, these modifications include:

1. Reduction in displacement (2.1 liter to 2.0 liter)
2. Substitution of synthetic engine oil
3. Reduction of accessory drive speed
4. Addition of a multi-spark capacitive discharge ignition system
5. Elevated engine coolant temperature
6. Turbocharging
7. Reduction of engine lubricant pumping losses
8. Reduction of crankcase pressure

It was anticipated, from the onset, that a reduction in engine displacement from 2.1 L to 2.0 L would be beneficial to the program. This would be accomplished by utilizing a B-19 engine block with a B-21 Lambda-Sond cylinder head. Therefore, initial break-in and running would be done with a B-19 block.

Engine development began with three B-19 engines being broken in and baselined. The engine break-in was accomplished by operating these engines on the engine dynamometer over a predetermined vacuum and RPM schedule. The schedule was arrived through the use of factory recommended break-in schedules. (The total break-in time for each engine was 30 hours.) All three engines, at completion of their break-in, were baselined to determine their relative horsepower, torque and brake specific fuel consumption (BSFC).

The third engine remained on the dynamometer to begin evaluation of the candidate modifications previously mentioned.

Simultaneously, engines #1 and #2 were disassembled to determine their dimensional consistency. After measuring, #1 engine was blueprinted and balanced. It should be noted that the machining of these internal engine parts were maintained within production tolerances but brought to a finer degree of precision than normally found in factory production.

For reference, the following describes some of the tolerances incorporated into the LRSV engine:

	<u>B-21</u>	<u>LRSV</u>
Cylinder Bores	+/- .0004"	+/- .0001"
Piston Diameter	+/- .002"	+0/-.002"
Piston Weight Variation	+/- .220 oz.	+0/-.010 oz.
Connecting Rod Weight	+/- .180 oz.	+0/-.004 oz.

Engine #1 was reassembled according to recommended Volvo procedure and subsequently broken in and baselined.

Concurrently, engine #2 was reassembled to serve as an installation mock-up for the turbocharging system. This turbocharging layout was then re-installed on engine number one.

The turbo air delivery pressure capability of the turbocharging system was matched according to operational requirements of the B-19 engine. Similarly, boost levels and knock suppression system (water injection) were matched and installed.

At conclusion of the testing program those modifications which were significant or necessary were incorporated onto #1. This engine was then installed into a 1978 244DL Volvo for final testing.

In addition to the engine modifications, a series of power train modifications were assessed and included into the final test chassis. These modifications include:

1. Reduction of engine rotating mass by reducing the flywheel, clutch and pressure plate size and weight.
2. Addition of synthetic lubricants in the transmission and rear axle.
3. Optimization of transmission and rear axle ratios with available ratio.

This engine and chassis were then tested at New York City Department of Environmental Protection, Air Resources Lab in Brooklyn, New York to optimize and confirm results on the EPA cycle.

To facilitate the final stages of development and tuning a series of hot starts, using the 1972 Federal Driving Cycle, were run. During these tests, the performance of the Lambda-Sond system, catalytic converter and engine were monitored by continuous reading of the HC and CO reading before the catalyst and HC, CO, CO<sub>2</sub> and NOx levels at the tailpipe. Analysis of these results returned sufficient data to reasonably predict performance of both emission and fuel economy on the FTP composite and highway cycle.

Final test verification was run on the 1978 EPA Test Procedure which required a 12 hour cold soak prior to the city and highway cycle.

## RESULTS:

(All figures referenced are included immediately following the result section of this report).

As stated from the Procedure Section of this report, it was desired to establish a steady state condition which could serve as a "modeling tool" to expedite technical trend analysis during initial stages of development.

The installed manifold vacuum transducer yielded a trace, a section of which is described on Figure 1, which when integrated manually, indicated a load corresponding to 13" Hg would approximate the transient conditions of the test cycle. Further, a speed trace of engine speed range yielded a test range of 1600 to 2800 Rpm.

Engines were broken in and baselined according to the "break-in" schedule described on Figures 2 and 3. The total break-in time was 30 hours each engine.

Using this modeling "tool", it was possible to evaluate a number of anticipated modifications in a fairly rapid manner. As stated in the previous section, the list of test modifications included:

1. Reduction in displacement (2.1 liter to 2.0 liter)
2. Addition of synthetic engine oil
3. Reduction of accessory drive speed
4. Addition of a multi-spark capacitive discharge ignition system
5. Elevated engine coolant temperature

The below modifications were tested but for reasons noted later in the report were not included into the final engine.

1. Turbocharging
2. Reduction of engine lubricant pumping losses
3. Reduction of crankcase pressure

Using the stated procedure in evaluating the above items, the following results were obtained:

Before continuing it should be emphasized that each candidate modification was in turn evaluated and compared against the baseline data from the stock B-19 engine. It should be understood that the results

of all the tests are not additive and the presence or effect of one modification will, in most circumstances, influence the results of the other modifications. Therefore, the combined effect of all these modifications will be diminished by the effect or change of engine operating characteristics caused by the other modifications.

To determine the effect of reduction of displacement from 2.1 L to 2.0 L under wide open throttle conditions (WOT), BSFC curves were generated for both engines. From these curves, Figure 4, it can be seen that there is a decrease in fuel consumption that varies from 3% at 1700 rpm to a maximum decrease of 8% at 4000 rpm.

The baselined B-19 BSFC curve is depicted in Figure 5; this curve is provided as a reference for comparison of following modifications.

Figure 6 is a graphical representation of the B-19 Lambda Sond engine emissions before and after the catalyst. For the remainder of this section, if emission levels are discussed, only emission levels before the catalyst will be considered.

The effect of the substitution of low viscosity synthetic lubricants was studied. Figure 7 shows the results of this test at 13" Hg manifold pressure. From the graph it can be seen that there was reduction in BSFC with a maximum decrease of 4% at 2200 rpm. This effect has been attributed to the reduced pumping loss from a lower viscosity oil and to a lesser extent, reduced friction in the main bearing, rod bearings and cylinder wall surfaces.

The alternator and water pump constituted the only engine driven accessories. Customarily, during the FTP cycle, the alternator would be driving no accessories and, therefore, at low load. However, it was anticipated that there would be a decrease in BSFC if the accessory drive speed was reduced.

This was accomplished with the installation of 3.75" diameter crank pulley as opposed to the stock pulley diameter of 5.50" diameter. This accounted for a 30% reduction of accessory drive speed. The largest decrease in BSFC, as shown on Figure 8, was 7% at 2200 rpm.

A commercially available multi-spark ignition system was installed and tested. This system is designed to spark repetitively over 30° of crankshaft rotation. Referring to Figure 9, there was a decrease in BSFC over the range of 1600 to 2500 rpm.

It was believed that emissions could be attenuated particularly during certain parts of the FTP (Bag 1), if the cooling system was modified to raise the coolant temperature above the standard 195°F. The two test temperatures were selected at 210°F and 220°F. The cooling system was modified by: removing the engine driven fan and replacing it with an electric fan activated by a temperature switch sensing coolant temperature, and the installation of a thermostat of the correct opening temperature.

By increasing the coolant temperature, it was speculated that there would also be a simultaneous improvement in cycle efficiency which would return correspondingly lower BSFC. However, only when the 220°F coolant temperature was used was there a noticed decrease in BSFC over the test range of 1600 to 2800 Rpm. Due to the risk of thermal degradation to the engine, the lower test temperature of 210°F was used. When evaluating the 210°F coolant temperature over the same test range, the change in fuel efficiency was only marginal.

The final system, as installed on the LRSV, utilized the mentioned electric fan with a thermostatic temperature setpoint of 210°F on, 200°F off.

Finally, fuel injectors were flowed to obtain matched sets of injectors ensuring consistent cylinder to cylinder A/F ratios. Eight sets of nozzles were flowed at A/F meter control arm openings of 1/4, 1/2, 3/4 and full open to determine flow rate consistency. Of all eight sets, one set would flow to within 2% variation up to a 1/2 control arm opening, and one more set would hold up to 3% variation in flow rates up to 3/4 A/F ratio control arm opening. In the other cases, variations of up to 4% were encountered.

Earlier exploration of BSFC curves and engine maps revealed that there would be a need to decrease the N/V ratio. It was further speculated that reduced rotational mass would reduce inertial losses and enhance fuel economy. This was accomplished via the following methods:

N/V ratio was lowered by utilization of overdrive ratio on 1st, 2nd as well as engaged 5th overdrive ratio on the highway cycle above 45 mph. The rear axle ratio was lower (numerically) to a 3.54 ratio as opposed to the standard 3.91 axle. Utilizing this, the N/V ratio was lowered to 51.8 at 4th. or 41.3 in 5th. (O.D.) compared to the stock N/V ratio of 57.2 in 4th. and 45.5 in 5th. (O.D.).

Inertial losses were reduced during acceleration through utilization of a lighten flywheel, clutch and pressure plate. To accomplish this, the stock flywheel was machined to reduce the flywheel weight to 11 lbs. A Borg Beck pressure plate and clutch was added, bringing the entire installed weight of the assembly to 23lbs. This compares to a stock flywheel, clutch, and pressure plate weight of 34 lbs.

As mentioned earlier, special attention was given to the control of the Lambda-Sond system. Before continuing, it is necessary to briefly describe the system. The system centers itself around controlling the HC, CO, NOx levels from the engine to a degree of accuracy so as to accommodate the very narrow operating conditions needed for the three-way catalyst to be effective in reducing the three pollutants. This is accomplished by sensing the oxygen present in the exhaust system and altering air/fuel ratio to make the appropriate change. A more detailed description of the system operation is presented in Appendix B.

During the EPA testing, it became evident that tighter and better control of the Lambda-Sond controller would be necessary for this application.

Initial findings indicated that it would be advantageous for emission reduction to lean the mixture during the cold start portion of the composite cycle.

To accommodate this, the sensor voltage was lowered according to coolant temperature. This was accomplished with a thermostat set to the correct temperature level making the appropriate change in the controller internally. The best results were achieved with a 400 mv sensor voltage during cold condition changing to 550 mv as coolant temperature reached 180°F.

During testing it was found helpful in reducing exhaust emission to insulate the exhaust header and catalytic converter. The insulation required a thermal conductivity of .55 BTU/hr/sqft/°F/in. and thickness of 1/2".

The specific results of the FTP testing which commenced 9/18/78 and was concluded on 8/2/79 are presented in Appendix D. The development program was concluded with a repeated cycle for verification of results.

As noted earlier, certain modifications were tested but for reasons described below were not included into the final engine. As these modifications were part of the initial program, the results obtained are discussed below.

When the program was initially proposed, it was felt that the additional hp and torque provided by turbocharge boosting would be necessary for meeting acceleration objectives. As stated previously, it was later found that the naturally aspirated version would meet the program objectives.

Initially when the turbocharger was fitted, it was fitted to an exhaust manifold with similar primaries, but no secondary exhaust head pipe.

The turbo and manifold were then installed and tested, but provided actually lower hp. at high manifold vacuum than the stock engine. The manifold was then redesigned to include the secondary exhaust head pipe. After investigation of the manifolding system, the best configuration was found to be the stock exhaust head pipe coupled with a fabricated "J" pipe which duplicates the secondaries of the stock engine.

The turbo was then matched to the engine such that positive pressure boost from the compressor was not utilized below 2500 rpm. This was accomplished by testing of various capacity exhaust housings. The engine was then dynamometer tested under load to determine the knock limited boost, which under these circumstances is 4 PSIG boost.

The maximum horsepower output was then tested and recorded under WOT conditions. The results are shown on Figure 11. Referring to this figure, maximum boosted turbo power is 122 hp. at 5000 rpm compared to the naturally aspirated version with 100 hp at 5000 rpm.

Knocking was suppressed via a modulated water injection system which would introduce water into the turbo compressor inlet according to engine load as determined by manifold pressure. Additionally, an independent manifold fuel injector was installed to both deter knocking and introduce additional fuel required for boost conditions.

Knocking was further deterred by a vacuum ignition retard system as described on Figure 12. Under boost conditions, the in-line check valve closes and supplies positive pressure to the diaphragm retarding the system. At a maximum boost of 4 PSIG, ignition can be retarded up to  $8^{\circ}$ .

Reducing engine lubricant pumping losses was next investigated. Most engine oil pressure levels are somewhat higher than necessary to maintain bearing life. Therefore, it was felt that if the oil pressure could be lowered to a level somewhat above a critical level, the oil pumping horsepower could be reduced increasing BSFC. This was accomplished by modifying the existing oil pump to output 35 PSI instead of 65 PSI.

After evaluation of oil pressure reduction, it was found there was only a marginal improvement in horsepower output and in lieu of the possible reduced bearing life, it was felt that this modification did not warrant installation onto the final LRSV engine.

Positive crankcase pressure increases the pumping losses induced by the piston movement. In certain instances, output horsepower increases if this pressure is reduced. This reduction in crankcase pressure is usually accomplished by "syphoning" the engine's crankcase into the intake manifold. In most cases, this type of system is working well if zero crankcase pressure is maintained. Referring to the Figure 12 which correlates crankcase pressure of a production Volvo B-19, operating at 13.0 inches Hg manifold vacuum and at wide open throttle full load, it can be seen that the production system functions extremely well. Therefore, crankcase pressure reduction was considered of marginal benefit and not included in the final engine.

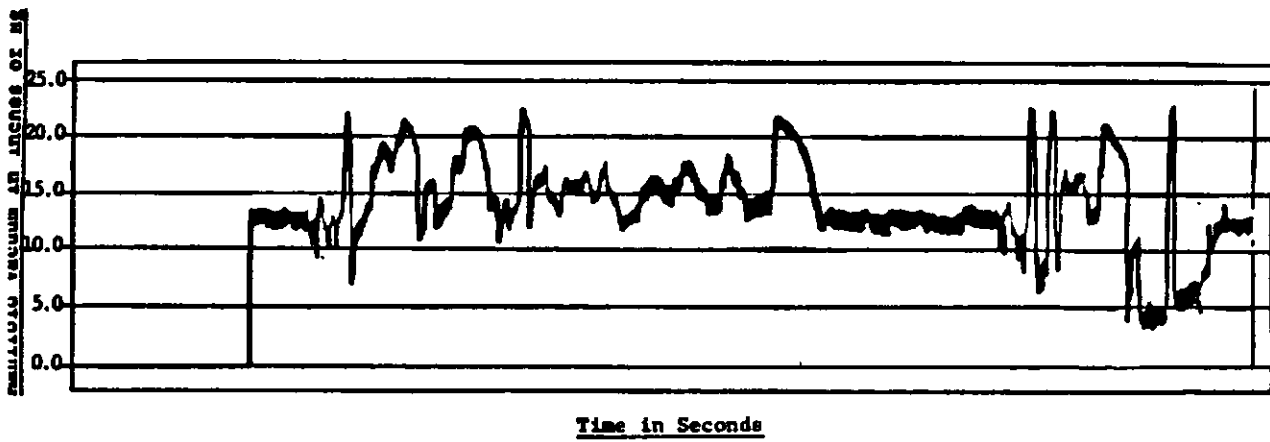


Figure No. 1. Manifold Vacuum vs. Time - 1978 B-21 Volvo Manifold  
Vacuum During 1978 FTP Driving Cycle

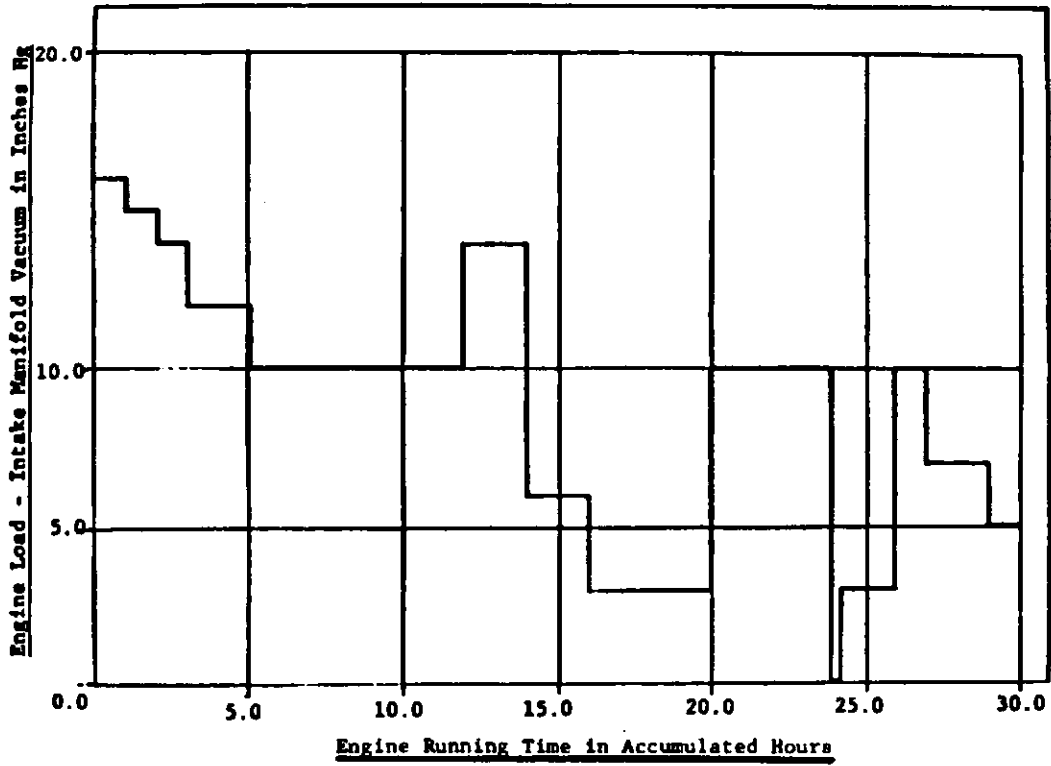


Figure No. 2. Engine break-in Schedule - Manifold Vacuum vs. Total Time

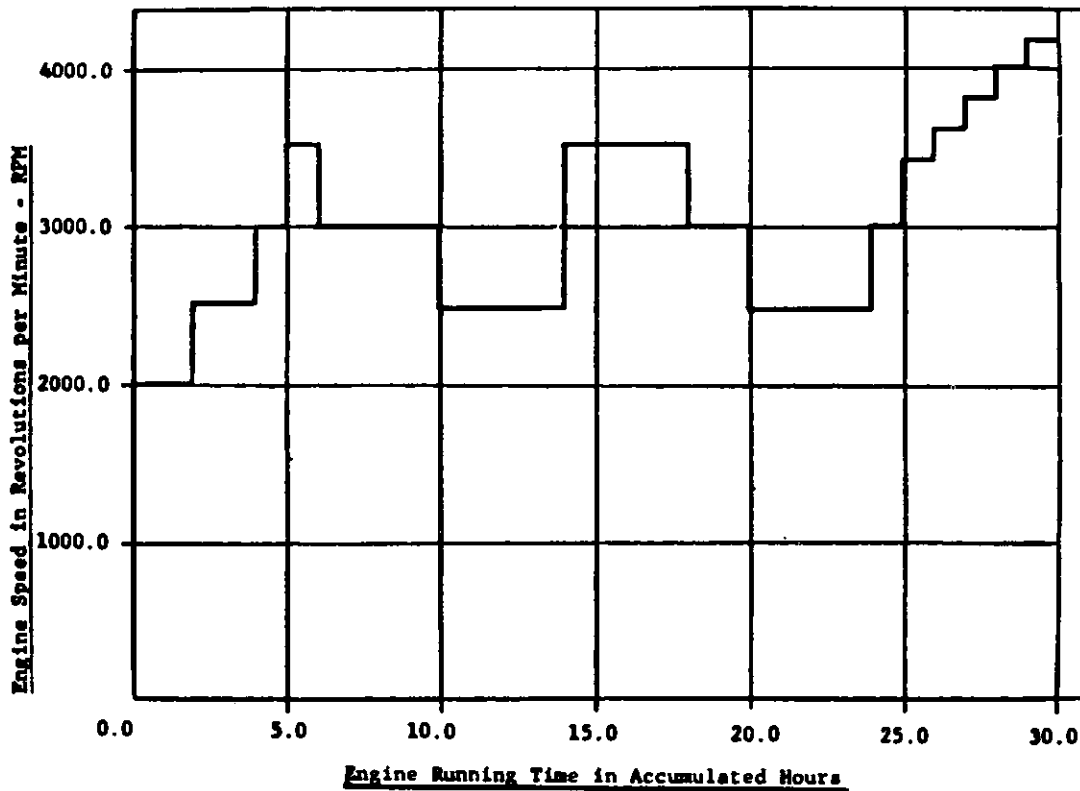


Figure No. 3. Engine Break-in Schedule - Engine Speed vs. Total Time

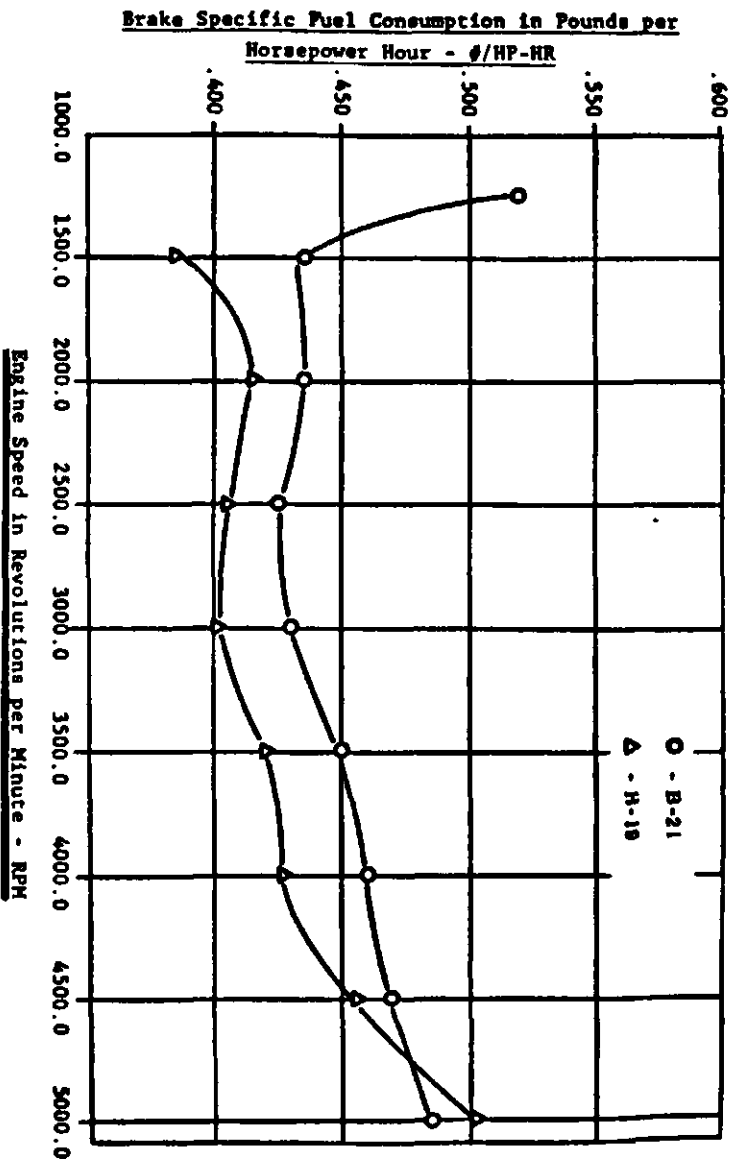


Figure No. 4 . Graph of Brake Specific Fuel Consumption vs. Engine Speed  
for Volvo B-21 & B-19 Engines Evaluated at Wide Open Throttle

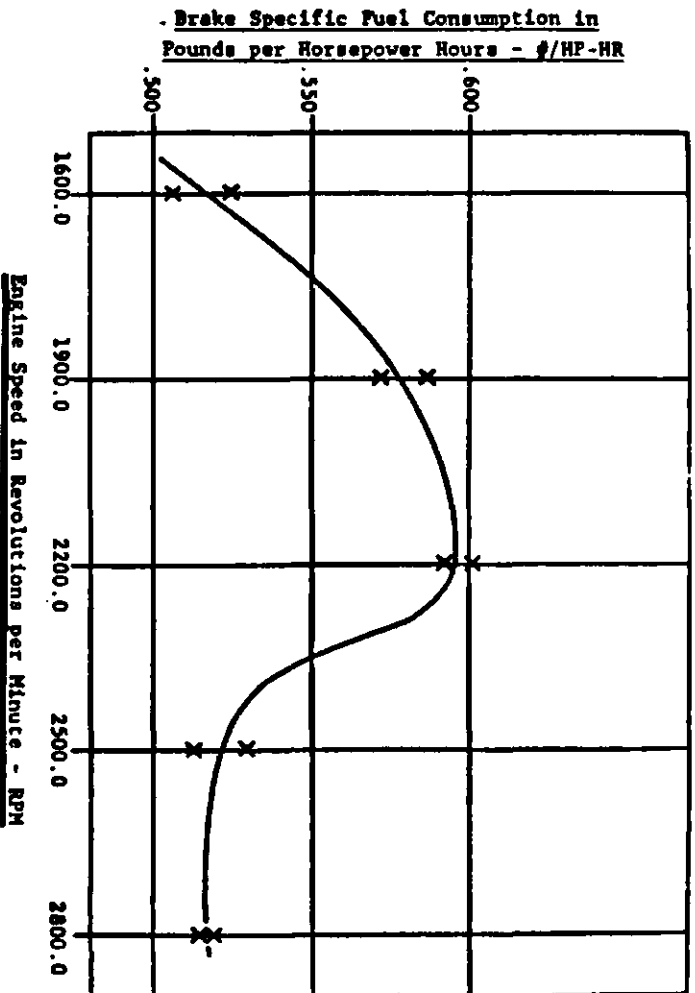


Figure No. 5 . Graph of Brake Specific Fuel Consumption vs.  
Engine Speed - Volvo B-19 Operated at 13.0 Inches (Hg) Intake Manifold Vacuum

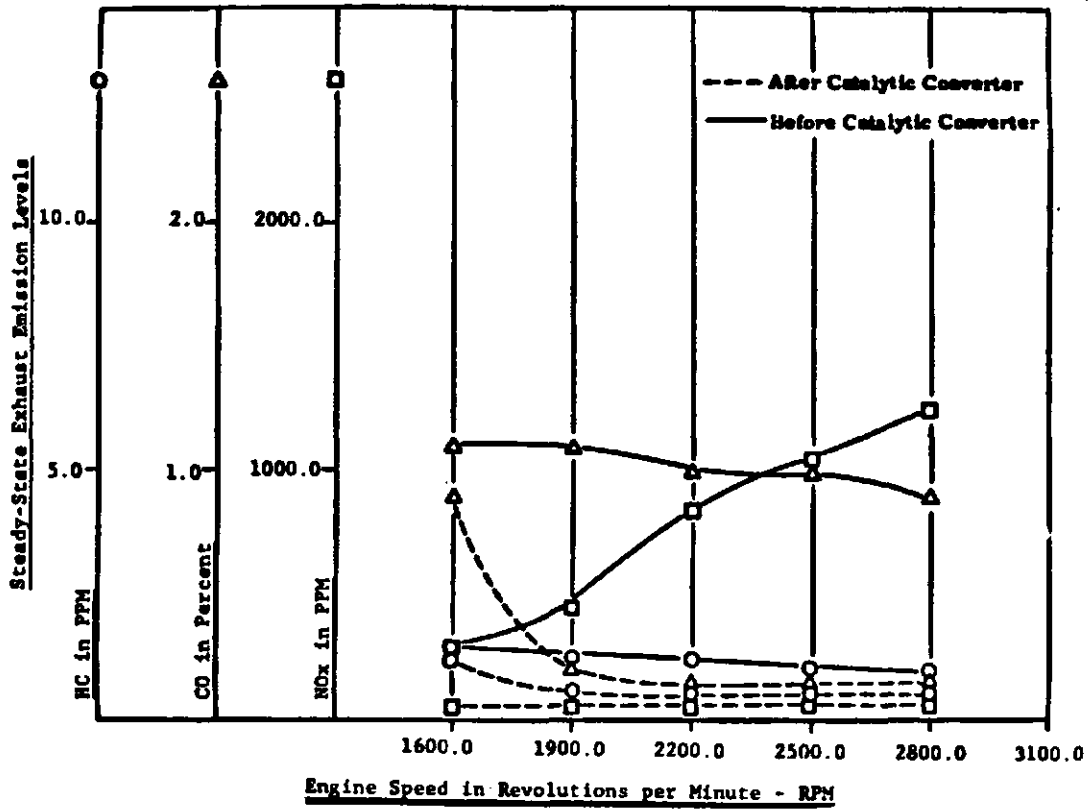


Figure No. 6 . Graph of Steady-State Exhaust Emission Levels vs. Engine Speed - Volvo B-19 Engine Operated at 13.0 Inches Hg Intake Manifold Vacuum

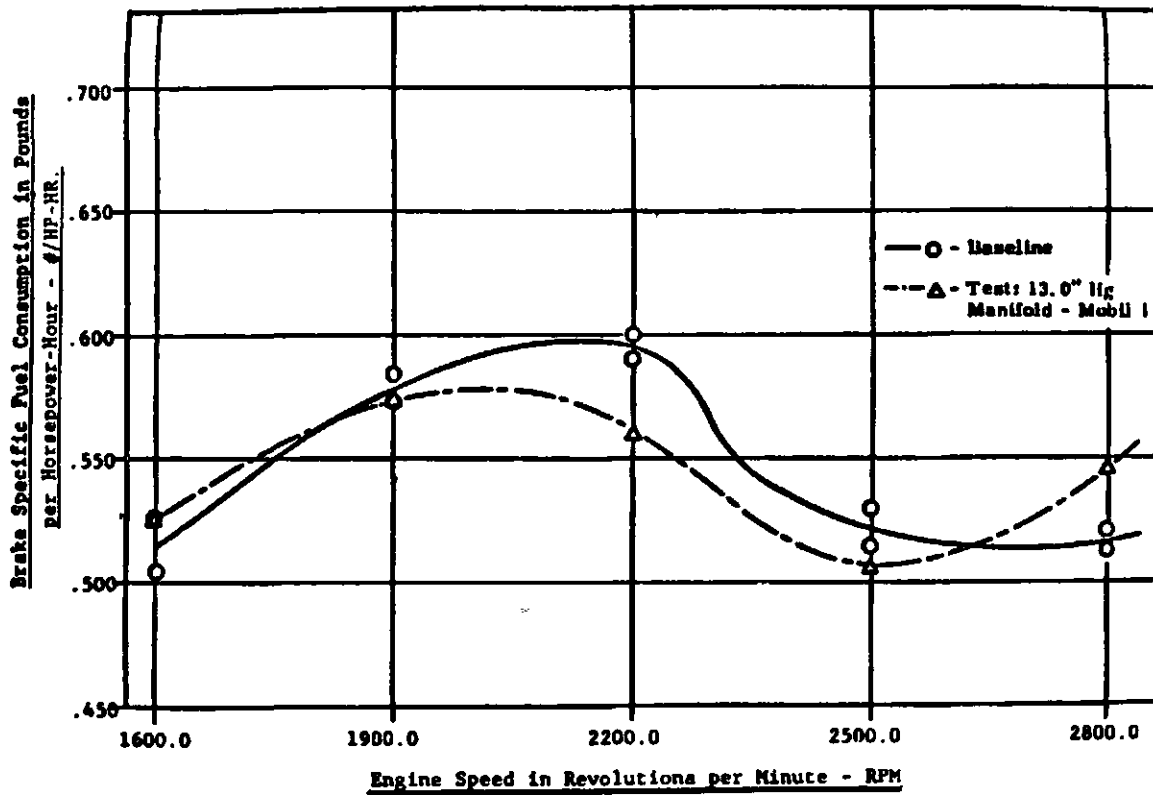
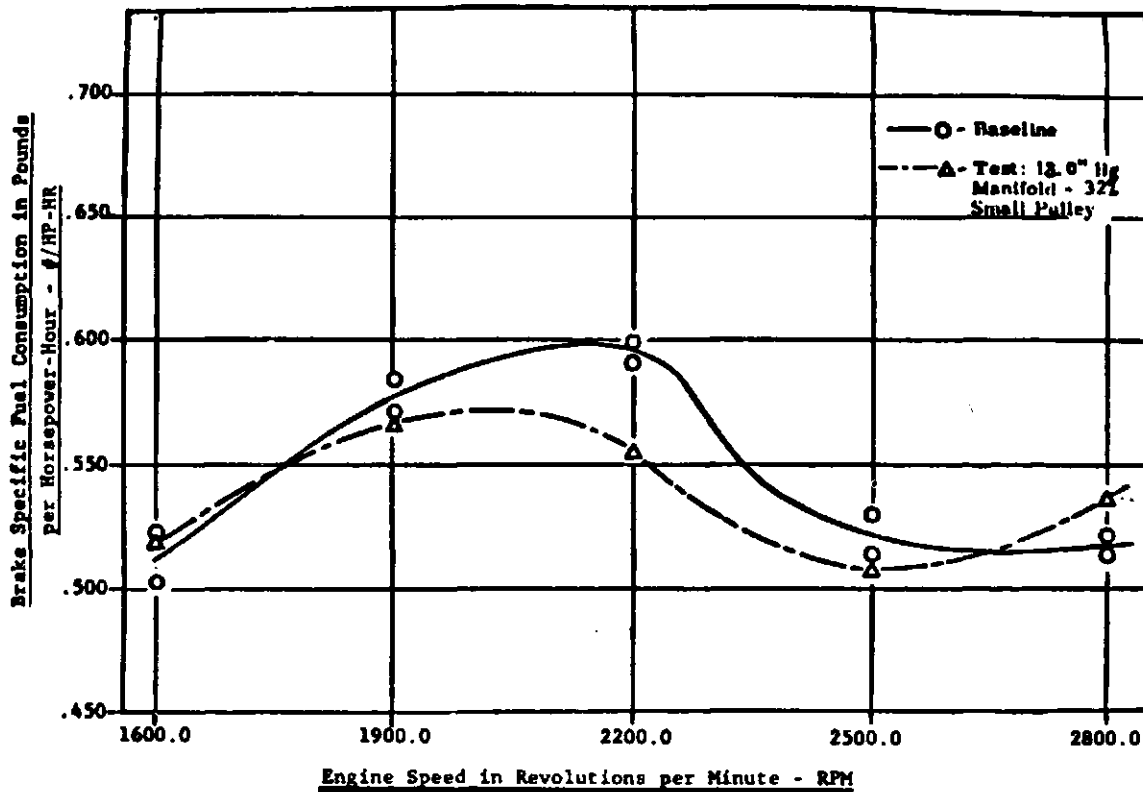
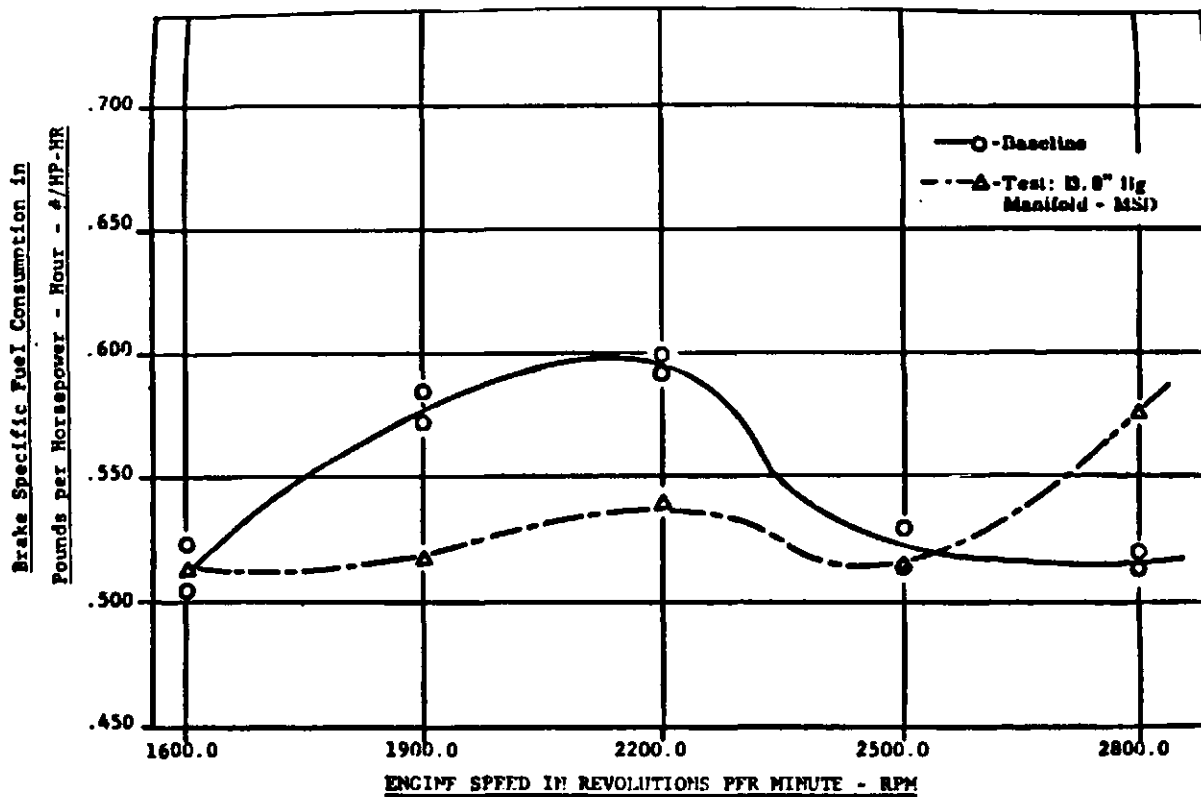


Figure No. 7 . Graph of Brake Specific Fuel Consumption vs. Engine Speed - Volvo B-19 Engine Operated at 13.0 Inches Hg Intake Manifold Vacuum with Synthetic Engine Oil



**Figure No. 8 Graph of Brake Specific Fuel Consumption vs. Engine Speed - Volvo B-19  
Operated at 13.0 Inches Hg Intake Manifold Vacuum with a 32% Reduced Diameter Crankshaft Pulley**



**FIGURE NO. 9 Graph of Brake Specific Fuel Consumption vs. Engine Speed  
Volvo B-19 Operated at 13.0 Inches Intake Manifold Vacuum With Multi-Spark  
Discharge Ignition**

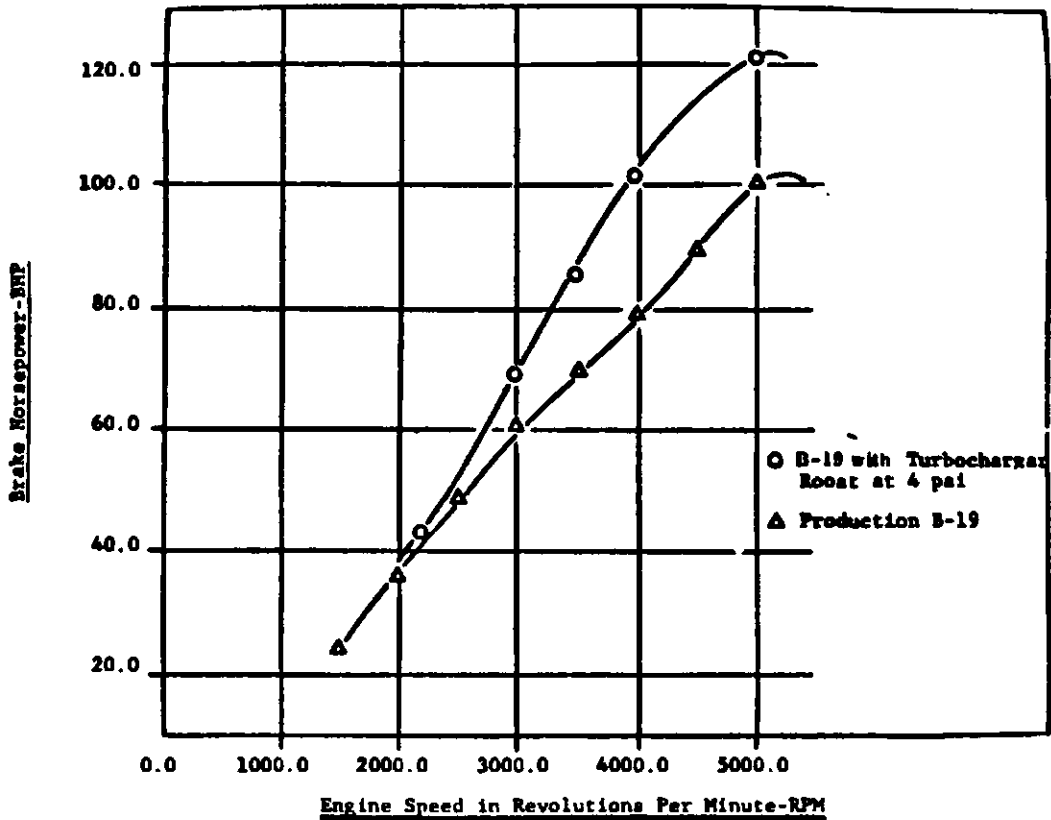


**Figure No. 10 Graph of Brake Horsepower vs. Engine Speed - Production Volvo B19 and Balanced-Blueprinted- Turbocharged Volvo B-19**

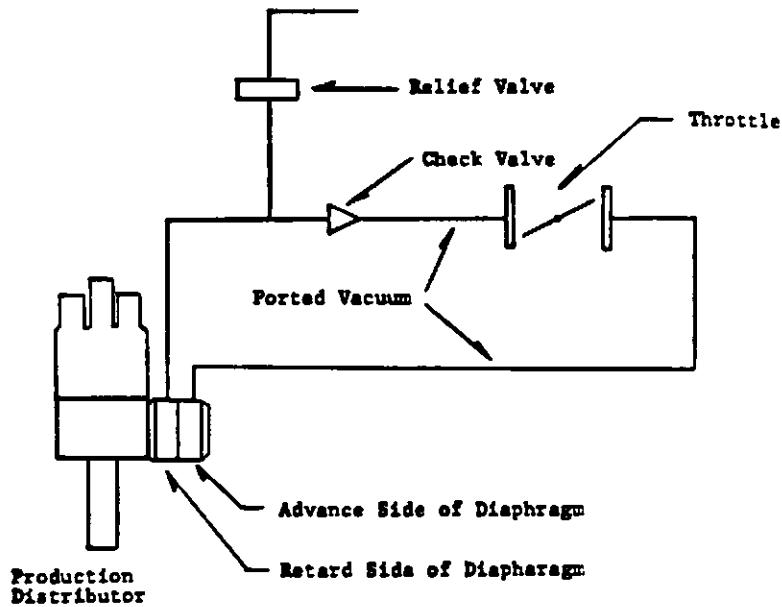


**Figure No. 11 Boost Pressure Retard System**

Figure 12

Crankcase Pressure as Recorded Against  
 Engine Speed at 13" Manifold Vacuum and  
 Wide Open Throttle

<u>Engine Speed-RPM</u>	<u>Load-Speed</u>	<u>Crankcase Pressure</u>
1600.0	13.0 in. Hg	0.0 in H <sub>2</sub> O
1900.0	"	"
2200.0	"	"
2500.0	"	"
2800.0	"	-.2 in
1500.0	WOT	1.2 in
2000.0	"	1.0 in
2500.0	"	.8 in
3000.0	"	.3 in
3500.0	"	.2 in
4000.0	"	0.0 in
5000.0	"	0.0 in



### Fuel Economy

The minimum acceptable fuel economy of the LRSV shall be 27.5 miles/gallon for combined EPA city and highway driving. The fuel economy performance is to be determined according to 1978 EPA Fuel Economy Test Procedures.

### Acceleration

As an objective, the LRSV shall accelerate from 0 to 60 mph in not more than 13.5 seconds. The maximum acceptable time for this acceleration shall not exceed 20.0 seconds.

### III. ENGINE SPECIFICATIONS

The Engine to be furnished for the LRSV shall be based on a modified design of the 1977 Volvo B21 engine. The specifications that follow describe the preliminary Volvo B21 engine configuration revised for LRSV use.

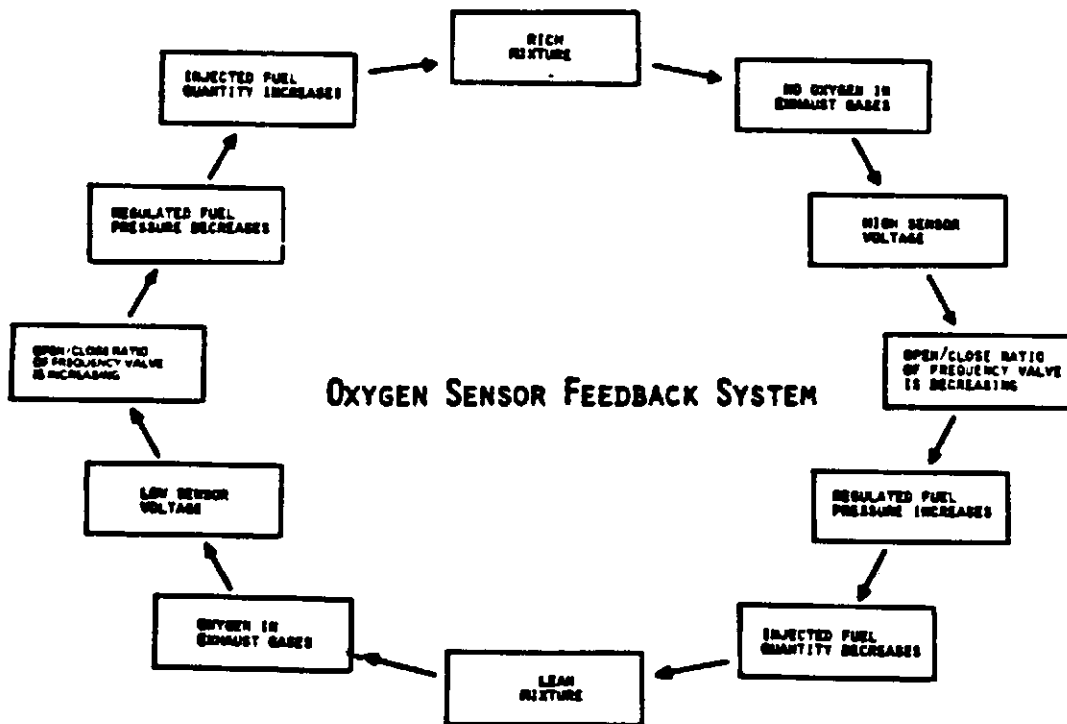
Type	Liquid cooled 4 cylinder in-line with cast iron block, light-alloy cylinder head of cross flow design; belt driven overhead camshaft
Displacement	2017cc
Bore	3.53" (89 mm)
Stroke	3.15" (80 mm)
Compression Ratio	10.4:1
Maximum Output	Estimated SAE net H.P.: 122 @ 5,000 rpm
Fuel Requirements	91 RON unleaded gasoline
Fuel Induction	Bosch K Jetronic continuously manifold injected system with exhaust oxygen sensing mixture correction and three-way catalyst
Ignition System	Autotronic Controls Corporation High energy multi spark capacitive Discharge system

Standard engine driven accessory equipment	770 watt (55 amp) alternator
Starter	810 watt, 1.1 HP
Cooling system	Positive pressure, closed system with cross flow radiator and separate expansion tank. Radiator fan and fan drive to be supplied by Minicars. System capacity: 10 qts. (9.5 liters) 50% water/glycol solution  Temperature activated electric fan, set point 210 <sup>o</sup> F
Clutch	Borg and Beck pressure plate and flywheel with lighter flywheel. Cable operated Borg and Beck dry plate type
Miscellaneous	Lubrication system adopted to synthetic oil plus other friction reduction modifications.  A three-way catalytic converter and an appropriately configured exhaust head pipe to connect it to the turbo charger discharge connection shall be provided.
Engine Weight	Estimated net, including engine mounted accessories and components as indicated excluding fluids, 380 lbs. max.

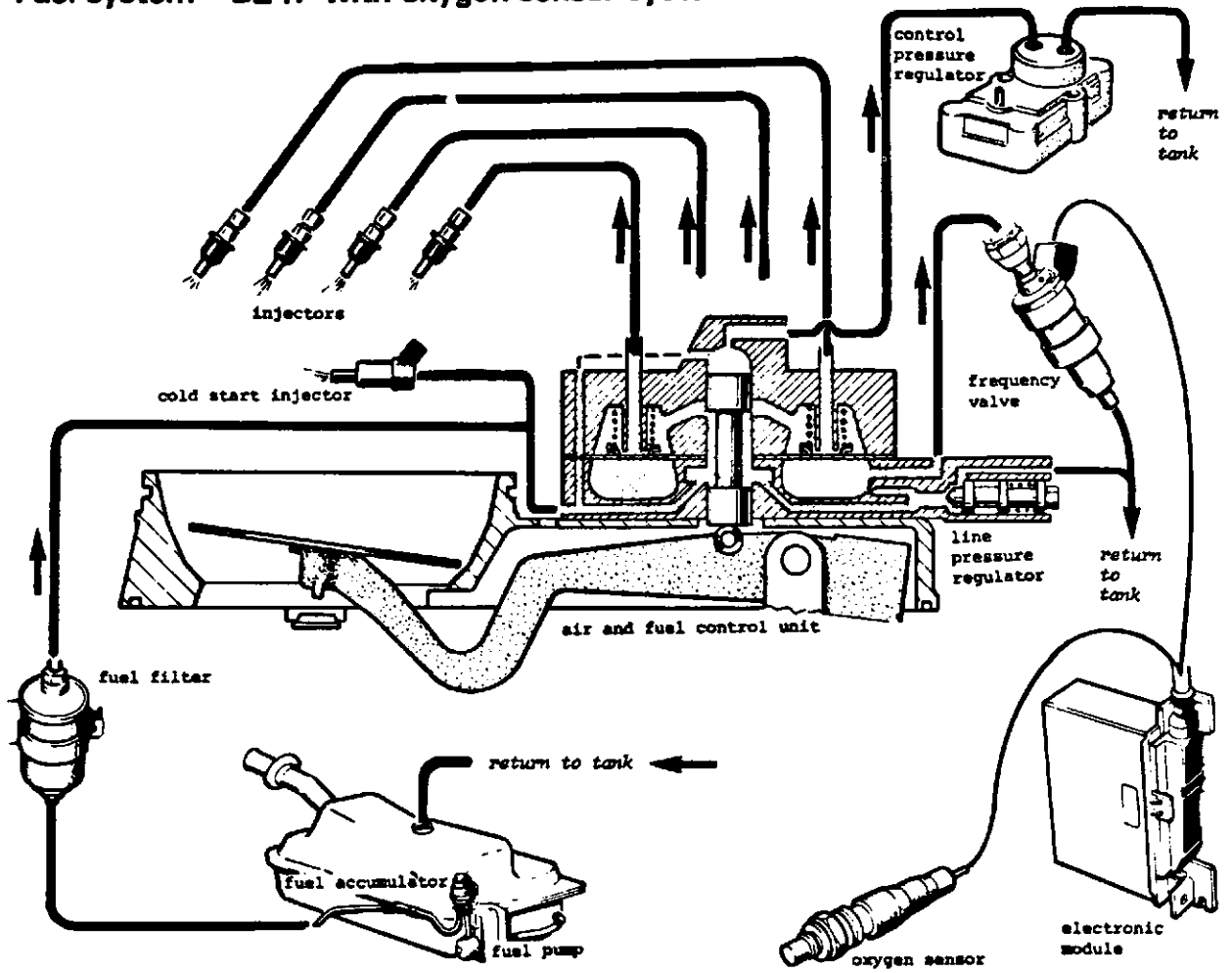
APPENDIX B—GENERAL DESCRIPTION LAMBDA-SOND  
AIR FUEL CONTROL SYSTEM

The following description has been excerpted from a Volvo Publication:

The Lambda-Sond oxygen sensor feedback system, described in the flow chart below, is a self-tuning engine control system designed to reduce emissions and improve fuel economy. An exhaust gas sensor, (oxygen sensor, also called Lambda Sensor) monitors the composition of the exhaust gases leaving the engine. The exhaust gas analysis is fed into a closed loop feedback system. This continuously adjusts the air/fuel ratio to provide optimum conditions for combustion and efficient elimination of all three of the major pollutants (HC, CO, NOx) by a 3-way catalytic converter.



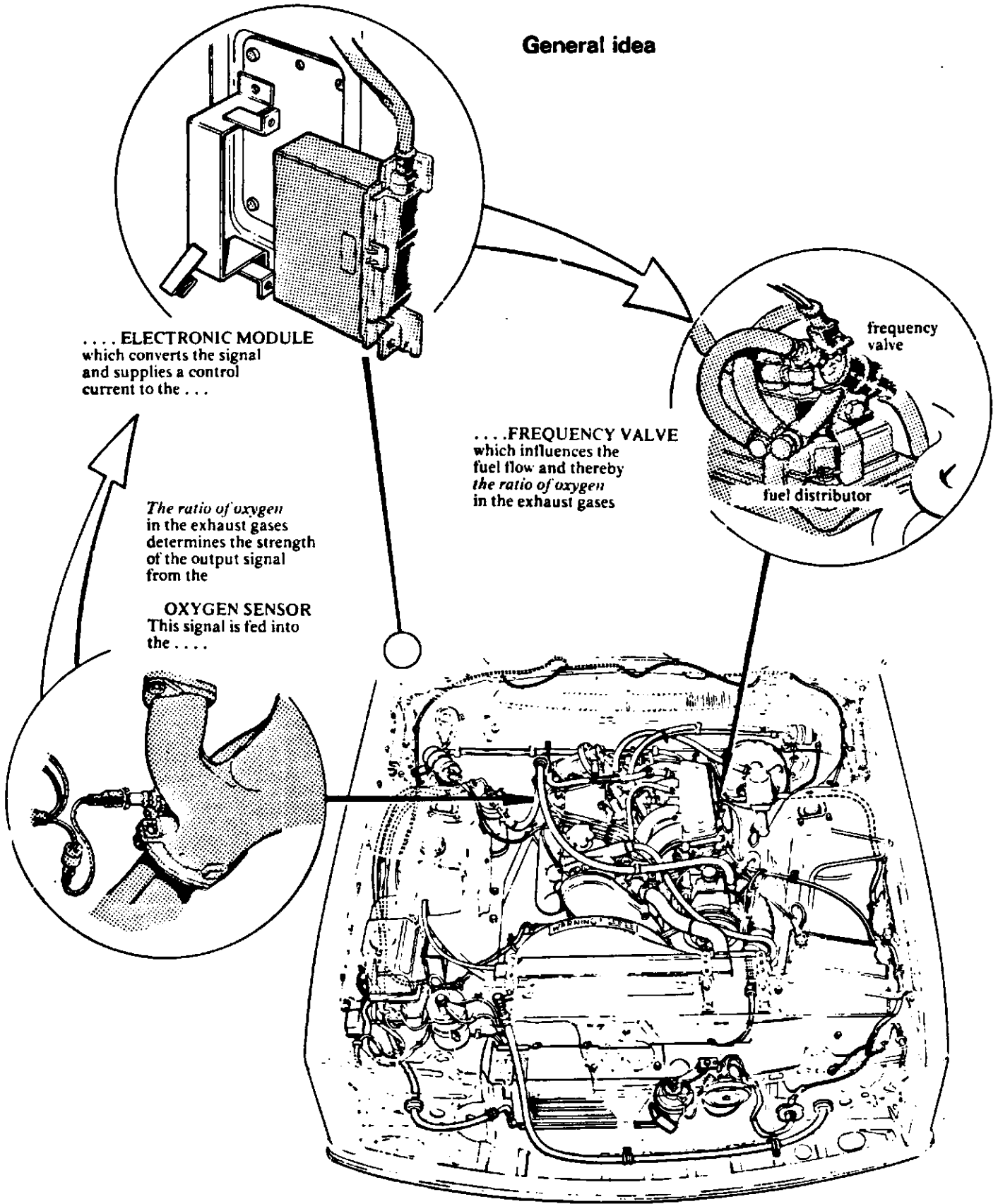
**Fuel system - B21F with oxygen sensor system**



120 004

# Description of Oxygen Sensor Feedback System

## General idea

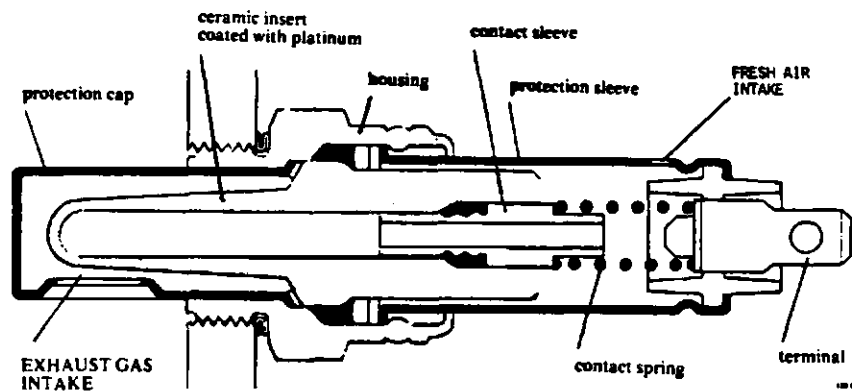


## OXYGEN SENSOR

The exhaust gas sensor, called oxygen sensor, is located in the exhaust manifold. It consists of a platinum coated ceramic tube. The inside is connected to atmosphere, while the outside extends into the exhaust gases.

An electrical potential is built up according to air/fuel ratio. There is a steep transition just at the point where the air/fuel ratio is ideal.

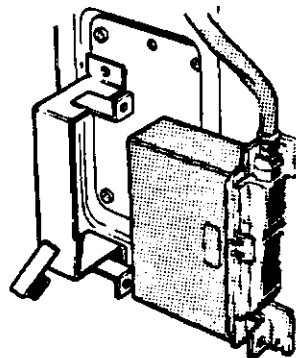
The electrical potential is high (approx. 1 volt) with low content of oxygen in the exhaust gases (= rich mixture) and low (approaching 0 volt) when the mixture is lean (= oxygen surplus).



## ELECTRONIC MODULE

The output from the oxygen sensor is fed into an electronic unit, called the electronic module. This device supplies a control current to the frequency valve. The control current has a set frequency and operates by varying the duty cycle.

The electronic module is located inside the vehicle, at the right side in front of the right door. In this position it is protected and is close to the oxygen sensor and the electrical system.

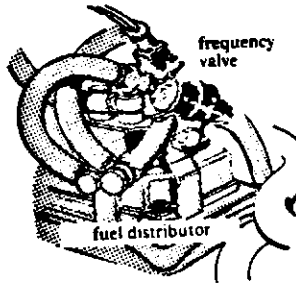


## FREQUENCY VALVE

This device influences the fuel flow by influencing the pressure on the underside of the diaphragm in the pressure regulating valves in the C1 System.

It is located on a bracket behind the fuel distributor on the left side of the engine.

The frequency valve operates on a set frequency and by varying the duty cycle (ratio of closed/open circuit).



## APPENDIX C DESCRIPTION ENGINE DEVELOPMENT APPARATUS

The testing apparatus as used in the engine dynamometer engine development can be divided into three basic systems:

1. Engine performance measurement
2. Engine fuel consumption measurement, and
3. Engine emission measurement.

Because direct correlation between FTP cycle results and engine dynamometer fuel economy and emission data is very difficult to obtain, the engine dynamometer measurement systems were used only for trend analysis of the effects of select modifications. This offered the ability to weigh the relative value of each modification. Considering the preceding, the following is a partial description of the test apparatus for information purposes.

The engine performance measuring system is shown in diagrammatic form in Figure No. 13. The engine parameters measured in this system are as follows:

1. Engine rpm
2. Engine torque
3. Engine air inlet temperature, dry bulb
4. Engine air inlet temperature, wet bulb
5. Barometric pressure
6. Engine oil pressure
7. Engine water temperature
8. Engine inlet oil temperature
9. Manifold vacuum/pressure

This system centers around a water absorption type dynamometer unit and is controlled by varying the flow of water through the unit using an analog pneumatic valve arriving at the engine's output horsepower. The absorption dynamometer's water supply consists of a 3,000 gallon capacity reservoir. The water is maintained at a constant temperature using an external water cooling tower. Engine torque was measured using a pressure transducer as a load cell. The torque measurement system was calibrated daily using a detachable arm and calibrated weights. Engine rpm was measured using a mechanical tachometer calibrated in place.

Oil pressure, manifold vacuum, and fuel pressure were measured using Bourdon Tube mechanical gauges. Oil and water temperatures were measured using resistance type electric gauges. Air inlet wet and dry bulb temperatures were continuously monitored throughout the testing series using thermistors. Finally, barometric pressure was measured using a temperature compensated Taylor aneroid barometer.

The fuel measurement system, shown in Figure No. 14, is calibrated to read engine fuel flow rate in pounds per hour. The system consisted of the following: An aircraft type fuel pump supplying fuel to one of three Rotometer type flow meters ranging: 3-30 lbs/hr, 20-190 lbs/hr and 50-350 lbs/hr. The use of any one of the flow meters was determined by opening and closing the appropriate valves. Fuel continues into a level controlled tank which acts as the fuel reservoir for the Volvo system.

The exhaust emission measurement system equipment was chosen to be of the infrared type. This measurement system, shown in Figure No. 15 is explained as follows: Exhaust gas, sampled from before and after the catalytic converter enters discreet stainless steel lines into an ice bath cooler. From the cooler the gases enter two inline 0.6 micron filters and into the systems' pump. From the pump, gases flow into two discreet flow meters and one line enters a NOx oven and the NOx cell, while the other enters a condenser, a HC cell, and CO cell.

This type of measurement allowed direct comparison of emission being produced from a Volvo engine with a select modification to the production Volvo engine.

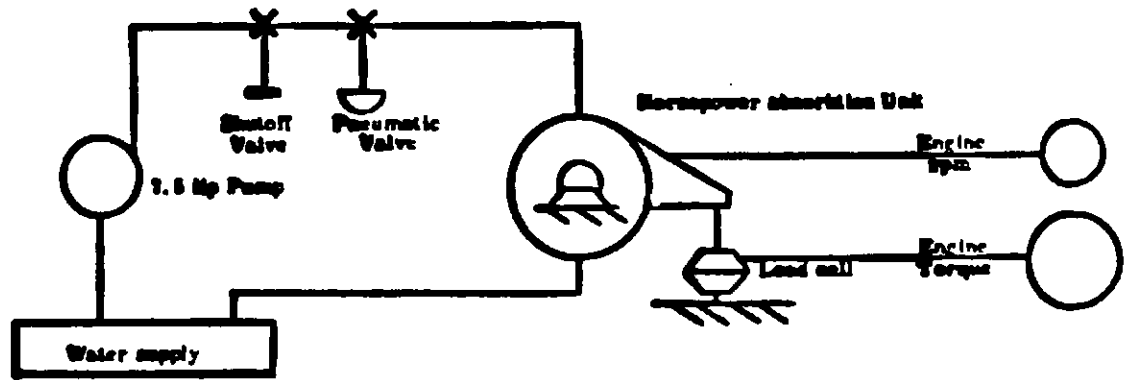


**Figure No. 13 Engine Performance Measurement System**

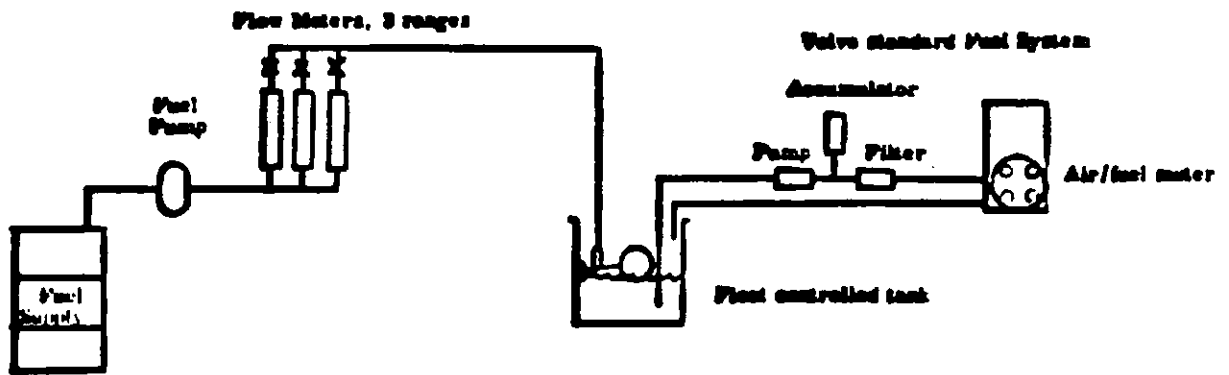


**Figure No. 14 Engine Dynamometer Fuel Measurement System**

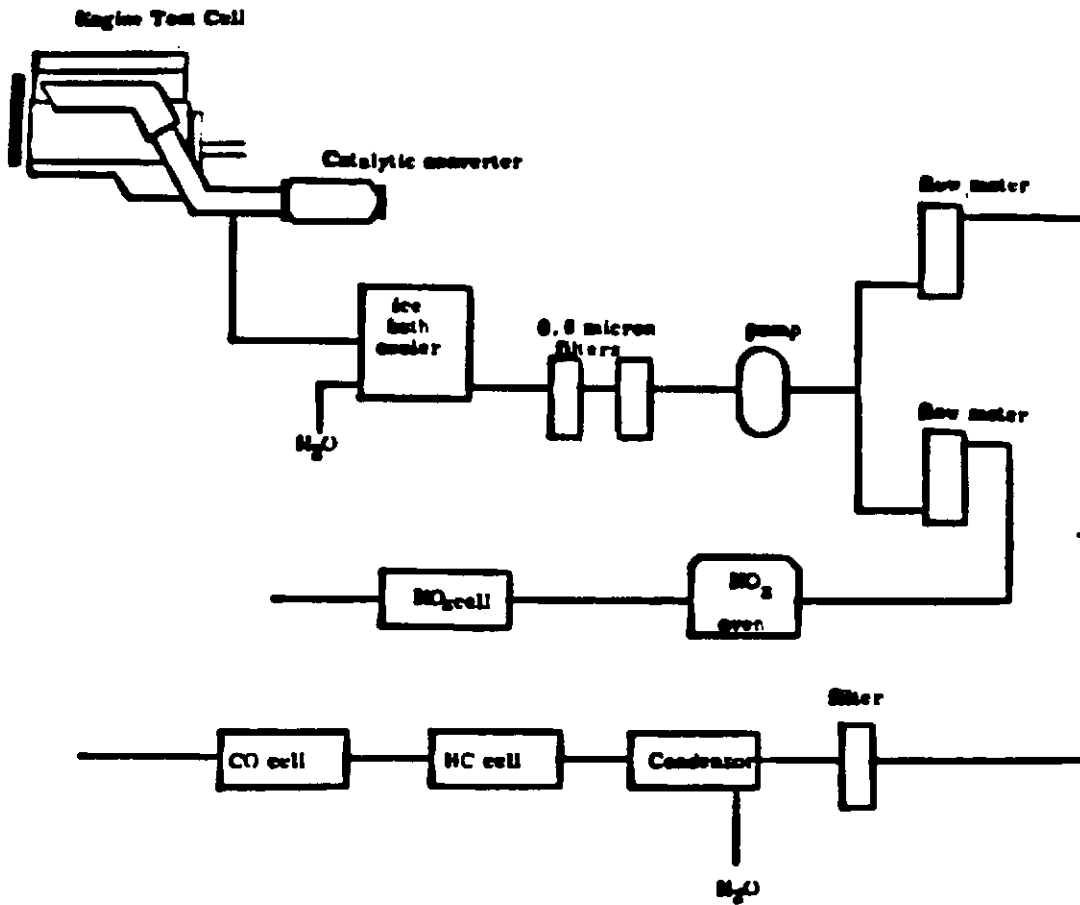


Figure No. 15 Engine Dynamometer Exhaust Emissions Measurement

APPENDIX D

VOLVO B19 LRS.

Brooklyn Air Resources Lab Test Results

Date	Run #	HC	CO	CO <sub>2</sub>	NO <sub>x</sub>	MPG	Notes
9/18	2871c	.56	11.16	437.	.12	19.3	As delivered
	2871c	.37	8.98	259.1	.10	32.0	
9/18	2872c	.39	9.27	368.4	.01	23.0	Trans & rear end lube installed
	2872h	.44	9.75	251.4	.10	32.8	
9/19	2873c	.51	10.83	375.3	.10	22.3	Run lean r
9/19	2874c	.53	4.79	373.5	.12	23.0	Lambda Sond Problems Overdrive used
	2874h	.28	6.17	241.9	.08	34.8	
	2874h	.35	8.43	231.8	.14	35.8	
9/29	Englehard	1.48	11.50	462.8	1.86	18.4	
10/23	2883c	.48	8.48	365.7	1.05	23.3	New cat. Engine as per Englehard Remove warm-up regulator/install ol cat. Fuel meter w/ large air meter
	2883h	.20	4.29	214.2	1.01	39.7	
	2884c	.24	3.69	364.4	.07	23.7	
	2884h	.20	2.56	214.0	.08	40.2	
	2885c	.53	7.17	364.5	.26	23.3	
10/30	2891c	.37	4.47	373.2	.20	23.1	CO high-repeat hot
	2891h	.20	2.27	222.4	.04	38.8	
	2892c	.24	3.68	373.2	.07	23.2	
	2892h	.16	2.53	218.6	.03	39.4	
	2893c	.22	3.98	373.4	.07	23.1	
	2893h	.14	2.28	218.0	.02	39.4	
10/31	2894comp	.57	6.42	392.0	.44	21.8	Cold start
	2894i	1.67	16.14	---	1.22	---	
	2894il	.19	3.67	---	.05	---	Average 27.22
	2894iil	.45	4.30	---	.58	---	
	2894c	.32	3.97	387.1	.30	22.3	
	2894h	.17	1.89	221.4	.12	30.1	

**VOLVO B10 LRSV Brooklyn Air Resources Lab Test Results Continued**

<b>Date</b>	<b>Run #</b>	<b>HC</b>	<b>CO</b>	<b>CO<sub>2</sub></b>	<b>NO<sub>x</sub></b>	<b>MPG</b>	<b>Notes</b>
<b>11/20</b>	<b>2902c</b>	<b>.20</b>	<b>2.11</b>	<b>394.0</b>	<b>.34</b>	<b>22.1</b>	<b>Weighted fuel meter</b>
	<b>2902h</b>	<b>.13</b>	<b>1.04</b>	<b>225.9</b>	<b>.06</b>	<b>38.8</b>	
	<b>2903c</b>	<b>.58</b>	<b>9.34</b>	<b>384.8</b>	<b>.49</b>	<b>21.9</b>	
	<b>2904c</b>	<b>.51</b>	<b>5.43</b>	<b>369.5</b>	<b>.98</b>	<b>23.2</b>	
	<b>2905c</b>	<b>.38</b>	<b>4.09</b>	<b>382.9</b>	<b>.73</b>	<b>22.5</b>	
<b>11/21</b>	<b>2906comp</b>	<b>.68</b>	<b>3.58</b>	<b>425.8</b>	<b>.32</b>	<b>20.3</b>	<b>Cold start test/ raised air meter disc. Too lean on start. Average 25.83</b>
	<b>2906l</b>	<b>2.39</b>	<b>8.58</b>	<b>---</b>	<b>1.14</b>	<b>---</b>	
	<b>2906ll</b>	<b>.15</b>	<b>2.21</b>	<b>---</b>	<b>.08</b>	<b>---</b>	
	<b>2906ill</b>	<b>.31</b>	<b>2.42</b>	<b>---</b>	<b>.15</b>	<b>---</b>	
	<b>2906h</b>	<b>.09</b>	<b>.84</b>	<b>225.8</b>	<b>.12</b>	<b>38.7</b>	
<b>12/18</b>	<b>2910c</b>	<b>.14</b>	<b>2.80</b>	<b>370.5</b>	<b>.71</b>	<b>23.4</b>	<b>New Lambda Sond computer set lower 500mv nom. added 2 oz wgt. fuel meter</b>
	<b>2911c</b>	<b>.24</b>	<b>3.77</b>	<b>364.8</b>	<b>.49</b>	<b>23.7</b>	
	<b>2912c</b>	<b>.12</b>	<b>2.61</b>	<b>364.8</b>	<b>.20</b>	<b>23.8</b>	
	<b>2913c</b>	<b>.19</b>	<b>3.38</b>	<b>364.4</b>	<b>.51</b>	<b>23.7</b>	
	<b>2913h</b>	<b>.04</b>	<b>.62</b>	<b>214.0</b>	<b>.09</b>	<b>40.8</b>	
	<b>2914</b>	<b>.10</b>	<b>2.99</b>	<b>385.7</b>	<b>.07</b>	<b>22.8</b>	
<b>12/19</b>	<b>2915comp</b>	<b>.47</b>	<b>4.77</b>	<b>398.8</b>	<b>.44</b>	<b>21.8</b>	<b>Set volt richer/600mv 500mv</b>
	<b>2915l</b>	<b>1.50</b>	<b>13.08</b>	<b>---</b>	<b>1.44</b>	<b>---</b>	
	<b>2915ll</b>	<b>.13</b>	<b>2.72</b>	<b>---</b>	<b>.14</b>	<b>---</b>	
	<b>2915lll</b>	<b>.33</b>	<b>2.41</b>	<b>---</b>	<b>.25</b>	<b>---</b>	
	<b>2915h</b>	<b>.08</b>	<b>1.11</b>	<b>218.0</b>	<b>.08</b>	<b>40.0</b>	
	<b>2916c</b>	<b>.48</b>	<b>3.84</b>	<b>371.5</b>	<b>.09</b>	<b>23.2</b>	
	<b>2917c</b>	<b>.12</b>	<b>2.29</b>	<b>377.8</b>	<b>.31</b>	<b>23.0</b>	
	<b>2918c</b>	<b>.10</b>	<b>2.67</b>	<b>365.8</b>	<b>.12</b>	<b>23.8</b>	
	<b>2918c</b>	<b>.12</b>	<b>3.45</b>	<b>377.8</b>	<b>.05</b>	<b>22.9</b>	
<b>12/20</b>	<b>2920comp</b>	<b>.45</b>	<b>5.22</b>	<b>383.2</b>	<b>.37</b>	<b>22.3</b>	<b>550 mv 10ms OD all gears</b>
	<b>2920l</b>	<b>1.53</b>	<b>12.75</b>	<b>---</b>	<b>1.33</b>	<b>---</b>	
	<b>2920ll</b>	<b>.13</b>	<b>3.69</b>	<b>---</b>	<b>.08</b>	<b>---</b>	
	<b>2920lll</b>	<b>.25</b>	<b>2.44</b>	<b>---</b>	<b>.19</b>	<b>---</b>	
	<b>2920h</b>	<b>.07</b>	<b>1.14</b>	<b>230.5</b>	<b>.08</b>	<b>37.8</b>	

**VOLVO H 19 Brooklyn Air Resources Lab Test Results Continued**

<b>Date</b>	<b>Run</b>	<b>HC</b>	<b>CO</b>	<b>CO<sub>2</sub></b>	<b>NO<sub>x</sub></b>	<b>MPG</b>	<b>Notes</b>
<b>12/27</b>	<b>SATRA comp</b>	<b>.27</b>	<b>4.33</b>	<b>---</b>	<b>.36</b>	<b>22.51</b>	<b>400 - 4 min.</b>
	<b>SATRA ih</b>	<b>.29</b>	<b>4.75</b>	<b>---</b>	<b>.49</b>	<b>21.62</b>	
	<b>lih</b>	<b>.29</b>	<b>4.46</b>	<b>---</b>	<b>.55</b>	<b>22.35</b>	
	<b>liih</b>	<b>.27</b>	<b>4.34</b>	<b>---</b>	<b>.46</b>	<b>22.06</b>	
	<b>lvh</b>	<b>.28</b>	<b>4.23</b>	<b>---</b>	<b>.40</b>	<b>21.90</b>	
<b>1/10</b>	<b>2921comp</b>	<b>.28</b>	<b>1.78</b>	<b>361.5</b>	<b>.55</b>	<b>24.1</b>	<b>Turbo charger removed</b>
	<b>2921i</b>	<b>1.14</b>	<b>7.44</b>	<b>---</b>	<b>.89</b>	<b>---</b>	
	<b>2921ii</b>	<b>.04</b>	<b>.23</b>	<b>---</b>	<b>.26</b>	<b>---</b>	
	<b>2921iii</b>	<b>.08</b>	<b>.36</b>	<b>---</b>	<b>.83</b>	<b>---</b>	
	<b>2921b</b>	<b>.06</b>	<b>.37</b>	<b>225.8</b>	<b>.15</b>	<b>36.8</b>	
<b>1/15</b>	<b>2924c</b>	<b>.05</b>	<b>.51</b>	<b>360</b>	<b>.11</b>	<b>24.4</b>	<b>Vac. retard No vac. retard 3250 inertia wheel</b>
	<b>2925c</b>	<b>.09</b>	<b>1.19</b>	<b>350.7</b>	<b>.11</b>	<b>24.9</b>	
	<b>2926c</b>	<b>.05</b>	<b>.51</b>	<b>366.1</b>	<b>.09</b>	<b>24.0</b>	
<b>1/16</b>	<b>2927comp</b>	<b>.28</b>	<b>2.42</b>	<b>367.8</b>	<b>.17</b>	<b>23.8</b>	
	<b>2927i</b>	<b>1.07</b>	<b>10.08</b>	<b>---</b>	<b>.51</b>	<b>---</b>	
	<b>2927ii</b>	<b>.04</b>	<b>.38</b>	<b>---</b>	<b>.04</b>	<b>---</b>	
	<b>2927iii</b>	<b>.08</b>	<b>.53</b>	<b>---</b>	<b>.17</b>	<b>---</b>	
	<b>2927h</b>	<b>.06</b>	<b>.26</b>	<b>222.8</b>	<b>.04</b>	<b>39.4</b>	

APPENDIX E--TASK RESULTS:

TASK 1 - Predict performance of an LRSV powered by the engine and an estimate of the maintenance required to preserve the performance levels over 50,000 miles.

A) LRSV engine output  
(Based on actual dynamometer data)

Engine: B-19 derived Lambda-sond emission control system  
Displacement: 2017 cc  
Compression Ratio: 10.4:1  
Max Turbo Boost: 4 Psig

Figure 16

<u>RPM</u>	<u>LRSV Turbo</u>		<u>LRSV (N.A.)</u>	
	<u>hp</u>	<u>Torque (ft.-lbs.)</u>	<u>hp</u>	<u>Torque (ft.-lbs.)</u>
1000	15.0	78.8	15.0	78.8
1500	25.4	88.9	25.4	88.9
2000	35.9	94.3	37.3	98.1
2500	52.0	109.2	49.0	102.9
3000	70.2	122.9	62.3	109.1
3500	86.2	129.3	71.5	107.2
4000	103.3	135.7	81.3	106.7
4500	115.0	134.2	91.9	107.2
5000	122.1	128.2	102.6	107.7

TASK 1 (cont'd)

B) LRSV Preliminary Performance Prediction  
Determined from following data:

- 1 Engine torque: turbo and normally aspirated from figure 16.
- 2 Maximum engine rpm 5000
- 3 Gear Box Ratio:

1st.	3.53
2nd.	1.45
3rd.	1.24
4th.	0.81
Final Drive	3.34
- 4 Assume transmission efficiency 96%
- 5 Wheel dimension P175/14 tire  
Rolling radius 11.5 in.
- 6 Coefficient of Drag = .42  
Frontal Area = 25 ft.<sup>2</sup>
- 7 Rolling Resistance = 36 lbs.
- 8 Curb weight = 3004 lbs.  
Test weight = 3304 lbs.

TASK 1 (cont'd)

Figure 17 LRSV Acceleration Prediction

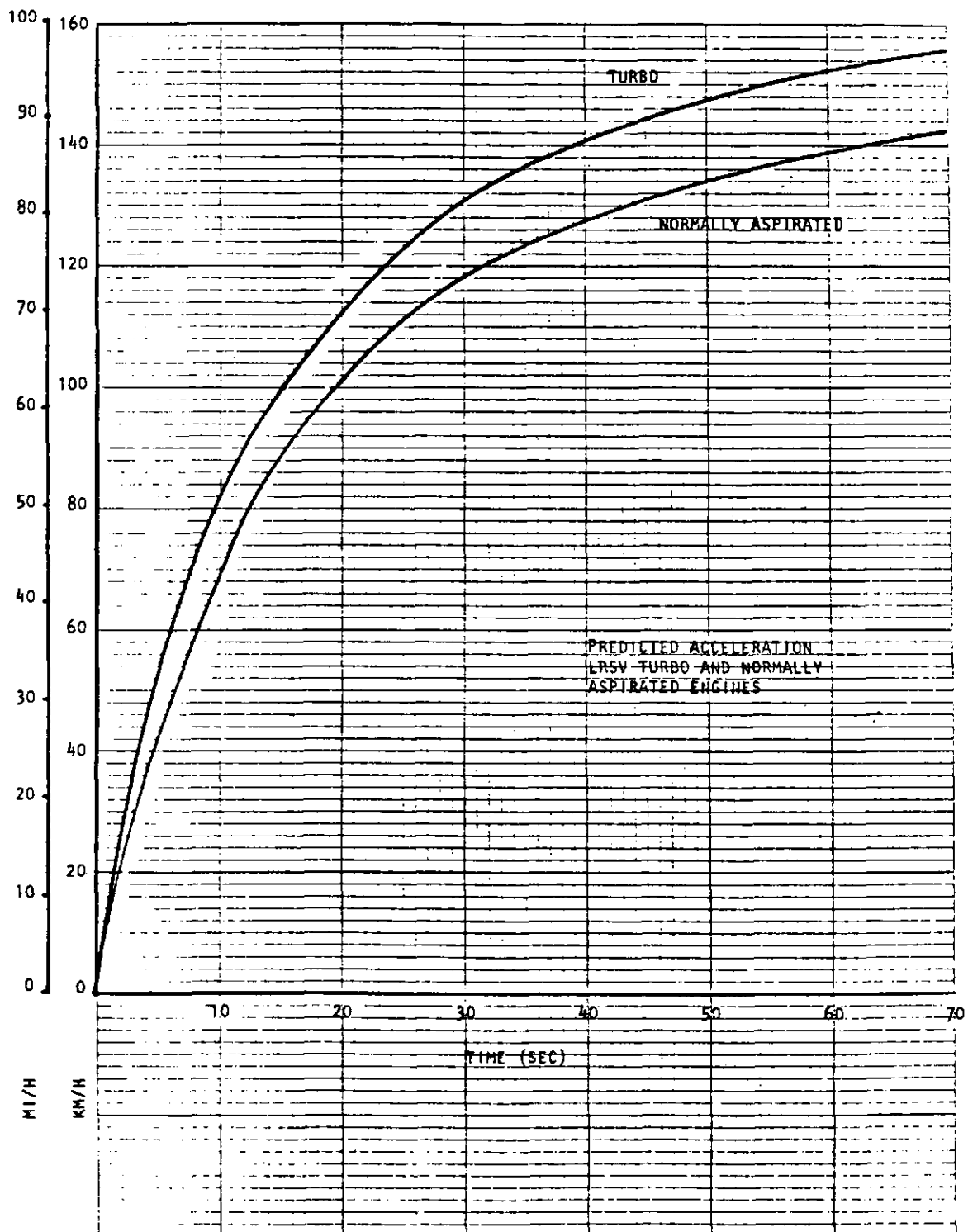
Turbocharged engine:

<u>MPH</u>	<u>TIME (Sec.)</u>	<u>DISTANCE (Ft.)</u>
10	1.20	6.01
20	2.46	36.20
30	4.25	115.73
40	7.50	246.70
50	9.50	417.48
60	13.80	793.74
70	19.75	1280.64
80	28.00	2302.26
90	44.50	5024.16

Normally aspirated engine:

10	1.50	11.30
20	3.30	47.52
30	6.00	137.54
40	9.00	300.79
50	12.40	521.57
60	17.75	1003.24
70	25.50	1702.02
80	40.50	3964.56
90	-----	-----

Figure 18 Predicted Acceleration Curve



TASK 1 (cont'd)

C) LRSV Maintenance Schedule

<u>Replace</u>	<u>Initially (miles)</u>	<u>Interval (miles)</u>
Engine oil and oil filter	600-1200	3,750
Oxygen sensor		30,000
Spark plug		30,000
Transmission oil	600-1200	
Rear axle oil	600-1200	
Air cleaner filter		30,000
Engine coolant		30,000
Camshaft belt (if required)		45,000
<u>Adjust</u>		
Engine drive belts	600-1200	
Torque manifold bolts	600-1200	
Camshaft drive belt	600-1200	
Oxygen sensor	600-1200	10,000
Catalytic converter mounting bolts	600-1200	
<u>Inspect</u>		
Cooling system and connection	600-1200	30,000
Engine drive belts		30,000
Valve clearance		30,000
Vacuum fitting	600-1200	30,000
Idle rpm	600-1200	10,000
Fuel system cap, tank, lines and connections	600-1200	30,000

**TASK 2** Furnish a description of procedure that will be followed in the tests and the type of test data to be acquired. Fabricate engine according to this procedure.

Test Procedure for LRSV Engine

- 1)
  - a) outfit 1978 244DL with vacuum transducer
  - b) run a 1978 FTP
  - c) determine steady state "modelling tool"
- 2)
  - a) construct B-19 Lambda-Sond engine
  - b) break in (three engines) 30 hours each according to load/engine speed schedule
  - c) baseline engine WOT test B-19 and production B-21
- 3)
  - a) test engine at steady state modelling tool conditions
  - b) record engine parameters for following:
    - 1) synthetic oil
    - 2) reduced accessory drive speed
    - 3) multi-spark capacitive discharge ignition system
    - 4) reduced oil pump pressure
    - 5) reduced crankcase pressure
    - 6) elevated coolant temperature
  - c) determine BSFC's of above modifications
- 4)
  - a) blueprint and balance engine
  - b) break in on dyno
  - c) baseline engine
- 5)
  - a) install turbocharging system from mock-up
  - b) break in, baseline
  - c) WOT test turbo engine
  - d) install boost retard system
  - e) match and install injectors

- 6)
  - a) assemble final engine with selected modifications from above test
  - b) install in 244DL test chassis
- 7)
  - a) test on FTP
  - b) drivetrain modifications
  - c) Lambda-Sond modifications

**TASK 3** Engine specifications shall be revised by the findings of TASK 2. Where revisions influence performance, trade off studies shall be conducted to assure that revisions do not unnecessarily compromise performance objectives.

Updated Engine Specifications - None at TASK 3, as actual dynamometer values were utilized for performance predictions, the need to revise the engine specifications are at TASK 3 not necessary. This is evidenced by the satisfactory acceleration data computed during TASK 1, Page 37, Figure 17.

TASK 4 Follow up testing, tests shall be conducted to determine acceleration performance of TASK 3 engine.

Actual Acceleration Times for LRSV - Volvo Chassis

A Data:

- 1 Engine torque: turbo and normally aspirated torque, see Figure 16 Page 35
- 2 Maximum engine speed 5,000
- 3 Gear Box Ratio

1st.	3.17
2nd.	2.16
3rd.	1.37
4th.	1.00
5th.	0.80
Final drive	3.54
- 4 Transmission efficiency 96%
- 5 Wheel dimensions 185/70 SR14  
Rolling radius 11.1 in.
- 6 Coefficient of drag = 0.51  
Frontal area = 22.6 ft.<sup>2</sup>
- 7 Rolling resistance = 37 lbs.
- 8 Curb weight = 3040 lbs.  
Test weight = 3340 lbs. (assumed)

Note: 1980 GL acceleration times are provided for comparison.

TASK 4 (cont'd)

Figure 19

Actual acceleration times:

Engine: LRSV-turbo

Chassis: Volvo 1978 244DL

<u>Zero to mph</u>	<u>Time to Speed LRSV-turbo</u>	<u>1980 Volvo GL</u>
20	2.23	2.15
30	3.40	3.56
40	5.09	5.60
50	6.80	8.10
60	9.50	12.03
70	13.00	16.46
80	16.60	24.03
90	22.10	-----

Note: This data reprinted with permission from Motor Trend Magazine, April 1980, Petersen Publishing Co., Los Angeles, California

**TASK 5**      The durability of the engine in maintaining the specified emission and fuel economy levels shall be extrapolated to 50,000 miles, using actual data and appropriate engineering data.

**Figure 20**

**Predicted Emission Levels and Fuel Economy at 50,000 Miles**

	Initial Level		Predicted Levels 50,000 miles	
	Turbo	Non-turbo	Turbo <sup>1</sup>	Non-turbo <sup>2</sup>
<b>Emission Data:</b>				
HC	0.37	0.19	0.49	0.19
CO	2.96	2.38	4.80	2.54
NOx	0.48	0.57	0.56	0.57
<b>Fuel Economy (Combined):</b>				
MPG	29.65	27.43	30.1	28.04

1) Based on "deterioration factors" for 1980 GLT Turbo,  
Chassis: Volvo LRSV  
Transmission: Volvo 5 Sp. Manual

2) Based on "deterioration factors" for 1978 244 DL Lambda-Sond engine,  
Chassis: LRSV  
Transmission: GM X-body 4 Sp. Manual

**TASK 6** Zero mile test, final drawing, final maintenance schedule, and raw data collected during dynamometer.

A) Zero mile test:

1976 Federal Urban Driving Cycle conducted at Air Resources Lab, Brooklyn, N.Y., August 2, 1979

Test #3021

Figure 21

	<u>HC</u>	<u>CO</u>	<u>CO<sub>2</sub></u>	<u>NOx</u>	<u>MPG</u>
Bag 1	1.24	10.08	---	1.93	---
Bag 2	0.13	1.23	---	0.06	---
Bag 3	0.18	0.94	---	0.22	---
Composite	0.37	2.96	363.2	0.48	24.0
Highway	0.06	0.32	225.8	0.17	39.1

Inertia weight: 3,000 lbs.

Dyno setting: 10.3 hp @ 50 mph.

Chassis: LRSV-Volvo

- B) Final drawing - see separate General Arrangement Drawing
- C) Final maintenance schedule - unchanged from preliminary specification, Page 39
- D) Raw data - see Appendix F, G

Appendix F. Observed and Calculated Data Recorded During Dynamometer Study

VAC. = in. Hg                      Temp. = Dry Bulb, °F  
 Torque = lbs.-ft.                Fuel Flow = lbs./hr.

Test 1:     Baseline  
 VAC:       WOT

<u>RPM</u>	<u>TORQUE</u>	<u>FUEL FLOW</u>	<u>TEMP.</u>	<u>Hp</u>	<u>CORRECTED Hp</u>	<u>BSFC</u>
1600	82.72	9.10	84	23.62	24.38	0.385
2000	91.91	14.60	84	35.00	36.12	0.417
2500	97.68	18.90	85	46.50	48.03	0.406
3000	100.05	22.80	86	57.15	59.09	0.399
3500	99.79	28.00	85	66.50	68.69	0.421
4000	98.46	32.00	86	75.00	77.55	0.427
4500	99.79	39.00	87	85.50	88.49	0.456
5000	99.79	48.00	86	95.00	98.23	0.505
5200	98.21	47.00	87	97.20	100.64	0.483

Test 2:     Baseline  
 VAC:       13.0"  
 Baro:       30.27"

1600	29.15	4.50	83	8.80	9.21	0.507
1900	30.46	6.30	83	11.02	11.02	0.572
2200	28.68	8.40	83	14.19	14.72	0.592
2500	34.14	8.60	83	16.25	16.86	0.529
2800	35.45	9.80	84	18.90	19.63	0.519

Test 3:     Baseline  
 VAC:       13"  
 Baro:       30.28

1600	31.25	5.00	86	9.52	9.90	0.525
1900	29.67	6.30	86	10.73	11.16	0.587
2200	33.35	8.40	86	13.97	14.52	0.601
2500	35.19	8.60	86	16.75	17.42	0.513
2800	35.71	9.80	86	19.04	19.80	0.515

Test 4: Multi-Spark Ignition  
 VAC: 13"  
 Baro: 30.4

<u>RPM</u>	<u>TORQUE</u>	<u>FUEL FLOW</u>	<u>TEMP.</u>	<u>Hp</u>	<u>CORRECTED Hp</u>	<u>BSFC</u>
1600	31.25	4.90	83	9.52	9.81	0.515
1900	32.56	6.10	83	11.78	12.23	0.518
2200	35.45	8.00	83	14.85	15.29	0.539
2500	35.19	8.60	84	16.75	17.26	0.513
2800	36.50	11.20	84	19.46	20.06	0.576

Test 5: Reduced Diameter Crank Pulley  
 VAC: 13"  
 Baro: 30.45

1600	32.03	5.10	81	9.76	10.01	0.523
1900	33.09	6.80	81	11.97	12.28	0.568
2200	35.19	8.20	81	14.74	18.12	0.556
2500	35.98	8.70	80	17.12	17.55	0.508
2800	36.76	10.50	80	19.60	20.09	0.536

Test 6: Synthetic Lubricant  
 VAC: 13"  
 Baro: 30.43"

1600	32.03	5.10	91	9.76	10.15	0.523
1900	32.83	6.80	91	11.87	12.35	0.573
2200	35.71	8.40	91	14.96	15.55	0.561
2500	35.97	8.70	91	17.12	17.81	0.508
2800	36.87	10.80	91	19.65	20.44	0.549

Test 7: Elevated Coolant 210°F Temp.  
 VAC: 13"  
 Baro: 30.80"

1600	28.36	4.70	82	8.64	8.85	0.544
1900	29.15	5.40	82	10.54	10.79	0.512
2200	34.14	6.80	82	14.08	14.41	0.438
2500	34.40	10.20	82	16.37	16.76	0.623
2800	35.19	10.50	82	18.76	19.21	0.560

Test 8: Elevated Coolant 220°F Temp.  
 VAC: 13"  
 Baro: 30.8

<u>RPM</u>	<u>TORQUE</u>	<u>FUEL FLOW</u>	<u>TEMP.</u>	<u>Hp</u>	<u>CORRECTED Hp</u>	<u>BSFC</u>
1600	29.94	4.20	83	9.12	9.34	0.461
1900	29.94	5.80	83	10.83	11.10	0.536
2200	33.09	7.80	83	13.86	14.20	0.563
2500	34.14	8.60	83	16.25	16.65	0.529
2800	35.45	11.00	83	18.90	19.37	0.582

Test 9: Turbocharged  
 VAC: 13"

1600	26.19	5.30	-	7.68	7.77	0.690
1900	29.41	6.30	-	10.64	10.77	0.592
2200	30.99	7.80	-	12.98	13.13	0.601
2500	34.66	8.50	-	16.50	16.70	0.515
2800	37.29	11.09	-	19.88	20.12	0.558

Test 10: Turbocharged  
 VAC: WOT (positive pressure)

2000	93.49	15.59	-	35.60	35.92	0.435
2200	101.70	17.97	-	42.60	43.06	0.422
2400	105.04	19.68	-	48.00	48.43	0.410
3000	121.85	28.81	-	69.60	70.22	0.414
3500	128.15	36.04	-	85.40	86.17	0.422
4000	134.45	25.60	-	102.40	103.32	0.250

Test 11: Blueprinted Engine  
 VAC: 13"

1600	21.00	5.00	-	6.40	6.56	0.781
1900	25.72	6.50	-	9.31	9.55	0.698
2200	30.46	7.90	-	12.76	13.09	0.619
2500	32.81	9.40	-	15.62	16.03	0.602
2800	35.19	11.11	-	18.76	19.24	0.592

Test 12: Blueprinted Engine  
 VAC: WOT

<u>RPM</u>	<u>TORQUE</u>	<u>FUEL FLOW</u>	<u>TEMP.</u>	<u>Hp</u>	<u>CORRECTED Hp</u>	<u>BSFC</u>
1500	86.67	9.99	-	24.75	25.39	0.404
2000	95.59	14.60	-	36.40	37.34	0.401
2500	102.41	19.80	-	48.75	38.31	0.406
3000	106.35	24.00	-	60.75	62.33	0.395
3500	104.97	28.12	-	69.95	71.46	0.402
4000	103.99	38.42	-	79.20	81.26	0.429
4500	104.51	38.00	-	89.55	91.87	0.424
5000	105.04	44.00	-	100.00	102.60	0.440
5200	101.10	45.04	-	100.10	102.70	0.450

Test 13:  
 VAC: 13" Hg

1600	24.94	6.75	-	7.60	7.78	0.888
1900	28.08	7.00	-	10.16	10.40	0.689
2200	31.25	8.19	-	13.09	13.40	0.626
2500	32.56	9.60	-	15.50	15.87	0.619
2800	35.71	11.25	-	19.04	19.49	0.591

Test 14: Blueprinted Engine  
 VAC: WOT

1500	87.18	10.51	-	24.90	25.49	0.422
2000	96.37	14.68	-	36.70	37.58	0.409
2500	103.72	19.70	-	49.37	50.56	0.399
3000	105.04	22.02	-	60.00	61.44	0.367
3500	105.56	36.02	-	70.35	72.03	0.512
4000	104.78	33.99	-	79.80	81.71	0.426
4500	103.20	38.02	-	88.42	90.54	0.430
5000	99.79	45.03	-	95.00	97.28	0.474
5200	102.94	44.03	-	101.92	104.36	0.432

Test 15: Blueprinted Engine  
 VAC: 13"

<u>RPM</u>	<u>TORQUE</u>	<u>FUEL FLOW</u>	<u>TEMP.</u>	<u>Hp</u>	<u>CORRECTED Hp</u>	<u>BSFC</u>
1600	19.95	4.90	-	6.08	6.28	0.806
1900	24.93	6.59	-	9.02	9.32	0.731
2200	29.41	8.30	-	12.32	12.72	0.674
2500	32.46	9.30	-	15.45	15.96	0.602
2800	35.19	11.34	-	18.76	19.38	0.605

Test 16: Blueprinted Engine  
 VAC: WOT

1500	86.38	11.20	-	24.67	25.48	0.454
2000	96.11	15.48	-	36.60	37.80	0.423
2500	102.14	19.59	-	48.62	50.23	0.403
3000	103.99	22.99	-	59.40	61.36	0.387
3500	103.99	28.00	-	69.30	71.58	0.404
4000	104.51	32.00	-	79.60	82.83	0.402
4500	103.46	38.03	-	88.65	91.57	0.429
5000	102.41	43.00	-	97.50	100.71	0.441
5200	100.05	45.96	-	99.06	102.32	0.464

Appendix G Steady State Emission Data Recorded During Dynamometer Study

VAC 13" Hg

Test 1: Baseline Before Catalytic Converter

<u>RPM</u>	<u>% CO</u>	<u>PPM/HC</u>	<u>PPM/NOx</u>
1600	1.10	1.55	300
1900	1.10	1.30	400
2200	0.98	1.39	840
2500	1.00	1.35	1020
2800	0.90	1.18	1220

Test 2: Baseline After Catalytic Converter

1600	0.90	1.30	75
1900	0.20	0.63	65
2200	0.17	0.65	80
2500	0.15	0.62	80
2800	0.13	0.61	20

Test 3: Reduced Diameter Crankshaft Pulley Before Catalytic Converter

1600	2.13	1.53	320
1900	1.60	1.10	520
2200	1.30	1.10	840
2500	1.05	1.00	1160
2800	0.90	0.80	1400

Test 4: Elevated Coolant Temp. - 210°F Before Catalytic Converter

1600	0.72	0.85	380
1900	0.70	0.60	560
2200	0.64	0.60	920
2500	0.70	0.61	1380
2800	0.78	0.44	1380

**Test 5: Elevated Coolant Temp. - 220°F Before Catalytic Converter**

<u>RPM</u>	<u>% CO</u>	<u>PPM/HC</u>	<u>PPM/NOx</u>
1600	1.23	1.15	430
1900	0.80	0.75	460
2200	0.65	0.79	940
2500	0.73	0.72	1240
2800	0.79	0.65	1380

**Test 6: Multi-Spark Ignition System Before Catalytic Converter**

1600	2.23	1.80	320
1900	1.85	1.50	500
2200	1.70	1.55	740
2500	1.40	1.40	1020
2800	1.27	1.29	1300

APPENDIX C

BENDIX AUTOMOTIVE CONTROL SYSTEMS GROUP FINAL REPORT

BENDIX ADAPTIVE BRAKING SYSTEM INSTALLATIONS  
ON MINICARS' RESEARCH SAFETY VEHICLE..... C-1

and

ADAPTIVE BRAKING SYSTEM FOR MINICARS' HIGH  
TECHNOLOGY RESEARCH SAFETY VEHICLE:  
DESCRIPTION AND OPERATING INSTRUCTIONS..... C-21

Final Test Report

Bendix Adaptive Braking  
System Installations on

Minicars'  
Research Safety Vehicles

March 1980

## Final Test Report

### Bendix Adaptive Braking System Installations on Minicars' Research Safety Vehicles

#### SUMMARY

This report summarizes test activities associated with the installation of four-wheel adaptive braking system (ABS) on Minicars' Ride and Handling Test Bed and High Technology Research Safety Vehicle (RSV). A recurring problem associated with insufficient front brake pressure consumed an inordinate amount of activity. However, this problem did not prevent the acquisition of substantial data and satisfactory demonstration of major test objectives.

Briefly, the Ride and Handling Test Bed was initially tested to a portion of MVSS-105 procedures; then, the ABS was installed and system function verified on a number of test surfaces. The system was then transferred to the High Technology RSV which was fitted with new Dunlop run-flat tire / wheel assemblies. Pre-and-post burnish effectiveness data was obtained. System function was verified and demonstrated via an eight-to-ten minute color movie. The balance of this report will discuss testing, results, and related events in more detail. Appendix "A" discusses the brake pressure problem.

#### DISCUSSION

##### Ride and Handling Test Bed

Prior to any vehicle testing, the four Chapman / McPherson strut assemblies were replaced with Minicars' supplied items to accommodate a higher GVW. The vehicle front and rear axles were realigned by a local chassis specialist. New brake pads (procured from local Fiat dealer) were installed with thermocouples per SAE J-46. The vehicle was equipped with a fifth wheel and instrumentation to monitor rear brake pressure, pedal effort, and vehicle deceleration.

The vehicle was loaded to GVW and MVSS-105 test procedures were followed through the second effectiveness portion. Figures 1 and 2 show results of these tests. As requested, a measurement of vehicle deceleration versus brake pressure was then conducted. Figure 3 shows the results.

Ride and Handling Test Bed (Continued)

The four-wheel adaptive braking system was then installed. In preparation for initial system tests, difficulties were experienced in obtaining sufficiently high front brake pressure to assure wheel lock prior to primary master cylinder runout. Many different solutions were attempted with only fair success. Appendix "A" (attached) will provide more details on these efforts.

In order to demonstrate ABS performance, all ballast was removed from the vehicle to reduce high brake pressure requirements. The vehicle was then tested periodically over a six week period at curb weight, plus two occupants, plus approximately 100 pounds of instrumentation.

In a typical test sequence, several alternate system ON and system OFF stops are made under the same test surface / speed condition. SAE J-46 procedures were used including rapid brake application to a high level of effort. Initial speed (0.1 ft./sec. resolution) and stopping distance (0.1 ft. resolution) were recorded. The data was reduced by correcting stopping distance for minor initial speed variations, and then averaging the groups of system ON and system OFF stops. Figure 4 summarizes the results of these ABS performance measurements. Please note the test surfaces changed over the time period due to wear, climate, and, in some cases, resurfacing; thus, no attempt should be made to dwell on absolute distances. In fact, it is for this type of reason that J-46 seeks to compare the system equipped vehicle only with itself in a locked wheel stop at the same surface / speed condition.

High Technology RSV

With satisfactory system function demonstrable on the Ride and Handling Test Bed, transfer to the High Technology RSV was accomplished. The vehicle was also equipped with new brake pads and thermocouples, instrumentation, and weighed with the following results:

	<u>Weight (Lbs.)</u>	
	<u>Front</u>	<u>Rear</u>
Left	576	765
Right	560	760
Totals	<u>1,136</u>	<u>1,525</u>
	<u>2,661</u>	

DISCUSSION (Continued)

High Technology (RSV) (Continued)

Pre-burnish effectiveness was measured at 30 and 60 mph (two occupants) and the results are plotted in Figures 5 and 6. The vehicle was then subjected to the 200 stop burnish schedule of SAE J-46 and 30 and 60 mph brake effectiveness again measured. See Figures 7 and 8.

A short movie was made of the High Technology RSV on a variety of surfaces. The movie sought to visually demonstrate the ABS contribution to vehicle performance, much like SAE J-46, by comparing vehicle behavior with and without the system in operation.

Attachments

Figure 1  
Ride and Handling Test Bed  
MVSS-105 Test Results

Conditions:

- Fuel tank 75 - 100% full.
- Tire inflation pressure correct.
- Weight: Front Axle - 1,440 Lbs.  
Rear Axle - 1,782 Lbs.

First Effectiveness - 30 MPH

<u>Stop Number</u>	<u>Maximum Line Pressure (psi)</u>	<u>Corrected Distance (Ft.)</u>	<u>Maximum Pedal Effort (Lbs.)</u>
1	1,470	41.7	128
2	1,510	41.0	137
3	1,550	40.7	142
4	1,440	42.1	139
5	1,500	40.1	137
6	1,470	42.7	135

(1) Corrected distance,  $D_C = D_A \left\{ \frac{V_0^2}{V_A^2} \right\}$

Where:  $D_A$  = actual distance, feet.  
 $V_A$  = actual velocity, feet/second.  
 $V_0$  = desired velocity, feet/second.

First Effectiveness - 60 MPH

<u>Stop Number</u>	<u>Maximum Line Pressure (psi)</u>	<u>Corrected Distance (Ft.)</u>	<u>Maximum Pedal Effort (Lbs.)</u>
1	1,400	184.9	128
2	1,500	171.5	131
3	1,300	176.4	125
4	1,460	182.4	128
5	1,470	176.0	128
6	1,490	183.6	125

FIGURE 2

Ride and Handling Test Bed  
MVSS-105 Test Results

Second Effectiveness - 30 MPH

<u>Stop Number</u>	<u>Maximum Line Pressure (psi)</u>	<u>Corrected Distance (Ft.)</u>	<u>Maximum Pedal Effort (Lbs.)</u>
1	1,550	44.6	133
2	1,580	41.5	136
3	1,600	40.6	142
4 *			
5	1,500	46.3	135
6	1,525	44.6	140

\* Both front wheels slide, midway.

Second Effectiveness - 60 MPH

<u>Stop Number</u>	<u>Maximum Line Pressure (psi)</u>	<u>Corrected Distance (Ft.)</u>	<u>Maximum Pedal Effort (Lbs.)</u>
1	1,560	176.0	133
2	1,650	170.1	145
3	1,600	174.9	132
4	1,510	175.5	115
5	1,530	181.3	107
6	1,550	179.5	102

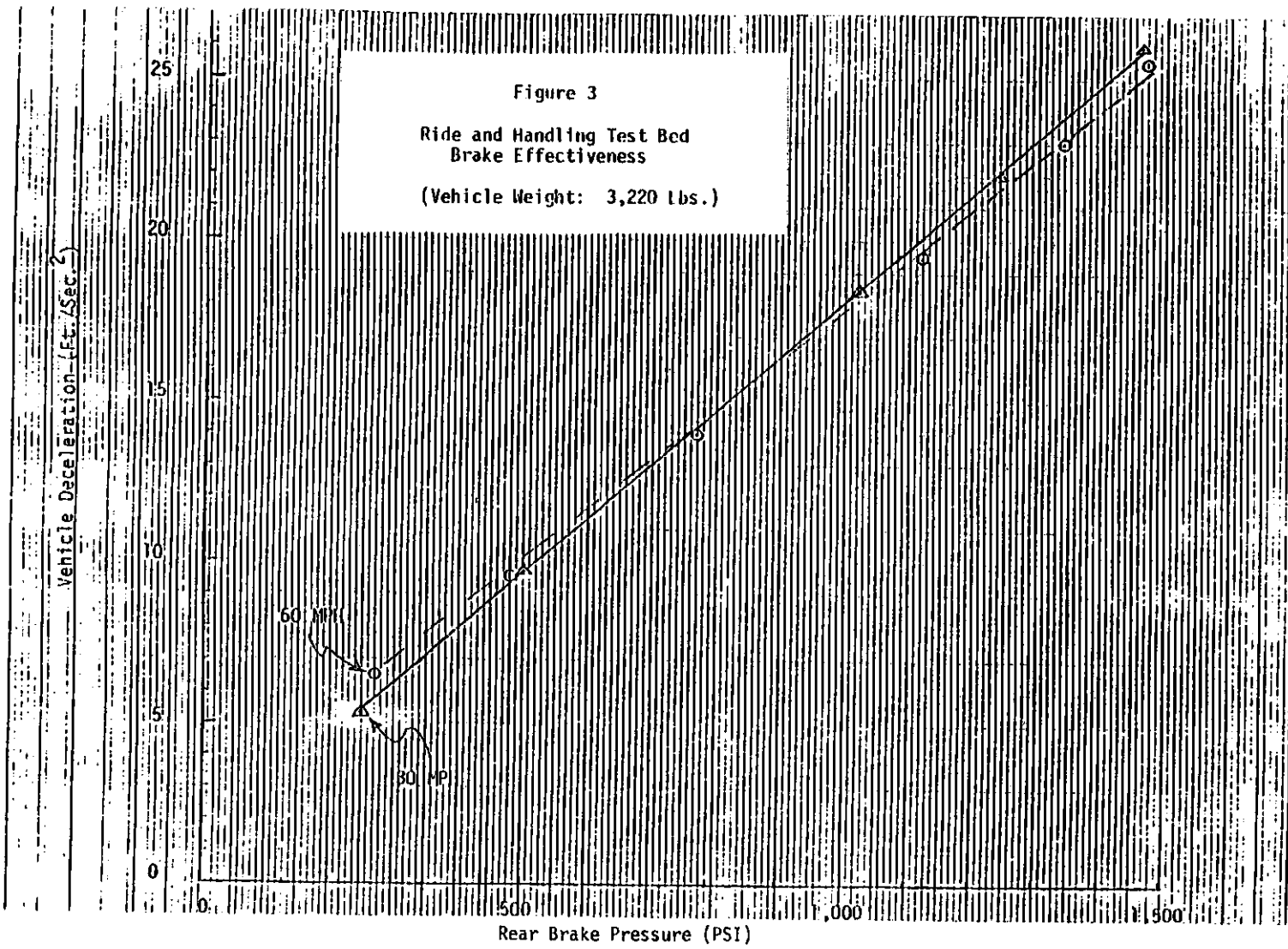


Figure 4

Ride and Handling Test Bed  
ABS Performance Summary

Surface (Skid Number Range)	Speed (MPH)	Corrected Stopping Distance		Improvement <sup>(1)</sup> (Percent)
		System ON (Ft.)	System OFF (Ft.)	
Wet X-10 (18 - 35)	30	76.1	92.6	+18.0
	30	76.8	90.6	+15.2
	30	75.3	90.6	+16.9
	30	117.8	158.7	+25.8
Wet Jennite (28 - 48)	30	73.5	90.0	+15.3
	30	68.3	85.6	+20.2
	40	137.9	177.9	+22.6
	45	118.7	150.6	+21.2
Wet Asphalt (55 - 65)	30	52.0	49.4	- 5.3
Dry Asphalt <sup>(2)</sup> (70 - 85)	30	41.0	38.5	- 6.5
	60	159.9	156.0	- 2.1

1. Percent improvement of system ON over system OFF.

2. Locking of both front wheels sometimes erratic.

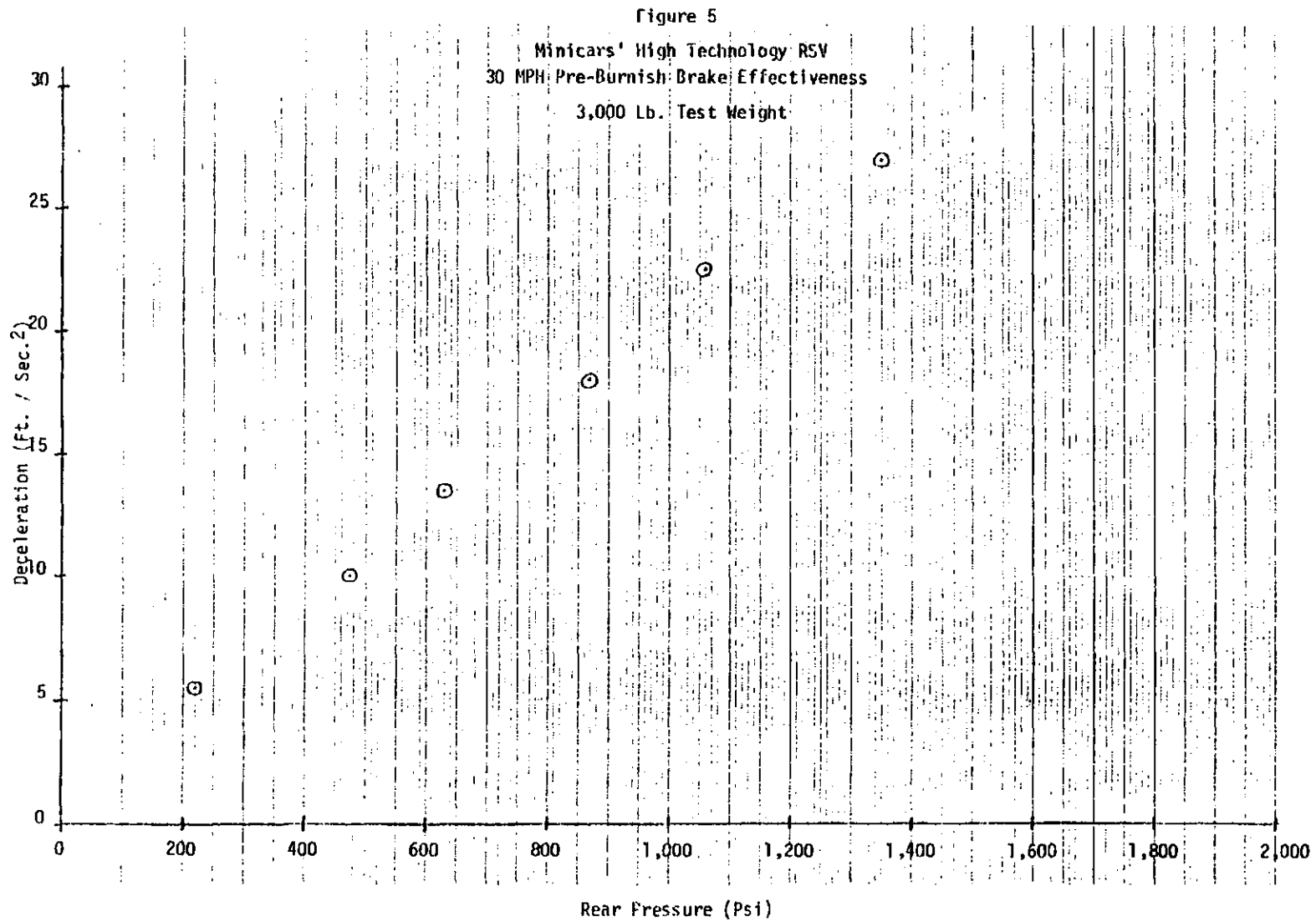
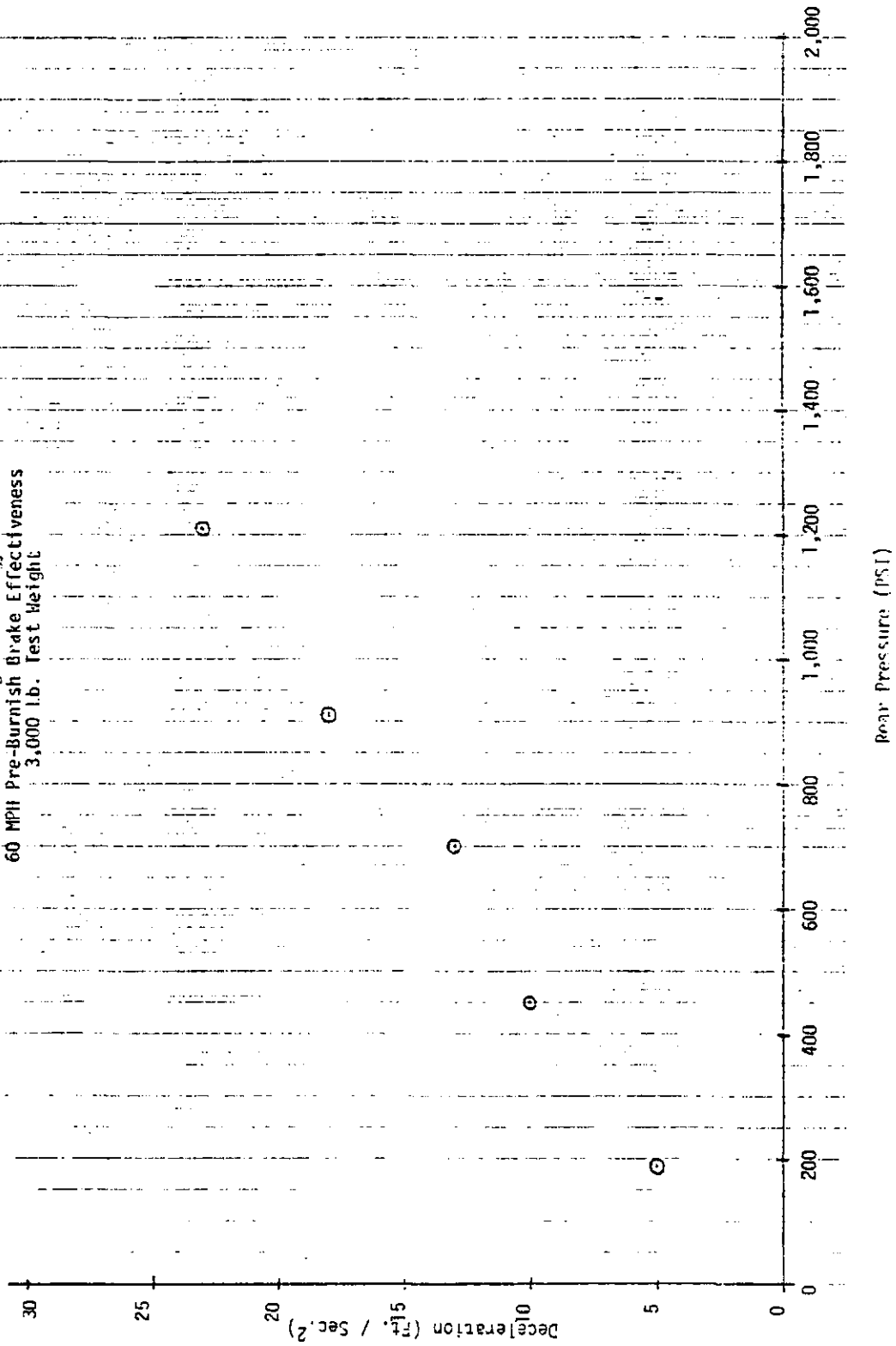
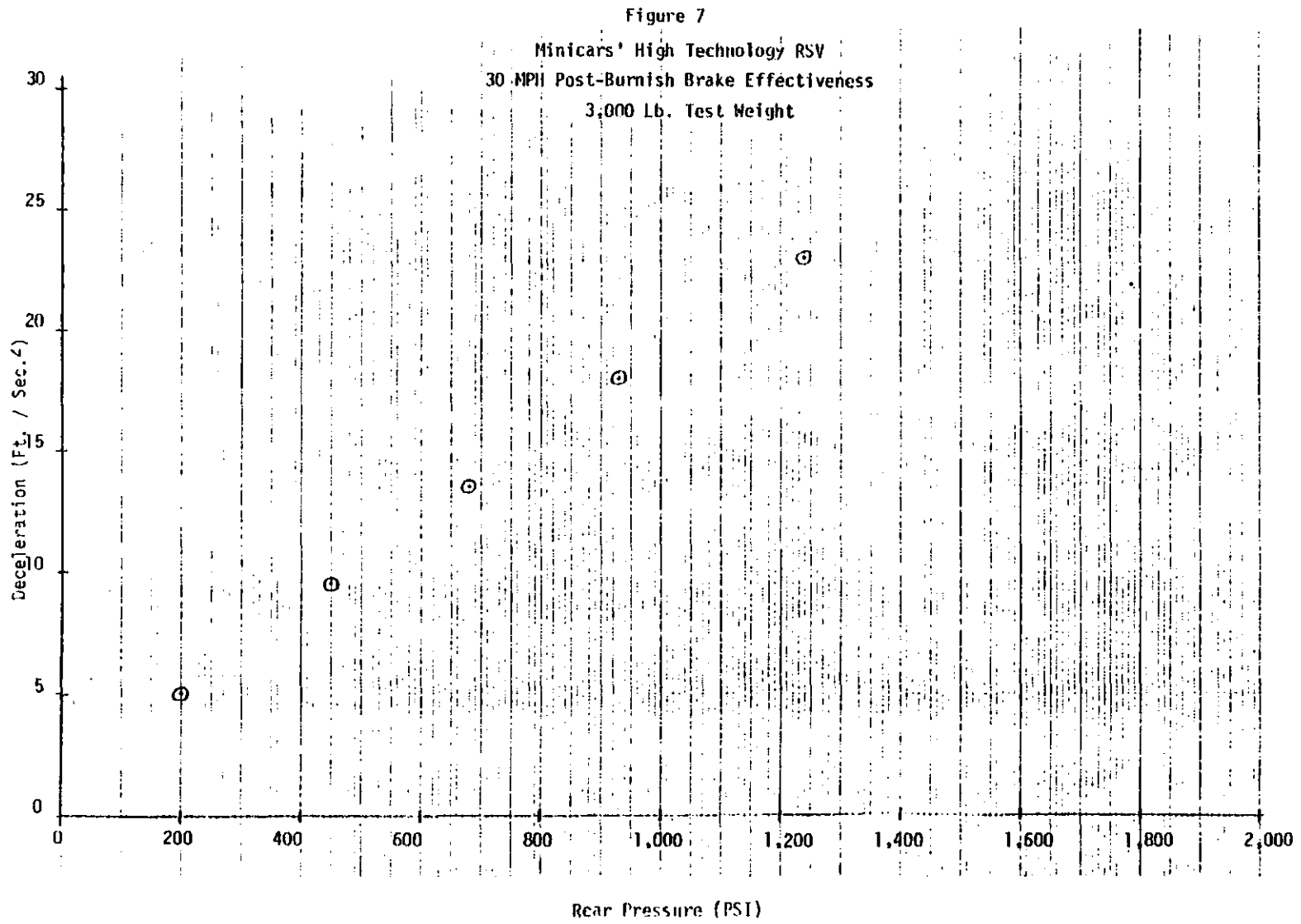
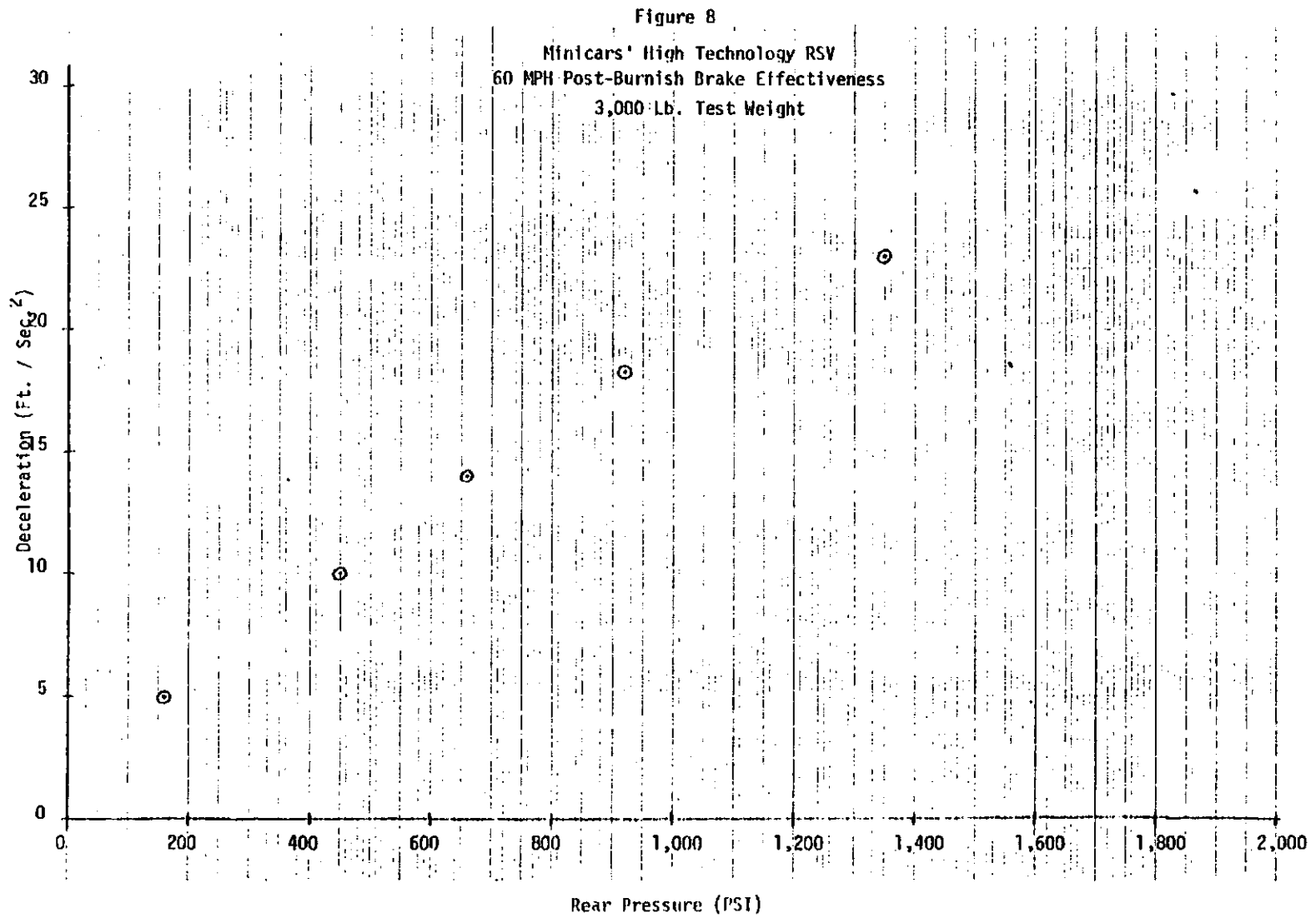


Figure 6

Mintecars' High Technology RSV  
60 MPH Pre-Burnish Brake Effectiveness  
3,000 lb. Test Weight







## Appendix A

### High Brake Pressure Limitation

#### SUMMARY

The ability to develop a given level of brake pressure in the foundation brake system for a given pedal stroke diminished in both vehicles. Thus, for full pedal stroke, peak brake pressure available diminished. No conclusive reason was identified although some attempted changes were helpful in mitigating the problem. This Appendix summarizes activities associated with this phenomena.

#### DISCUSSION

Figures A-1 and A-2 illustrate the changes observed in the stroke / pressure relationship. Figure A-1 demonstrates the relationship of travel and pressure versus pedal effort before any test activity had been conducted on the High Technology RSV. Note that with a pedal travel of four inches, both front and rear pressures in excess of 2,000 psi were demonstrable. Figure A-2 represents data from the same vehicle at a later time. Note here that pedal travel of almost five inches provides pressures of 1,500 psi or less. This reduced maximum pressure produced two effects:

- A. On high coefficients, sufficient torque to quickly lock the front wheels was marginal; thus, a meaningful comparison of OFF versus ON stopping distances was difficult.
- B. With the pedal fully stroked, the primary master cylinder piston (front axle) was also fully stroked. In ABS operation, desired pressure balance in the front regulator was uncertain since even minute motion of the regulator piston could have a substantial effect on front master cylinder pressure in the full stroked situation.

Examination of Figures A-1 and A-2 reveal a difference which suggested an insight into cause of the phenomena. Note on Figure A-1, the initial knee of the pedal stroke application curve occurs at around 0.9" of stroke with an application force of around 12 pounds. By contrast, Figure A-2 shows that 12 pounds of force results in approximately two inches of pedal travel. Thus, this "loss" of an inch of stroke is thought to be a direct casual factor of the diminished high pressure capability.

## DISCUSSION (Continued)

Although the bulk of activity investigating this phenomena was directed at the Ride and Handling Test Bed, both vehicles demonstrated quite similar behavior; therefore, it is concluded that differences between the two vehicles were insignificant. (This dispells the earlier hypothesis that the pressure differential switch, which was only present on the Ride and Handling Test Bed, was a major contributor.)

Presence of ABS was widely examined as a factor on the Ride and Handling Test Bed even though the same system had been installed on several earlier vehicles without incident. However, this hypothesis was ruled out when the phenomena continued to manifest itself on the Ride and Handling Test Bed after the vehicle was returned to standard in preparation for return.

Speculations on the principle cause and subsequent investigations can be grouped broadly into two categories: air in the brake system and some added source of hydraulic compliance.

### Air

Various bleeding techniques were utilized on many different occasions including those suggested by the local Fiat Service Manager and those used by Minicars during vehicle assembly. None of these techniques proved superior. In all cases, pumping the brakes rapidly produced higher peak pressure. The following summarizes these techniques:

Standard Pressure Bleeding - This technique is widely used by Bendix test vehicle support personnel and with only minor variations was suggested by both Minicars and the local Fiat representative. A source of brake fluid, under pressure of 30 - 50 psi, is connected to the master cylinder remote reservoir or to the reservoir lines. A transparent tube is attached to the individual caliper bleed screws; the screw is turned and flow out of the caliper is continued until the flow is free of bubbles or foam. An alternative was used on many occasions where, during the time that flow was under way, the pedal was exercised to promote higher flow rates, intended to dislodge air in the lines which might be stationary due to high surface adhesion.

Reverse Pressure Bleeding - In this technique, flow through the brake system is reversed by connecting the brake fluid pressure source to the caliper bleed screw port and monitoring flow out of the reservoir lines.

## DISCUSSION (Continued)

Vacuum Bleeding - In this technique, a vacuum pump capable of producing approximately 29 In. Hg. is connected to the master cylinder reservoir. After the brake system is thoroughly evacuated, reservoir pressure is returned toward atmospheric. By intent, air removed during evacuation is replaced by fluid from the reservoir.

Manual Bleeding - Mild pressure is applied to the pedal and maintained while the caliper bleed screw is opened and closed. The pedal is then released allowing the master cylinder to be recharged with fluid from the reservoir. The process is continued until the flow out of the bleed screw port is free of bubbles or foam.

Service Bleeding - This technique from the Fiat X-1/9 Service Manual is a variation of manual bleeding. A transparent hose is attached to the bleed screw and the other end is immersed in clean brake fluid. After the bleed screw is opened, the brake pedal is rapidly depressed, then allowed to return slowly. This process is continued until bubble and foam-free fluid is obtained; then, while the pedal is depressed, the bleed screw is tightened.

Other - The master cylinder has two outlet ports in the primary bore, which normally are connected to individual front brake lines. Because only one line was necessary from the master cylinder to the front regulator / modulators assembly, one of the primary ports was plugged. During activities directed at the High Technology RSV, the master cylinder was removed and the two primary outlet ports were plumbed together. The master cylinder was bled in the laboratory and reinstalled. This change made no detectable difference in high pressure capability.

As installed, the master cylinder bore axis is not horizontal; the outlet ports are higher than the reservoir ports. To test the hypothesis that air could be trapped in the top of the master cylinder bore, the front of the High Technology RSV was raised to reverse the inclination of the bore axis with the horizontal. The brake pedal was actuated repeatedly in an effort to flow any air trapped in the master cylinder back into the reservoir. No benefits were detected from this exercise.

### Additional Hydraulic Compliance

This hypothesis came into being because of the apparent diminishment of high pressure capability after the vehicles had been exercised and was strengthened when bypassing of the ABS showed no improvement in pressure capability.

Master Cylinder Replacement - From vehicle instrumentation, it was sometimes observed that the master cylinder front piston would reach a limiting pressure before the pedal had full stroked. This situation allowed rear master cylinder pressure to continue to increase with stroke. This phenomena was not visible during the initial testing (MVSS-105) of the Ride and Handling Test Bed since only rear pressure was monitored. Thus, it was hypothesized that an anomaly might exist with the primary piston seal and / or compensating arrangement. Disassembly of the master cylinder did not reveal any problems. A new master cylinder was procured and installed with no benefits detectable.

Pedal Linkage Hinge Pin - After noting that the hinge pin was made of Delrin tubing, it was hypothesized that high stresses had caused it to yield. A new solid pin was fabricated from aluminum. However, no improvements were noted after installation on the High Technology RSV.

Caliper Mounting Influence - Since the calipers had been removed during speed sensor installation, it was suggested that they had been remounted in a fashion that caused the pads to not be parallel with the contact surface of the new rotors. The calipers were removed from the High Technology RSV hub assemblies and pie shaped sections of a spare rotor were inserted between the pads. However, no change in high pressure capability was observed.

Front Brake Hoses - Under pressure, a slight swelling of the front brake hoses was observed. New hoses were provided by Minicars. However, after installation, no significant improvement was detected.

Master Cylinder Modification - The Fiat X-1/9 brake system includes 48mm front calipers and 34mm rear calipers, meaning that the fronts require essentially twice the fluid displacement as the rears for a given amount of piston travel. The X-1/9 master cylinder has a 50 / 50 split, i.e., front and rear sections displace the same amount of fluid, which is measured as 0.186 cubic inches on the original master cylinder from the Ride and Handling Test Bed. Data from another program indicated that a pair of 48mm calipers would require 0.223 cubic inches at 2,000 psi. As an experiment, the primary piston stroke on the Ride and Handling Test Bed was increased by cutting .122 inches off the piston snout. This change provided an increase in maximum pressure on the front axle sufficient to reliably lock the front wheels. However, this change was not pursued on the High Technology RSV because of MVSS-105 split system implications.

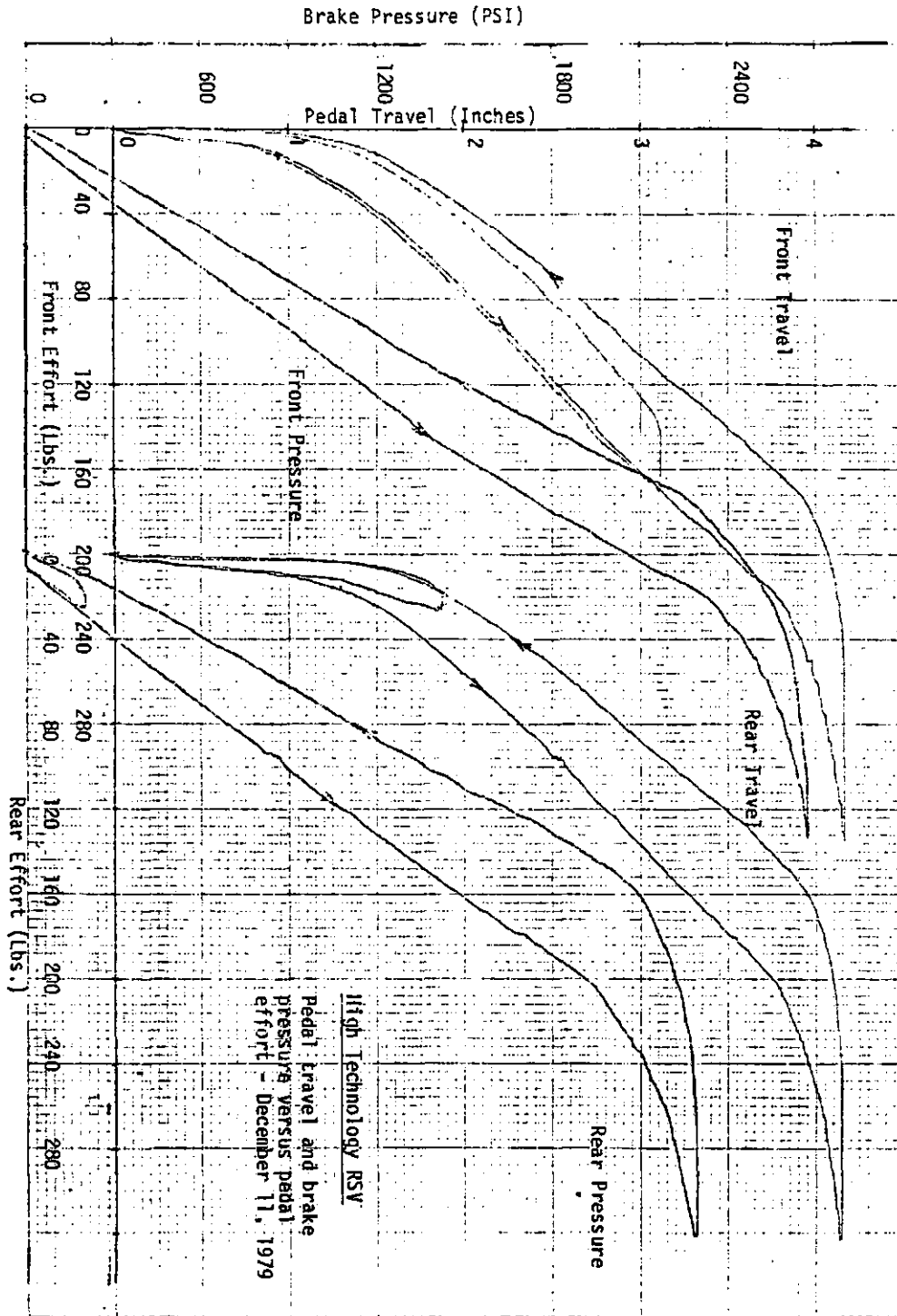


Figure A-1

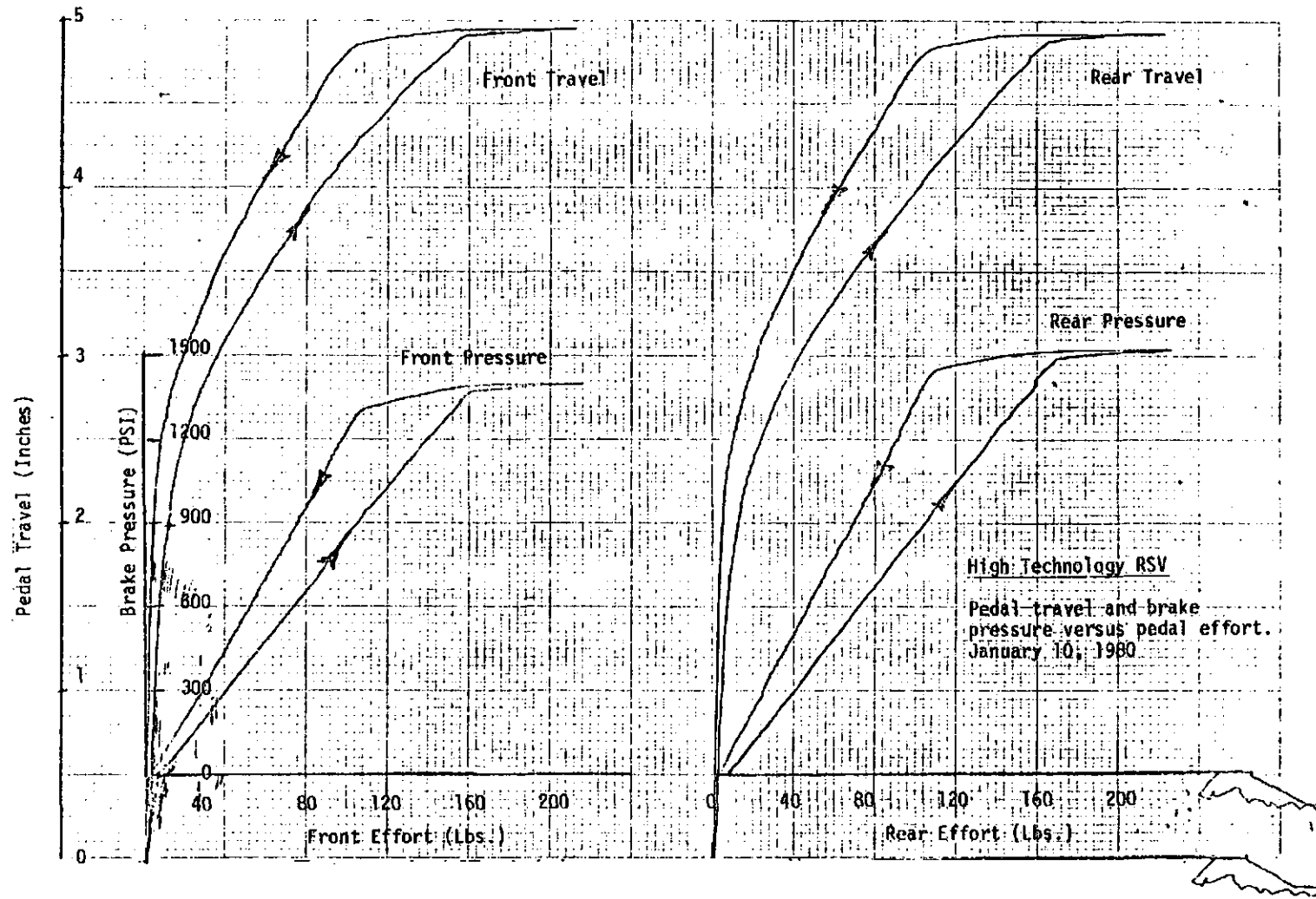


Figure A-2

Adaptive Braking  
System

for

MINICARS  
HIGH TECHNOLOGY  
RESEARCH SAFETY  
VEHICLE

Description

and

Operating Instructions

March, 1980

## INTRODUCTION

This booklet provides operating instructions and describes the four-wheel Adaptive Braking System (ABS) installed in Minicars' High Technology Research Safety Vehicle, DOT License Number 80141. The system is quite similar to other systems installed by Bendix Automotive Control Systems Group (ACSG) in an earlier feasibility program for commercial application, and is also similar to the system utilized in another RSV application.

Briefly, the system consists of wheel speed sensors in each wheel, an electronic control unit, a brake pressure modulator for each front wheel and the rear axle, and a hydraulic power supply which consists of an electric motor driven brake fluid pump and two brake fluid accumulators. Except for the speed sensors, Figure 1, all components are mounted on a common bracket in the right rear corner of the trunk, Figure 2.

The system has no effect on routine braking and requires no participative action by the operator. However, because of the prototype nature of this system and, as well, to allow vehicle evaluation without the system, an ON / OFF switch has been provided. In the OFF position, electrical power to the system pump and solenoid valves is denied by a specially installed relay. When the switch is in the ON position, it is internally illuminated while the ignition key is ON. With the system switch in the ON position and with a brake light signal present, the system continuously monitors for imminent wheel lock. Should this be detected, brake pressure to the affected wheel(s) is decreased and reapplied in order to maximize braking performance and avoidance of wheel lockup at all speeds above approximately five miles per hour. Avoidance of wheel lockup allows for significant vehicle steerability and stability characteristics not otherwise possible.

A red warning light on the instrument panel is connected to the system. This light will illuminate (with the ignition key ON) should the system detect any of several undesirable conditions or if the system switch is in the OFF position. When the warning light is illuminated, the system is inoperable.

Since the system does not require any servicing or periodic maintenance, no special tools or equipment are necessary for support.

The remaining sections of this booklet will describe the system components and function in greater detail.

## SYSTEM COMPONENT DESCRIPTION

### General

The four-wheel Adaptive Braking System (ABS) is designed to prevent any wheel from locking due to excessive brake pressure above a speed of approximately five miles per hour. The system reduces the skid potential of a locked wheel but still maintains brake pressure for maximum stopping effort available with the existing tire / road condition. The end result is to improve the directional control and steerability of the vehicle and, in many cases, to reduce the distance required to bring the vehicle to a stop.

The major components of the ABS are:

1. A speed sensor at each front and rear wheel.
2. An electronic control unit (ECU) located inside the trunk right side adjacent to the fuse panel.
3. An electric motor driven brake fluid pump located in the trunk below the ECU.
4. Two accumulators which are located on the forward side of the ABS mounting bracket inside the right side of the trunk, along the firewall.
5. Two regulators which are attached to the modulators inside the right rear of the vehicle trunk.
6. Three pressure modulators mounted inside the right rear of the vehicle trunk. They are attached to the aft side of the ABS mounting bracket.

Figure 3 illustrates the basic plumbing arrangement of the ABS components.

## SYSTEM COMPONENT DESCRIPTION

### Speed Sensors

Each wheel speed sensor consists of a variable reluctance pickup placed in close proximity to a rotating toothed wheel. The pickup includes a permanent magnet and coil in a case which is attached to the mounting bracket. In this installation, the toothed wheel is formed by teeth cut on the outside diameter of the brake rotor. Clearance between the pickup and toothed wheel is adjustable and is nominally set for .020-inch air gap.

### Electronic Control Unit

The electronic control unit (ECU) is essentially a small computer and contains various electronic components. The unit is encased in a container and includes the necessary cables and connectors. Electronically, the ECU contains three channels, one for each of the three pressure modulators, as well as failure detection logic.

### Wiring System

The wiring system consists of one major wiring harness plus the leads from the speed sensors and the pressure modulators. Figure 4 shows a schematic of the harness and the other electrical leads that make up the wiring system.

### Brake Fluid Pump

This assembly is an electric motor driven single piston pump. The motor is activated by the pump relay. The pump relay coil is powered by ignition voltage; coil current flows when the pump switch provides a ground (low pressure). The pump accepts fluid from the master cylinder reservoir and provides brake fluid under pressure to the two system accumulators. The accumulators are maintained at about 1,700 psi by the pressure sensitive pump switch which turns the pump motor ON and OFF via the pump relay.

## SYSTEM COMPONENT DESCRIPTION

### Accumulators

The two accumulators are spring loaded devices which store pump output fluid under pressure for replenishment of caliper fluid during ABS function. One accumulator is provided for each half of the brake system to preserve the hydraulically split brake system. The accumulators have a check valve at their pump inlets and a filter is provided at their output to the regulators. Also, internal to the accumulators is a relief valve which vents the accumulator to master cylinder reservoir, should the internal pressure exceed approximately 2,700 psi. Attached to the top of the accumulators are low pressure switches which provide an electrical signal (ground) to the ECU when stored pressure is greater than 1,000 psi. This signal is used for failsafe purposes described later.

### Regulators

The regulators receive fluid from the accumulators and provide the modulators with a fluid pressure source equivalent to master cylinder pressure for use during ABS cycling. There are two regulators, a front and a rear, to maintain the brake system split.

### Pressure Modulators

The system includes three pressure modulators. There is a pressure modulator for each front brake and one pressure modulator for the two rear brakes.

The hydraulic brake tubes are routed as follows: (See Figure 3.)

- a. Front Wheels - From the master cylinder primary outlet port to both front brake modulators; from each modulator to an individual front disc brake caliper.
- b. Rear Wheels - From the master cylinder secondary outlet port to the rear brake modulator; from the modulator to the disc brake calipers of both rear brakes.

## SYSTEM COMPONENT DESCRIPTION

### Pressure Modulators (Continued)

The pressure modulators are simply an assembly of two two-way electrically operated solenoids and two flow rate control orifices. The two valves are called "isolation" and "decay" and function as follows: (Refer to Figure 5.)

Isolation Valve - As the name implies, this valve can, when energized, isolate the master cylinder from communicating with the wheel caliper. Normally, the valve is de-energized and master cylinder pressure comes in and passes the open ball seat and passes on to the decay valve. The regulator supply pressure is sealed off by the closed ball seat of this valve.

Decay Valve - Again, as the name implies, this valve can, when energized, allow wheel caliper fluid to bleed to reservoir, decreasing caliper fluid pressure. Normally, the valve is de-energized and master cylinder pressure comes in the top center of the valve seat, passes the open ball seat, and out to the caliper.

The two orifices, build and decay, control the flow rate of the brake fluid during pressure build and decay. Their function will be described in the ABS Function section of this document.

Speed sensor layout drawings, AEXD-10540 and 10541, were provided earlier. Remaining major packaging drawings are attached.

## ABS FUNCTION

### Warning System (Continued)

If the ABS OFF / ON switch is illuminated and the ABS failure lamp is illuminated, then a failure is being detected by the ECU. The conditions under which the ECU will cause the ABS failure lamp to illuminate are as follows:

1. No low I (e.g. fuse blown) - five millisecond delay - non-latching.\*
2. Low pressure switch open (e.g. low accumulator pressure) - 35 millisecond delay - non-latching.\*
3. Any isolation or decay valve continuously energized (e.g. solenoid driver transistor shorted) - 6.8 seconds delay - latching.\*\* Fail only if no brake signal present.
4. Any isolation or decay valve or its conductive path to the ECU open (e.g. connector unplugged) - 6.8 second delay - latching.\*\* Fail only if no brake signal present.
5. Any processed speed sensor signal 15 MPH less than other speed sensor signals (e.g. connector unplugged) - differential must exist for 7.0 seconds - latching.\*\* Fail only if no brake signal present.

\* Non-latching: ABS warning lamp lit only for duration of failure.

\*\* Latching: If failure is detected, ABS warning lamp is lit continuously until ignition switch is turned off.

## ABS FUNCTION

### Ignition OFF

With the ignition switch in the OFF position, the system relay is de-energized and, therefore, no voltage is supplied to the motor / pump or to the ECU for powering solenoids. If the brakes are applied, master cylinder pressure is applied to the calipers as shown in Figure 5, passed the two normally open ports of the solenoid valves.

### Ignition ON

When the ignition is turned ON and the system OFF / ON switch is in the ON position, the system relay is energized providing voltage to the ECU for solenoid power and to the motor / pump. If the vehicle has been sitting for any length of time, the accumulators may have lost some fluid charge; therefore, the ABS warning lamp may be lit, due to low pressure, and the motor will run to charge the accumulators. Within approximately ten seconds, the pump motor will normally have recharged the accumulators, causing the ABS warning lamp to extinguish.

### Engine Running - Vehicle Stationary

The speed sensors do not generate any signals while the vehicle is stationary. In the absence of speed signals, the ECU does not send any commands to the pressure modulators.

If the brake pedal is depressed, master cylinder pressure is applied to the calipers as shown in Figure 5, passed the two normally open solenoid valve ports in each modulator.

### Engine Running - Vehicle in Motion

When the vehicle is in motion, an alternating voltage (AC) is generated at each speed sensor and is sent to the ECU. The frequency of the AC voltage is directly proportional to the speed of the wheel.

The ECU converts the signals received from the speed sensors to a DC voltage which is proportional to wheel speed. If the brakes are not applied, or if they are applied lightly, the ECU sends no commands to the pressure modulators.

## ABS FUNCTION

### Engine Running - Vehicle in Motion (Continued)

When the brakes are applied with greater force, the ECU, based on the signals received from the speed sensors, determines the rate at which each wheel is decelerating. If the rate of deceleration is great enough to produce excess wheel slippage or wheel lockup and a brake light signal is present, the ECU sends commands to the pressure modulator of the slipping wheel(s).

The command from the ECU initially performs two functions at the pressure modulators: (Refer to Figure 6.)

1. It energizes the isolation valve. This shuts off the fluid communication path from the master cylinder to wheel caliper.
2. It energizes the decay valve. This provides a path for now trapped wheel caliper fluid to flow to master cylinder reservoir. The rate of pressure drop is controlled by the decay orifice.

As the caliper pressure decreases, and brake torque consequently reduces, the wheel speed stops decreasing and starts to increase back toward vehicle speed. The ECU, which is continuously monitoring wheel speeds, detects the increase in wheel speed. At the appropriate time, the ECU de-energizes the decay valve. The isolation valve is maintained in an energized condition for a pre-determined fixed period of time. This action results in the following:

1. Isolation Valve Energized - Communication is denied to master cylinder. However, a path is now provided across the lower isolation valve seat to regulator supply. Regulator fluid is supplied from the accumulator at master cylinder pressure.
2. Decay Valve De-energized - Regulator supply is now communicated to the wheel caliper (see Figure 7). The rate of flow from the regulator supply, and therefore the rate of pressure increase at the caliper, is controlled by the build orifice.

## ABS FUNCTION

### Engine Running - Vehicle in Motion (Continued)

This controlled resupply of brake fluid to the caliper increases hydraulic pressure to reapply the brakes at a controlled rate.

The cycle described above is repeated during a hard brake application until the vehicle has stopped or the driver reduces force on the brake pedal below a level which will cause wheel(s) lock. Pressure decay may not occur below five miles per hour due to wheel speed signal resolution.

Under some conditions, the ECU timed isolation valve command, which is set by a decay command, may expire causing the isolation valve to de-energize. If this happens, the driver may notice a slight drop in the brake pedal as the master cylinder is again able to provide fluid to the caliper.

After the ABS stop, when the isolation valve timer in the ECU times out, the isolation valve will de-energize. When this happens, the brake pedal may drop slightly as noted above.

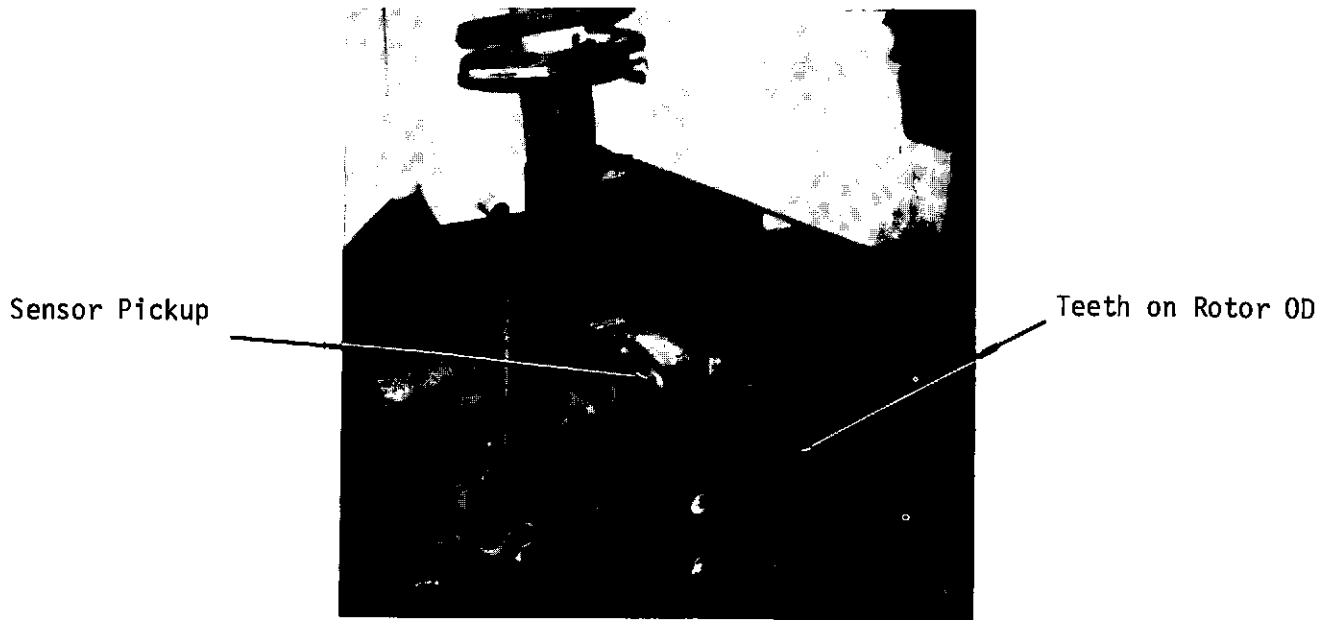
If either accumulator pressure drops below approximately 1,500 psi during ABS cycling, the pump switch will detect this event and provide a ground to the pump relay, causing the electric motor to start and continue to run until the low accumulator is replenished.

### Warning System

The ABS includes a warning sub-system to warn the driver of certain types of failures or undesired conditions in the system. The warning system illuminates the ABS warning lamp to warn the driver that an anomaly exists and inhibits system cycling for the duration of the warning.

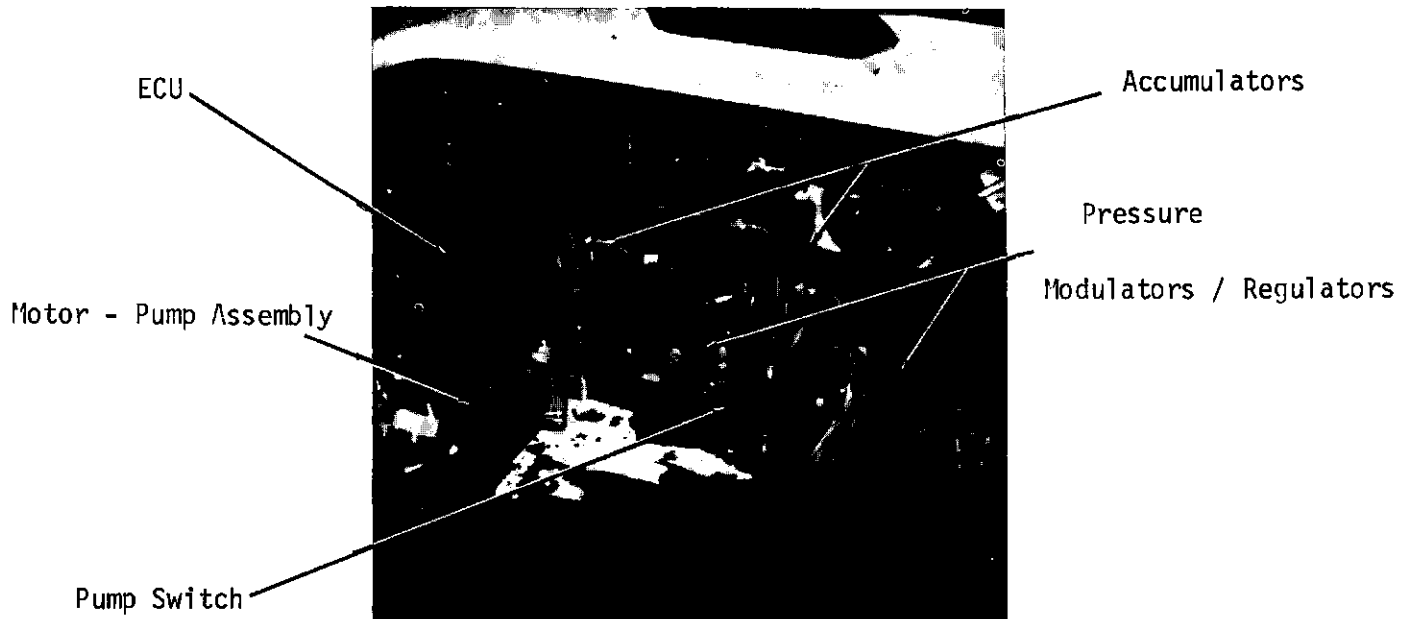
Note that on the wiring diagram, Figure 4, there is an ABS OFF / ON switch. When the switch is ON, the switch's internal lamp is illuminated and the ABS is active. When the switch is OFF, the switch's internal lamp is extinguished and the ABS warning lamp is illuminated. Also when the switch is OFF, the system relay is de-energized, which denies power to the electric motor driven pump and all power required to energize solenoid valves in the pressure modulators (Hi I conductor).

Figure 1

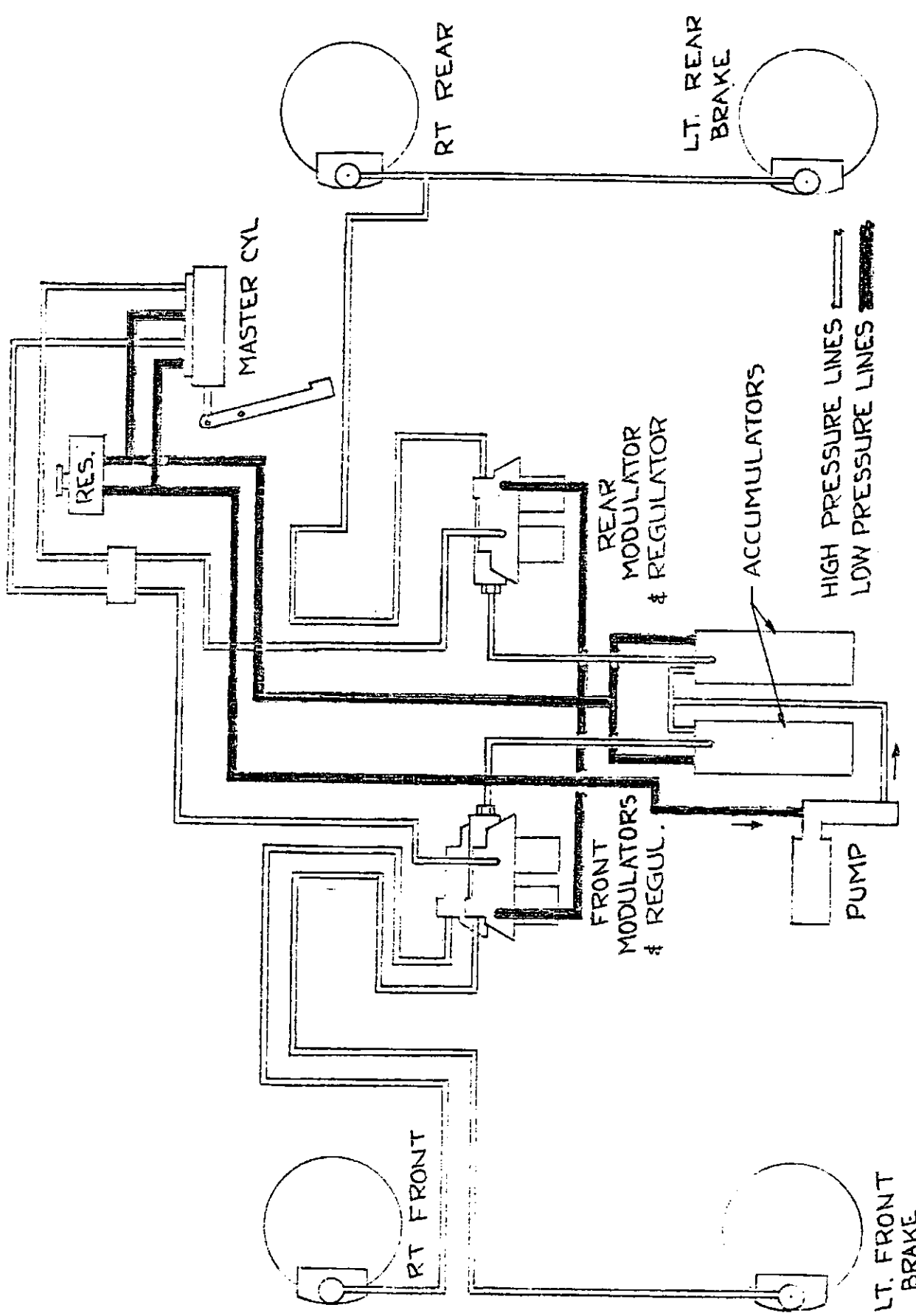


TYPICAL WHEEL SPEED SENSOR

Figure 2

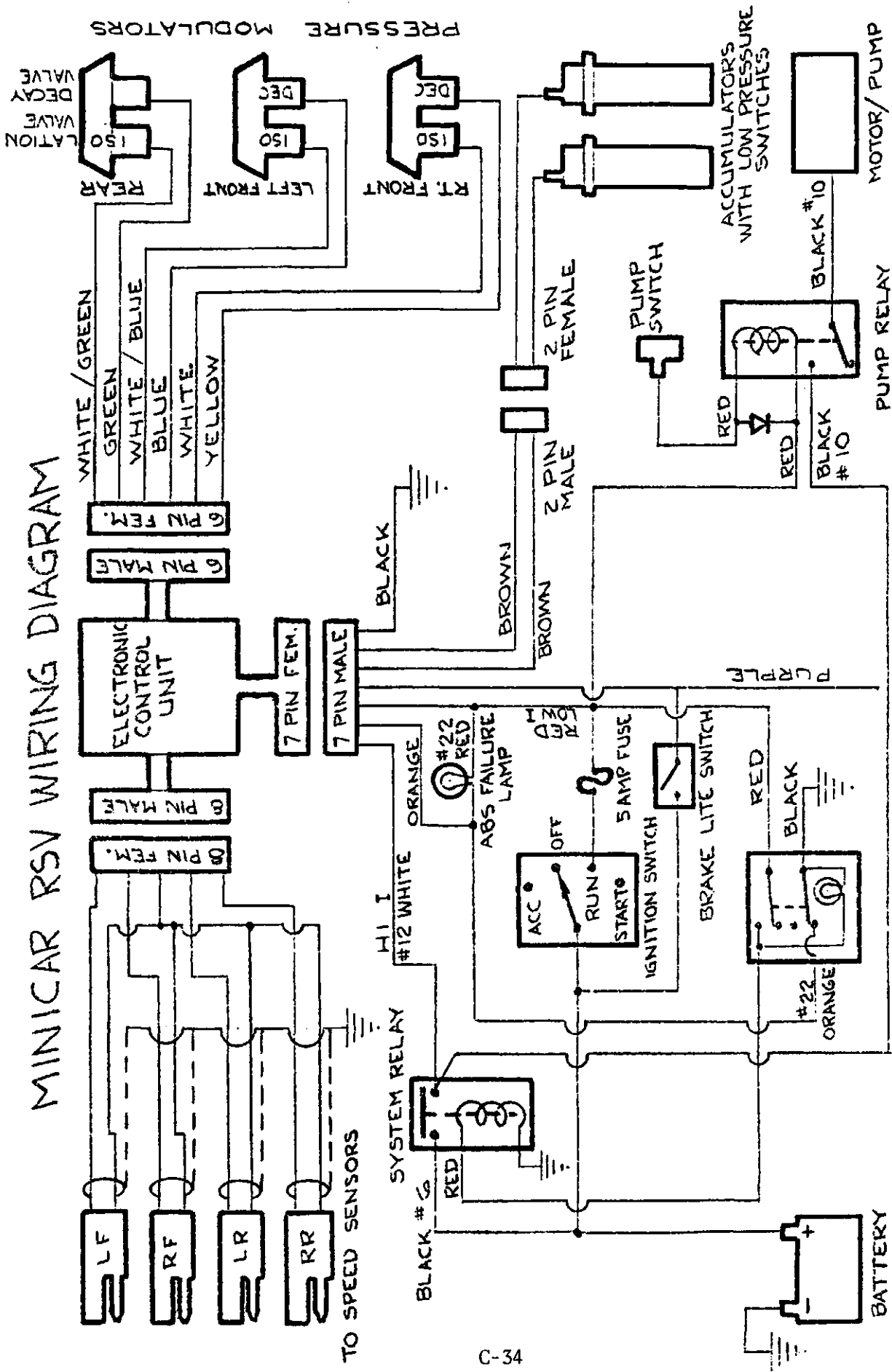


ABS TRUNK LAYOUT



MINICAR RSV HYDRAULIC DIAGRAM  
 FIGURE 3

# MINICAR RSV WIRING DIAGRAM



#18 WIRE UNLESS OTHERWISE NOTED

TO STOP LIGHTS

FIG. 4



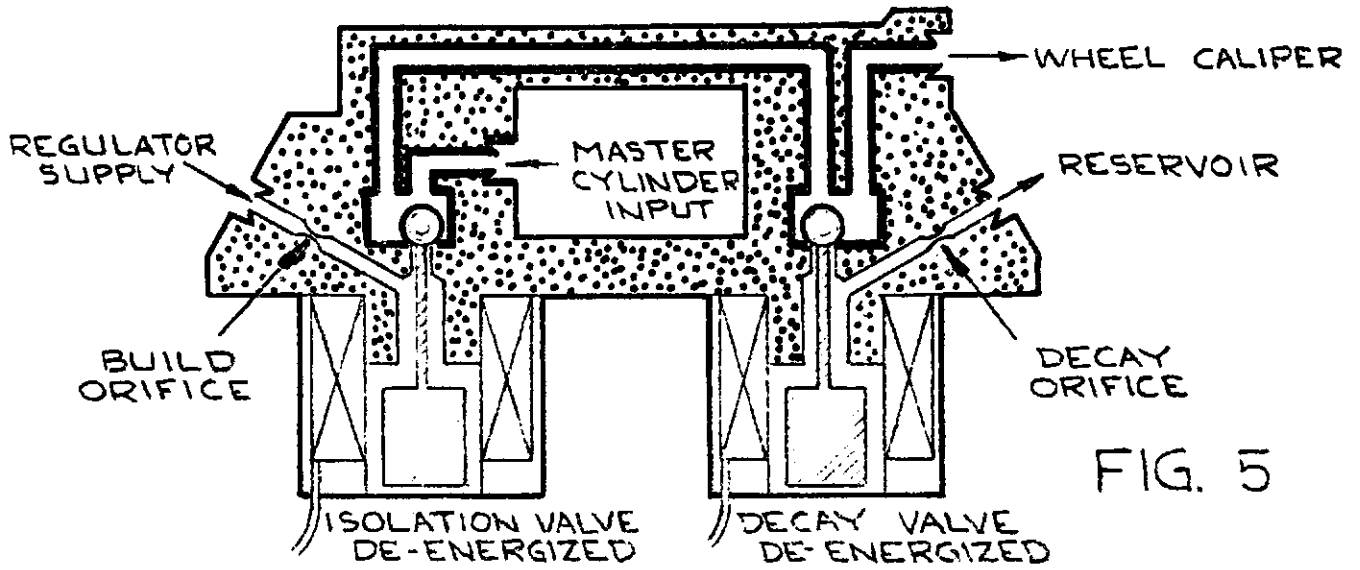


FIG. 5

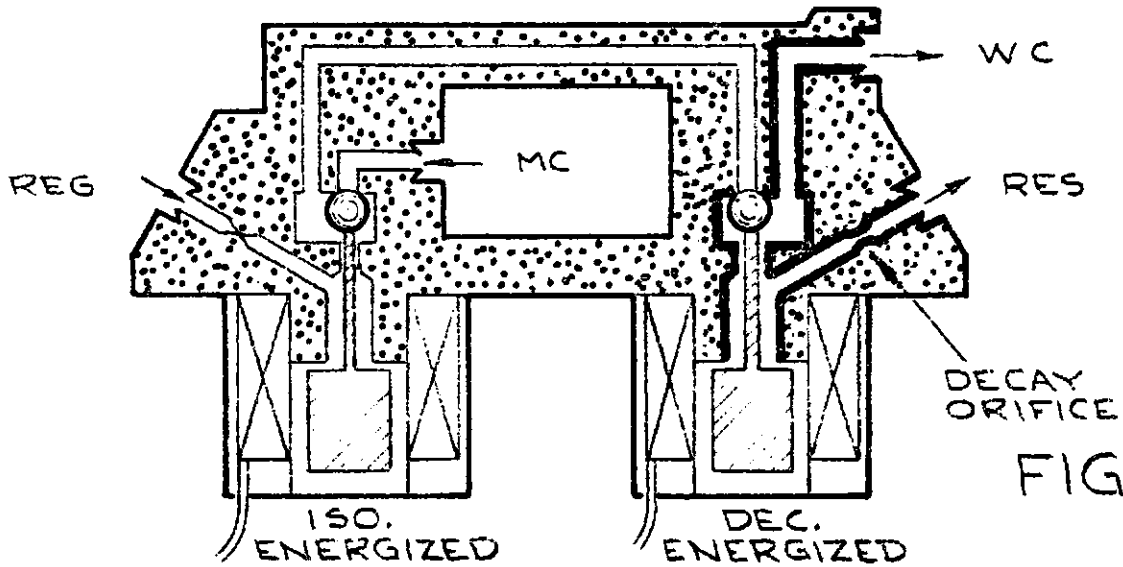


FIG. 6

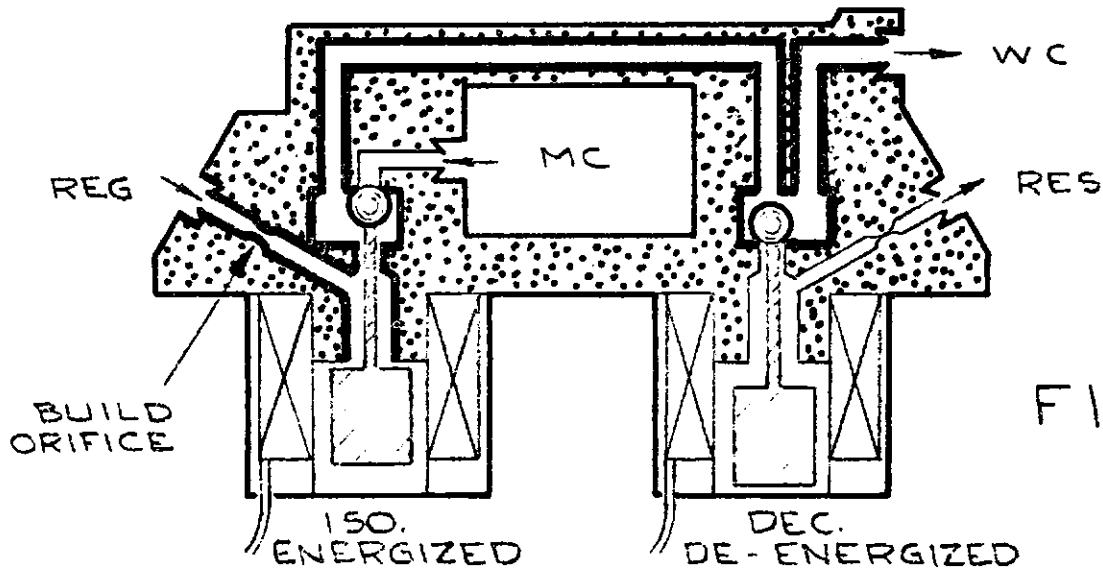
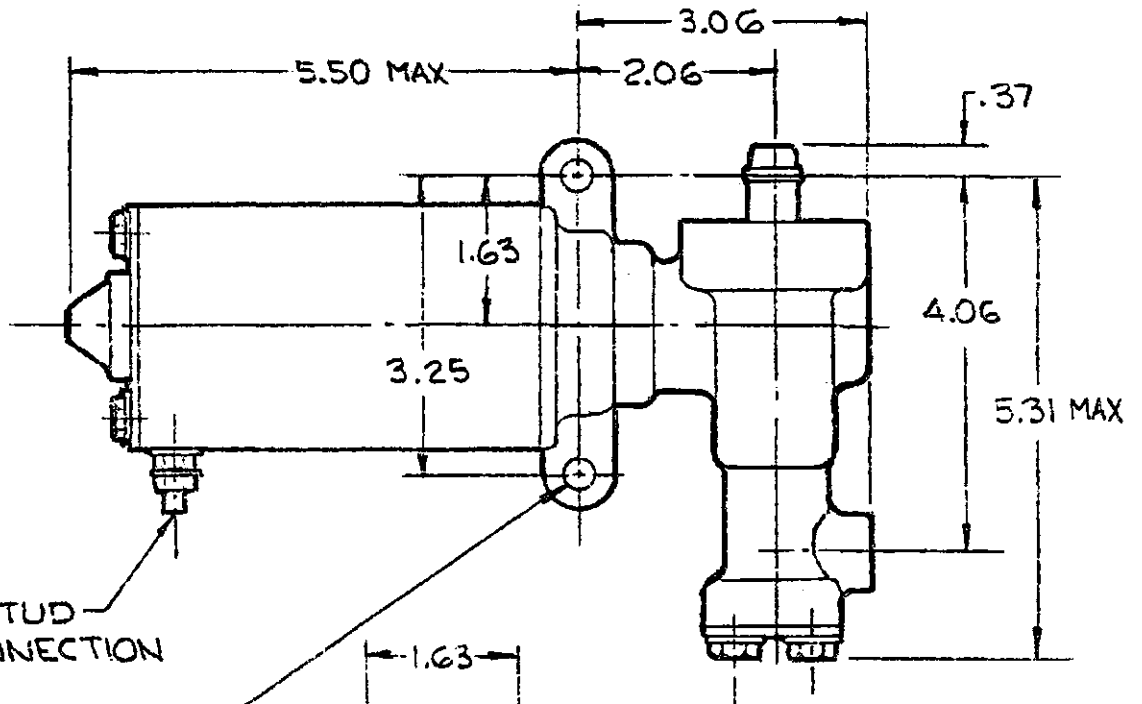
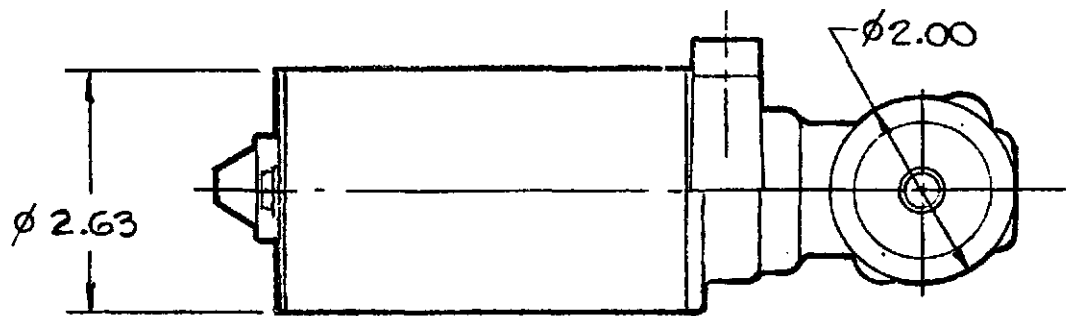


FIG. 7

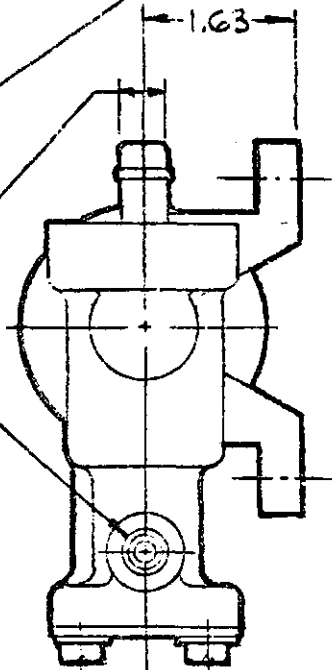


#10-32 STUD  
12 V. CONNECTION

.34 DIA - 2 HOLES  
FOR MOUNTING

INLET FITTING  
FOR 1/2" I.D.  
FLEXIBLE HOSE

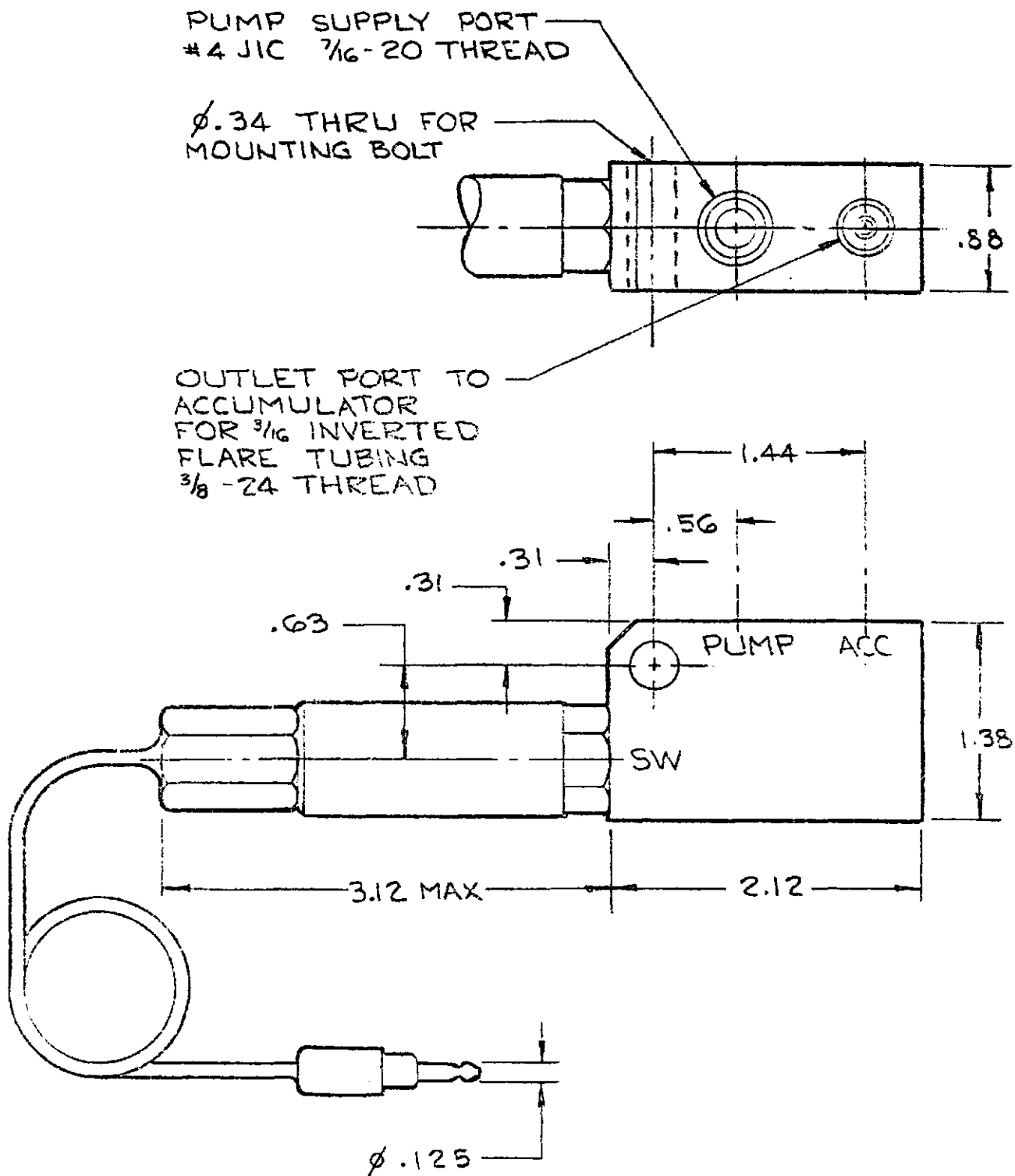
OUTLET PORT  
#4 JIC  
1/16-20 THREAD



ABS MOTOR/PUMP ASSEMBLY

C-36





# ABS PUMP SWITCH ASSEMBLY





